

USAAMRDL-TR-76-13



PROGRAM FOR EXPERIMENTAL INVESTIGATION OF FAILURE PROGNOSIS OF HELICOPTER GEARBOXES

Northrop Research and Technology Center
3401 West Broadway
Hawthorne, Calif. 90250

2000 AD

August 1976

Final Report



Approved for public release;
distribution unlimited.

Prepared for

EUSTIS DIRECTORATE
U. S. ARMY AIR MOBILITY RESEARCH AND DEVELOPMENT LABORATORY
Fort Eustis, Va. 23604

EUSTIS DIRECTORATE POSITION STATEMENT

The work reported herein is part of a continuing effort at the Eustis Directorate, USAAMRDL, to conduct investigations directed toward advancing the state of the art of diagnostics and prognostics for Army aircraft. The object of this particular effort was to identify useful sensed parameters and analysis techniques that would provide prognostic information on the mechanical condition of helicopter power train components. The contractor instrumented five UH-1 90° gearboxes and tested them for more than 4,600 hours. Vibration sensing and analysis techniques as well as both conventional and new oil monitoring techniques were included in the investigation.

The trend analysis of the data collected from the gearboxes was hampered by the fact that the majority of the gearboxes did not fail catastrophically during the testing.

A related contract has been awarded to Northrop Corporation (DAAJ02-75-C-0019) by the Eustis Directorate to conduct additional prognostic investigations using UH-1 90° gearboxes. The findings of this reported effort are being used to conduct an improved controlled prognostic data acquisition and analysis effort under the new contract.

The technical monitor for this contract was Mr. G. William Hogg, Military Operations Technology Division.

ACCESSION NO.	EUSTIS DTC	CHART NUMBER	JESTIFICATION	BY	TYPE SPECIFIC SERIAL NUMBER	SPECIAL CODES

DISCLAIMERS

The findings in this report are not to be construed as an official Department of the Army position unless so designated by other authorized documents.

When Government drawings, specifications, or other data are used for any purpose other than in connection with a definitely related Government procurement operation, the United States Government thereby incurs no responsibility nor any obligation whatsoever; and the fact that the Government may have formulated, furnished, or in any way supplied the said drawings, specifications, or other data is not to be regarded by implication or otherwise as in any manner licensing the holder or any other person or corporation, or conveying any rights or permission, to manufacture, use, or sell any patented invention that may in any way be related thereto.

Trade names cited in this report do not constitute an official endorsement or approval of the use of such commercial hardware or software.

DISPOSITION INSTRUCTIONS

Destroy this report when no longer needed. Do not return it to the originator.

Unclassified

SECURITY CLASSIFICATION OF THIS PAGE (When Data Entered)

DD FORM 1473 EDITION OF 1 NOV 68 IS OBSOLETE

Unclassified

SECURITY CLASSIFICATION OF THIS PAGE (When Data Entered)

Unclassified

SECURITY CLASSIFICATION OF THIS PAGE(When Data Entered)

2.0 Abstract - continued

During this program five gearboxes were tested for a composite total of over 4600 hours. The gearboxes were loaded at 40 hp torque on the output shaft, and the entire test and data collection system was automatically controlled by a computer. Of the five gearboxes tested, one was a high time unit, three had incipient bearing failure and one had an incipient gear failure. Data from temperature sensors, ultrasonic and low-frequency accelerometers, oil debris monitors, a shock pulse analyzer and the sensors which monitored the test cell itself was collected automatically at 4-minute intervals. All sensors were not used on all gearboxes. Spectroscopic oil analysis (SOA) of gearbox oil was conducted on a routine basis. Gearboxes were disassembled and wear inspections were made before and after each test. Some gearboxes were tested and disassembled three times during the program. Polynomial and exponential trending and least-mean-square prediction techniques were used to determine if the low-frequency vibration signals provided useful trends for predicting future wear in these gearboxes. Only a limited amount of vibration data was selected for trend analysis, and the data selected did not show trends which could be related to gearbox wear.

None of the real-time sensors provided data which indicated the wear condition of a gearbox. Ultrasonic vibration signals might have been more meaningful if a broadband accelerometer had been available. The spectroscopic oil analysis (SOA) and dynamic noise tests gave the most useful information on the condition of the gearbox components. If more appropriate analysis techniques were developed, the low-frequency vibration data might prove to be the most useful prognostic tool.

Unclassified

SECURITY CLASSIFICATION OF THIS PAGE(When Data Entered)

SUMMARY

The objective of this program was to run five different UH-1 helicopter 90° gearboxes for a total of 5000 hours to determine if the output of the sensors attached to the gearboxes contained information that would allow us to predict the future mechanical condition of the gearboxes. A test cell to operate the gearboxes was built. An automatic computer-controlled data collection, reduction, processing and storage system was designed. The computer also automatically controlled the operation of the test cell so that the gearboxes could be operated unattended. This automated system allowed the gearboxes to be run continuously. This resulted in the collection of more data than could be analyzed under the contract. A variety of sensors was used to monitor the wear occurring in the gearboxes, including oil debris monitors, accelerometers, a shock pulse analyzer, and temperature sensors. Spectroscopic oil analysis (SOA) of the gearbox oil was conducted at regular intervals. The gearboxes were disassembled and inspected for wear prior to and following each test. Wear measurement techniques included visual inspection by an expert, measurements of ball and ball track wear, dynamic noise testing of bearings, and scanning electron microscope photographs of the surface of one ball from each bearing.

Polynomial and exponential trending techniques were applied to some of the vibration data. The least-mean-square (LMS) prediction technique was also used on the vibration data.

The most useful sensors for future prognostic programs appear to be the ultrasonic and low-frequency accelerometers and the shock pulse analyzer. The SOA is extremely useful for determining when the gearbox is experiencing a period of excessive wear. The dynamic noise test is a reliable and consistent measurement of bearing wear patterns. The tentative conclusion is that information related to the wear of the mechanical components is present in the output signals from some of the sensors and that, with further effort, it may be possible to successfully predict the remaining useful lifetime of mechanical components.

PREFACE

This program was carried out for the Eustis Directorate, U. S. Army Air Mobility Research and Development Laboratory under Contract DAAJ02-72-C-0118, Task 1F162203A43405. Mr. William Hogg served as the principal technical monitor for this program. His enthusiastic support of this program and contract guidance are deeply appreciated.

TABLE OF CONTENTS

	<u>Page</u>
SUMMARY	3
PREFACE	4
LIST OF ILLUSTRATIONS	11
LIST OF TABLES	22
INTRODUCTION	23
TEST INSTRUMENTATION AND PROCEDURES	24
TEST CELL AND CONTROLLER	24
Test Stand	24
Test Cell Controller (TCC)	27
Computer-Test Cell I/O	28
SENSORS AND SENSOR LOCATIONS	32
Temperature Sensors	32
Oil Debris Monitors	32
Chip Detector	33
Capacitance Type ODM	33
X-Ray Fluorescence Type ODM	36
Spectroscopic Oil Analysis	36
Low-Frequency Accelerometers	39
Ultrasonic Accelerometers	43
Shock Pulse Analyzer	44

TABLE OF CONTENTS (Continued)

	<u>Page</u>
Torque Sensing	48
RPM Sensor	48
DETERMINATION OF BEARING CONDITION AND SURFACE WEAR	50
Visual Inspection	50
Ball Bearings Wear Measurements	53
Dynamic Noise Testing of Ball Bearings	53
Radial Play Measurements of Ball Bearings	56
Cross-Groove Profile of Inner Race of Ball Bearings	56
Roller Bearing Wear Measurements	60
Roller Crown Measurement	60
Roller Axial Play	61
SCANNING ELECTRON MICROSCOPE SURFACE INSPECTION	61
Secondary Emission Mode (SEC)	61
Backscatter Emission Mode (BSE)	61
AUTOMATIC COMPUTER-CONTROLLED DATA COLLECTION AND REDUCTION	64
OVERVIEW OF MAIN COMPUTER SOFTWARE	64
START-UP SEQUENCE ROUTINE	64
SENSOR SELECT AND PROCESSING ROUTINE	64
DATA ANALYSIS - THEORY AND PROCEDURES	73

TABLE OF CONTENTS (Continued)

	<u>Page</u>
VIBRATION DATA REDUCTION	73
STATISTICAL ANALYSIS OF VIBRATION DATA	77
POLYNOMIAL TRENDING	80
EXPONENTIAL TRENDING	83
TRENDING BY LEAST-MEAN-SQUARE PREDICTION . .	91
EXPERIMENTAL RESULTS	95
HIGH TIME (HT) GEARBOX TESTS	97
Mechanical Condition of HT Gearbox	97
Spectroscopic Oil Analysis (SOA)	99
Oil Debris Monitors (ODM)	100
Temperature Sensors	101
Ultrasonic RMS Accelerometers	101
Shock Pulse Analyzer	102
Low-Frequency Vibration Data	104
Correlation of Sensor Outputs With Mechanical Condition	111
Summary of HT Gearbox Test Results	111
BAD BEARING (BB) GEARBOX TESTS	112
Mechanical Condition of BB Gearbox	112
Spectroscopic Oil Analysis (SOA)	113
Oil Debris Monitors (ODM)	114
Temperature Sensors	116

TABLE OF CONTENTS (Continued)

	<u>Page</u>
Ultrasonic RMS Accelerometers	116
Shock Pulse Analyzer	117
Low-Frequency Vibration Data	117
Correlation of Sensor Outputs With Mechanical Condition	121
Summary of BB Gearbox Test Results	122
BAD GEAR (BG) GEARBOX TESTS	122
Mechanical Condition Summary for BG Gearbox	123
Spectrochemical Oil Analysis (SOA)	124
Oil Debris Monitors (ODM)	124
Temperature Sensors	124
Ultrasonic RMS Accelerometers	124
Shock Pulse Analyzer	126
Low-Frequency Vibration Data	126
Correlation of Sensor Outputs With Mechanical Condition	132
Summary of BG Gearbox Test Results	132
BAD BEARING TWO (BBT) GEARBOX TESTS	133
Mechanical Condition of BBT Gearbox	133
Spectroscopic Oil Analysis (SOA)	135
Oil Debris Monitors (ODM)	138
Temperature Sensors	138

TABLE OF CONTENTS (Continued)

	<u>Page</u>
Ultrasonic RMS Accelerometers	138
Shock Pulse Analyzer	139
Low-Frequency Vibration Data	145
Correlation of Sensor Outputs With Mechanical Condition	154
Summary of BBT Gearbox Test Results	157
BAD BEARING THREE (BB3) GEARBOX TESTS	157
Mechanical Condition of BB3 Gearbox	158
Spectroscopic Oil Analysis (SOA)	158
Oil Debris Monitors (ODM)	159
Temperature Sensors	159
Ultrasonic RMS Accelerometers	159
Shock Pulse Analyzer	159
Low-Frequency Vibration Data	165
Correlation of Sensor Outputs With Mechanical Condition	172
Summary of BB3 Gearbox Test Results	172
VIBRATION DATA - BEARING FREQUENCIES	172
CONCLUSIONS	174
RECOMMENDATIONS	177
LITERATURE CITED	182

TABLE OF CONTENTS (Continued)

	<u>Page</u>
APPENDIXES	
A DEVELOPMENT OF Z-SCORE AND LMS PREDICTION TECHNIQUES	183
DEVELOPMENT OF Z-SCORE TEST	183
CORRECTED Z-SCORE	186
DERIVATION OF LMS PREDICTION TECHNIQUE . .	189
B DETAILED DOCUMENTATION OF GEARBOX TESTS .	195
HIGH TIME (HT) GEARBOX (ABC-1329)	195
BAD BEARING (BB) GEARBOX (ABC-3398)	227
BAD GEAR (BG) GEARBOX (B13-6884)	246
BAD BEARING TWO (BBT) GEARBOX (B13-3395) .	265
BAD BEARING THREE (BB3) GEARBOX (B13-9974)	302
LIST OF SYMBOLS AND ABBREVIATIONS	325

LIST OF ILLUSTRATIONS

<u>Figure</u>		<u>Page</u>
1	Overall View of Test Stand	25
2	Test Stand - Mechanical and Hydraulic Circuit Diagram	26
3	Block Diagram of Test Cell Controller	29
4	Interactive Computer Graphics System	30
5	Block Diagram of Computer - Test Cell I/O Signal Conditioning	31
6	Capacitance Type ODM Sensor Assembly	34
7	Capacitance Type ODM, Electronics and Sensor Head	35
8	X-ray Fluorescence Type ODM, Electronics and Sensor Head	37
9	Example of SOA Data for Defective Gear	38
10	Accelerometer Locations	41
11	Accelerometer Locations	42
12	Sixth-Order Butterworth High-Pass Filter	44
13	SKF Shock Pulse Analyzer	46
14	Shock Emission Profile Curve Types	49
15	Cross-Sectional View of 90° Gearbox	51
16	Partial Disassembly of a 90° Gearbox	52
17	Schematic Diagram of Dynamic Noise Test	54
18	Schematic Diagram of Cross-Groove Profile Measurement	57

LIST OF ILLUSTRATIONS (Continued)

<u>Figure</u>		<u>Page</u>
19	BBT-3 Cross-Groove Profile at Zero Test Hours	58
20	BBT-3 Cross-Groove Profile at 1022 Test Hours	59
21	Roller Crown Parameters	60
22	SEM Micrographs of BBT-2 (407 Hours)	62
23	Timing Diagram for Data Collection Effort	65
24	Macro Flow Chart for Data Collection Program	66
25	Flow Chart for Start-up Sequence Routine	67
26	Flow Chart for Sensor Select and Processing Routine	68
27	Flow Chart for Compute Ensemble PSD Routine	69
28	Flow Chart for Comparison Checks and Tests Routine	70
29	Example of the Reduction of DFT Sidelobe Structure by Hamming Weighting an Input Time Domain Signal	75
30	Example of Ensemble Averaging of PSD Functions	76
31	Structure of PSD Mean - Standard Deviation Data Base	79
32	Type Z-Score Linear Discriminant Plot	81
33	Wideband RMS Vibration Level of Input Longitudinal Accelerometer (UH-1 Helicopter Transmission)	84
34	Trending of PSD Vibration Data, Bad Bearing 2, Sensor 4, Frequency 1016 Hz	86
35	Trending of PSD Vibration Data, Bad Bearing 2, Sensor 5, Frequency 4219 Hz	87

LIST OF ILLUSTRATIONS (Continued)

<u>Figure</u>		<u>Page</u>
36	Trending of PSD Vibration Data, Bad Gear, Sensor 5, Frequency 1094 Hz	88
37	Trending of PSD Vibration Data, Bad Gear, Sensor 5, Frequency 2031 Hz	89
38	Trending of PSD Vibration Data, High Time, Sensor 3, Frequency 6250 Hz	90
39	Prognostic Trend of BB3 Gearbox, Sensor 4, Bin 53	94
40	Summary of HT Gearbox SOA	98
41	Typical HT Gearbox Temperature Data	102
42	Typical HT Ultrasonic RMS Data	103
43	Typical HT Gearbox Peak Shock Pulse Level Data .	104
44	Overall View of HT Vibration Data Base, Input Lateral Accelerometer	105
45	Overall View of HT Vibration Data Base, Skew Accelerometer	106
46	Overall View of HT Vibration Data Base, Output Lateral Accelerometer	107
47	PSD Vibration Path, HT Vibration Data, Input Lateral Accelerometer, 3202 Hz	109
48	Prognostic Trend of HT Vibration Data, Input Lateral Accelerometer, 3202 Hz	110
49	Summary of BB Gearbox SOA	113
50	Output of X-ray Fluorescence ODM	115
51	Oil Debris Found in Measurement Capacitor of Capacitance Type ODM	115

LIST OF ILLUSTRATIONS (Continued)

<u>Figure</u>		<u>Page</u>
52	Ultrasonic Data From Output Ultrasonic Accelerometer	116
53	Overall View of BB Vibration Data Base, Input Lateral Accelerometer	118
54	Overall View of BB Vibration Data Base, Skew Accelerometer	119
55	Overall View of BB Vibration Data Base, Output Lateral Accelerometer	120
56	Summary of BG Gearbox SOA	125
57	Overall View of BG Vibration Data Base, Input Lateral Accelerometer	127
58	Overall View of BG Vibration Data Base, Skew Accelerometer	128
59	Overall View of BG Vibration Data Base, Output Lateral Accelerometer	129
60	Prognostic Trend of BG Gearbox, Output Lateral Accelerometer, 2031 Hz	130
61	Prognostic Trend of BG Vibration Data, Output Lateral Accelerometer, 4140 Hz	131
62	Cutaway Sectional Illustration of Failed Input Coupling	134
63	Comparison of Failed Input Coupling With Good Coupling	136
64	Summary of BBT Gearbox SOA	137
65	Shock Emission Profile - BBT Start-up, First Test Period	140

LIST OF ILLUSTRATIONS (Continued)

<u>Figure</u>		<u>Page</u>
66	Shock Emission Profile - BBT Start-up, Second Test Period	141
67	Shock Emission Profile - BBT, 75 Hours Into Second Test Period	142
68	Shock Emission Profile - BBT, 300 Hours Into Second Test Period	143
69	Shock Emission Profile - BBT, Peak of Wear Period	144
70	Shock Emission Profile - BBT, 599 Hours Into Second Test Period	146
71	Shock Pulse Value for BBT	147
72	Overall View of BBT Vibration Data Base, Input Lateral Accelerometer	148
73	Overall View of BBT Vibration Data Base, Skew Accelerometer	149
74	Overall View of BBT Vibration Data Base, Output Lateral Accelerometer	150
75	Prognostic Trend of BBT Gearbox, Output Lateral Accelerometer, 4219 Hz	152
76	Aliasing Errors in Plot of BBT Vibration Data, 4219 Hz	153
77	Prognostic Trend of BBT Gearbox, Skew Accelerometer, 4297 Hz	155
78	Prognostic Trend of BBT Gearbox, Input Lateral Accelerometer, 1172 Hz	156
79	Spectroscopic Oil Analysis Summary, BB3	160
80	Shock Pulse Data for BB3 at the 62-Hour Point . .	161

LIST OF ILLUSTRATIONS (Continued)

<u>Figure</u>		<u>Page</u>
81	Shock Pulse Data for BB3 at the 800-Hour Point . . .	162
82	Shock Pulse Data for BB3 at the 980-Hour Point . . .	163
83	Shock Pulse Data for BB3 at the 1100-Hour Point . . .	164
84	Shock Pulse Value Data, BB3	166
85	Overall View of BB3 Vibration Data Base, Input Lateral Accelerometer	167
86	Overall View of BB3 Vibration Data Base, Skew Accelerometer	168
87	Overall View of BB3 Vibration Data Base, Output Lateral Accelerometer	169
88	Prognostic Trend of BB3 Gearbox, Input Lateral Accelerometer, 4140 Hz	170
89	Prognostic Trend of BB3 Gearbox, Skew Accelerometer, 4140 Hz	171
90	Cross-Sectional View of 90° Gearbox	196
91	Partial Disassembly of a 90° Gearbox	197
92	HT-1 Cross-Groove Profile at Zero Test Hours . . .	205
93	HT-1 Cross-Groove Profile at 877 Test Hours . . .	206
94	HT-1 Cross-Groove Profile at 1454 Test Hours . . .	207
95	HT-2 Cross-Groove Profile at Zero Test Hours . . .	208
96	HT-2 Cross-Groove Profile at 877 Test Hours . . .	209
97	HT-2 Cross-Groove Profile at 1454 Test Hours . . .	210
98	HT-3 Cross-Groove Profile at Zero Test Hours . . .	211

LIST OF ILLUSTRATIONS (Continued)

<u>Figure</u>		<u>Page</u>
99	HT-3 Cross-Groove Profile at 877 Test Hours . . .	212
100	HT-3 Cross-Groove Profile at 1454 Test Hours . . .	213
101	HT-4 Cross-Groove Profile at Zero Test Hours . . .	214
102	HT-4 Cross-Groove Profile at 877 Test Hours . . .	215
103	Cross-Groove Profile at 1454 Test Hours	216
104	SEM Micrographs of HT-1 (Zero, 877 Hours) . . .	217
105	SEM Micrographs of HT-1 (1454 Hours)	218
106	SEM Micrographs of HT-2 (Zero, 877 Hours) . . .	219
107	SEM Micrographs of HT-2 (1454 Hours)	220
108	SEM Micrographs of HT-3 (Zero, 877 Hours) . . .	221
109	SEM Micrographs of HT-3 (1454 Hours)	222
110	SEM Micrographs of HT-4 (Zero, 877 Hours) . . .	223
111	SEM Micrographs of HT-4 (1454 Hours)	224
112	SEM Micrographs of HT-5 (Zero, 877 Hours) . . .	225
113	SEM Micrographs of HT-5 (1454 Hours)	226
114	BB-1 Cross-Groove Profile at Zero Test Hours . .	233
115	BB-1 Cross-Groove Profile at 166 Test Hours . . .	234
116	BB-2 Cross-Groove Profile at Zero Test Hours . .	235
117	BB-2 Cross-Groove Profile at 166 Test Hours . . .	236
118	BB-3 Cross-Groove Profile at Zero Test Hours . .	237
119	BB-3 Cross-Groove Profile at 166 Test Hours . . .	238

LIST OF ILLUSTRATIONS (Continued)

<u>Figure</u>		<u>Page</u>
120	BB-4 Cross-Groove Profile at Zero Test Hours . . .	239
121	BB-4 Cross-Groove Profile at 166 Test Hours . . .	240
122	SEM Micrographs of BB-1 (Zero, 166 Hours) . . .	241
123	SEM Micrographs of BB-2 (Zero, 166 Hours) . . .	242
124	SEM Micrographs of BB-3 (Zero Hours)	243
125	SEM Micrographs of BB-4 (Zero Hours)	243
126	SEM Micrographs of BB-5 (Zero, 166 Hours) . . .	244
127	SEM Micrographs of BB-3 or BB-4 (166 Hours) . .	245
128	BG-1 Cross-Groove Profile at Zero Test Hours . .	252
129	BG-1 Cross-Groove Profile at 1000 Test Hours . .	253
130	BG-2 Cross-Groove Profile at Zero Test Hours . .	254
131	BG-2 Cross-Groove Profile at 1000 Test Hours . .	255
132	BG-3 Cross-Groove Profile at Zero Test Hours . .	256
133	BG-3 Cross-Groove Profile at 1000 Test Hours . .	257
134	BG-4 Cross-Groove Profile at Zero Test Hours . .	258
135	BG-4 Cross-Groove Profile at 1000 Test Hours . .	259
136	SEM Micrographs of BG-1	260
137	SEM Micrographs of BG-2	261
138	SEM Micrographs of BG-3	262
139	SEM Micrographs of BG-4	263
140	SEM Micrographs of BG-5	264
141	BBT-1 Cross-Groove Profile at Zero Test Hours . .	273

LIST OF ILLUSTRATIONS (Continued)

<u>Figure</u>		<u>Page</u>
142	BBT-1 Cross-Groove Profile at 407 Test Hours . . .	274
143	BBT-1 Cross-Groove Profile at 1022 Test Hours . . .	275
144	BBT-2 Cross-Groove Profile at Zero Test Hours . . .	276
145	BBT-2 Cross-Groove Profile at 407 Test Hours . . .	277
146	BBT-2 Cross-Groove Profile at 1022 Test Hours . . .	278
147	BBT-3 Cross-Groove Profile at Zero Test Hours . . .	279
148	BBT-3 Cross-Groove Profile at 407 Test Hours . . .	280
149	BBT-3 Cross-Groove Profile at 1022 Test Hours . . .	281
150	BBT-4 Cross-Groove Profile at Zero Test Hours . . .	282
151	BBT-4 Cross-Groove Profile at 407 Test Hours . . .	283
152	BBT-4 Cross-Groove Profile at 1022 Test Hours . . .	284
153	SEM Micrographs of BBT-1 (Zero Hours)	285
154	SEM Micrographs of BBT-1 (407 Hours)	286
155	SEM Micrographs of BBT-1 (1022 Hours)	287
156	SEM Micrographs of BBT-2 (Zero Hours)	288
157	SEM Micrographs of BBT-2 (407 Hours)	289
158	SEM Micrographs of BBT-2 (1022 Hours)	290
159	SEM Micrographs of BBT-3 (Zero Hours)	291
160	SEM Micrographs of BBT-3 (407 Hours)	292
161	Fatigue Pit on Inner-Ring Raceway, S/N BBT-3 . .	293
162	Magnified View of Fatigue Pit, S/N BBT-3	294

LIST OF ILLUSTRATIONS (Continued)

<u>Figure</u>		<u>Page</u>
163	SEM Micrographs of BBT-3 (1022 Hours)	295
164	SEM Micrographs of BBT-4 (Zero Hours)	296
165	SEM Micrographs of BBT-4 (407 Hours)	297
166	SEM Micrographs of BBT-4 (1022 Hours)	298
167	SEM Micrographs of BBT-5 (Zero Hours)	299
168	SEM Micrographs of BBT-5 (407 Hours)	300
169	SEM Micrographs of BBT-5 (1022 Hours)	301
170	BB3-1, Cross-Groove Profile at Zero Test Hours .	308
171	BB3-1, Cross-Groove Profile at 1086 Test Hours .	309
172	BB3-2, Cross-Groove Profile at Zero Test Hours .	310
173	BB3-2, Cross-Groove Profile at 1086 Test Hours .	311
174	BB3-3, Cross-Groove Profile at Zero Test Hours .	312
175	BB3-3, Cross-Groove Profile at 1086 Test Hours .	313
176	BB3-4, Cross-Groove Profile at Zero Test Hours .	314
177	BB3-4, Cross-Groove Profile at 1086 Test Hours .	315
178	SEM Micrographs of BB3-1 (Zero Hours)	316
179	SEM Micrographs of BB3-1 (Addition View Zero Hours)	317
180	SEM Micrographs of BB3-1 (1086 Hours)	318
181	SEM Micrographs of BB3-2 (Zero Hours)	319
182	SEM Micrographs of BB3-2 (1086 Hours)	320

LIST OF ILLUSTRATIONS (Continued)

<u>Figure</u>		<u>Page</u>
183	SEM Micrographs of BB3-3 (Zero Hours)	321
184	SEM Micrographs of BB3-3 (1086 Hours)	322
185	SEM Micrographs of BB3-4 (Zero Hours)	323
186	SEM Micrographs of BB3-4 (1086 Hours)	324

LIST OF TABLES

<u>Table</u>		<u>Page</u>
I	Accelerometer Characteristics, ENDEVCO Model 2217-M3	40
II	Dynamic Analysis Bearing Condition Levels	55
III	Summary of Data Collected	95
IV	Level of Confidence, β , Versus Confidence Coefficient, Z_C	184
V	Level of Significance, α , Versus Required Z-Score, Z	185
VI	Confidence Level, β , Versus Correction Factor, ζ .	188
VII	Mechanical Measurements for HT Ball Bearings .	203
VIII	Mechanical Measurements for HT Roller Bearings .	204
IX	Mechanical Measurements for BB Ball Bearings .	231
X	Mechanical Measurements for BB Roller Bearings .	232
XI	Mechanical Measurements for BG Ball Bearings .	250
XII	Mechanical Measurements for BG Roller Bearings .	251
XIII	Mechanical Measurements for BBT Ball Bearings .	271
XIV	Mechanical Measurements for BBT Roller Bearings .	272
XV	Mechanical Measurements for BB3 Ball Bearings .	306
XVI	Mechanical Measurements for BB3 Roller Bearings .	307

INTRODUCTION

This report is organized into four major sections and two appendixes. The first section, "Test Instrumentation and Procedures," includes a description of how the test cell was constructed and how it is controlled. The sensors used and where they were located on the gearbox are also discussed. A brief description of the measurement techniques used to determine degree of component wear in the pre- and post-test teardown inspection is also given.

The second section, "Automatic Computer-Controlled Data Collection and Reduction" describes the main computer program which controls the data collection process. Included are discussions of the start-up sequence, automatic fault detection and sensor selection and processing.

The third section, "Data Analysis - Theory and Procedures," discusses computational algorithms used to reduce the collected vibration data and the development of the statistical analysis and trending techniques which were applied to selected portions of the data.

The last section, "Experimental Results," contains an extensive discussion of the experimental results obtained for each gearbox. Summaries of the data collected by each sensor are given, and attempts are made to correlate significant changes in sensor data with changes in mechanical condition of the gearbox.

Appendix I is devoted to a theoretical discussion of the statistical signal processing used to identify significant frequency components for trending. A derivation of the LMS prediction technique is also given.

Appendix II contains all of the documentation obtained on the pre- and post-test wear condition of the mechanical components in each gearbox. The documentation includes visual wear observations as determined by expert, mechanical measurements, and SEM photographs of one ball from each bearing in each gearbox.

TEST INSTRUMENTATION AND PROCEDURES

TEST CELL AND CONTROLLER

Test Stand

A special test cell was constructed for this prognostic effort. This test cell was designed to provide constant torque loads to the gearbox for extended periods of time at constant rpm. Figure 1 is an overall view of the test stand with the major mechanical components identified. The test stand is inclined 42° to simulate the actual mounting position of the gearbox in the UH-1 helicopter and to guarantee proper operation of its splash-type internal lubrication system.

Figure 2 shows the mechanical and hydraulic circuit diagrams of the test stand. Torque loading of the gearbox is supplied by a hydraulic feedback process. The circuit operates as follows:

- a) The electric motor operates on 440 V 3Ø AC power and rotates at a fixed speed of 1185 rpm.
- b) To obtain the 4150 rpm required to drive the gearbox, the output of the electric motor is stepped up 3.5:1 by a pulley arrangement.
- c) Due to its internal gearing, the gearbox itself provides a 2.5:1 speed reduction. Its output rotation rate of 1650 rpm is used to drive a fixed-displacement hydraulic pump.
- d) The hydraulic pump, of the inner-vane type of construction, delivers 44.8 gallons per minute (gpm) of hydraulic fluid.
- e) The hydraulic motor is mechanically connected to the shaft of the electric motor. Since the primary source of power in the test cell is the electric motor, and since its rpm is fixed at 1185, the hydraulic motor must also turn at 1185 rpm. This specific hydraulic motor was chosen because it requires only 38.2 gpm of input oil to turn at 1185 rpm. The hydraulic motor is a fixed-displacement design, and will accept only 38.2 gpm of hydraulic fluid at 1185 rpm.
- f) The relief valve is a manually adjustable pressure regulating device. Excess oil flow (about 6.6 gpm in this case) above the maximum of 38.2 gpm required by the hydraulic motor to turn at 1185 rpm is directed by this valve to the reservoir.

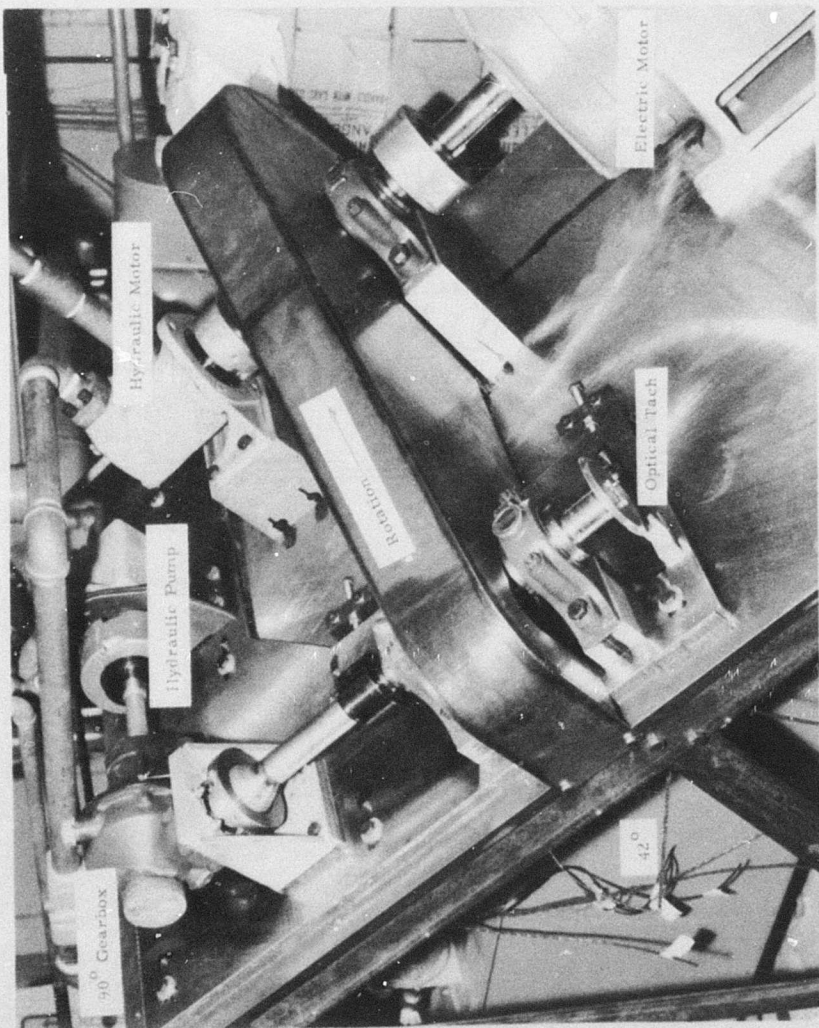


Figure 1. Overall View of Test Stand

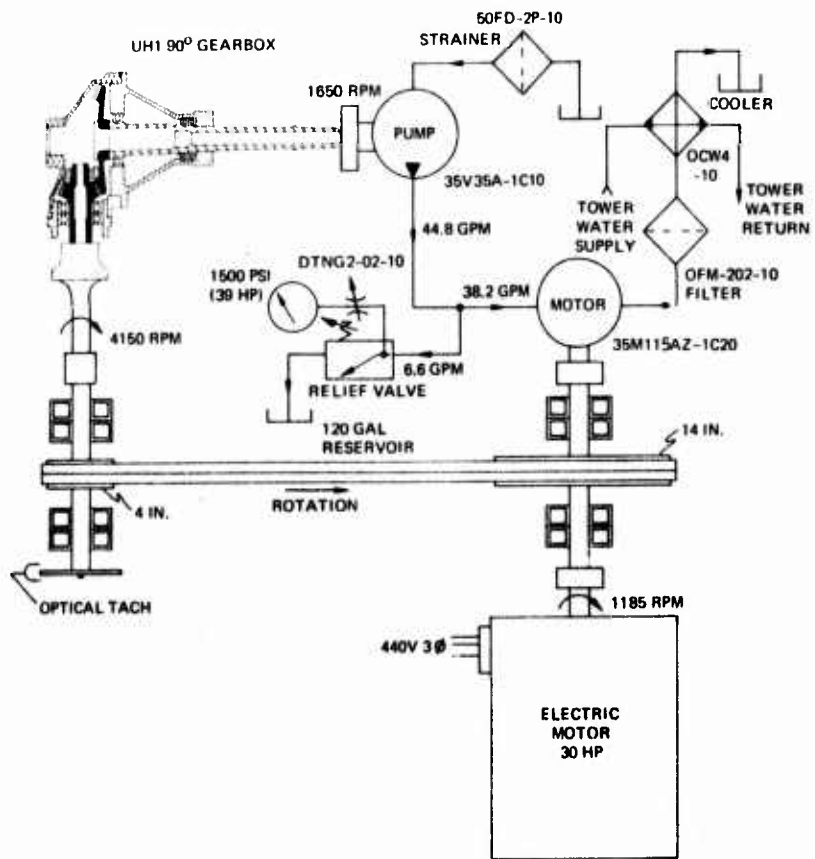


Figure 2. Test Stand - Mechanical and Hydraulic Circuit Diagram.
(All hydraulic components manufactured by Vickers, Inc.)

The relief valve further serves to maintain a constant operating pressure across the hydraulic motor.

g) To calculate the output torque of the gearbox we must find the power flowing through the hydraulic circuit. This is given in horsepower by

$$hp = \frac{gpm \times psi}{1714} \quad (1)$$

Since the relief valve is set for 1500 psi and the flow rate through the motor is 38.2 gpm, the power out of the hydraulic motor = $(38.2)(1500)/1714 = 33.4$ hp. Therefore, the hydraulic motor returns 33.4 hp to the input of the gearbox. The relief valve consumes 6.6 gpm at 1500 psi, or 5.8 hp. The sum of the power used by the hydraulic motor and by the relief valve is provided by the hydraulic pump, which equals the load applied to the gearbox under test. The output torque (τ) of the gearbox is

$$\tau(\text{lb-ft}) = \frac{5252 \times hp}{\text{rpm}} = \frac{(5252)(39)}{1650} = 124.1 \text{ lb-ft} \quad (2)$$

In summary, the output power of the gearbox is fed back into its input by a closed mechanical-hydraulic system. Since the electric motor must make up for all frictional losses in the system plus the 5.8 hp lost over the relief valve, it need only be large enough to drive the gearbox and make up for these losses.

Test Cell Controller (TCC)

The test cell controller is composed of all of the electronics required for automatic command and control of every phase of the test cell operation. The controller provides the interface between the sensors and test stand control system and the computer.

Considerable attention has been given to the design of the test stand for unattended, fully automatic operation. The test cell controller (TCC) has built-in checks and tests which operate independently of the tests and checks made by the computer.

Figure 3 shows the block diagram of the TCC. The functions performed by the signal conditioning and sensor interface circuitry will be discussed in detail in the next section. It is sufficient for the

present discussion of the TCC to note that the signal conditioning and sensor interface block provides the TCC with rpm measurements from the test cell.

Should the drive belt break or a bearing seize, this event is sensed by the rpm low limit detector in the TCC, and an AUTO STOP command is relayed to the test stand interlocks, which immediately shut down the test stand.

The TCC also checks for proper operation of the computer. The computer is programmed to process and record the outputs of each of the 16 sensors every 4 minutes. The Channel Increment Detector is a timing circuit which is reset every time the computer updates the multiplexer channel. If the computer fails to update the multiplexer within a 5-minute interval, another AUTO STOP command is generated to shut down the test cell.

The TCC also accepts commands directly from the computer. In the event that the computer senses a severe malfunction in either the test stand or the gearbox, or when the current test interval is completed, an AUTO STOP command is sent to the test stand interlocks and overrides to shut down the test stand.

The TCC is designed so that unattended operation is not possible unless the computer is monitoring the operation. Furthermore, the test stand cannot be automatically restarted after a stop command has been issued. The start-up sequence must be performed manually.

Computer-Test Cell I/O

The computer shown in Figure 4 is used to monitor the activities of the test stand and to collect the prognostics data. It is located some 500 feet from the test cell area. Special precautions were taken to ensure that reliable communications are maintained between the computer and the test cell.

Figure 5 shows the block diagram for the computer-test cell I/O signal conditioning circuitry.

Analog data from the test cell is sent to the computer through a double-shielded 50Ω balanced coaxial cable (RG22B/U). A differential amplifier removes any common mode signals and converts the analog data into an unbalanced signal. A 10 kHz sixth-order Butterworth low-pass filter provides protection against aliasing of the data. The filtered data is digitized at a 20 kHz rate by a 10-bit analog-to-digital

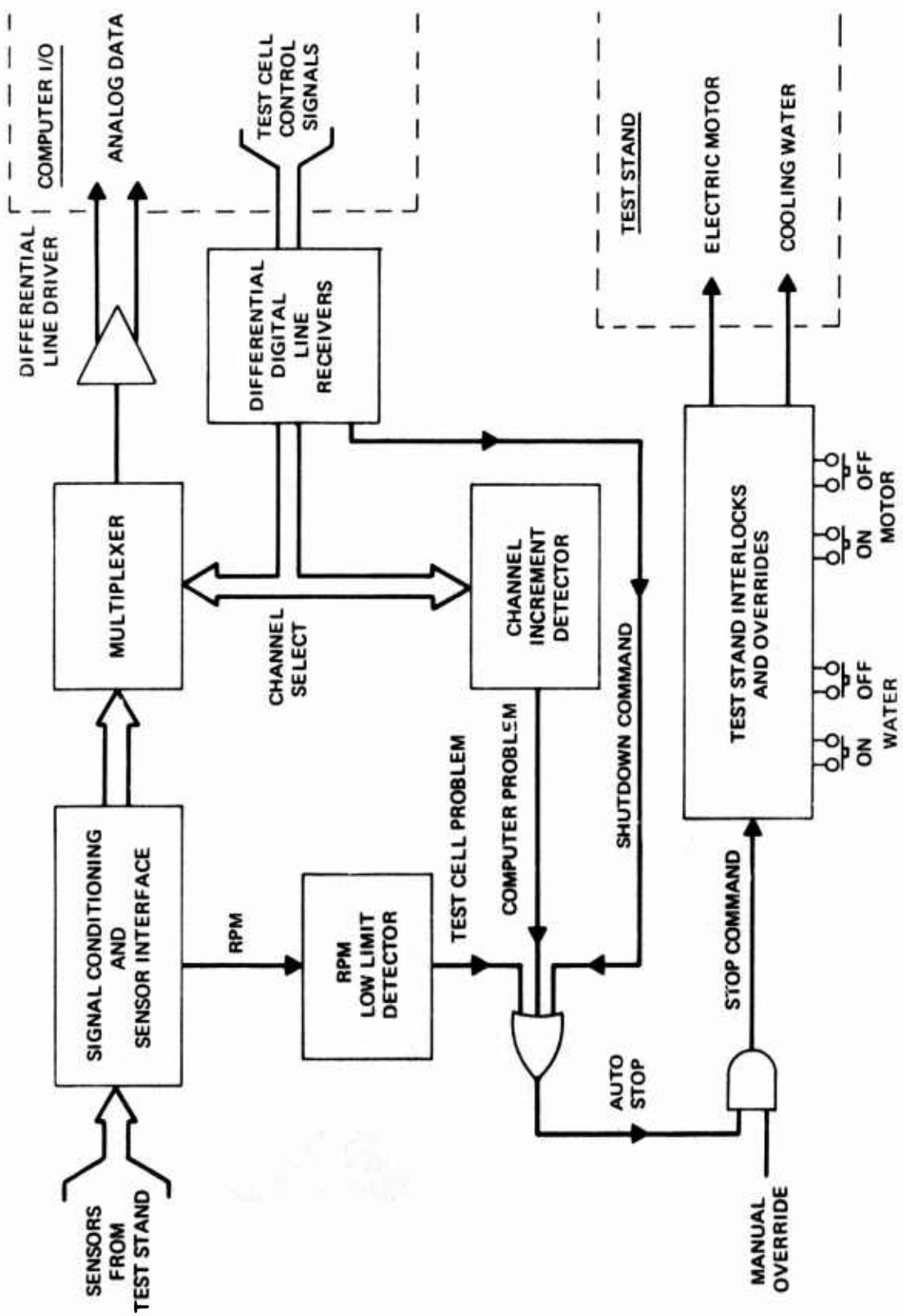


Figure 3. Block Diagram of Test Cell Controller.



Figure 4. Interactive Computer Graphics System.

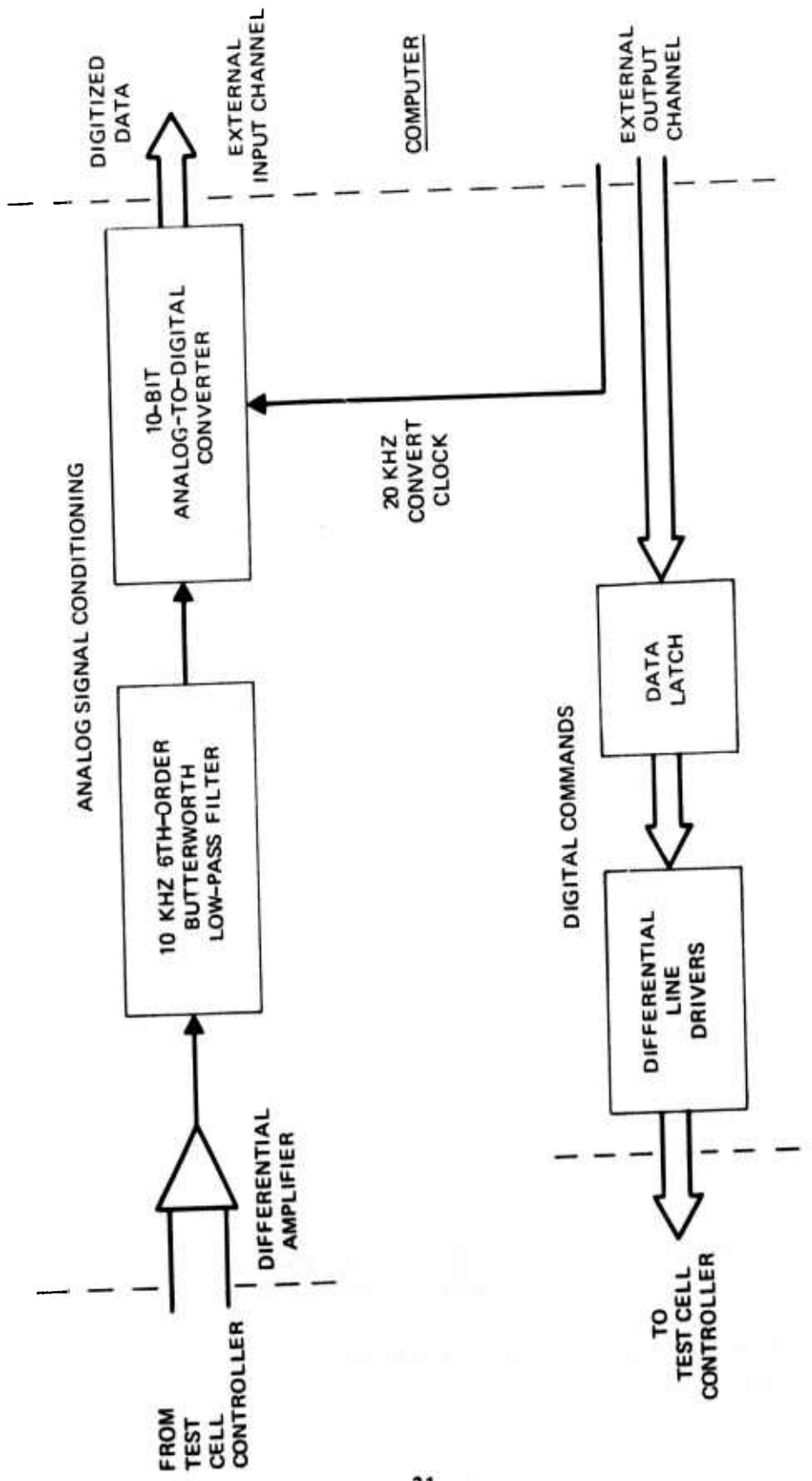


Figure 5. Block Diagram of Computer - Test Cell I/O Signal Conditioning.

converter. The computer controls the sampling rate for the ADC. The digitized data is brought directly into core memory via the external input channel. Digital commands originating from within the computer are sent via the external output channel to a data latch. The data latch stores the computer's commands, allowing the computer to accomplish other functions while the test cell controller is busy interpreting the latest command. To ensure reliable command transmission to the test cell, differential line drivers are used to drive $130\ \Omega$ twisted pairs to the test cell controller.

SENSORS AND SENSOR LOCATIONS

This section deals with the types of sensors used to monitor the gearbox under test, their locations, and any special signal conditioning required for that sensor. All the sensors used in this program are discussed even though all the sensors were not used on every gearbox tested. Some sensors were replaced during the course of the program because they were unreliable or furnished data of no value to this effort, and others which offered promise of providing the desired data were added after the program started. The usefulness of the data from each type of sensor for each gearbox is discussed in the section on "Experimental Results."

Temperature Sensors

Two platinum type temperature sensors were used in this program. One sensor was placed on the inside of the sight-glass of the 90° gearbox to measure gearbox oil temperature. The second temperature sensor was placed near the filler cap and exposed to the ambient air. This latter sensor did not provide any useful information for the analysis program. It was omitted from all gearboxes tested after HT, and its data reduction channel was used to monitor the SKF shock pulse analyzer for the rest of the gearboxes tested.

Oil Debris Monitors

A circulating oil system was installed on the gearbox to allow the use of two advanced oil debris monitors (ODM). These monitors were designed to provide on-line, real-time quantitative measurements of the absolute cumulative metal content in the oil and the rate of change in the generation of metal chips.

The two ODM's are based upon two completely different measurement techniques.

The following is a brief description of the two units and their operational concepts.

Chip Detector

The standard UH-1 helicopter 90° gearbox has a chip detector mounted as an insert in the oil drain plug. The gearboxes selected for testing in this program did not have chip detectors since operational experience has shown that these devices are relatively unreliable diagnostic tools and are not sufficiently sensitive to use as prognostic tools. Since spectroscopic oil analysis (discussed in a following section) is a much more sensitive indicator of oil contamination of all types than the chip detector, it was agreed that the chip detector could be omitted from the test program.

In any case, the chip detector would have had to be removed in order to accommodate the oil circulating system, which was designed to flow oil through the gearbox to the two externally mounted oil debris monitors. This circulation system was attached to the gearbox at the oil drain and fillercap.

Capacitance Type ODM

The "Advanced Capacitative Oil Debris Monitor" was developed by the Franklin Institute Research Laboratories under an Army contract.¹ This concept is based on collecting particulate debris in an annular space between the plates of a cylindrical capacitor. Debris is removed from the oil stream by centrifugal action caused by tangential introduction of the oil flow into the monitor cell, and by passing the flow through a 50-micrometer screen which is continually washed by the fluid flow. The particulate material settles into the measuring capacitor. The fluid which passes through the screen is allowed to flow through a reference capacitor with the same dimensions as the measuring capacitor. The measuring capacitor and the reference capacitor are compared by a bridge circuit so that the undesired capacitance effects due to changes in oil properties (temperature, water content, and dielectric constant) can be cancelled. Measured capacitance differences at the output of the bridge should therefore be due only to metallic debris buildup on the measurement capacitor.

Figure 6 shows a cross-sectional view of the sensor assembly. The electrical signals generated by the bridge circuit were monitored and periodically sampled by the computer. Figure 7 is a picture of the capacitance type sensor head and electronic controller.

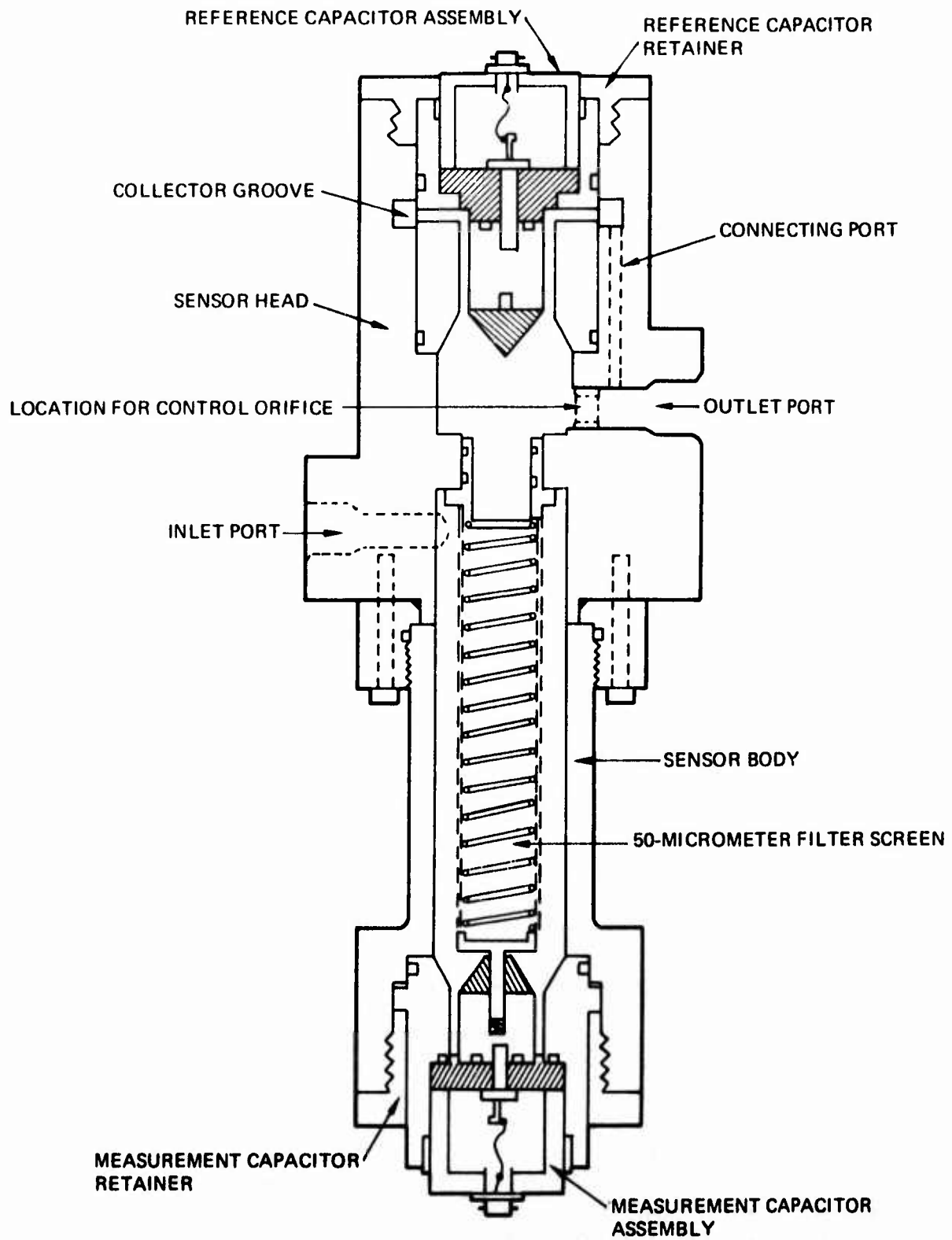


Figure 6. Capacitance Type ODM Sensor Assembly.

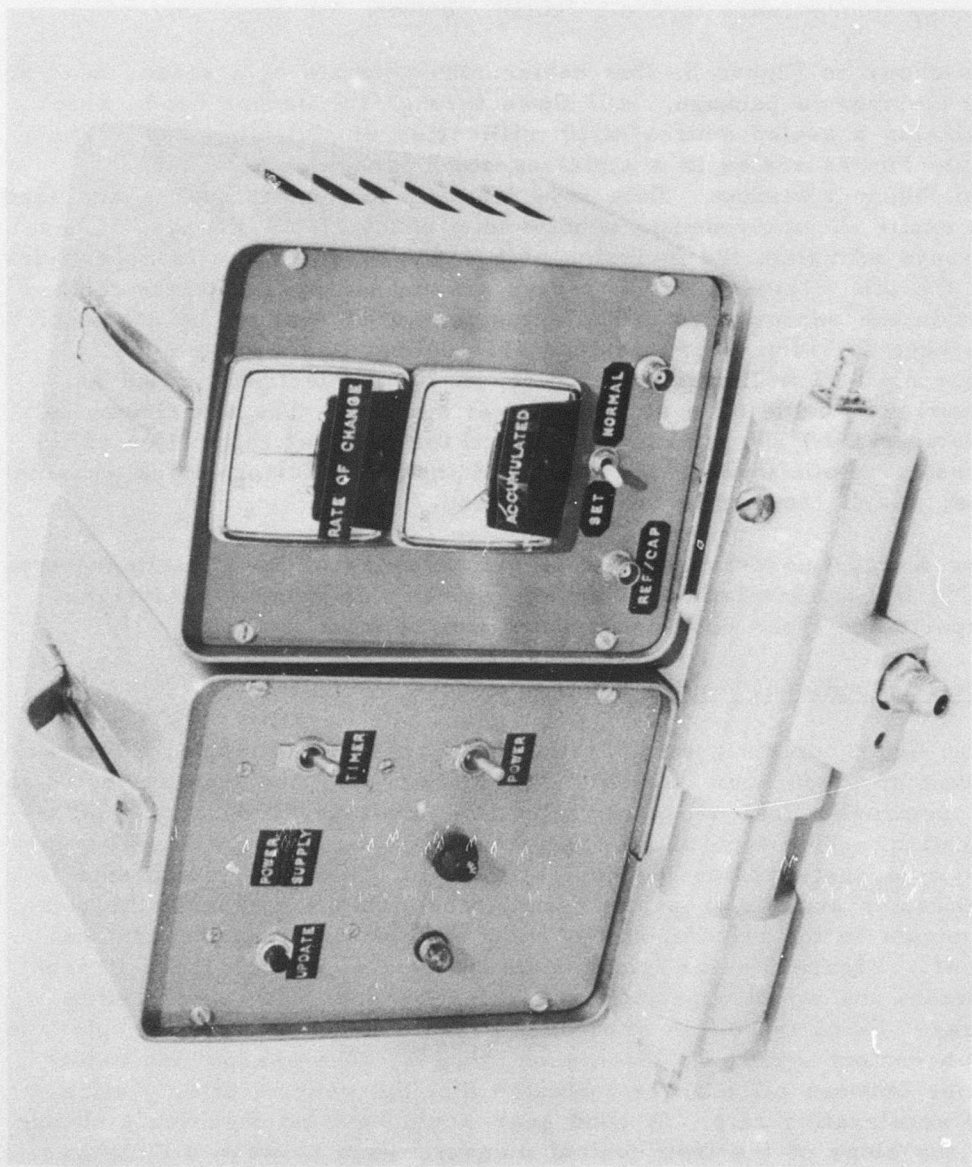


Figure 7. Capacitance Type ODM, Electronics and Sensor Head.

X-Ray Fluorescence Type ODM

Under a separate contract² Nucleonic Data Systems developed an X-Ray fluorescence type oil debris monitor.

As shown in Figure 8, this device also consists of a sensor head and an electronics package. Oil flows through the sensor head, which contains a sealed source of 10 millicuries of plutonium 238. The plutonium is sealed in a stainless steel capsule with a 5-mil molybdenum window. Beta rays from the plutonium source are used to excite the molybdenum window to produce 17 KV X-rays. These X-rays stimulate the emission of 6.4 KV X-rays from iron particles in the oil. These 6.4 KV X-rays are sensed by a detector located within the sensor head. The output signal is sent to the electronics package for further processing. In addition to the plutonium 238 source, 0.03 millicurie of americium 241 is electrodeposited as americium oxide on a stainless steel support. The americium 241 provides a 60 KV gamma ray source for internal calibration of the sensor. Both sources are contained inside a 1/2-inch-thick aluminum box, which constitutes the sensor head.

The X-ray fluorescence ODM is placed ahead of the capacitance type ODM in the circulating oil system, since this sensor, unlike the capacitance type, does not remove debris from the oil.

Spectroscopic Oil Analysis

The Army currently samples the oil from UH-1 helicopter 90° gearboxes at 25-30 hour intervals. These samples are then subjected to a spectrochemical or spectroscopic oil analysis (SOA) at a remote location. This type of oil analysis has proven to be a useful technique for determining mechanical wear of oil-wetted components in helicopter engines, gearboxes and transmissions. Iron is the contaminant in the oil which is of most use in diagnosing mechanical wear. Figure 9 is an example of the type of upward trend in iron content one would expect from a defective gear with accelerating wear. Since the oil is changed every 100 hours in this example, the iron content decreases after each change. The sharply increasing slope between oil changes indicates that the gear is deteriorating at an accelerating rate. A good gear would have no significant change in the slope of the iron content measurements between oil changes.

In this program, 3-ounce samples of gearbox oil were usually taken every 16 hours, which was the daily run time. However, due to an unfortunate misinterpretation of the Army oil changing schedule, the

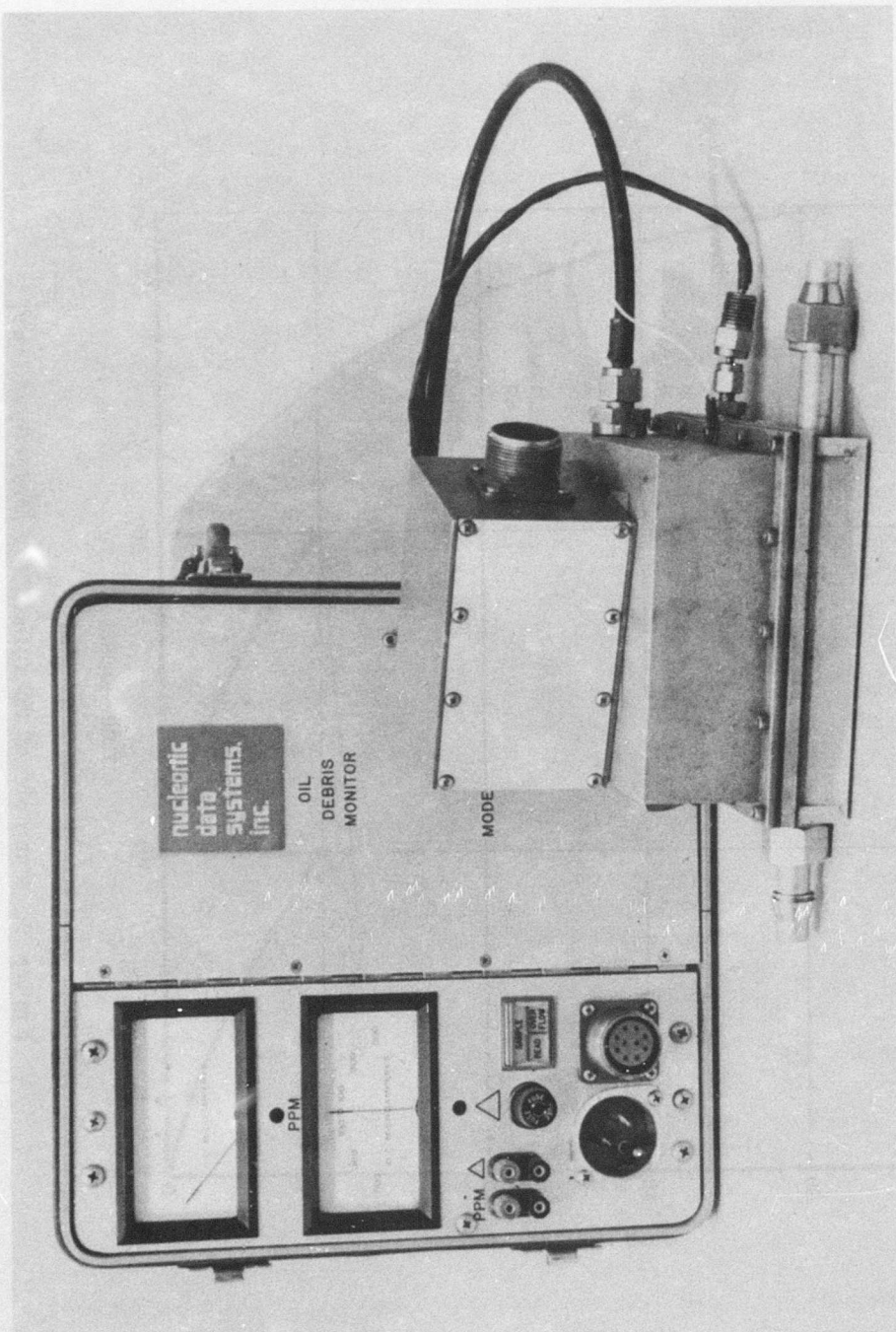


Figure 8. X-ray Fluorescence Type ODM, Electronics and Sensor Head.

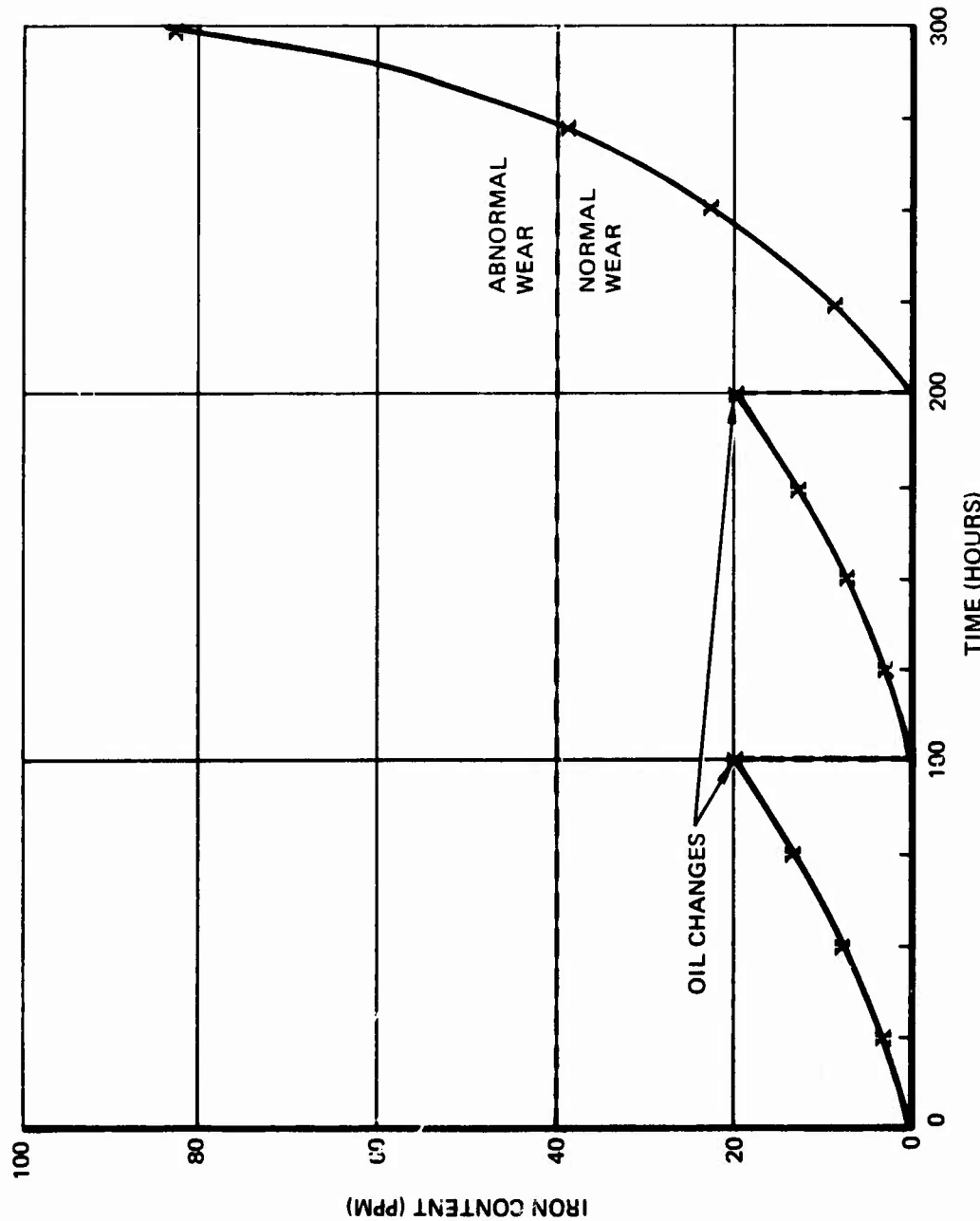


Figure 9. Example of SOA Data for Defective Gear.
 X = Oil Sample.

oil was changed in the test gearboxes in this program every time an oil sample was taken, or about every 16 hours instead of the normal 100 hours. Therefore, each oil sample usually represented only 16 hours of gearbox operation, which in many cases was insufficient operating time to observe the buildup of oil debris.

Another reason for our failure to obtain good trendable data from the SOA early in the program was the design of the circulation system for the oil debris monitor (ODM). The circulating system was required to channel the oil flow from the gearbox reservoir through the two oil debris monitors. The circulating system required 720 ml of oil, while the gearbox reservoir holds 80 ml of oil. This represented a 10:1 dilution of the oil and oil contaminants. However, after the ODM's proved to be too unreliable to use and were eliminated from further testing, a major change in oil contaminants which could be correlated with bearing wear was observed in gearbox BB3. This data is discussed in the section on "Experimental Results."

Low-Frequency Accelerometers

Endevco Model 2217M3 accelerometers were used for sensing low-frequency (< 10 kHz) vibration signals. Table I gives the characteristics of this type of accelerometer.

Five of these accelerometers were used: three to monitor the gearbox and two to monitor the hydraulic system.

The three gearbox-mounted accelerometers were used to sense input (shaft) lateral vibrations and output (shaft) lateral vibrations. Figures 10 and 11 are photographs of two different perspectives of the gearbox and show the locations of the accelerometers.

The other two accelerometers were connected to the hydraulic motor and the hydraulic pump. These accelerometers were included as a precaution in case the hydraulic components began to deteriorate in some manner not detectable by the TCC.

Two techniques were used to attach the accelerometers to the gearbox. The initial method was to use epoxy to attach small mounting pads to the gearbox at the desired locations. The accelerometers were then screwed into the mounting pads. This technique was selected because it did not require that holes be drilled in the gearbox and allowed for rapid attachment of the sensors to the pads. This mounting technique worked satisfactorily for the first gearbox tested (HT), but proved to be unreliable during the testing of the

TABLE I. ACCELEROMETER CHARACTERISTICS,
ENDEVCO MODEL 2217-M3

PHYSICAL	
DESIGN	Single-Ended Compression
WEIGHT	35 grams (1.3 ounces)
CRYSTAL MATERIAL	Piez-te® Element Type P-8
CASE MATERIAL	Stainless Steel
CONNECTOR TYPE	Coaxial, 10-32 thread
MOUNTING	Hole for 10-32 ENDEVCO® Mounting Stud. Recommended Mounting Torque: 18 in.-lb
GROUNDING	Case grounded
ACCESSORIES INCLUDED	Model 3090A-36 Low Noise Cable Assembly, 3 ft., 100 pF nominal. Model 2981-3 Mounting Stud.
ACCESSORIES AVAILABLE	Model 2980B or 2986B Insulated Mounting Stud.
ENVIRONMENTAL	
ACCELERATION LIMITS	
VIBRATION	1000 pk g, sinusoidal, any direction.
SHOCK	2000 g, any direction.
TEMPERATURE	-54°C to +177°C (-65°F to +350°F)
BASE STRAIN SENSITIVITY	10 equivalent g at 250 μ strain, nominal.
ACOUSTIC SENSITIVITY	Approximately 0.007 equivalent rms g at 140 db. ¹
MAGNETIC SENSITIVITY	Approximately 0.05 equivalent g/psi, up to 1000 Hz.
ALTITUDE	0.00005 equivalent g/gauss at 60 Hz, nominal.
HUMIDITY	Not affected
SALT SPRAY	All-welded hermetic seal. Meets MIL-E-5272C (with sealed cable connector)
DYNAMIC	
CHARGE SENSITIVITY	40 pC/g, nominal
VOLTAGE SENSITIVITY ¹	90 mV/g, nominal 70 mV/g, min.
MOUNTED RESONANCE FREQUENCY	27,000 Hz, $\pm 15\%$
FREQUENCY RESPONSE ($\pm 5\%$) ²	Charge: ³ 4 to 6000 Hz Voltage: 2 to 5000 Hz
TRANSVERSE SENSITIVITY	5%, max.
AMPLITUDE LINEARITY	Sensitivity increases approximately 1% per 70 g, 0 to 250 g.
TRANSDUCER CAPACITANCE	350 pF, $\pm 20\%$
RESISTANCE	20,000 M Ω , min. at 75°F. 1000 M Ω min. at 350°F.
NOTES	
<p>¹With 100 pF external capacitance. ²In shock measurements, minimum pulse duration for half-sine or triangular pulses should exceed 0.2 msec to avoid excessive high frequency ringing. (See Endevco Piezoelectric Accelerometer Manual.) ³Use ENDEVCO® 2700 Series or 2640 Series Charge Amplifiers.</p>	
TYPICAL TEMPERATURE RESPONSE	
<p>The solid line is the nominal charge-temperature response. The broken lines show the nominal voltage-temperature response with the indicated external capacitances.</p>	
TYPICAL FREQUENCY RESPONSE	
<p>The solid line shows the charge-frequency response. The broken line shows the voltage-frequency response with 100 pF external capacitance and the indicated loads. Estimated calibration errors: 5 to 900 Hz: $\pm 1.5\%$ 900 to 10,000 Hz: $\pm 2.5\%$</p>	

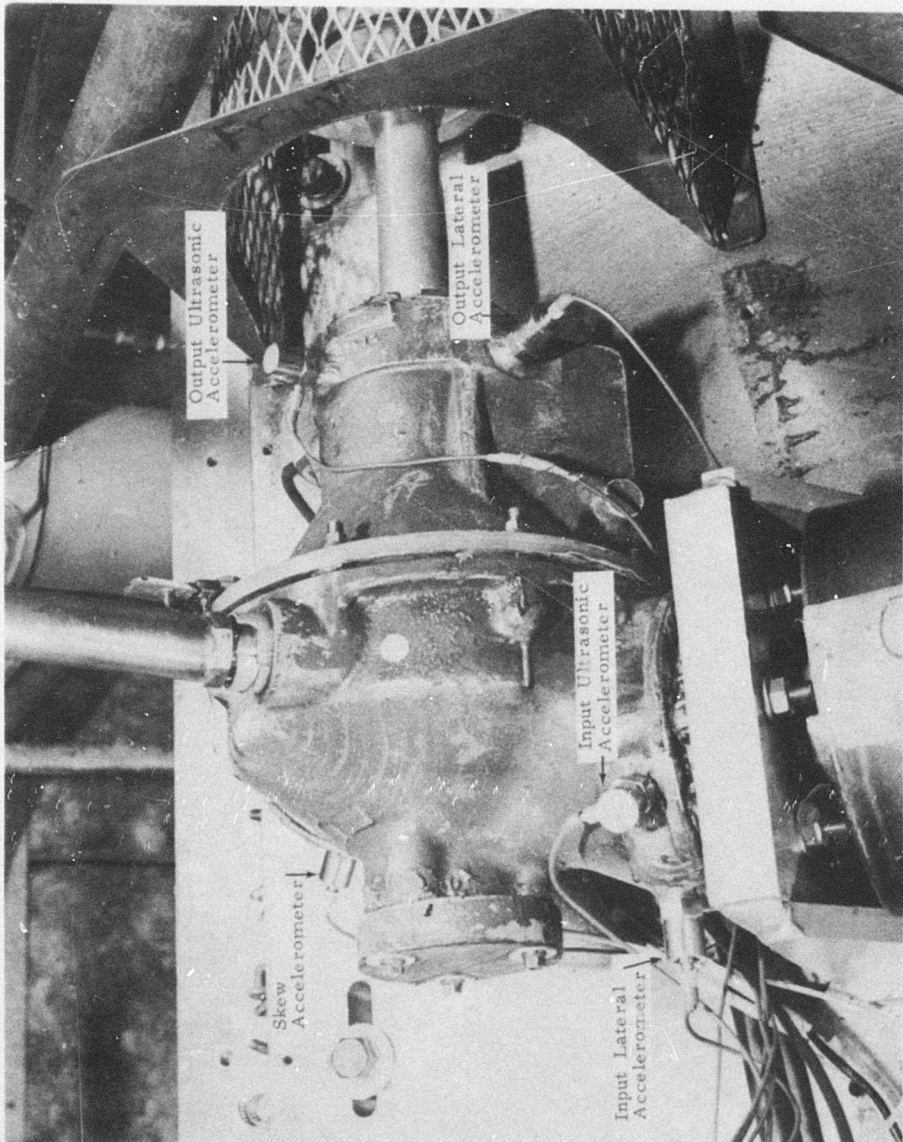


Figure 10. Accelerometer Locations.

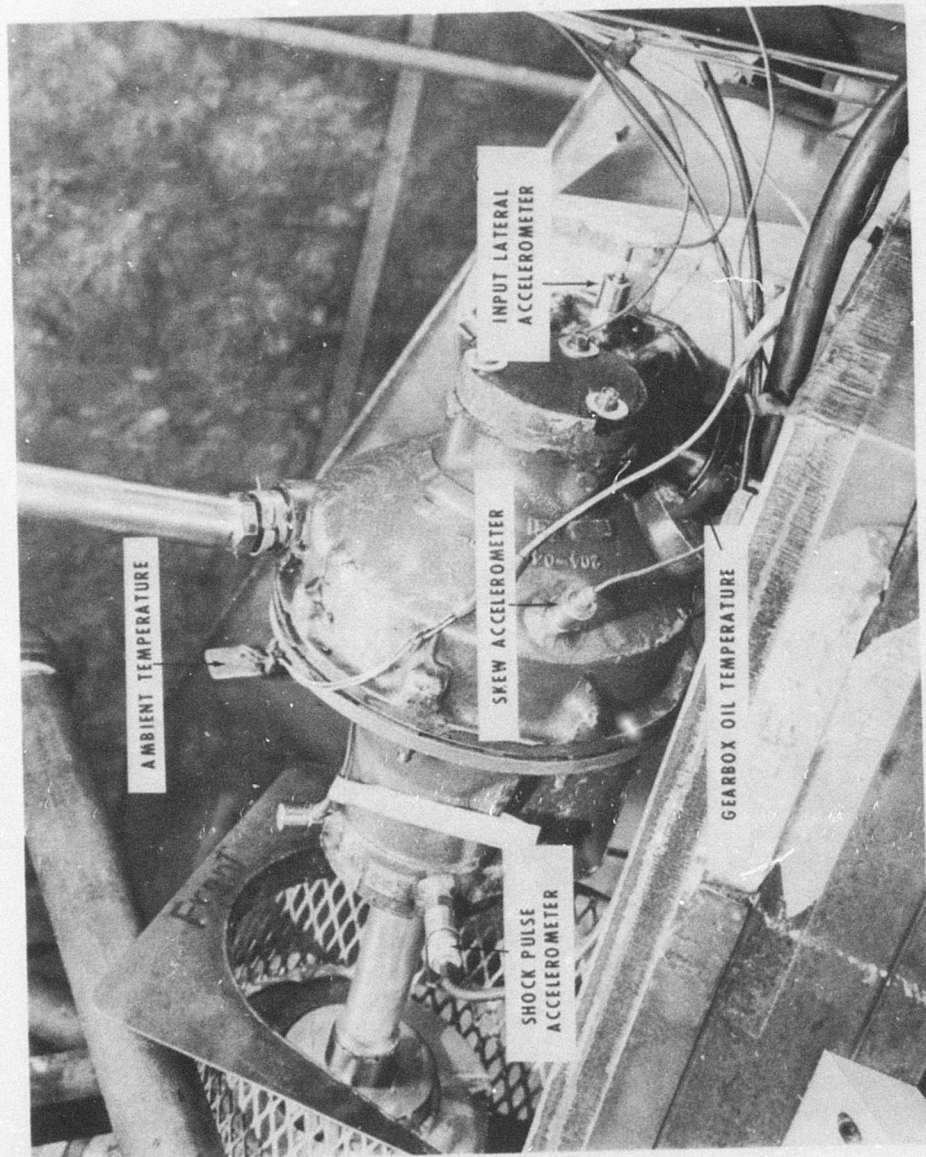


Figure 11. Accelerometer Locations.

second gearbox (BB), which failed catastrophically after a short period of operation.

The BB gearbox was obviously on the verge of catastrophic failure prior to testing, and the high vibration level experienced from the onset of testing, combined with the moment arm formed by the protruding accelerometer, generated sufficient force to break the epoxy bond and cause the accelerometer mounting pad to detach from the gearbox.

On the third gearbox (BG) tested, the accelerometer pads were welded to the desired locations on the gearbox and the accelerometers were screwed into the pads as before. This mounting technique worked satisfactorily for the last three gearboxes tested in this program.

It is worth mentioning that the idea of drilling and tapping holes directly into the gearbox for the purpose of mounting the accelerometers directly to the housing was considered. However, the input and output accelerometers were located extremely close to the input and output bearings, and it was felt that drilling accelerometer mounting holes in the thin magnesium housing might lead to structural failure of the gearbox.

Mounting tabs were also considered, but the concept was not implemented due to our concern that the secondary resonances of the tab would mask or modulate the vibration signals of interest to this program. Also, the design of the gearbox housing does not provide for optimum placement of mounting tabs.

Ultrasonic Accelerometers

Much has appeared in the literature regarding the diagnostic usefulness of ultrasonic emissions (< 20 kHz) from mechanical components. At the beginning of this program ultrasonic monitoring equipment was not commercially available. In order to study the prognostic value of ultrasonic vibration data, an ultrasonic monitoring system was designed and fabricated. Though broadband accelerometers were not commercially available when the initial design was developed for the ultrasonic detection system, the design anticipated the availability of a broadband accelerometer during the course of the test program. Therefore, a sixth-order 20-kHz Butterworth high-pass broadband active filter was used instead of a narrowband filter to remove the low-frequency gear-mesh vibration signals. These low-frequency signals, which are characteristic of the mechanical design of the gearbox, have amplitudes which are a factor of 1000 or so larger

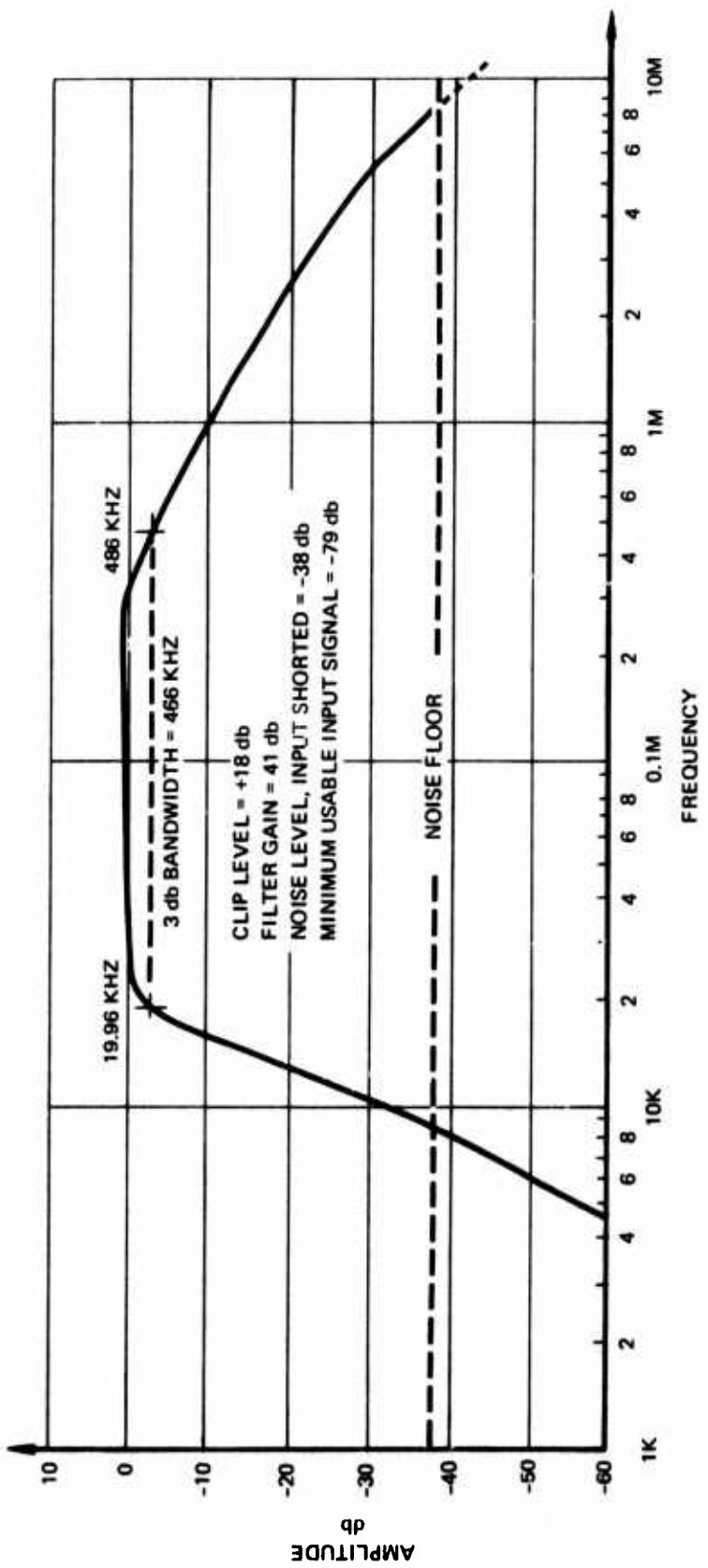


Figure 12. Sixth-Order Butterworth High-Pass Filter.

than the ultrasonic signals to be monitored. The frequency response of this filter is shown in Figure 12. The output of the high-pass filter drives a quasi-peak detector. The peak detector has a relatively slow attack time of 10 ms and a release time of several seconds. This detector was designed with a slow response time in order to discriminate against occasional large spurious amplitude pulses. The output of the detector provides an indication of the overall ultrasonic signal generated as sensed by the accelerometer.

The broadband accelerometer was not available at the start of the test program and in fact could not be obtained during the life of the contract. Therefore, a low-frequency accelerometer with a resonant frequency of 32 kHz when mounted on the gearbox was used to allow us to obtain some ultrasonic vibration data. The locations of these "ultrasonic accelerometers" directly above the input and output duplex bearings are shown in Figure 10.

The use of a low-frequency accelerometer with the broadband Butterworth filter resulted in a modified filter characteristic which was similar to a narrowband filter centered at 32 kHz, the mounted resonant frequency of the accelerometer. Therefore, most of the energy which passed through the filter to the peak detector was concentrated about this frequency. This represented a severe limitation on the type of data collected and its ultimate usefulness.

Shock Pulse Analyzer

The shock pulse monitor is manufactured by SKF Industries, Inc. This instrument uses an accelerometer to sense the ultrasonic shock pulses emitted by bearing defects in order to determine bearing health. Figure 13 shows a picture of the electronic unit.

The shock pulse analyzer was not available until testing began on gearbox BBT, but its usefulness as an important diagnostic tool became quite apparent after its incorporation into the automatic data collection system. It is for this reason that a discussion of how this device operates is included in this report. This discussion relies heavily upon the user's manual for the principles of operation.^{3, 4} The interaction between the rolling element of a bearing and discontinuities in the contact ellipse gives rise to mechanical impacts, which in turn release discrete emissions of energy within the bearing elements. These mechanical impacts create two different kinds of shock pulses within the bearing: a transient shock pulse and an elastic resonance shock pulse.

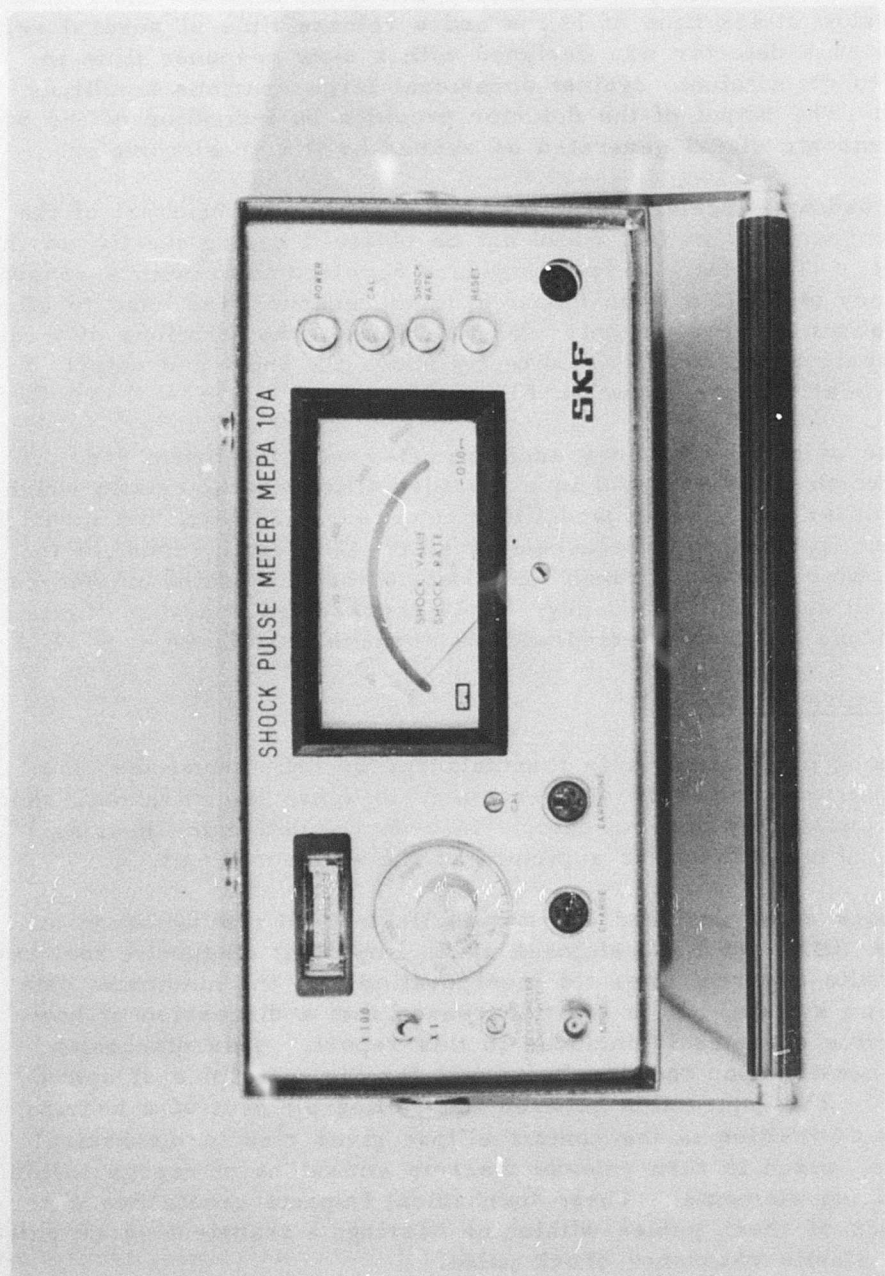


Figure 13. SKF Shock Pulse Analyzer.

A transient shock pulse of very short rise time ($< 1\mu\text{s}$) radiates from the point of impact. The rise time and amplitude of this initial shock wave are essentially determined by the impact velocity and the speed of sound through the material, and are independent of the mass of the interacting bodies.

This initial shock pulse sets up a multitude of different transients of relatively high frequencies in the different parts of the machinery. The amplitude, frequency and damping of these transients are determined by the material and the design of the machine parts.

The second type of shock pulse, the elastic resonance shock pulse, is generated by the total kinetic energy of the original impact. The amplitude and frequency of this wave will be determined by the impact velocity and the mass and rigidity of the bodies involved. These types of pulses are associated with the mechanical resonances of the bearing. Most current bearing diagnostic techniques model the bearing physical and operational characteristics to predict the frequency of these elastic shock pulses.

The SKF shock pulse analyzer, however, uses the transient shock pulse instead of the elastic shock pulse for the following reasons:

1. The transient shock pulse is a sharp-rise, short-duration pulse of energy which is directly related to the severity of the discontinuity in the bearing element contact ellipse.
2. The transient shock pulse depends only upon the speed of sound in the structure for its propagation velocity and is independent of the spring/mass characteristics of the structure. Therefore, it is not dependent on modeling of the mechanical system for data interpretation.
3. The transient shock pulse is markedly attenuated at mechanical interfaces (empirical data indicates about 14 dB per interface). Because of this, with careful sensor placement, the shock pulse analyzer can discriminate between a faulty bearing and a good bearing (and vice versa) when the two bearings are in close proximity to each other. The electronic signal processing used in the shock pulse analyzer is somewhat involved, and the interested reader is referred to the user's manual for these details. The net effect of the electronic signal processing is to provide a means for obtaining the cumulative amplitude distribution function of the shock pulses (integrated over sufficient time to ensure

proper statistics) which SKF calls a "shock emission profile." The shock emission profile is a plot of the total cumulative rate of shock pulse emissions above a given amplitude level (for a given unit of time) against the given amplitude level (potentiometer level). Figure 14 shows the three basic curve shapes (shock emission profiles) obtained by SKF in their testing of mechanical systems.

Curve A is a typical shock emission profile obtained when foreign particulate matter is present in the bearing lubricant. This curve is characterized by having high rates of very small shock levels, but no shocks above a level of 3 to 5.

Curve B is typical data obtained from dry bearings or when there is rolling element damage. This curve is characterized by very low rates of very high shock levels.

Curve C, characterized by high shock rates at high levels, indicates a damaged bearing. The spread in shock level is caused by the specific characteristics of each rolling element as it interacts with the damaged portions of the bearing.

Curve C' is an example of the shock emission profile one would expect to observe as the damaged bearing, represented by the data in Curve C taken at an earlier time, continues to degrade. The shock emission profile should reflect an increase in both shock rate and shock level.

All of the shock pulse data collected on this program had shock emission profiles similar to Curves C and C'.

Torque Sensing

The torque load on the gearbox was not sensed directly nor was it automatically measured during the computerized data collection. The torque load on the gearbox was calculated using the parameters of the operational hydraulic system as described in the earlier discussion of the "Test Stand" components and operational parameters.

RPM Sensor

The rpm of the gearbox was measured at the input shaft (see Figure 2) by an optical tachometer. Ten 1/8-inch holes evenly spaced near the rim of a 4-inch disc were used to mechanically interrupt the optical path between an infrared light emitting diode (LED) and a

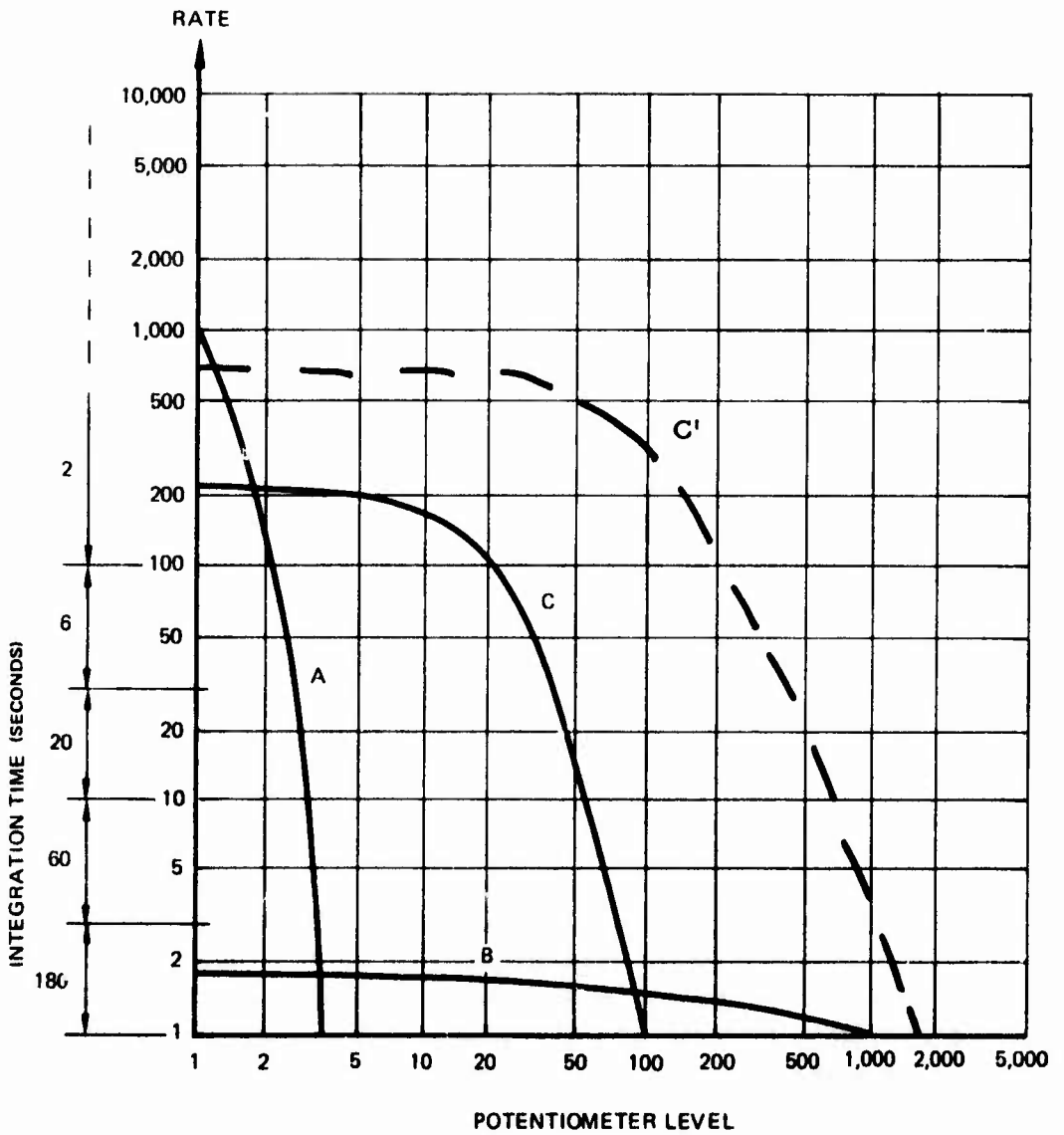


Figure 14. Shock Emission Profile Curve Types.

photo-detector. The detector output was used to drive a one-shot multivibrator, which in turn produced a constant-amplitude constant-width pulse for each interruption of the light source. A constant-amplitude constant-width pulse contains constant energy, and since the number of pulses per second is directly proportional to the rpm of the test cell, the average energy per second (average power) of the pulses is also directly proportional to the rpm of the test cell. The average power of the pulses is obtained by low-pass filtering the individual pulses with a 1-Hz filter. The resulting analog signal is directly proportional to rpm and is suitable for digitization.

DETERMINATION OF BEARING CONDITION AND SURFACE WEAR

Except for the scanning electron microscope studies, the tests for mechanical wear discussed in this section were performed by Bearing Inspection Incorporated of Santa Fe Springs, California. Bearing Inspection is authorized by the FAA to repair or recondition aircraft bearings.

Documentation of the initial condition of the bearings in each test gearbox and inspection of wear after testing were done only on the bearings.

No quantitative measurement technique was available for monitoring gear wear. Early in the program we requested that Bell Helicopter provide us with gear profiles, but they could not make profiles on spiral bevel gears. The condition of the gears was determined by a subjective assessment of their visual appearance as discussed in the section on "Experimental Results."

In all of the bearing wear measurements, the bearing condition after testing was compared to its condition prior to testing. Since all of the gearboxes were already in a worn condition, and no measurement data was available on new bearings, the very important data point on zero wear is missing.

Figure 15 shows a cross-sectional view of a UH-1 90° gearbox and the location of the gears and bearings to be discussed in this and following sections. Figure 16 is a photograph which shows most of the mechanical components of the gearbox.

Visual Inspection

Visual inspection involves the complete disassembly of the bearing.

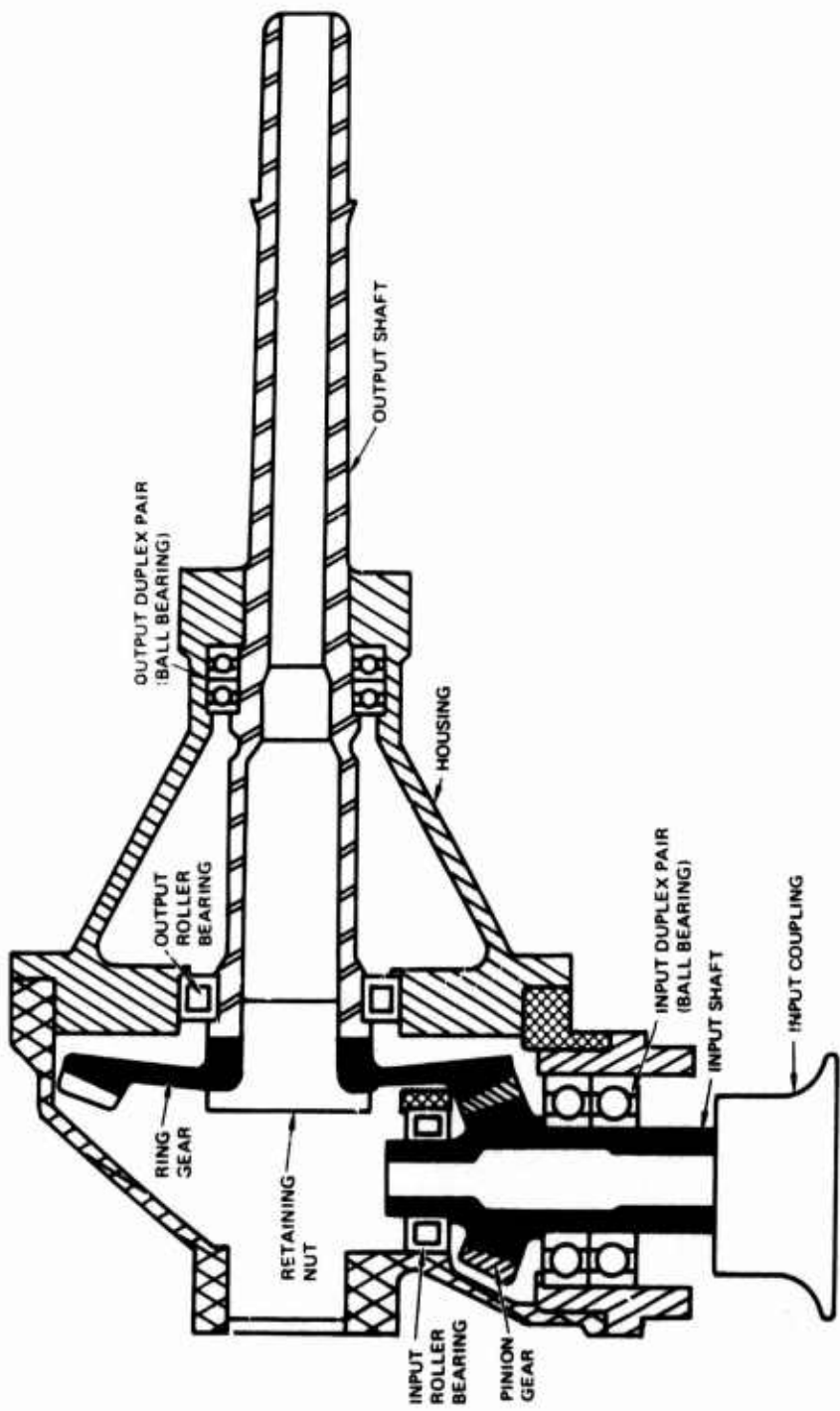


Figure 15. Cross-Sectional View of 230 Gearbox.

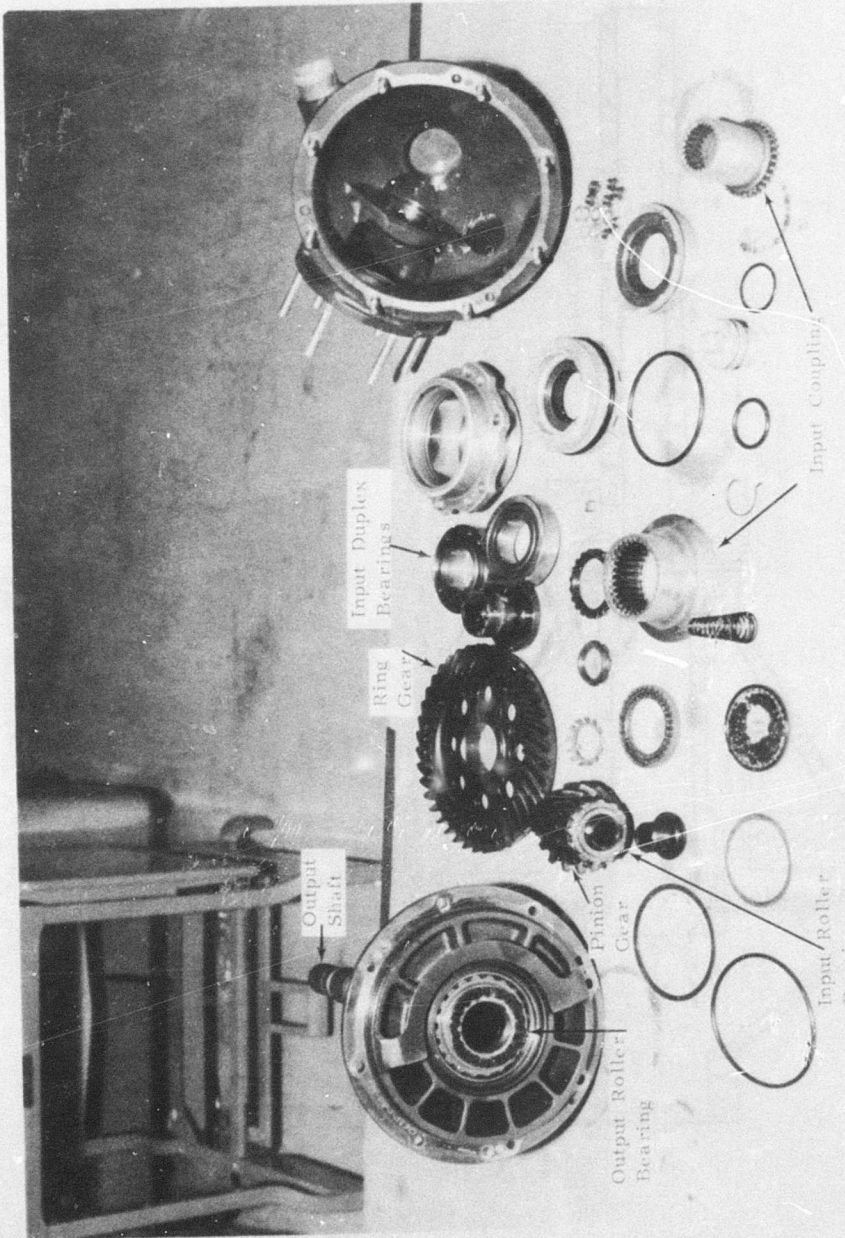


Figure 16. Partial Disassembly of a 90° Gearbox.

The subjective opinion of a highly trained bearing inspector is used to evaluate the mechanical condition of the bearings. This test helps to identify reasons why the bearings are in their present condition. The presence of large-scale contaminants, pits, grooves or other irregularities is noted and documented.

Ball Bearings' Wear Measurements

Three separate quantitative measurements were made to determine the wear condition of each bearing in the gearboxes prior to and after each phase of the test program.

Dynamic Noise Testing of Ball Bearings

This test characterizes the bearing as an operational dynamic unit. The results of this test give an accurate picture of the overall health of the bearing and are found to correlate well with visual and microscopic inspections of the individual components.

The test bearing is mounted on a shaft and is caused to rotate at low speeds by the application of a rotating rubber wheel to the outer casing of the bearing. Vibrations set up in the bearing are transferred to the (stationary) shaft and are sensed by a piezoelectric crystal as shown in Figure 17. The shaft and its support mechanism have a mechanical resonance of about 800 Hz. After amplification, the bearing vibrations are low-pass filtered to 2 kHz and the RMS noise level is determined. The RMS noise level is an overall indication of degree of wear in the bearing. This level is compared with the vibration noise level of known good bearings, and should not exceed 0 dB for a new bearing.

Table II is an excerpt from Bearing Inspection's "Product Specification" and gives a summary of how the (RMS) noise level compares with the physical condition of the bearing.

Another parameter derived from the noise test is the relationship between the peak-to-peak vibration noise level and the RMS

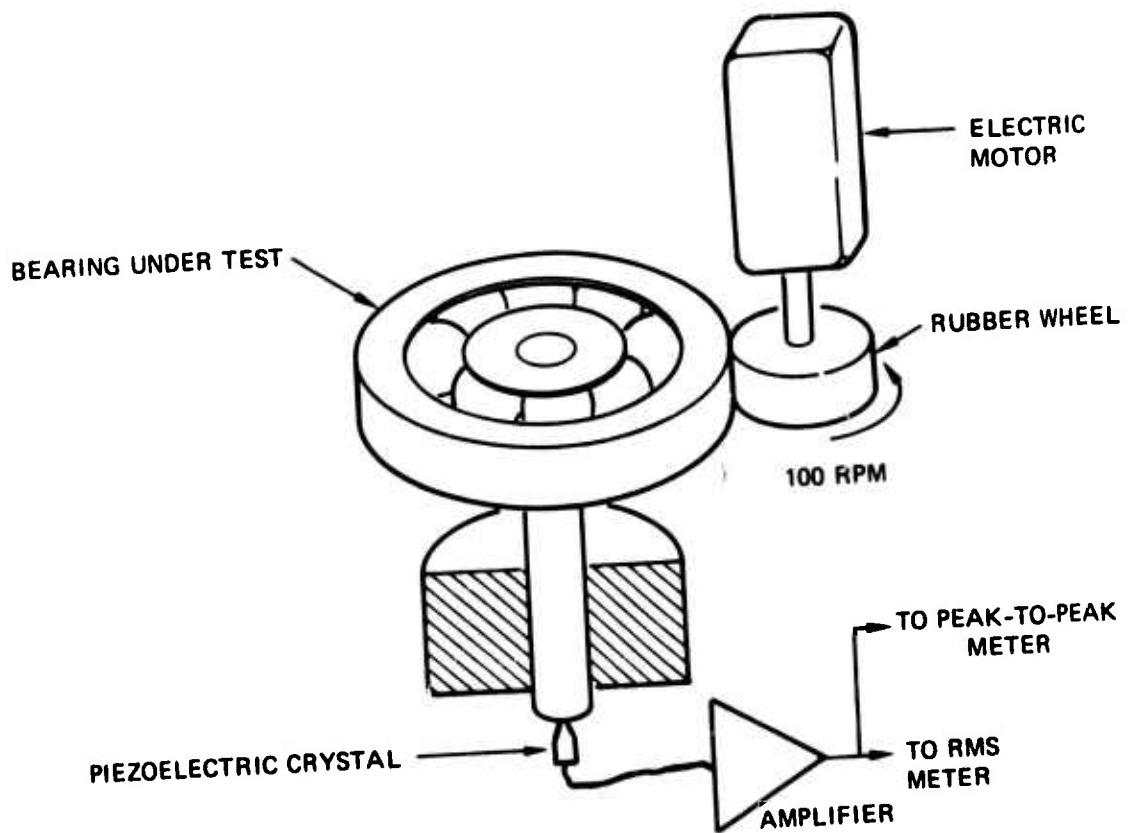


Figure 17. Schematic Diagram of Dynamic Noise Test.

TABLE II. DYNAMIC ANALYSIS BEARING CONDITION LEVELS
(Bearing Inspection Inc.)

Bearing Noise Level Range	Condition	Visual	Microscopic	Common Conditions
Below -7 dB	EXCELLENT	Like new	Smooth polish	N. A.
-7 to -5 dB	GOOD	Like new	Polish	N. A.
-5 to -3 dB	FAIR	Like new	Polish	N. A.
-3 to 0 dB	ACCEPTABLE NEGIGLIGIBLE Wear	Like new	Slight pitting and denting	Slight wear
0 to 3 dB	LIGHT Wear	Like new	Light pitting and denting	Light wear
3 to 7 dB	MODERATE Wear	Well defined wear tracks	Pitting and denting	Moderate wear
7 to 12 dB	HEAVY Wear	Wear tracks with pitting and denting	Heavy pitting and denting	Fatigue spalling
12 dB and above	EXTREME Wear	Very rough	Gross surface dis- turbance	Heavy electric current damage; extensive smear- ing and material transfer

noise level*. This relationship is called "peak rise" and is a measure of how uniformly the wear is distributed around the bearing. A peak rise of 0 dB is normally found in good bearings. A peak rise of -3 dB indicates an exceptionally uniform wear pattern, while a peak rise of +7 dB indicates considerable local damage.

In order that a bearing be considered acceptable as new, both the noise level and the peak rise must be below 0 dB.

Radial Play Measurements of Ball Bearings

Radial play is defined as the maximum total clearance between the inner and outer races of the bearing. It is measured by first pushing the inner race as close to the outer race as possible (this ensures intimate contact between the inner race, the ball, and the outer race) and then by pushing the inner race radially in the opposite direction as far as possible. The total distance traveled is called "radial play" and is a measure of running clearances and overall material wear (race and balls) in the bearing.

Cross-Groove Profile of Inner Race of Ball Bearings

This test measures the actual shape of the inner race of the bearing. A stylus with a very fine diamond tip is pressed lightly against the surface of the inner race. The other end of the stylus is connected to a linear displacement sensor. As the stylus is moved across the race, a profile of the bearing is plotted out. Figure 18 illustrates in principle how this measurement is performed.

A polar plot is usually made to show differences in curvatures across the inner race. As a bearing wears, the balls wear a groove (called a ball track) into the races. Examples of typical polar plots are shown in Figures 19 and 20. These measurements were taken on the inner races of bearing number three of gearbox BBT. Figure 19 shows a cross groove profile of BBT-3 prior to testing.

*This parameter is closely related to the so-called "Crest Factor", developed by the General Electric Company (see Houser, Donald R., et al, VIBRATION SIGNAL ANALYSIS TECHNIQUE, p. 78, Ohio State University Research Foundation, USAAMRDL Technical Report 73-101, December 1973.

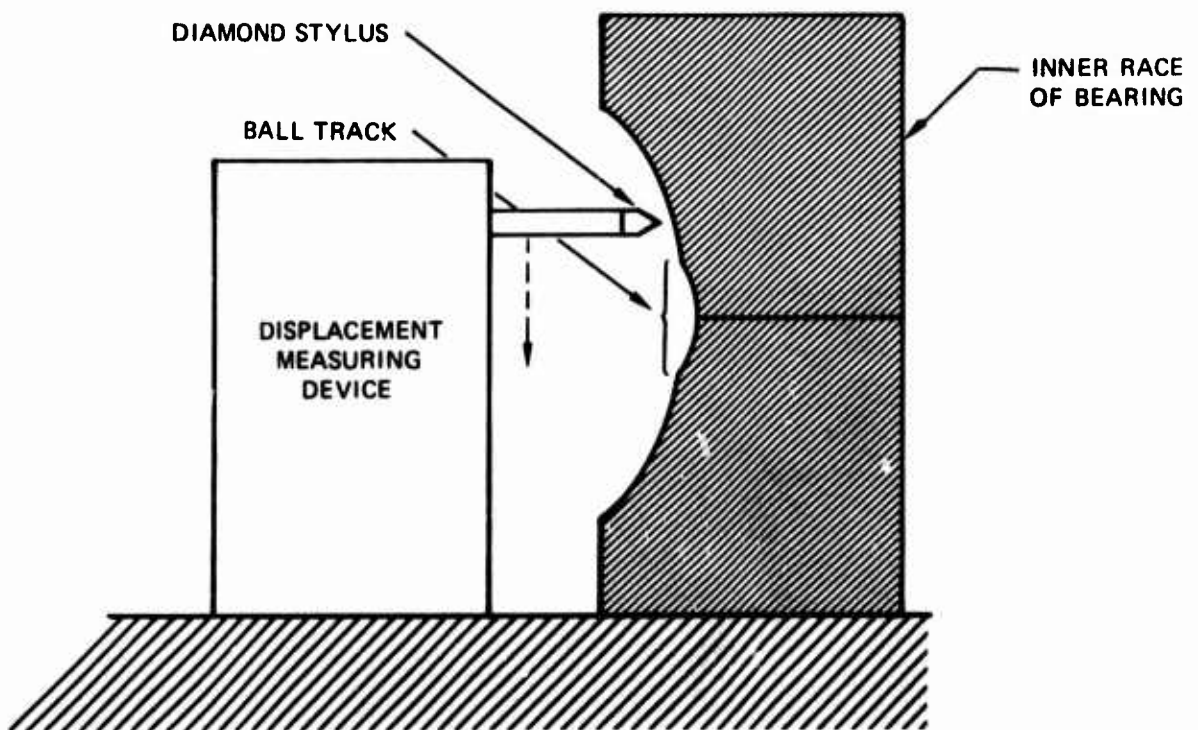


Figure 18. Schematic Diagram of Cross-Groove Profile Measurement.

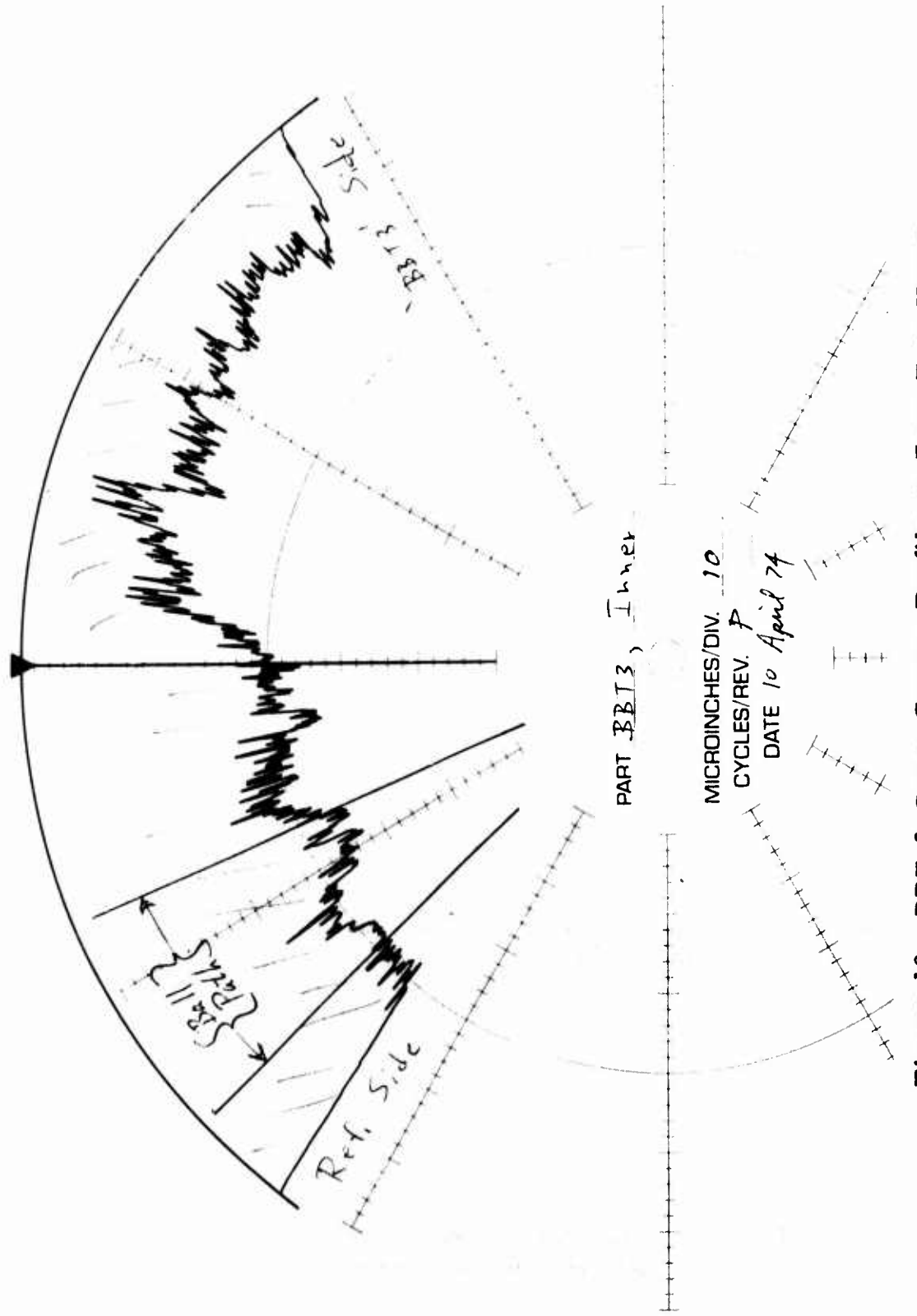


Figure 19. BBT-3 Cross-Groove Profile at Zero Test Hours.

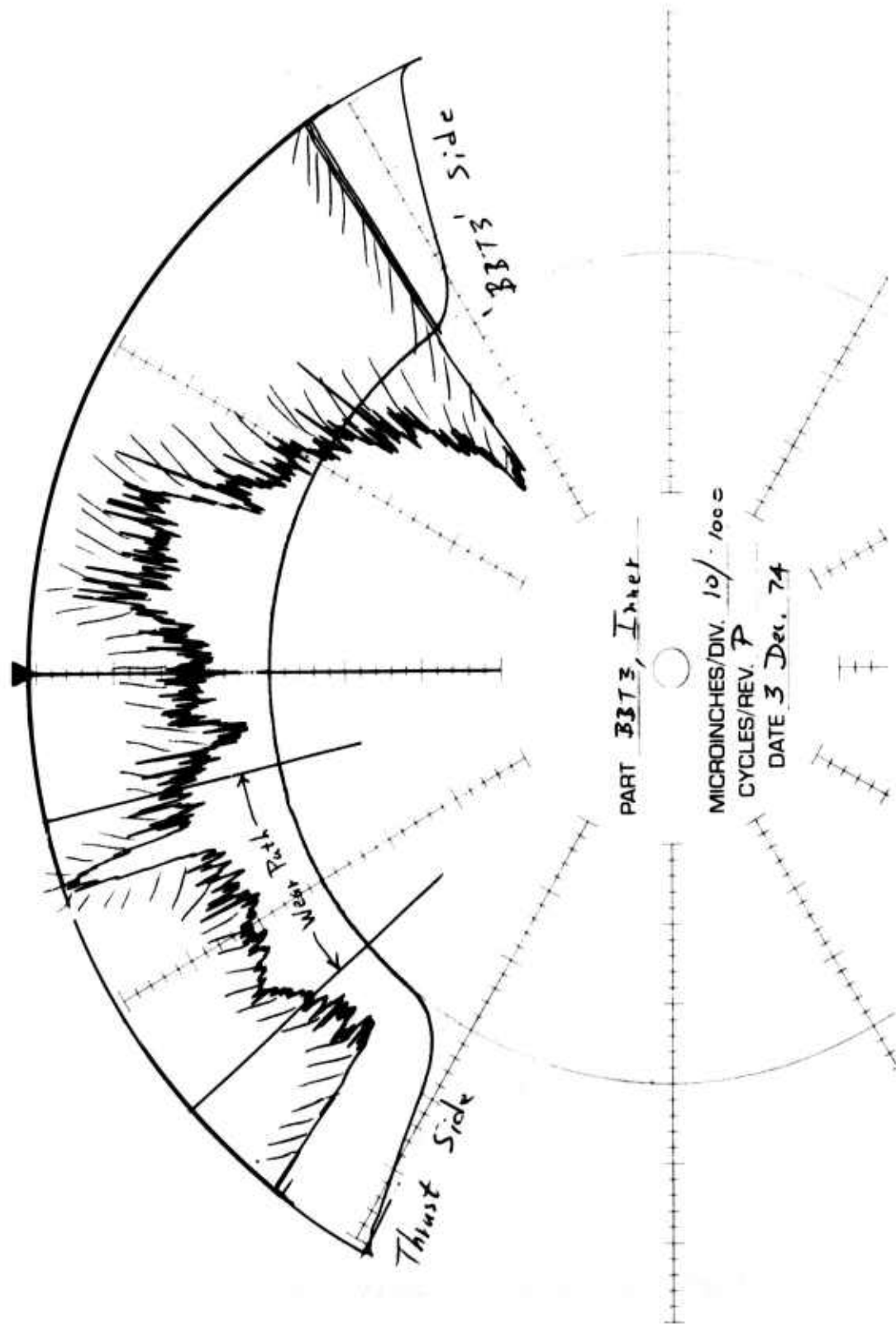


Figure 20. BBT-3 Cross-Groove Profile at 1022 Test Hours.

The radius plot has a scale of 10 microinches per division. The "reference side" and "BBT-3 side" refer to the orientation of the bearing in the gearbox. The cone of interest is marked "ball path." This is where the changes are expected to occur as the bearing deteriorates. Due to the bearing design, the ball contacts only the inner race at this point. Figure 20 is a cross-groove profile plot of the same bearing at 1022 hours of testing. Notice how the depth of the ball track has increased during testing. The cross-groove profile measurement is a very sensitive indicator of inner race wear.

Roller Bearing Wear Measurements

Only the ball bearings were completely disassembled. The output roller had only one roller removed in order to preserve its overall characteristics. The input roller was not disassembled at all since the rollers were pinned in place. Two separate quantitative measurements were made to determine the wear condition of gearbox roller bearings.

Roller Crown Measurement

A new roller is designed to be slightly tapered on the ends, as shown in Figure 21. This taper, called a crown, serves to relieve stress concentration from the ends of the roller during normal load conditions. As the roller wears, the crown becomes smaller. Crown wear measurements are sensitive measures of actual roller wear.

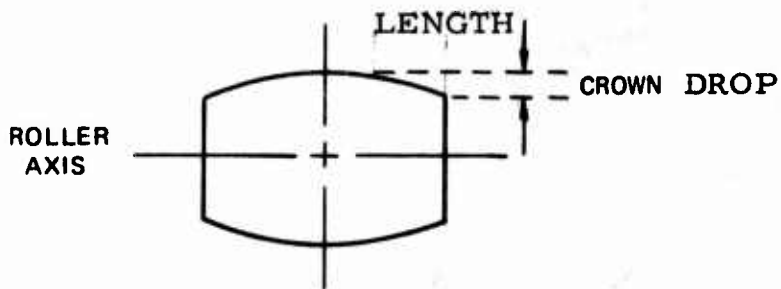


Figure 21. Roller Crown Parameters.

Roller Axial Play

The axial play of a roller is the amount of movement available to the roller along its axis. This measurement determines the amount of wear occurring on the ends of the roller. Excessive axial play can lead to skewing of the roller and unequal load distribution along the bearing. This causes nonuniform wear of the roller and eventual failure of the bearing.

SCANNING ELECTRON MICROSCOPE SURFACE INSPECTION

For completeness in determining the overall condition of the bearings, one ball and one roller from each bearing, except for the pinned roller bearing number 6 which was not disassembled in any gearbox, were examined with the scanning electron microscope. Each part was thoroughly cleaned in acetone before examination to remove fingerprints, excess oil and extraneous surface debris. The microscope has two modes of operation: the secondary emission (SEC) mode and the backscatter emission mode (BSE). The two modes produce different types of view of the same surface area because one mode (SEC) operates with low-energy electrons and the other (BSE) with high-energy electrons.

Secondary Emission Mode (SEC)

The secondary emission mode utilizes a low-energy (100 ev) focused electron beam to scan the surface of the specimen. The surface structure responds to the electron beam by emitting secondary electrons which, in turn, are collected for display purposes. Irregularities in the surface cause corresponding irregularities in the number of secondary electrons, in turn giving rise to a picture of the topography of localized portions of the surface. The SEC mode detects the structure of the first several angstroms (10^{-8} cm) of the specimen. The major advantage of the SEC mode is its ability to look around corners or into depressions and provides the viewer with a picture which appears to have three-dimensional characteristics. The SEC mode produces surface pictures which have no obscuring shadows around raised or depressed areas, making it somewhat difficult to differentiate between these two surface characteristics.

Backscatter Emission Mode (BSE)

The backscatter emission mode utilizes a high-energy (10 kev) focused electron beam to scan the specimen. The high-energy electrons

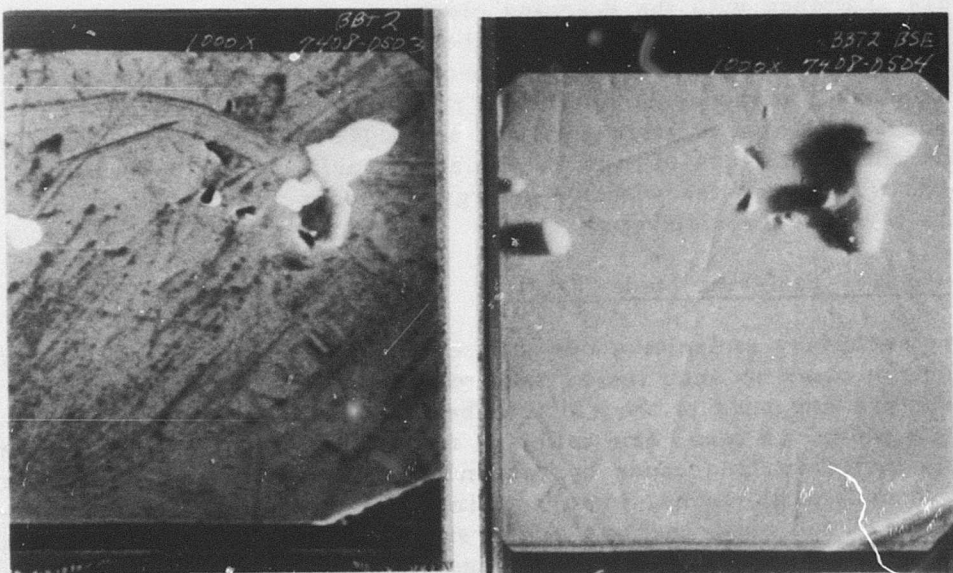


Figure 22. SEM Micrographs of BBT-2 (407 Hours).

penetrate the specimen's surface to a depth of about 10-20 microns. Some of these electrons are scattered back out of the specimen, where they are collected for display purposes. These high-energy electrons travel in straight lines which cause the BSE photo to be characterized by shadows around raised or depressed surfaces. The BSE mode is often the only way one can positively identify a raised or depressed surface. The BSE mode is most useful when surface films (e.g., oil stains) must be penetrated to view the surface underneath.

Examples of SEM pictures using the SEC and BSE modes are given in Figure 22. These were obtained from the surfaces of a ball from bearing number 2 in gearbox BBT. Both photographs are of the same surface area on the ball and both are taken at a magnification of 1000 to 1. Note the sharpness but lack of surface detail in the BSE picture.

For the gearbox bearing data given in this report, the SEM pictures were obtained using the SEC mode, unless specifically designated as BSE pictures. The SEC mode was selected for most of the data presented because, from our subjective viewpoint in determining surface abnormalities, the SEC mode produced the most useful pictures.

AUTOMATIC COMPUTER-CONTROLLED DATA COLLECTION AND REDUCTION

This section describes the computer-controlled data collection system and the documentation procedures for the gathering and initial reduction of the real-time test cell data.

OVERVIEW OF MAIN COMPUTER SOFTWARE

The data collection program was written to implement the data collection timing diagram shown in Figure 23. This diagram shows a data collection period of 16 hours, with each sensor being sampled every 4 minutes. The fundamental flow chart of Figure 24 describes how this timing diagram was implemented in the data collection program.

START-UP SEQUENCE ROUTINE

The "Start-Up-Sequence" (SUS) block in Figure 24 is a series of computer-generated requests which guide the user in defining the appropriate input parameters. The flow chart for this routine is given in Figure 25. The initial conditions referred to by the "Start-Up-Sequence" routine are later used by the "Comparison Checks and Tests" routine. Provisions have been made in the software to use either the first 4 minutes of any prior 16-hour test period on the same gearbox as the initial condition for comparison with each new data interval, or the first 4 minutes of data of the current 16-hour test period. For most of the data collected on this program, comparison was made with the first 4-minute interval of the current 16-hour test period.

SENSOR SELECT AND PROCESSING ROUTINE

The "Sensor Select and Processing" (SSP) block in Figure 24 contains the data acquisition and data processing operations of the program. Figure 26 shows the flow chart for this routine, which operates under control of the real-time clock. The real-time clock ensures accurate program timing according to the timing diagram of Figure 23.

Vibration data is processed by the "Compute Ensemble PSD*" block in Figure 26. Figure 27 shows the flow chart for this routine. To ensure statistical reliability, 128 (short-term) PSD's are combined into an ensemble.

*PSD = Power Spectral Density

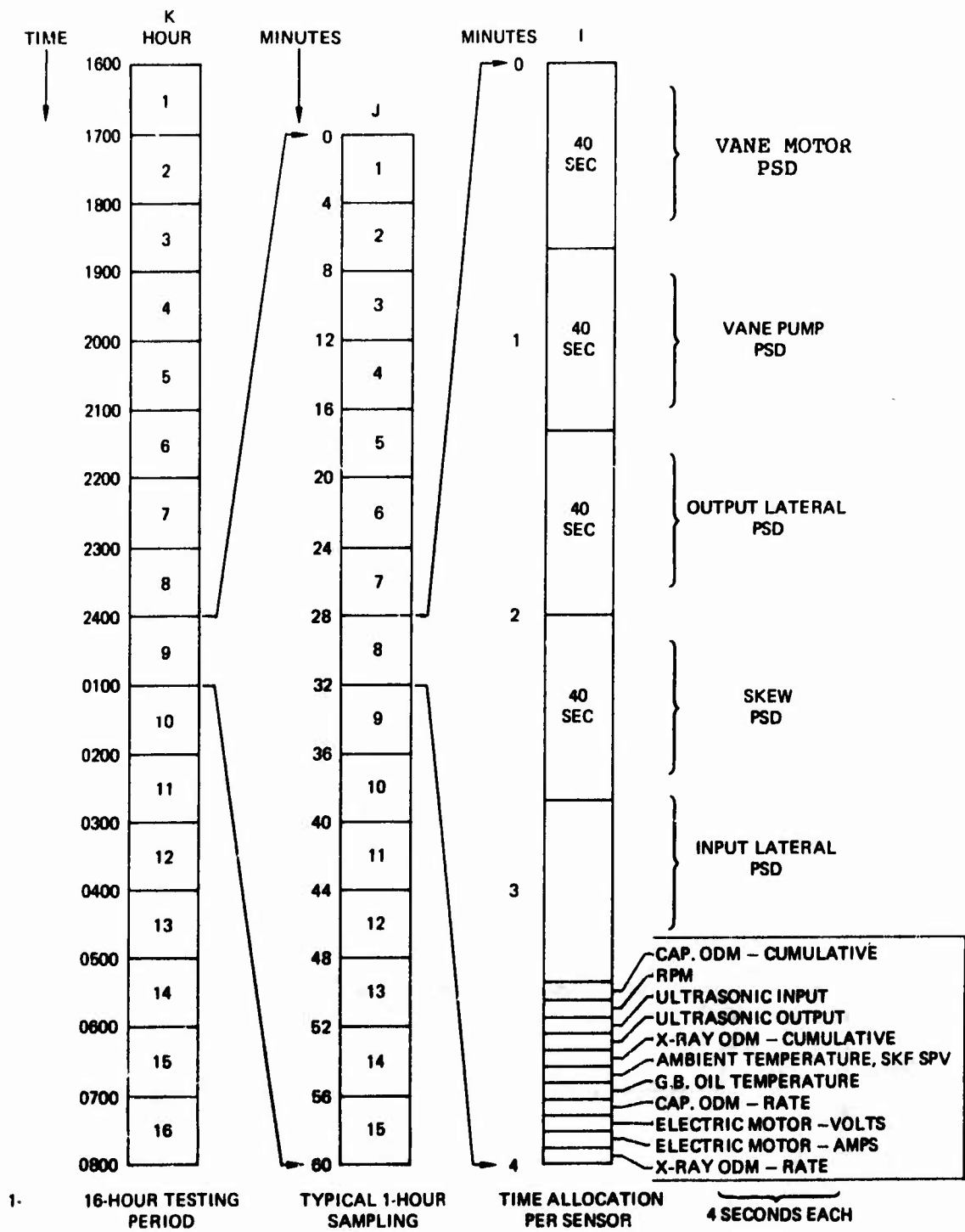


Figure 23. Timing Diagram for Data Collection Effort.

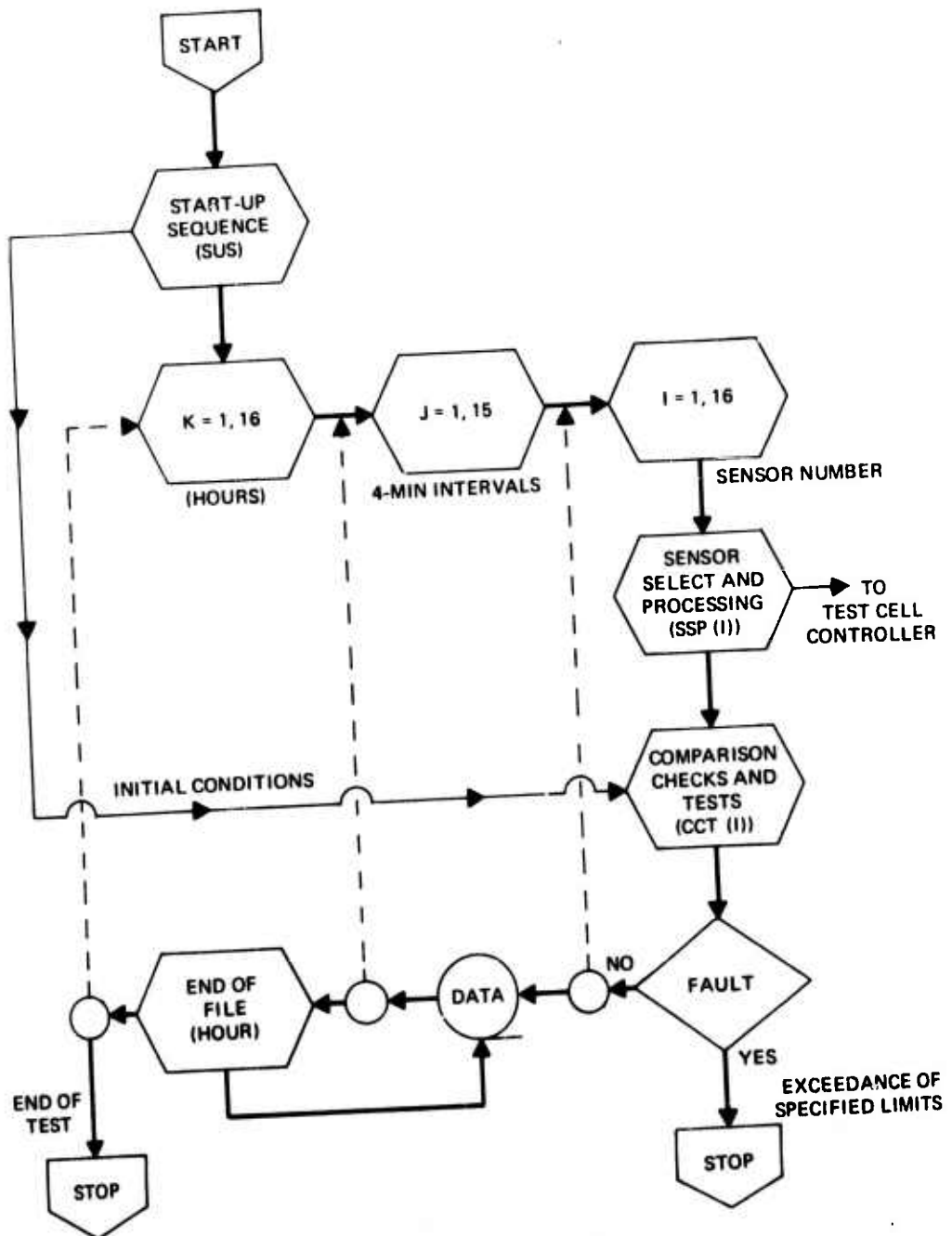


Figure 24. Macro Flow Chart for Data Collection Program.

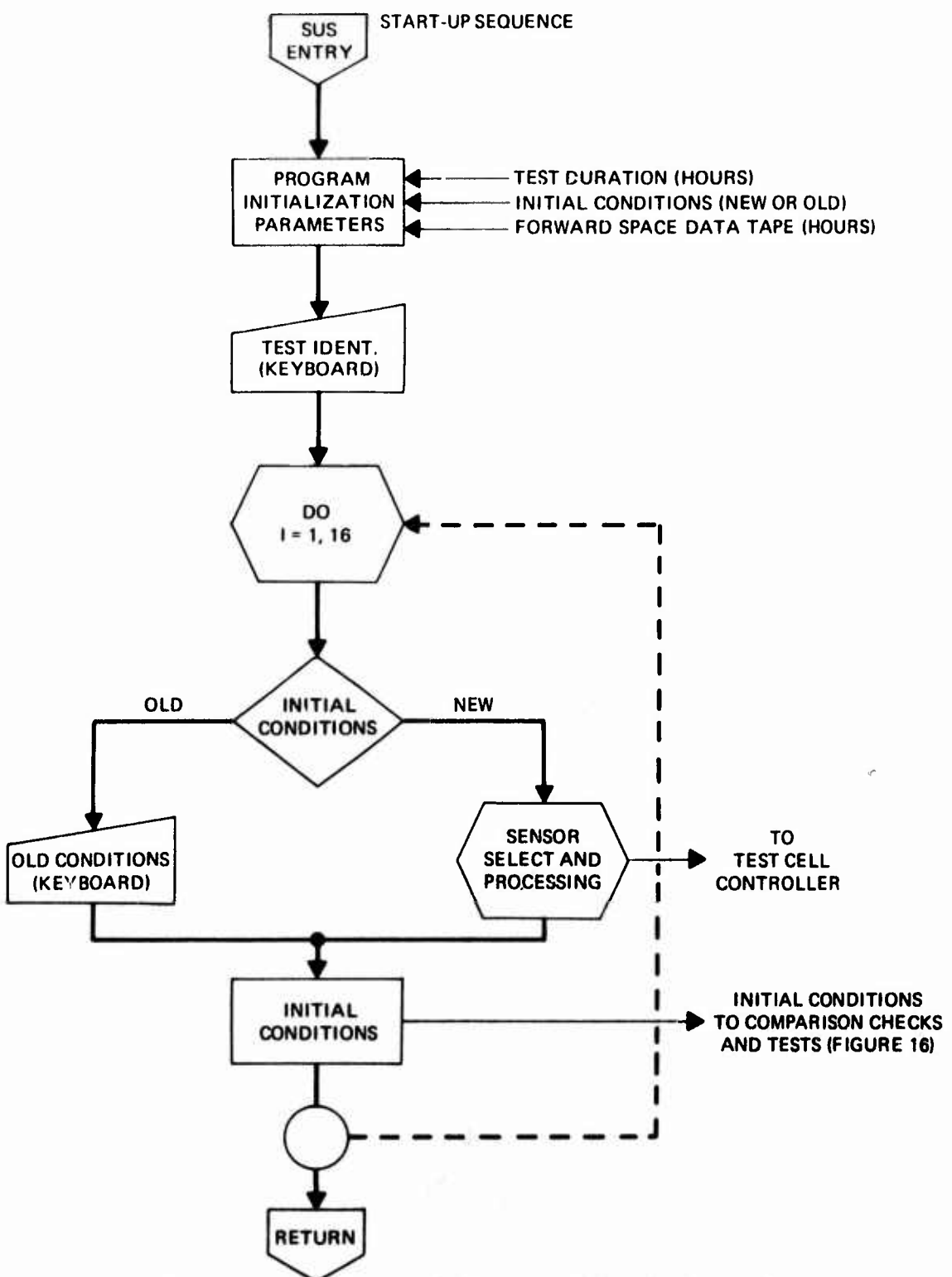


Figure 25. Flow Chart for Start-up Sequence Routine.

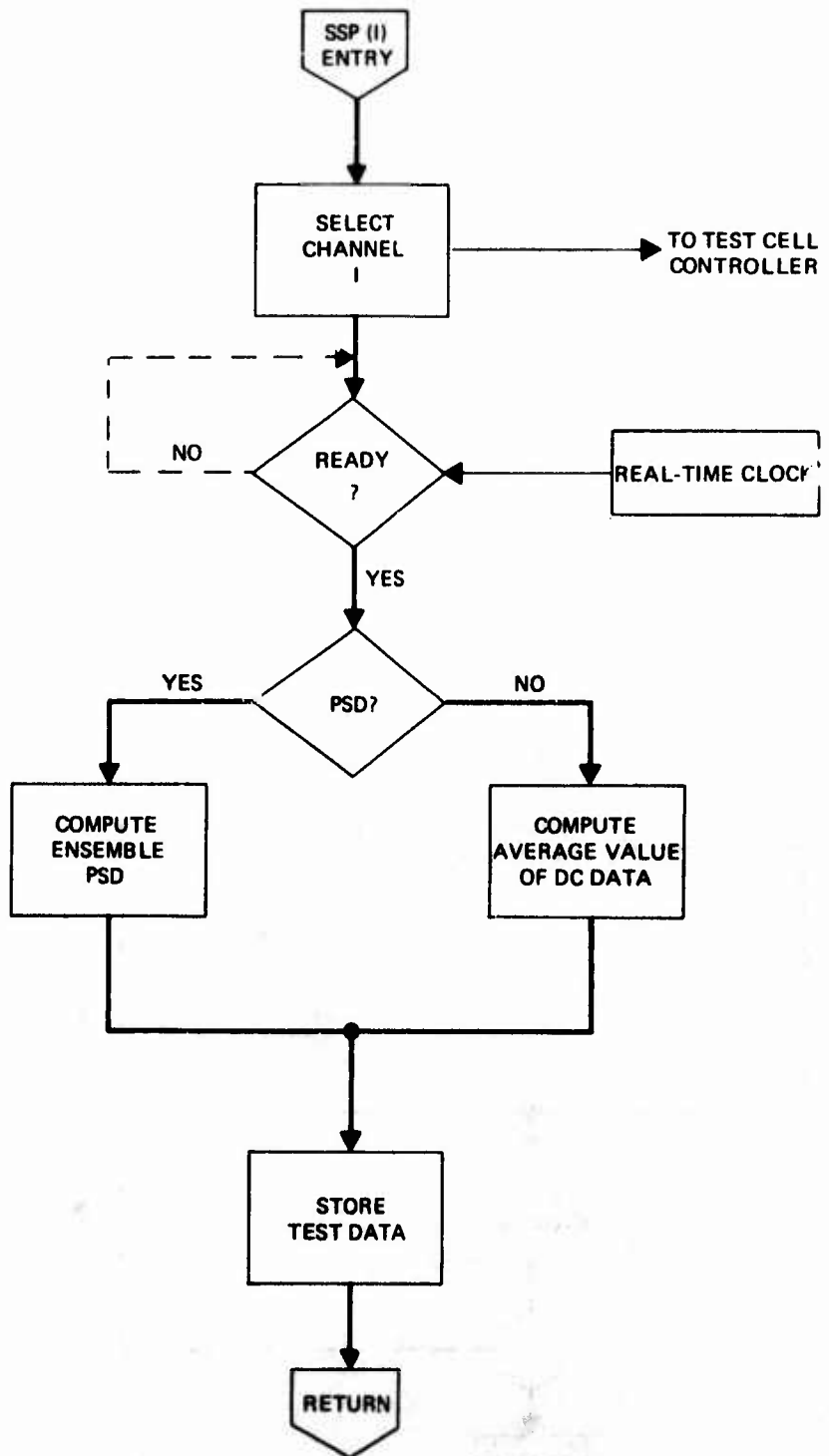


Figure 26. Flow Chart for Sensor Select and Processing Routine.

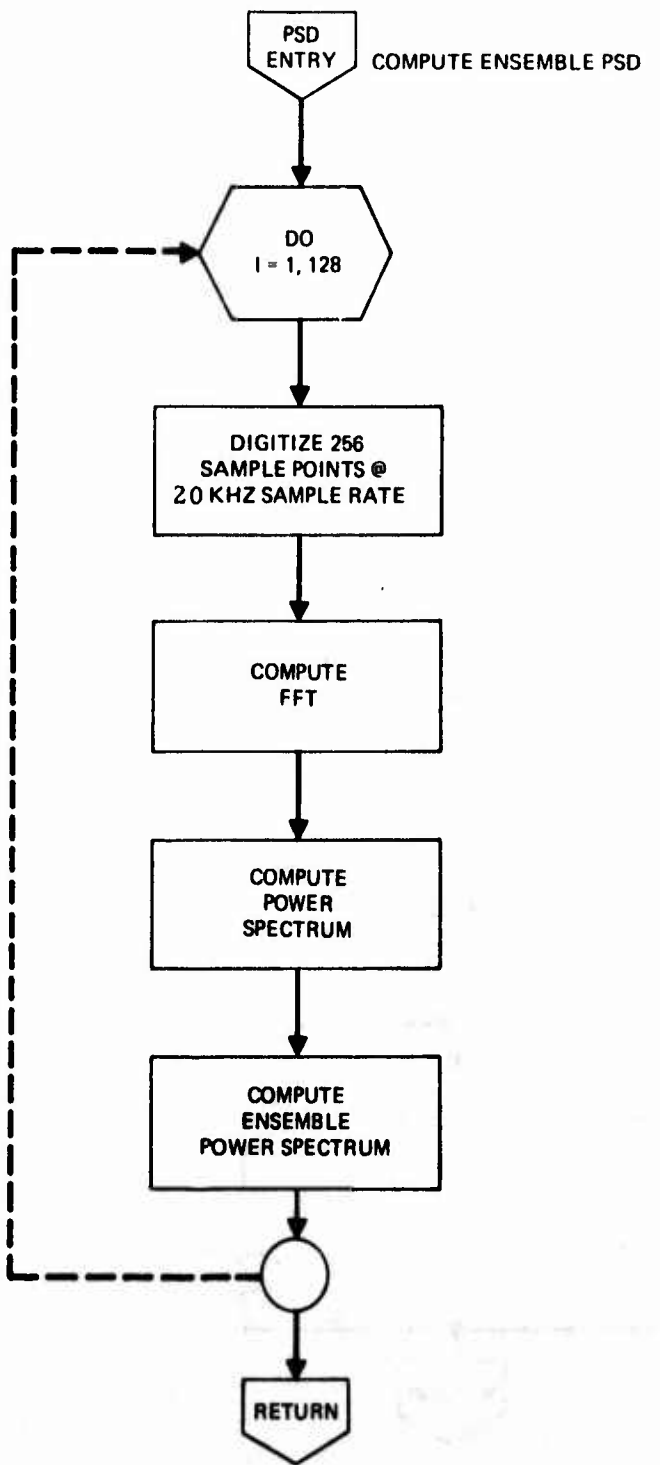


Figure 27. Flow Chart for Compute Ensemble PSD Routine.

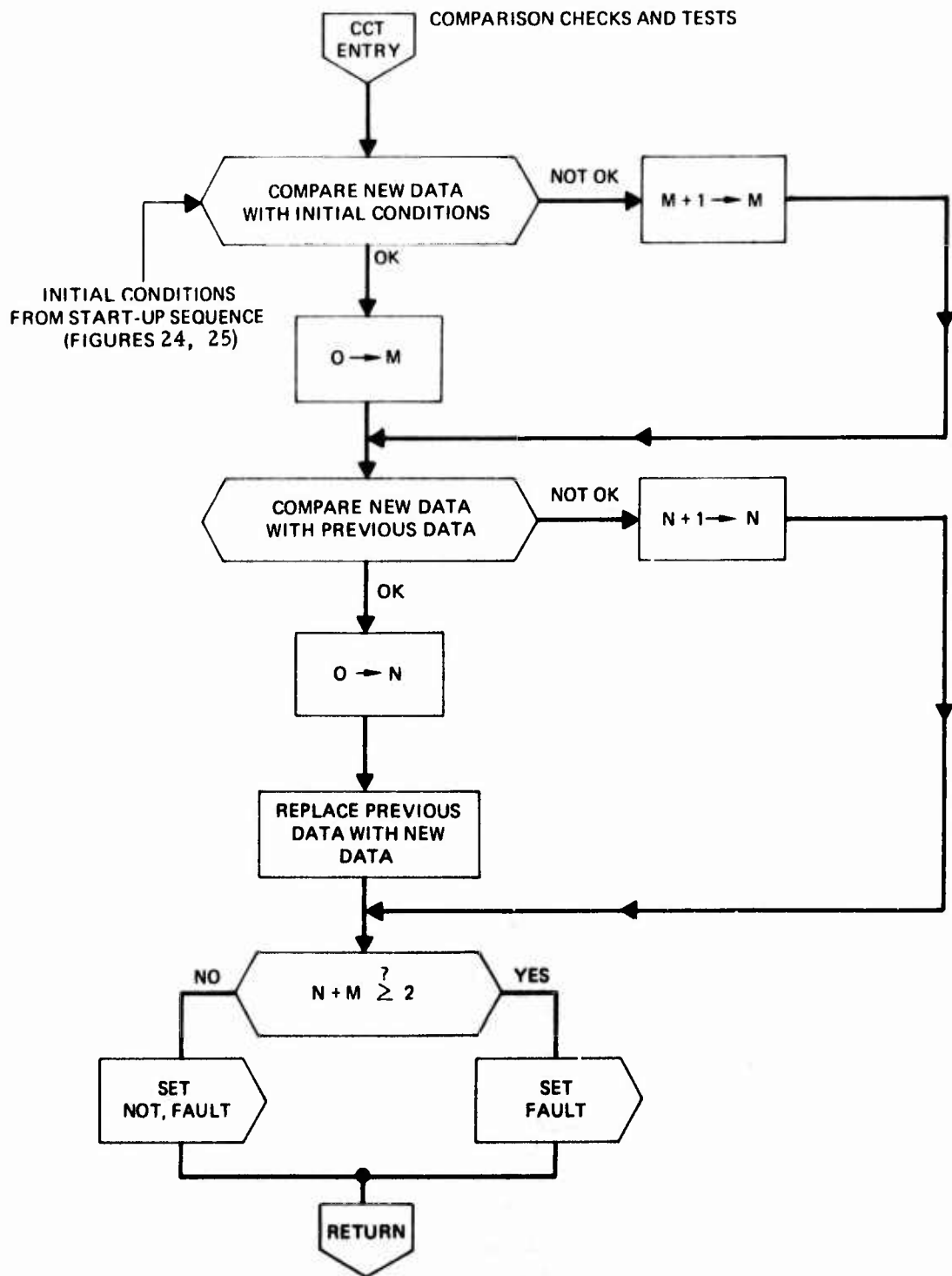


Figure 28. Flow Chart for Comparison Checks and Tests Routine.

The DC data (temperature, rpm, etc.) are similarly combined into an ensemble (128 times) for statistical reliability.

Figure 28 shows the flow chart for the comparison checks and test routine.

Comparison checks and tests are made:

- a) to determine (by comparison) when a significant mechanical change has occurred in the gearbox,
- b) to verify (test) that the change is not a transient condition, but is a valid, stable state, and
- c) to generate a shutdown command to the test cell controller to terminate testing in case an abnormality appears in any of the signals from the test cell.

Two comparisons were made of each 4-minute interval during each 16-hour test period to make certain that an abrupt change in any of the signals from the test cell was not a one-time transient, but a true indication that the gearbox was indeed on the verge of catastrophic failure. The objective was to shut down the test cell before the gearbox failed catastrophically so that the gearbox could be disassembled and the mode of failure determined.

The long-term comparison of the 4-minute data intervals consisted of comparing the amplitude of the data from any sensor in the current 4-minute interval with the amplitude of the data from the first 4-minute interval of the same 16-hour test period. This comparison was made to monitor the long-term mechanical condition of the gearbox during the test period. The limit on the allowable change in signal amplitude in this comparison was set at ± 10 dB.

The short-term limit was a comparison of the amplitude of the data from any particular sensor in two consecutive 4-minute intervals. This check was made to insure that the abrupt increase in signal was consistent from interval to interval and did represent a trend toward failure. The allowable change in signal amplitude for this comparison was set at 6 dB.

To insure that any abrupt changes in signal structure observed were positive indicators that the gearbox was failing catastrophically or at least undergoing a significant deviation from its past operating point, one of the following conditions had to be satisfied:

- a) The long-term limit must be exceeded in two consecutive 4-minute measuring periods.
- b) The short-term limit must be exceeded in two consecutive 4-minute measuring periods.
- c) Both the long-term limit and the short-term must be exceeded during one 4-minute measuring period.

If any one of these conditions was satisfied, the test cell was shut down.

During the early stages of data collection it was observed that low-amplitude PSD components fluctuated considerably more than 6 dB, and these fluctuations led to premature shutdown due to exceedance of the short-term limit. In retrospect, this behavior is not at all unreasonable, since a component whose amplitude is 1 need only increase to 2 to be recognized as a 6-db change in level; and if during the next 4-minute measuring interval it increases to 3 or 4, both the 10-db long-term limit and the 6-db short-term limit is exceeded and consequently a shutdown command is generated. All of the data processing was done using 16-bit integer arithmetic (2's complement), so these low-amplitude components are subject to large roundoff errors, and it is impossible to distinguish between actual increases in signal levels and apparent increases due to numerical roundoff. Since the comparison checks and test program was intended to stop testing only when an abnormally large long-term trend was encountered and/or when an abnormally large parameter rate of change occurred, the original comparison decision had to be modified. It was decided not to compare amplitude signals which were below an arbitrary threshold of 32. This modification did prevent premature shutdown from occurring due to low-amplitude fluctuations, but unfortunately, because of the particular manner in which the threshold was implemented, it also prevented the shutdown from occurring when gearbox BB failed catastrophically. As discussed in the section on "Experimental Results", the data from this gearbox was unusable for prognostic analysis due to undetected sensor detachment.

DATA ANALYSIS - THEORY AND PROCEDURES

This section describes the data reduction procedures used to analyze the data collected under this contract. Five different gearboxes were tested for a cumulative test period of over 4600 hours. Each sensor was sampled every 4 minutes. These samples were statistically reduced by the on-line computer via the procedures described below. The reduced samples were stored on nine-track IBM compatible magnetic tape, which were later edited and put into the CDC Library for trend analysis.

Although the data base contains sensor samples taken every 4 minutes, only the hourly sensor points were used for the trending analysis discussed in the section on "Experimental Results" and in Appendix A.

VIBRATION DATA REDUCTION

Vibration measurements for this contract were taken from three low-frequency accelerometers. The locations of these accelerometers are shown in Figures 10 and 11. The frequency range of analysis was DC to 10 kHz. This range was divided into 128 frequency bins which were 78.125 Hz wide.

Each accelerometer signal was low-pass filtered to 10 kHz by a sixth-order Butterworth filter before being digitized by a 10-bit analog-to-digital converter. The resulting digital signals were pre-processed in the following manner.

First the discrete Fourier transform (DFT) of each signal was computed. The DFT converts time domain signals into frequency domain spectra. The DFT is defined as

$$F(k) = \sum_{i=0}^{N-1} [W(i) \cdot f(i)] \exp [-j(2\pi ik/N)], \quad k = 0, \dots, N-1 \quad (3)$$

where

$F(k)$ = k th Fourier transform coefficient

k = frequency bin index

N = transform size

$f(i)$ = i th time domain signal sample

i = time signal sample index

$$W(i) = \text{Hamming weighting function} \\ = 0.54 - 0.46 \cos [2\pi i/(N - 1)]$$

The DFT was computed using the "fast" Fourier transform (FFT) technique.

The purpose of Hamming weighting the time domain vibration signal prior to computing the DFT is to reduce the sidelobe structure of the transform caused by abrupt time domain transitions associated with transforming over a finite time interval. Without the Hamming weighting, the sidelobes would obscure low-amplitude transform coefficients.

Figure 29a shows a finite-length time domain sine wave without Hamming weighting and the magnitude of its DFT. Note the high sidelobe levels (down from the main lobe by only 13.2 dB). Figure 29b shows the same signal with Hamming weighting. Here the sidelobes have been reduced to 42 dB.

Next the power spectral density (PSD) function of each signal was computed. The PSD is obtained from the DFT by the relation

$$P(k) = |F(k)|^2 = F(k) \cdot F(k)^*, \quad k=0, 1, \dots, N/2-1 \quad (4)$$

where

$P(k)$ = power spectral density in frequency bin k

$F(k)^*$ = complex conjugate of $F(k)$

The vibration signals were sampled at a 20-kHz rate, and the sample duration was 12.8 ms, which corresponds to a DFT size, N , of 256. A short-term PSD was computed over this interval. The computation time by the computer was about 200 ms.

To increase the statistical accuracy and our confidence level that the true PSD values were being calculated, we ensemble averaged 128 short-term PSD's to form a statistically averaged PSD. The sample standard deviation of the ensembled PSD's approaches the true PSD value as the ensemble becomes larger. The selection of the ensemble size is a trade-off between the need for statistical accuracy and reasonable computation time. Since the relative statistical accuracy

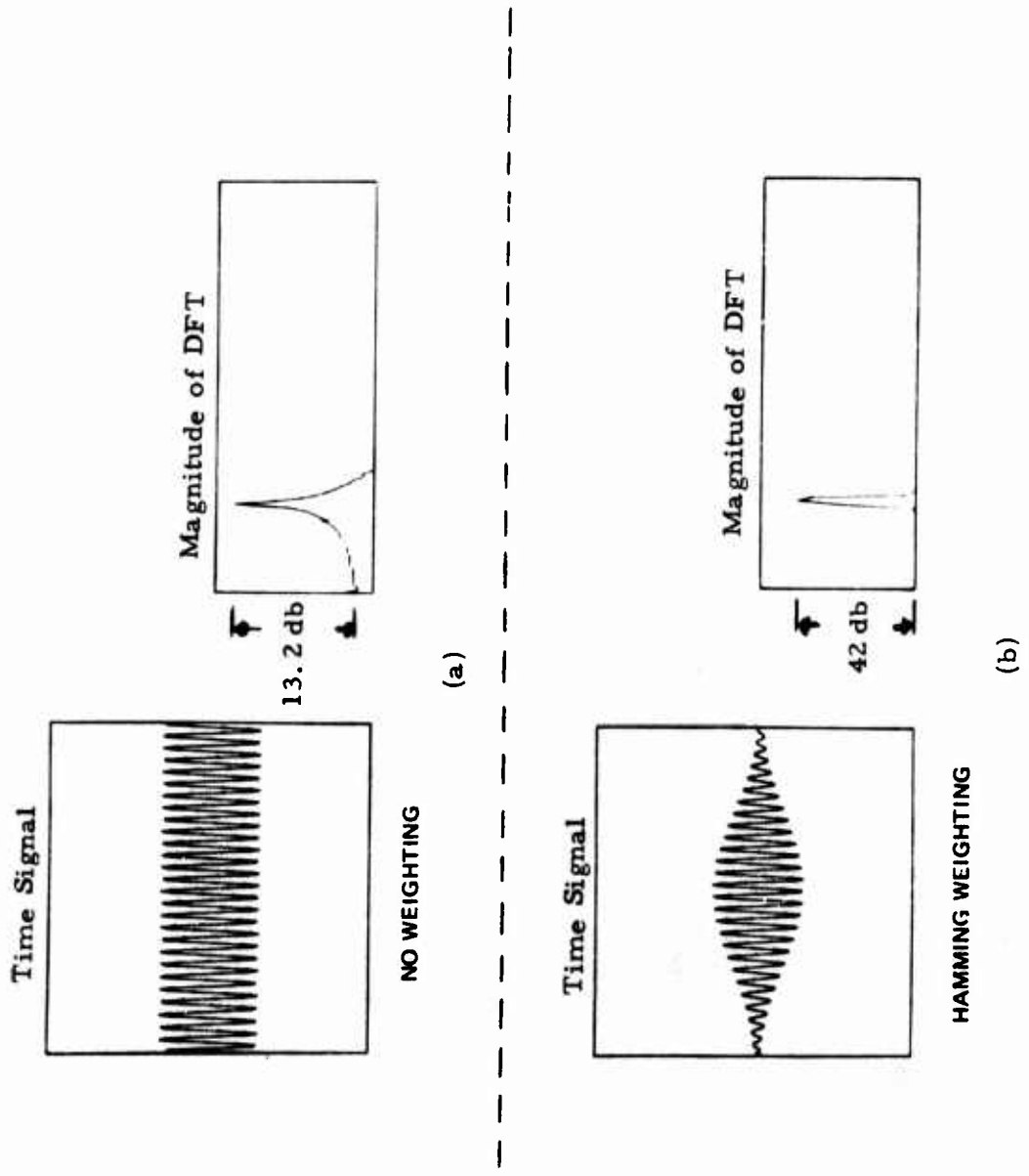


Figure 29. Example of the Reduction of DFT Sidelobe Structure by Hamming Weighting an Input Time Domain Signal.

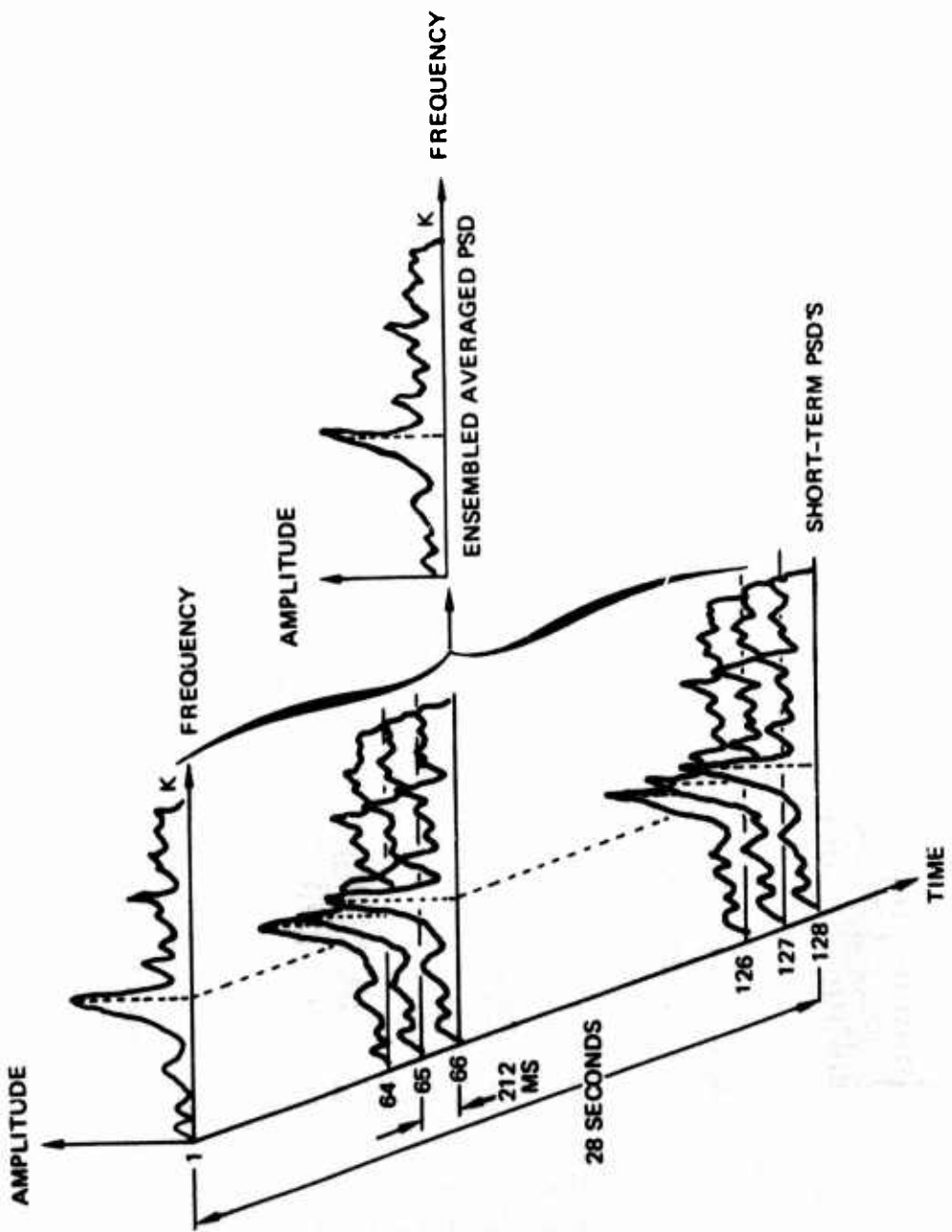


Figure 30. Example of Ensemble Averaging of PSD Functions.

increases in proportion to the square root of the sample size, a sample size of 128 yields a statistical accuracy of 0.5 dB and a computation time of 28 seconds. Figure 30 shows how the 128 PSD's are ensemble averaged to obtain the statistically averaged PSD, which is then stored as reduced data on magnetic tape for off-line processing.

STATISTICAL ANALYSIS OF VIBRATION DATA

As mentioned at the beginning of this section, the original data base was edited to utilize only the hourly sample points for further statistical processing. An hourly sample point is defined as the ensemble PSD taken during the 4-minute interval which occurred at the beginning of an exact hour of testing. This edited data was placed in a Control Data "Cybernet" library, where it could be accessed by the CDC 6600 scientific computer.

The statistical processing performed on the edited data was designed to identify those frequency bins which showed a statistically significant growth (or decay) over the test period.

The first phase of the statistical processing involved the computation of the means and standard deviations of the edited data in groups of 50 hours. The mean is computed using equation (5), and the standard deviation is computed using equation (6).

$$M_\ell(k) = \frac{1}{T+1} \sum_{t=a}^{t=b} P_t(k) \quad (5)$$

$$S_\ell(k) = \sqrt{\left[\frac{1}{T+1} \sum_{t=a}^{t=b} P_t^2(k) - M_\ell^2(k) \right] \left[\frac{T}{T-1} \right]} \quad (6)$$

where

$M_\ell(k)$ = ℓ_{th} mean of $P_t(k)$ over T hours

$S_\ell(k)$ = ℓ_{th} standard deviation of $P_t(k)$ over T hours

k = frequency bin index

t = time index for hourly PSD data

$P_t(k)$ = k_{th} PSD coefficient at hour t

T = time interval over which mean and standard deviation are computed (T = 50 hours).
a = starting time in hours
b = stopping time in hours = a + T
l = reference time index for means and variances of PSD data = (a+b)/2

For $T > 30$ hours, there is practically no difference between the standard deviation of the total population and the standard deviation of a sample drawn from the population. To ensure that this condition was met, we used $T = 50$ hours in this analysis.

The means and standard deviations of the different sensor PSD data were computed at the following intervals: for those sensors which provided less than 1000 hours of usable test data, the computation was done at 50-hour intervals; for those which provided over 1000 hours of usable test data, the computation was done at 100-hour intervals.

Figure 31 is an example of the results obtained from calculating the group PSD means and standard deviations for different groups at different times during a test period. The example in the figure shows the first 50-hour group PSD mean which is computed using the 50 hourly ensembled PSD's obtained for test hours 26 to 75. This computation is performed for each subsequent group of 50 hourly PSD's throughout the test period for each gearbox. The only exception to this method of calculating 50-hour group PSD means was the calculation of the baseline group PSD mean against which all 50-hour group PSD means were compared for the Z-score statistical test described in the following paragraphs. The baseline group PSD mean is called the 25-hour group PSD mean and was computed using the hourly ensembled PSD's obtained for test hours 1 to 50.

The second phase of the statistical analysis involved the determination of statistically significant differences between the mean and standard deviation of the reference group (25-hour point) and each subsequent 50-hour group. The methods of statistical decision theory were applied to the mean and standard deviation statistics to identify those differences which might indicate that the mechanical condition of the gearbox is changing.

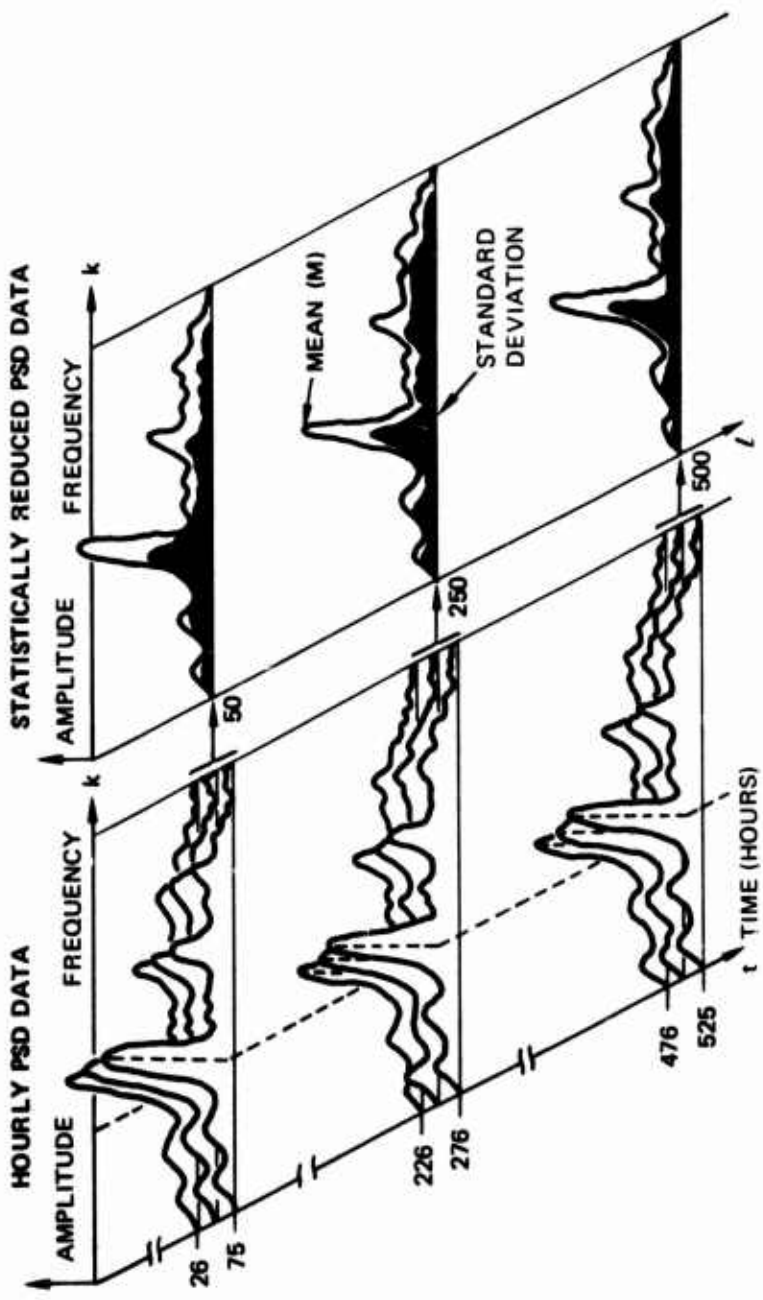


Figure 31. Structure of PSD Mean - Standard Deviation Data Base.

In order to develop any trending technique, it must be assumed that the sampled data does change in some manner with time and that this change is statistically significant.

In this analysis the following basic assumption is made:

As the mechanical condition of an operating gearbox with an incipient failure continues to degrade in time toward catastrophic failure, the group PSD means $M_l(k)$, $l = 50, 100, 150, \dots$ (from equation 6) will differ significantly from an earlier reference group PSD mean (M_{25}) at certain frequency bins, k .

A Z-score (or linear discriminant) statistical test was used to identify those frequency bins for which the differences in group PSD means were statistically significant. The derivation of the Z-score test is rather involved, but is included for completeness in Appendix A.

Figure 32 is a typical Z-score plot for a 90° gearbox which compares the data in one 50-hour PSD group with the data in the 25-hour baseline reference group. A Z-score magnitude of 4.3 or greater for a particular frequency bin means that 95% of the time we can be 95% confident that the mean value of the current data in the selected frequency bin is significantly different from the mean value of the data in the corresponding reference frequency bin. It can be seen that in example Figure 32, none of the frequency bins meet the Z-score criteria. This was the case for much of the data analyzed. When the Z-score test failed to identify appropriate frequency bins to use, frequency bins with the largest Z-scores were selected for the trend analysis.

POLYNOMIAL TRENDING

Once we have identified the frequency bins in the PSD data that meet the Z-score criteria for change, we use these frequencies from each hourly ensembled PSD for our trend analysis. The objective of conducting a trend analysis on the vibration data is to determine in a quantitative manner the time history of the data in each frequency bin over the test period of the gearbox. It is hoped that trends found in this data can be correlated with gearbox wear as determined by other sensors or post-test wear measurements. Since an enormous amount of data was collected in this program, we selected data from ensembled PSD's taken every 5 to 10 hours for use in the trend analysis. After the frequency bins of interest were determined and the data in these bins plotted with time, second- and third-degree polynomial curves were fitted to the data on a minimum mean-square error

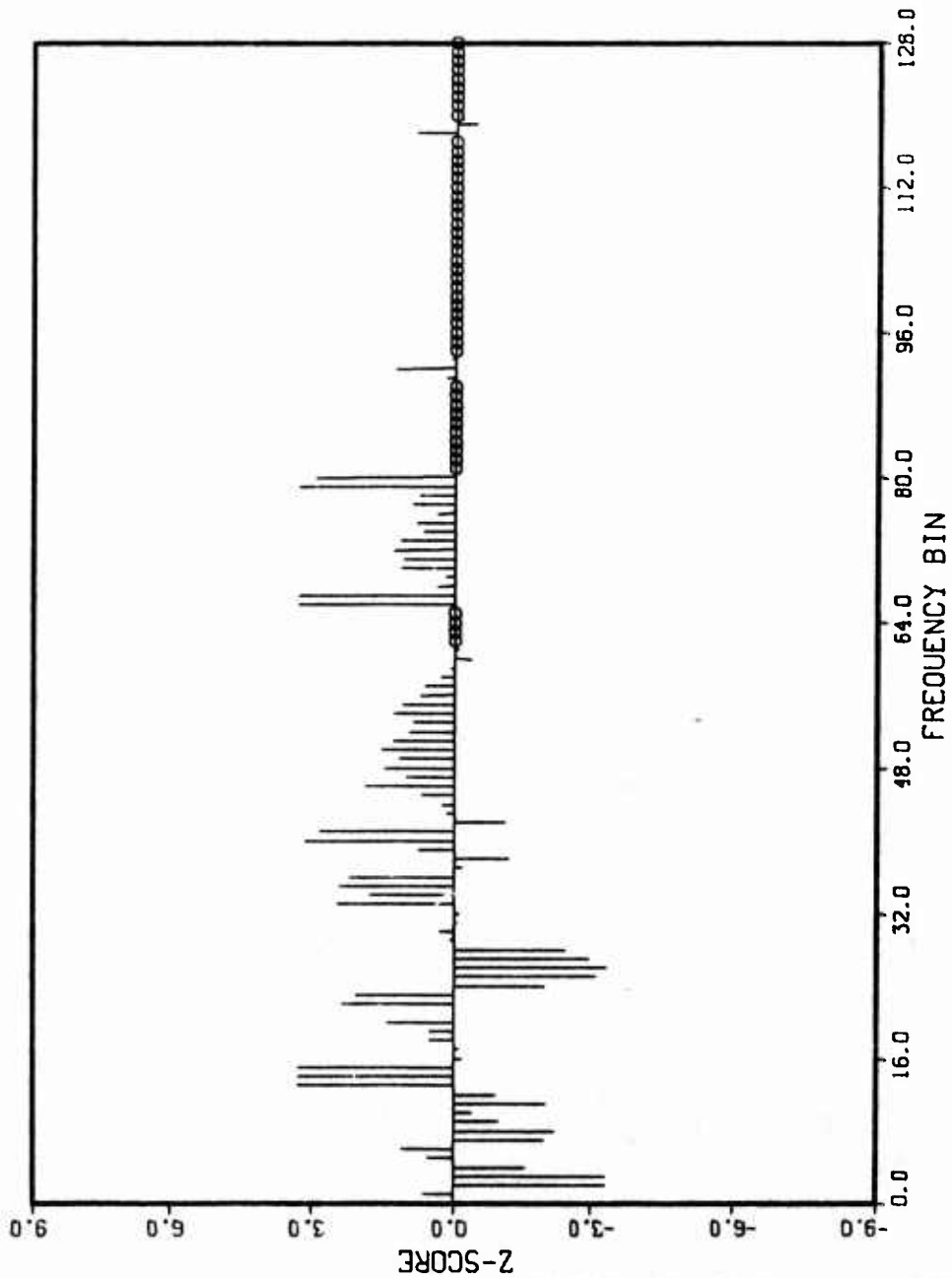


Figure 32. Typical Z-Score Linear Discriminant Plot.

$$Z = \frac{\text{Mean (Ref)} - \text{Mean (Test)}}{\sqrt{S_r^2 + S_T^2}}$$

$S = \text{Std. Dev.}$

(least-squares) basis. These smooth trend curves are used to determine whether or not there is any long-term trend to the data irrespective of the fact that the data would probably exhibit short-term deviations from the long-term trend line. A standard polynomial curve-fitting procedure was used on the data collected in this program. Let $P_m(k)$ be the value of the PSD data in the selected frequency bin k at the plotting times $m = 0, 10, \dots, M$ hours of a gearbox test period. We wish to match a third-degree polynomial $y_3(m)$ to this data on a mean-square error basis. Then

$$y_3(m) = a_0 + a_1 m + a_2 m^2 + a_3 m^3, \text{ for } 0 \leq m \leq M \quad (7)$$

The mean-square error criteria is defined as

$$Y_k(a_0, a_1, a_2, a_3) = \sum_{m=0, 10, \dots}^M [P_m(k) - y_3(m)]^2 \quad (8)$$

For Y_k to be a minimum, the partial derivative of Y_k with respect to the a 's must be zero.

$$\frac{\partial Y_k}{\partial a_\ell} = -2 \sum_{m=0, 10, \dots}^M [P_m(k) - y_3(m)] m^\ell = 0 \text{ for } \ell = 0, 1, 2, 3. \quad (9)$$

This reduces to

$$\sum_{m=0, 10, \dots}^M P_m(k) m^\ell = a_0 \sum_{m=0, 10, \dots}^M m^\ell + a_1 \sum_{m=0, 10, \dots}^M m^{\ell+1} \quad (10)$$

$$+ a_2 \sum_{m=0, 10, \dots}^M m^{\ell+2} + a_3 \sum_{m=0, 10, \dots}^M m^{\ell+3}$$

This represents four independent equations (ℓ 's) in four unknowns (a 's) and can be solved by standard techniques. Once the a 's are known, the initial equation $y_3(m)$ can be superposed on the data from frequency bin k .

The results of polynomial trending as applied to the gearbox are discussed in the next section on "Exponential Trending" and in the section on "Experimental Results".

EXPONENTIAL TRENDING

Exponential trending is another approach studied under this contract. If we assume that the rate of change of a fault in a gearbox component at a particular time is directly proportional to the magnitude or extent of the fault at that time, then as the fault changes it produces an exponentially increasing time function which has a magnitude and time constant determined by the gearbox structure, extent of initial fault, gearbox load, etc.

Though vibration signals caused by a fault will be modified by the mechanical structure of the gearbox, some of the vibration frequencies generated should be more or less directly related to the extent of the fault and also increase exponentially with time. This behavior was observed by Northrop during the UH-1 Test Bed Program*. Under this contract, a UH-1 helicopter transmission was implanted with a defective (innermost) input triplex quill bearing and run for some 30 hours in a test cell at full load. At the start of the test, the defective bearing had a (man-made) 1-inch spalled area on the outer race. Figure 33 shows the wideband (100 Hz to 5 kHz) RMS vibration level of the input longitudinal accelerometer as a function of test time and the parameters needed to fit an exponential curve to the data.

After 28 hours of testing, bronze chips were found in the chip detector and the oil temperature increased 8 degrees. The bronze chips were part of the bearing cage. After 30 hours of testing, the transmission was torn down and the implanted bearing was found to have a 2-inch spalled area on the outer race and a 1/8-inch spall on one ball, and the bearing cage was fractured in 3 places. During the first 25 hours of testing, the overall vibration level doubled every 5 hours. The vibration level grew exponentially until the bearing cage fractured, at which time the overall vibration level flattened out (saturation).

*Final Report Contract DAAJ01-70-C-0828(P3L) AVSCOM UH-1 Test Bed Program. Final Report Northrop Corporation, Electronic Division, December 1971.

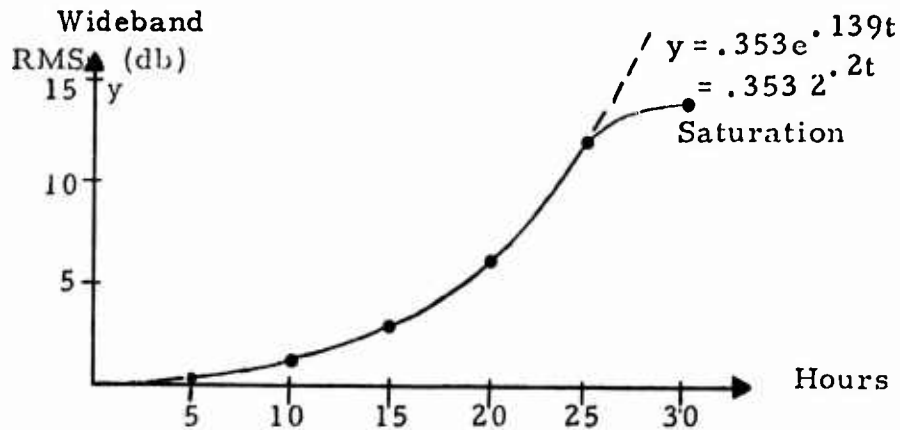


Figure 33. Wideband (100 Hz to 5 kHz) RMS Vibration Level of Input Longitudinal Accelerometer (UH-1 Helicopter Transmission).

Although this was an isolated example, it was sufficiently encouraging for us to attempt to apply exponential trending to the gearbox vibration data obtained on this contract.

The Z-Score criterion was used to select the PSD frequency bins to be used for exponential trending. If none of the data met this criterion, those frequency bins with the largest Z-Score were selected. In exponential curve fitting of the PSD data, it is assumed that the data points can be represented by a single exponential

$$P_m(k) = A \exp[y_3(m)], \quad m = 0, 10, \dots M \quad (11)$$

where

$$y_3(m) = a_1 m + a_2 m^2 + a_3 m^3$$

and A is some scalar constant.

To find the a 's and A , we first take the natural logarithm of each side of the equation to obtain

$$\ln[P_m(k)] = \ln(A) + y_3(m) . \quad (12)$$

Then we form the error criterion

$$X_k(A, a_1, a_2, a_3) = \sum_{m=0,10,\dots}^M \ln[P_m(k)] - \ln[A] - y_3(m) \quad (13)$$

To find the least-mean-square error, we take the partial derivatives of this error criterion and set them equal to zero as was done for polynomial curve fitting. The resulting equations are

$$\begin{aligned}
 \sum_{m=0, 10, \dots}^M \ln \left[P_m(k) \right] m^l &= \ln(A) \sum_{m=0, 10, \dots}^M m^l + a_1 \sum_{m=0, 10, \dots}^M m^{l+1} + \\
 a_2 \sum_{m=0, 10, \dots}^M m^{l+2} + a_3 \sum_{m=0, 10, \dots}^M m^{l+3}, \\
 l &= 0, 1, 2, 3 \dots
 \end{aligned} \tag{14}$$

This again represents four equations (l 's) in four unknowns (a's, A) which can be solved for the unknowns. If $a_1 \gg a_2, a_3$, then $P_m(k)$ should be essentially exponential in nature.

The results of applying long-term exponential and polynomial curve fitting to the data collected in this program were not particularly encouraging. The only gearbox which reached the same stage of failure as the example given for the UH-1 helicopter transmission in Figure 33 was gearbox BB, and no usable vibration data was obtained from this gearbox due to instrumentation failures.

Figures 34, 35 and 36 are rare examples of data which appeared to be long-term trendable with curve fitting. Unfortunately, Figures 37 and 38 are much more typical of the results obtained. The gearbox vibration data is characterized by short-term oscillations and amplitude discontinuities. These discontinuities are themselves characterized by a short-term (50 to 100 hours) exponentially increasing vibration level followed by very rapid (less than an hour) decrease in amplitude. An example of this behavior can be seen in Figure 35 between hours 200 and 280.

Because of the short-term instabilities and oscillatory behavior of the gearbox vibration data, lower order polynomials cannot be fitted to the data. Polynomial fitting can be used on small intervals of the data, but cannot be applied to the data outside this interval.

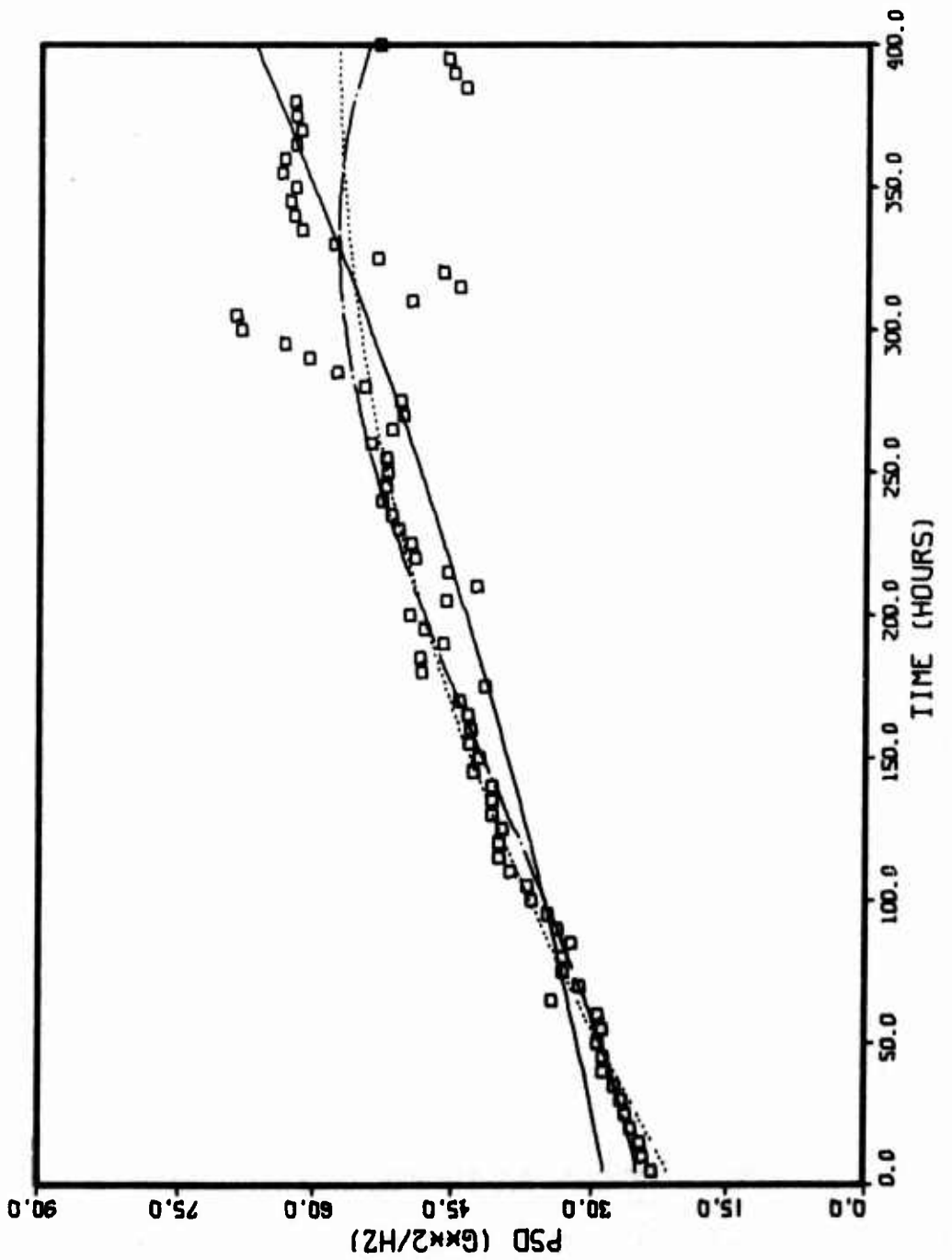


Figure 34. Trending of PSD Vibration Data, Bad Bearing 2, Sensor 4, Frequency 1016 Hz.
Data Point □ Quadratic Fit . . . Cubic Fit - - - Exponential Fit —

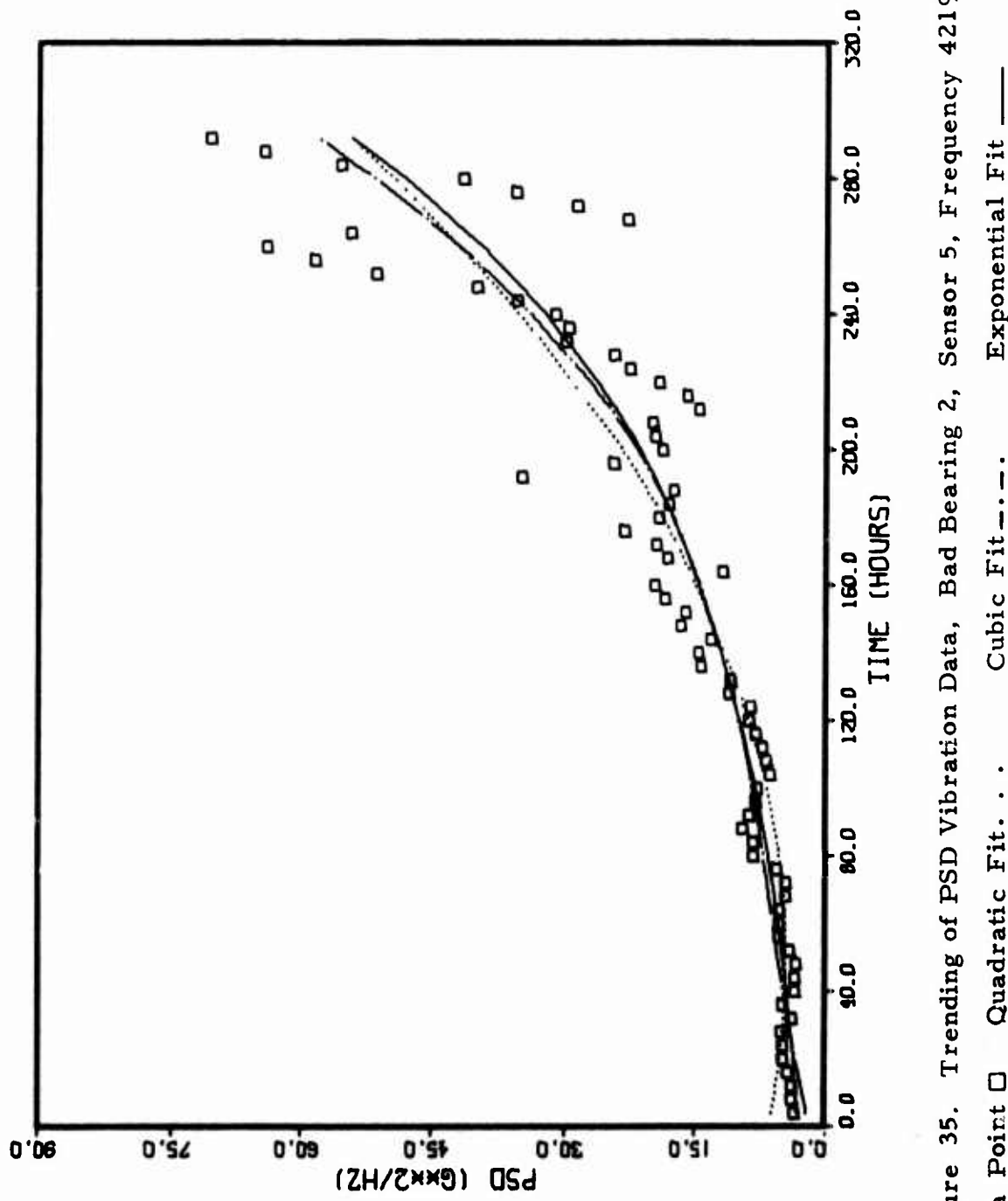


Figure 35. Trending of PSD Vibration Data, Bad Bearing 2, Sensor 5, Frequency 4219 Hz.
Data Point □ Quadratic Fit . . . Cubic Fit - - - Exponential Fit —

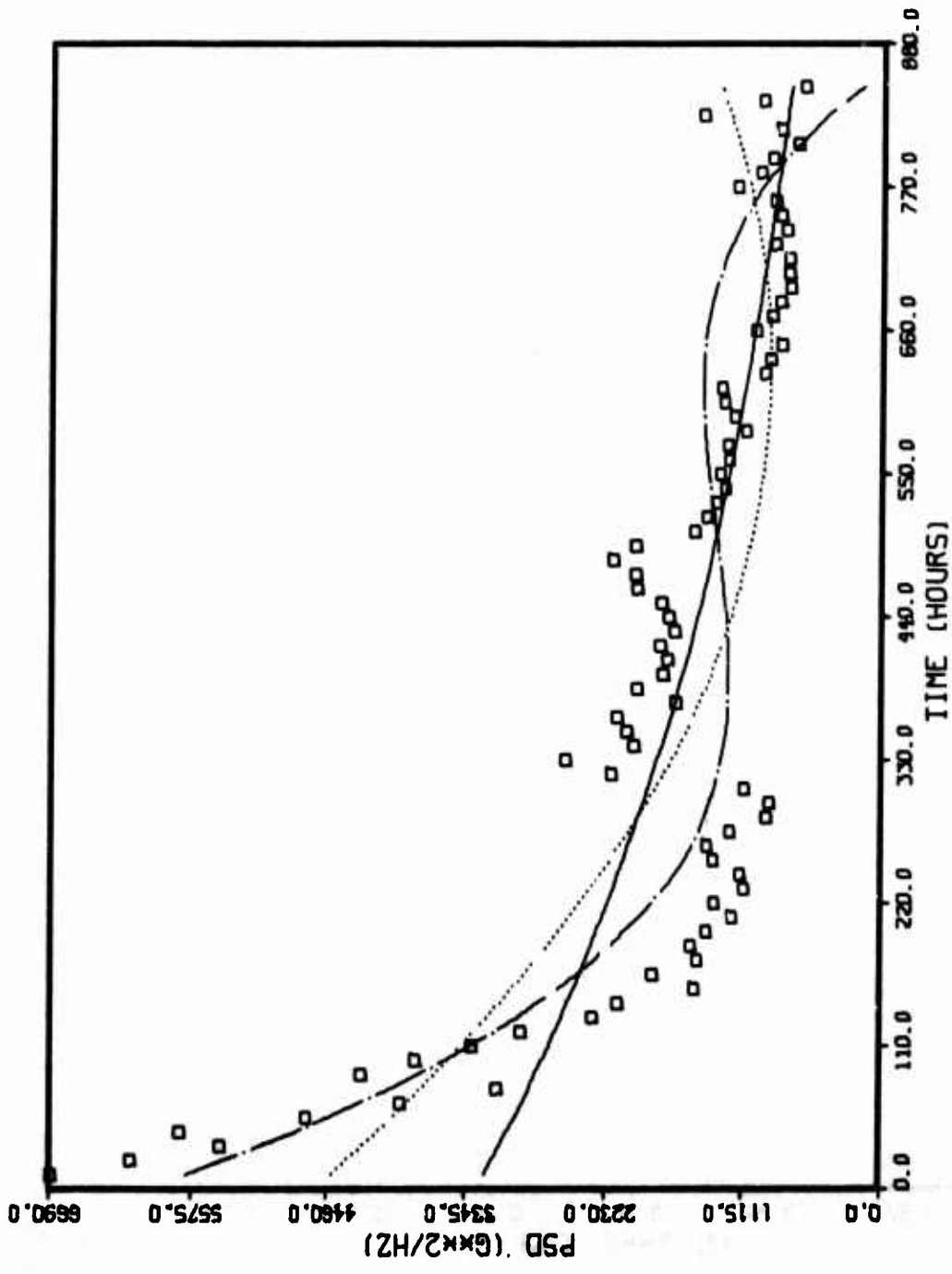


Figure 36. Trending of PSD Vibration Data, Bad Gear, Sensor 5, Frequency 1094 Hz.

Data Point	□	Quadratic Fit	...
		Cubic Fit	---
		Exponential Fit	—

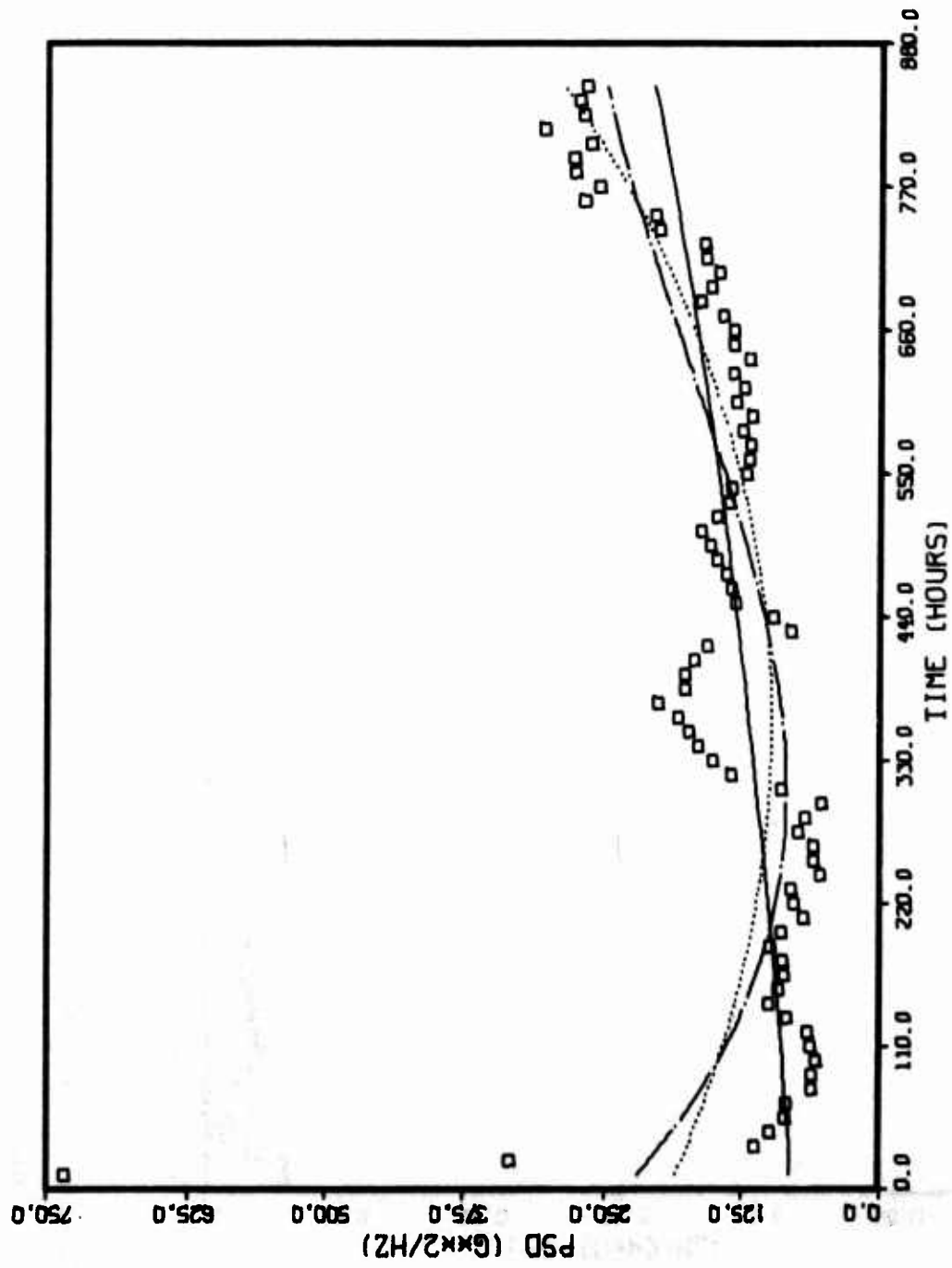


Figure 37. Trending of PSD Vibration Data, Bad Gear, Sensor 5, Frequency 2031 Hz.
Data Point \square Quadratic Fit . . . Cubic Fit ---. Exponential Fit —

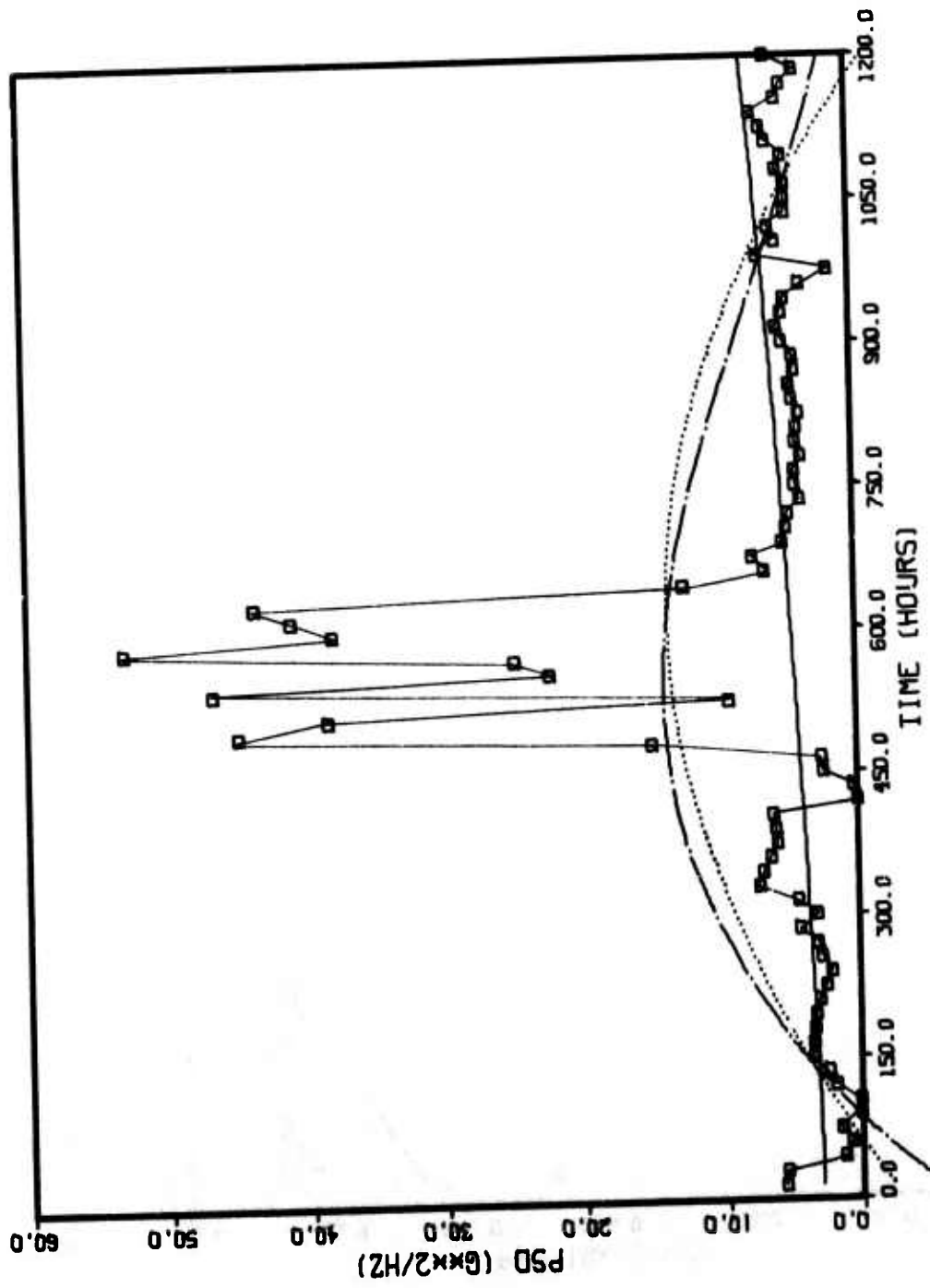


Figure 38. Trending of PSD Vibration Data, High Time, Sensor 3, Frequency 6250 Hz.
 Data Point \square Quadratic Fit . . . Cubic Fit - - - Exponential Fit —

Some combination of different data reduction, processing and analysis techniques and frequency bin selection might result in more meaningful trending of gearbox vibration data. However, it is considered that with the present stage of wear in the gearboxes tested and the observed short-term instabilities in the vibration data, it is not possible to predict the long-term behavior of the gearboxes using exponential or polynomial curve fitting of data selected from a single frequency bin.

Due to this observation on our trending results, we studied a third approach: trending by least-mean-square predictions.

TRENDING BY LEAST-MEAN-SQUARE PREDICTION

The least-mean-square (LMS) prediction technique was developed in order to account for short-term oscillations in the data and to estimate the data outside the fit interval based on data statistics within the fit interval. The LMS prediction technique as developed in Appendix I is given below.

Given a PSD signal $s(t)$ which is known for $t > 0$, the optimum prediction of $s(t)$ at time $t + \lambda$, where $0 < \lambda < t$, is given by

$$s(t+\lambda) = a_0 s(t) + a_1 s'(t) \quad (15)$$

where

$$a_0 = \frac{R(\lambda)}{R(0)} \quad (16)$$

$$a_1 = \frac{R'(\lambda)}{R''(0)} \quad (17)$$

and

$$R(\lambda) = \frac{1}{t-\lambda} \int_0^{t-\lambda} s(t+\lambda) s(t) dt, \quad 0 < t < T \quad (18)$$

is the autocorrelation function of $s(t)$, for finite t .

The prediction is optimum in the sense that the mean-square error between $s(t+\lambda)$ and $a_0 s(t) + a_1 s'(t)$ is a minimum for a stationary and ergodic process (stationarity and ergodicity are discussed in Appendix A).

For small prediction intervals λ , it is shown in Appendix A that the LMS prediction, $s(t+\lambda)$, is identical to the Taylor expansion of the data signal. However, for prediction intervals which are not small, the LMS prediction differs from the Taylor prediction in that the LMS weights the derivatives of the data signal by the past data values whereas the Taylor expansion coefficients are a function only of λ and cannot account for the past behavior of the signal. Consequently, the LMS prediction technique will always be more accurate than the Taylor prediction (for the same number of approximating derivatives) when λ is large, so long as the data remains stationary and ergodic.

In comparing the LMS prediction technique to the polynomial trending technique, there are two important points to consider. The first and most important is that there is no well-developed theory, such as exists for stationary random processes, which allows one to confidently predict future data values by polynomial extrapolation. Consequently, polynomial estimators are not guaranteed to give the least-mean-square prediction error for well-behaved physical processes, as does the LMS prediction technique. The second point is that polynomials in general are not efficient approximators of periodic phenomena; i.e., many polynomial terms are required to represent rapidly changing periodic signals. In situations where the PSD data has a large periodic component, polynomial estimation of the trend will yield large estimation errors.

We have shown that the LMS prediction technique gives the best estimate of what $s(t+\lambda)$ should be in the sense of minimum mean-square prediction error using all past $s(t)$ data up to time t and assuming that the gearbox operating condition has not appreciably changed (stationarity condition not violated).

As the gearbox condition deteriorates appreciably, the LMS technique cannot be used with confidence since the process is nonstationary. However, a difference between the actual $s(t+\lambda)$ values and the predicted $s(t+\lambda)$ values based on a continuation of the stationary process after time t can be interpreted as meaning that a significant change in gearbox operating condition is taking place. This change will also be reflected in the Z-score, which is a measure of how much the statistics have actually changed. We can bring into play nonstationary trend analysis techniques (e.g., mean and standard deviation trend test based on reverse arrangements⁵) to determine the important statistics and duration of the nonstationary trend. Such nonstationary trends can be isolated in this way for a collection of gearboxes undergoing incipient failure. The set of trend data can be analyzed to establish the existence of patterns involving mean and

standard deviation statistics and the relationships of one trend to another, and thereby attempt to predict what nonstationary trends will occur and when. The determination and characterization of nonstationary gearbox trends over a suitable collection of gearboxes using the LMS prediction technique and elementary pattern classification methods were beyond the scope of this contract, but its usefulness should be studied in future efforts.

The LMS algorithm developed and applied to a limited data set on this contract is a weighting of the signal and its first derivative at time t based on the autocorrelation function and its derivatives of the known data. As such, it is sensitive to errors in calculating the derivatives of the signal at time t , and errors in derivative computations are especially troublesome when the signal data is noisy (measurement noise, noise due to short-term changes in environment, etc.) and discrete in nature. To overcome this noise sensitivity, there exists a different formulation of the LMS prediction algorithm which does not involve computing derivatives of the autocorrelation function. In mathematical terms, the new algorithm solves the following problem: Predict $s(t+\lambda)$ in terms of a linear combination of $s(t_0)$, $s(t_1)$, ---, $s(t)$, where $t_0 < t_1 < \dots < t$, with minimum mean-square error. The solution of this problem will be weights which depend only on the autocorrelation function itself and not on its derivatives, and should be more accurate than the above LMS algorithm if more than three weights are used. This formulation of the LMS prediction algorithm is particularly well-suited to implementation as a variable weight tapped delayline matched filter. Because of funding and time considerations, this formulation has not been tried on experimental data, but in view of the encouraging results obtained in applying the previous LMS formulation (Equation 15), this formulation should be given prime consideration in any future analytical effort devoted to solving the prognostic problem.

The LMS technique based on the stationary integration process was applied to a few samples of gearbox data. The results obtained from analyzing one frequency bin from the vibration data obtained from gearbox BB3 is shown in Figure 39. Note that though both time intervals contain short-term instabilities, the LMS prediction of the signal in the second time interval based on the data obtained in the first interval was within 3 db of the actual data values. A 3-db change is not usually considered to be significant. Additional results using the LMS analysis technique are given in the next section, "Experimental Results".

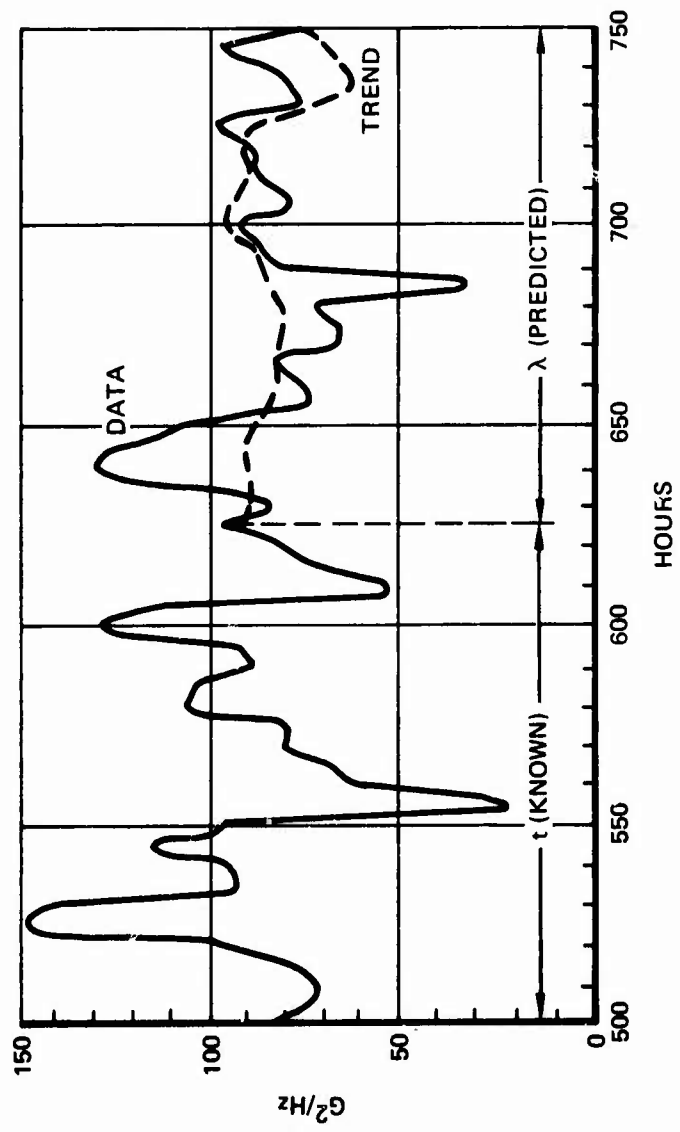


Figure 39. Prognostic Trend of BB3 Gearbox, Sensor 4, Bin 53.

EXPERIMENTAL RESULTS

This section discusses the experimental results obtained for each gearbox tested and how each sensor signal was trended. Five gearboxes were tested for a total of 4743 hours. Table III summarizes the data obtained for each gearbox. Due to instrumentation problems, not all of the data collected could be considered usable for trend analysis.

TABLE III. SUMMARY OF DATA COLLECTED

Gearbox	No. Test Hours	Trendable Hours
High Time (HT)	1438	1277
Bad Bearing (BB)	166	0
Bad Gear (BG)	1031	951
Bad Bearing Two (BBT)	1022	1022
Bad Bearing Three (BB3)	1086	1086
Totals	4743	4336

The gearboxes that were tested were hand-selected from those about to undergo repair at ARADMAC in Corpus Christi, Texas. These gearboxes were selected for specific incipient failures, with the intent of gaining insight into how sensor signals relate to various mechanical conditions. Since this program emphasized prognostics as opposed to diagnostics, man-made incipient failures would not be suitable for testing. Only those gearboxes which had reached incipient failure as a result of actual field use were used in this effort. Because of this, the data collected in the test cell represents information on how mechanical components deteriorate under normal operating conditions due to incipient failure.

Three different types of incipient failures were considered: high operational time, bad bearing, and bad gear. Selecting gearboxes with

the desired incipient failure is not a simple task. Since very little work has been done in the area of prognosis, it is difficult to determine just how incipient the failure should be in order to minimize test time, but still be able to monitor the component as it degrades from incipient failure to failure and on to catastrophic failure. If a gearbox with too early an incipient failure is selected, several thousand hours of testing may be required before the component degrades sufficiently to be considered failed. If a gearbox is chosen with an incipient failure bordering on complete failure, too little test time is available before the gearbox fails catastrophically to obtain good prognostic trending data. The data obtained from the early failure of gearbox BB could be used only for diagnostics, which is not the primary objective of this investigation.

Another difficulty in selecting the proper gearboxes for testing was the inability to make a quantitative evaluation of the mechanical condition of the gearbox components during the process of selecting the test gearboxes at ARADMAC. The reason for this is that ARADMAC is primarily a production repair depot and not a research center, so the gearboxes had to be selected on a noninterference basis. This resulted in the selection of gearboxes on a best-guess basis as to the stage of incipient failure in each gearbox chosen. Our inability to obtain quantitative information on each gearbox before it was selected, coupled with the fact that there were usually less than 50 gearboxes available for inspection at any one time, considerably reduced the odds for obtaining test gearboxes which were in an optimized stage of incipient failure for the test program. All of the gearboxes selected had completed the time between overhauls (TBO) of 1200 hours specified for this type of gearbox, and none of the gearboxes showed any signs of catastrophic failure (e.g., spalling of ball and roller bearings or chipped or missing gear teeth). Our selection of the bad gear (BG) gearbox proved to be less than optimum since the gear had already failed, though not catastrophically, and our selection of bad bearing (BB) gearbox resulted in catastrophic failure in 166 test hours.

In general, the quality of the data collected is good, with the exception of the vibration data on BB. The advance state of wear of this gearbox resulted in initially high vibration levels which caused the accelerometer mounting pads to detach from the gearbox at an early stage in the testing. The limited amount of vibration data obtained from this gearbox was not usable for analytical purposes. Most of the prognostic value of the oil analysis data was lost due to improper collection procedures and the attachment of the external oil debris monitors. A more detailed discussion of these problems is given in

the section on "Sensors and Sensor Locations" earlier in this report.

As discussed in this section, it was originally intended that all data be collected automatically. As the testing program progressed, the shock pulse analyzer became available and was added to the test cell. This sensor required manual tabulation and plotting of the shock emission profiles on a daily basis. Due to funding constraints, shock pulse data and oil samples were not taken on holidays and weekends, when the test cell ran continuously and unattended.

HIGH TIME (HT) GEARBOX TESTS

The high time gearbox (HT) was the first gearbox to be tested. The total cumulative test time of 1438 hours was broken up into two test intervals. The first test interval lasted 861 hours and yielded 715 hours of trendable data. Of the 146 hours of nontrendable data, the first 50 hours of test were taken at different operating conditions due to minor test cell irregularities (slipping belts, relief valve adjustment slippage, etc.). Although not suitable for trending, these test hours did constitute a "green run." The remaining 96 hours occurred at various times throughout the testing sequence and were attributed to test cell controller malfunctions and operator error. The second test sequence lasted 577 hours and yielded 562 hours of trendable data. The 15 hours of data which was not trendable was due to accidental erasure of the data during the following day's test.

Mechanical Condition of HT Gearbox

The HT gearbox was inspected three times during the program, and a detailed account of the inspection results is given in Appendix B.

The first inspection was conducted prior to testing and served to document the initial condition of the gearbox. Visual examination of the ball and roller bearings indicated that they were all in good condition, showing minor pits and dents with only light abrasive wear. Dynamic noise tests verified that there was negligible to light wear with light local damage.

At the end of the first test interval (861 hours), another gearbox inspection was performed. Visual inspection of the ball and roller bearings showed increased wear in the output duplex ball bearing and a significant deterioration in the condition of the input roller bearing. Noise testing of the ball bearings shows moderate wear with light local damage.

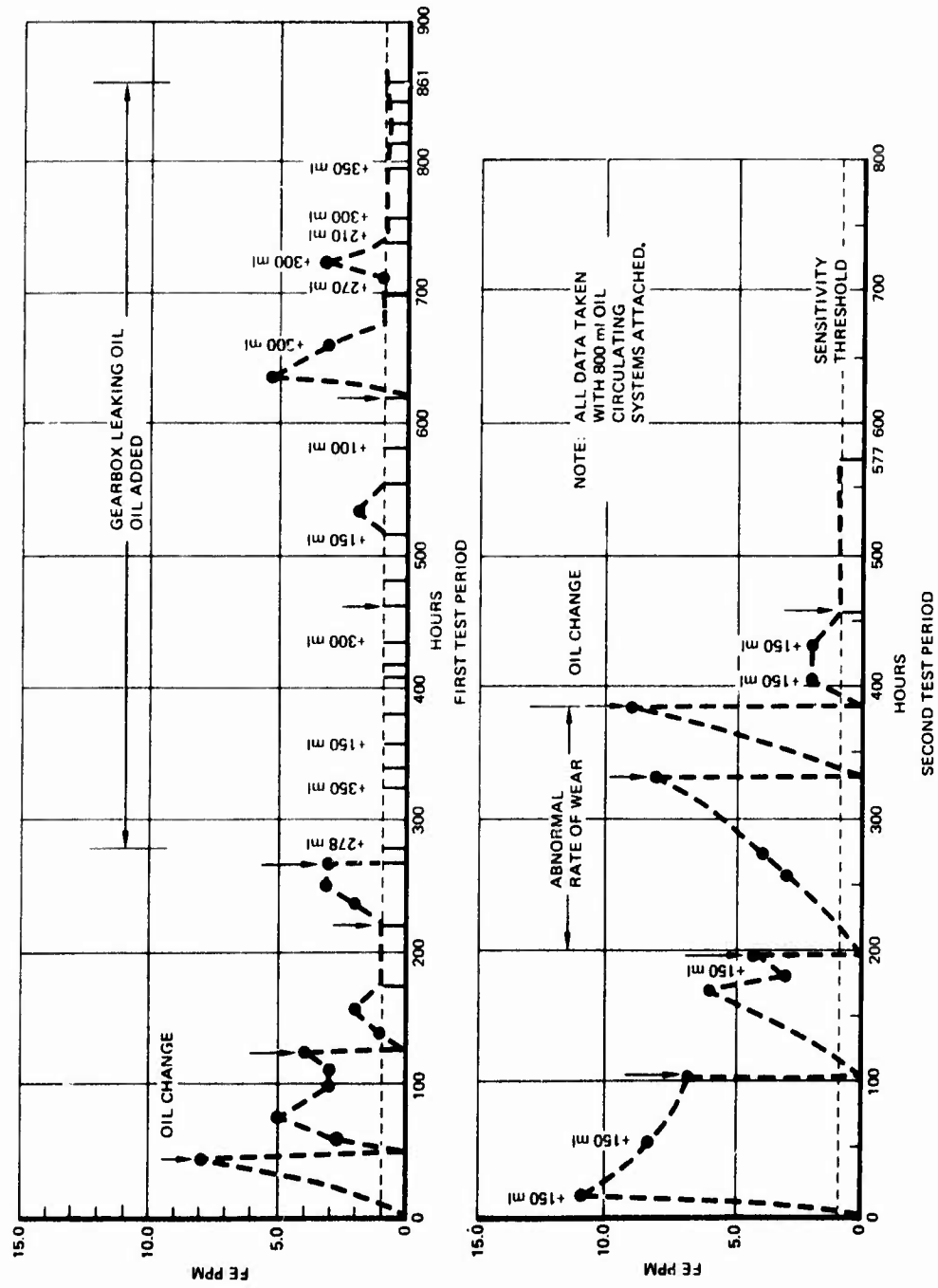


Figure 40. Summary of HT Gearbox SOA.

The final gearbox examination occurred at the end of the second test interval (577 hours). By then the gearbox had been subjected to over 1400 hours of testing at a 40 hp load. Visual inspection of the ball and roller bearings revealed that they were in fair to poor condition, showing dents and extensive fine electrical pitting. The ball retainers for the output duplex pair were visibly out-of-round. Dynamic noise testing of the ball bearings indicated heavy wear with negligible local damage.

In summary, the bearings in the HT gearbox deteriorated from good to moderate to bad over the course of testing. However, the wear was uniform and proceeded in what could be called a normal manner for the applied torque load. Due to the absence of abnormal wear we should not have expected these deteriorating bearings to produce any significant changes in the measured vibration levels from the high time gearbox. Therefore, it should be difficult to detect this wear by analyzing the low-frequency accelerometer vibration spectrum. This is discussed more fully at the end of this section under "Vibration Data-Bearing Frequencies."

Spectroscopic Oil Analysis (SOA)

Oil samples were taken at various times during the course of testing the HT gearbox. As discussed in the earlier section on "Test Instrumentation and Procedures," the attachment of the oil debris monitors resulted in the installation of a circulating oil system which increased the total gearbox oil from 80 ml to 800 ml.

Figure 40 summarizes the results of spectrochemical analysis of the oil samples taken during the testing of the HT gearbox. Except for the presence of silicon which came from a sealing compound used to stop the gearbox from leaking oil, iron was the only metal detected in abnormal quantities. Oil changes are indicated by downward-pointing arrows (↓). The gearbox developed an oil leak after 280 hours of testing which persisted throughout the duration of the first test interval despite our efforts to control it. The leak could be stopped only by replacing the gasket between the two housings, a procedure which we felt would disturb the present alignment of the gearbox and invalidate the vibration data for trending purposes. The amount of oil we had to add to the gearbox and the time at which it was added to compensate for the leak are also shown in Figure 40.

The SOA has an iron sensitivity of 1 ppm. This is adequate for determining iron concentration increases due to normal wear in standard UH-1 90° gearboxes. However, the gearboxes in this test

program were modified to include the two oil debris monitors. The standard gearbox requires 80 ml of oil, and the oil circulation system for the ODM's required 800 ml of oil. This 10:1 dilution of any iron particles produced by the gearbox was sufficient in many cases to reduce the iron concentration below the detectable threshold of the SOA. Though much data was collected on this program from the SOA, it is impossible, with any confidence, to adjust the data to account for the 10:1 dilution of the iron concentration.

From the mechanical measurements that were performed, we know that during the first test period the gearbox degraded only slightly, but during the second test period the gearbox degraded significantly. We can infer from Figure 40 that most of this wear occurred during the first 400 hours of the second test period. The iron content in the oil increased in a well-behaved manner over the 130 hours of operation between the time the oil was changed at 200 hours and 330 hours.

In the 55 hours after the oil change at test hour 330, the iron concentration rose to a higher level than it had reached during the preceding 130 hours of testing. This represents an exponential increase in wear and indicates the onset of significant degradation. For an as yet unknown reason, the wear process significantly subsided after the oil change at 385 hours, and the SOA failed to detect any further changes in the wear process.

Oil Debris Monitors (ODM)

Calibration of the oil debris monitors was the responsibility of the vendors who supplied the devices. No functional check of the monitors was performed prior to their use in the test cell since these devices were supplied as "black boxes" for evaluation. Unfortunately, these sensors failed to operate properly from the outset.

Since there was no method available for evaluating the performance of the ODM's once they were connected to the gearbox, it was assumed that they were performing satisfactorily during the first few hundred hours of testing on the HT gearbox. However, in studying the first SOA results received from the vendor, it was apparent that the Nucleonics ODM was not performing to its specifications. This X-ray fluorescence ODM was reported to have a sensitivity of 5 ppm and should have detected the 8 ppm of iron concentration discovered in the SOA after 50 hours of testing. Because of the time which elapsed in collecting enough oil samples to send a minimum quantity to the vendor and his turnaround time, the nonperformance

of the Nucleonics ODM was not verified until well into the test program. At the 219-hour point this ODM was removed from the test cell and returned to the vendor for service. Since the capacitance type ODM had a much lower sensitivity, it was assumed that the iron concentration measured in the SOA during the first test period of 861 hours was never high enough to be detectable. Thus, neither ODM provided any useful information during the first test period of the HT gearbox.

After completion of the first test period, the HT gearbox was disassembled for inspection and measurement of component wear. During this time the BB gearbox was installed in the test cell. Even though this gearbox failed catastrophically, the capacitance type ODM did not detect the enormous concentration of metal which was later found in the oil. After this occurrence, this ODM was removed from the test cell and returned to the supplier for repair.

The second HT test period started without the Nucleonic ODM since it had failed again during the test of gearbox BB and was not repaired. The capacitance type ODM was available at the start of the second test period; but after the first SOA results were received, it was determined that again it was not functioning properly. In summary, no useful data was collected from either the x-ray fluorescence or the capacitance type ODM's during tests conducted on the HT gearbox.

Temperature Sensors

Ambient and gearbox oil temperature were monitored continuously during the testing of gearbox HT. At no time was any abnormal temperature rise detected in the gearbox. Figure 41 shows typical temperature data taken between hours 181 and 331 of the second HT test period.

The spikes in the oil temperature plot of Figure 41 correspond to the start-up transients ($\sim 30^{\circ}\text{F}$) observed as the gearbox oil warms up. Ambient air temperature was held at 75°F by the test cell air-conditioning system.

Ultrasonic RMS Accelerometers

As mentioned in the section on "Instrumentation", ultrasonic data was collected from the input and output gearbox bearing locations. No significant ultrasonic data was collected during either of the HT test intervals. Figure 42 shows typical ultrasonic RMS data taken

TEST DATA FROM DC SENSORS LINEAR PLOT MARCH 24, 1974
SENSOR NUMBER 00012 CB OIL TEMP
NUMBER OF HOURS PLOTTED = 00150
DATA PLOTTED AT INTERVALS OF 00060 MINUTES
VERT SCALE = 00010 / 10

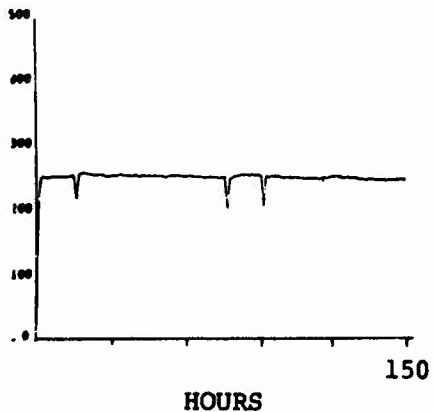


Figure 41. Typical HT Gearbox Temperature Data.

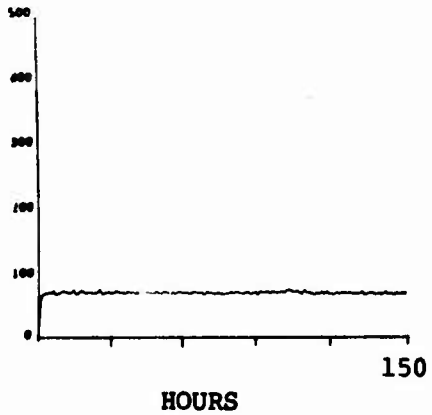
between hours 181 and 331 of the second HT test period for the sensors on the input and output bearings.

Note the existence of the start-up transients in the output ultrasonic transducer. It is speculated that this transient (which lasted several hours) is due to minute changes in temperature-sensitive mechanical tolerances. These changes could cause the bearing ball paths to change and generate different amounts of ultrasonic energy. Apparently, as the oil and gearbox warm up, the bearings return to their normal condition.

Shock Pulse Analyzer

The shock pulse analyzer was not available during the first HT test period. We obtained the analyzer during the second test period. In order to incorporate the shock pulse analyzer into the automatic data collection system, it was necessary to disconnect one of the existing sensors to provide a data channel. It was decided to remove the ambient air temperature sensor from the collection process since this sensor provided no useful data. The shock

TEST DATA FROM DC SENSORS LINEAR PLOT MARCH 24, 1974
 SENSOR NUMBER 00009 ULTRASONIC INPUT
 NUMBER OF HOURS PLOTTED = 00140
 DATA PLOTTED AT INTERVALS OF 00060 MINUTES
 VERT SCALE = 00010 / 10



TEST DATA FROM DC SENSORS LINEAR PLOT MARCH 24, 1974
 SENSOR NUMBER 00009 ULTRASONIC OUTPUT
 NUMBER OF HOURS PLOTTED = 00140
 DATA PLOTTED AT INTERVALS OF 00060 MINUTES
 VERT SCALE = 00010 / 10

Figure 42. Typical HT Ultrasonic RMS Data.

pulse analyzer is a manually operated device, so it was not possible to automate the entire data collection process. We were able to continuously monitor the peak shock pulse level, which SKF calls the "shock pulse value", since it was available as an analog voltage at a connector on the shock pulse analyzer. Figure 43 shows typical peak shock pulse data collected during hours 181 and 331 of the second HT test period.

Start-up transients are apparent in the shock pulse data and correlate with the start-up transients observed in the gearbox oil temperature as shown in Figure 42.

Note the nearly linear long-term increase in peak shock pulse level despite the oil change at the 196-hour point. The analog voltage from the shock pulse analyzer is proportional to the logarithm of the peak shock pulse value as plotted in Figure 43. This linear increase in the logarithmic value of the peak shock pulse level corresponds to an exponential growth in the absolute peak shock pulse value. This exponential increase correlates with the spectrochemical oil analysis as shown in Figure 40.

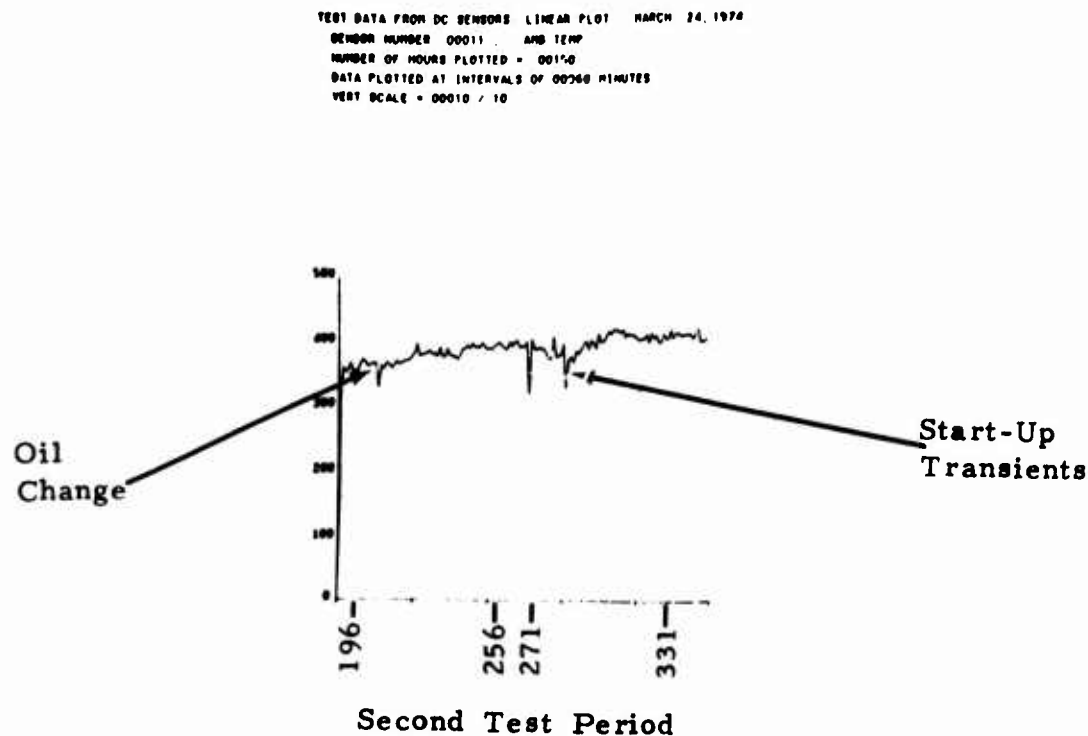


Figure 43. Typical HT Gearbox Peak Shock Pulse Level Data.

It appears from this data that the shock pulse analyzer may be a very sensitive indicator of the condition of the gearbox oil and may well prove to be a sensitive indicator of the overall mechanical condition of the gearbox itself.

Low-Frequency Vibration Data

A significant amount of low-frequency vibration data was collected for the HT gearbox. Figures 44, 45 and 46 provide an overview of the entire HT vibration data base at a single glance. These plots allow the analyst to quickly spot the significant characteristics of the gearbox as it was tested.

This type of plot enables the analyst to quickly determine the vibration frequencies which are characteristic of the operation of the particular gearbox under test and its mechanical condition. It also provides a rapid method for detecting changes in the operational

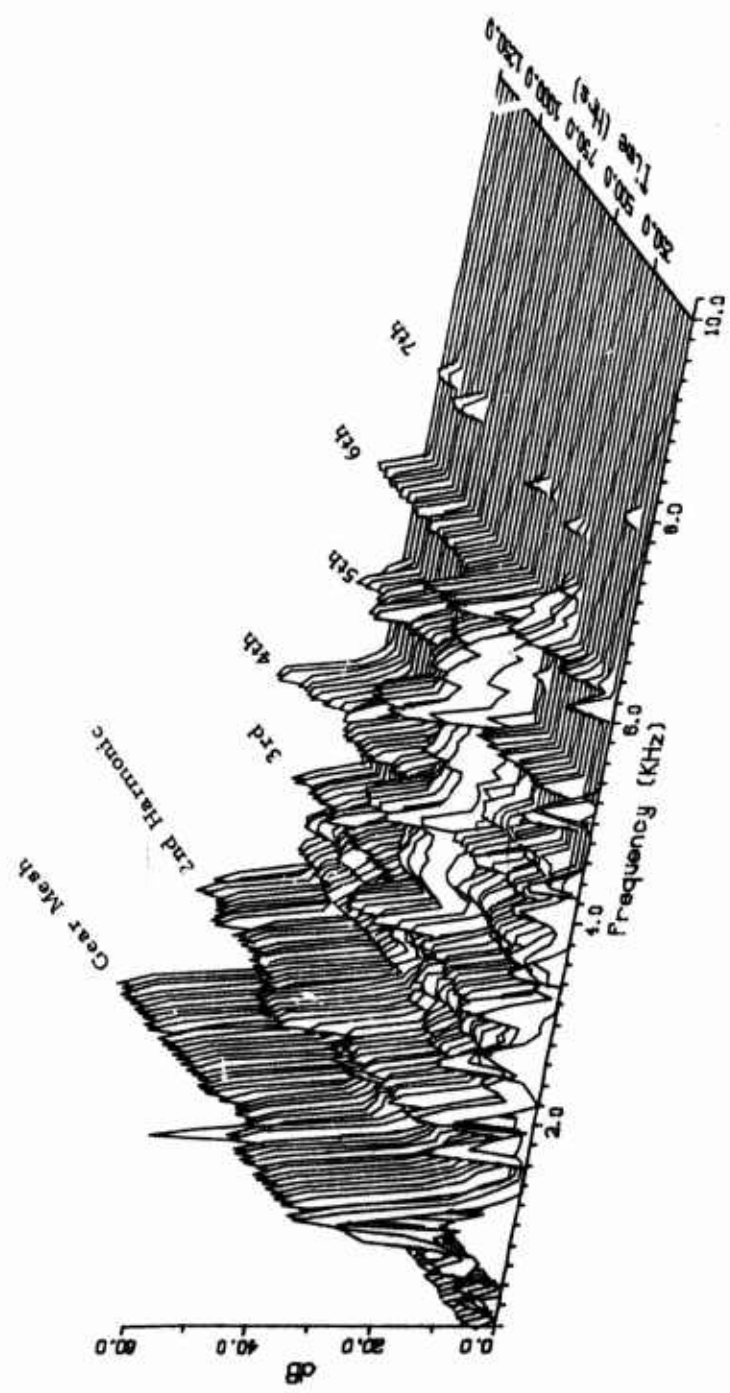


Figure 44. Overall View of Hi Vibration Data Base,
Input Lateral Accelerometer.

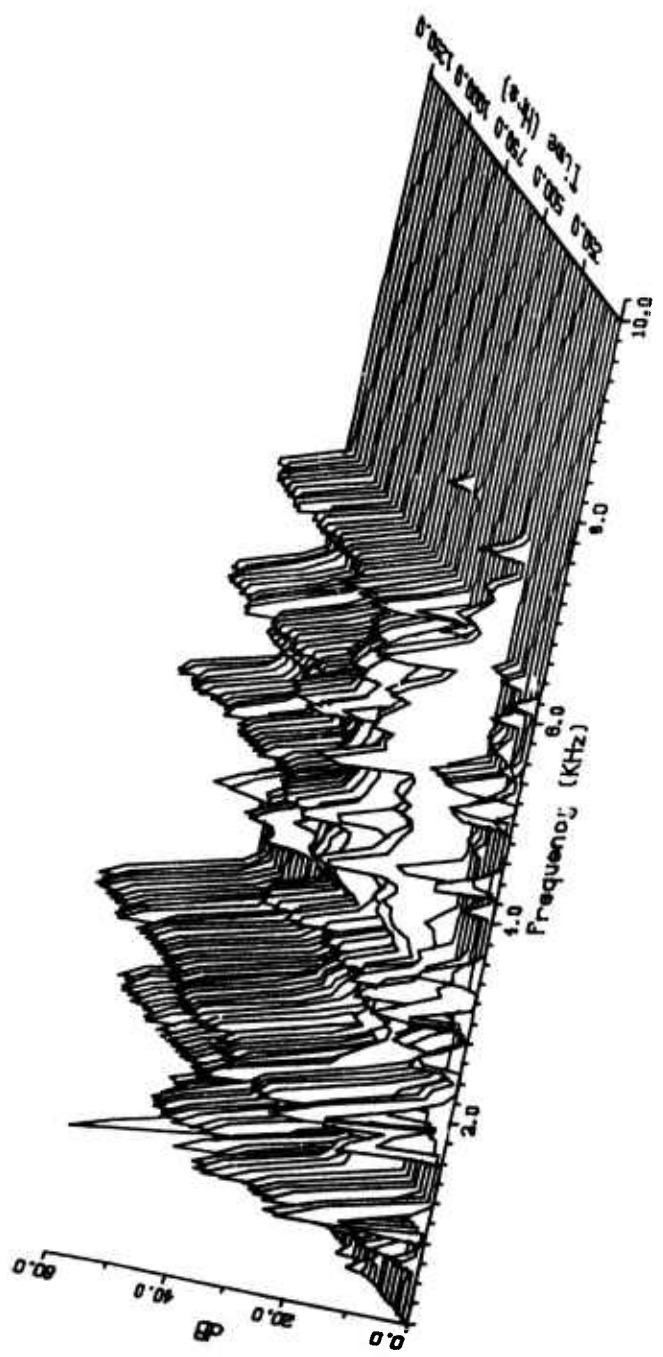


Figure 45. Overall View of HT Vibration Data Base,
Skew Accelerometer.

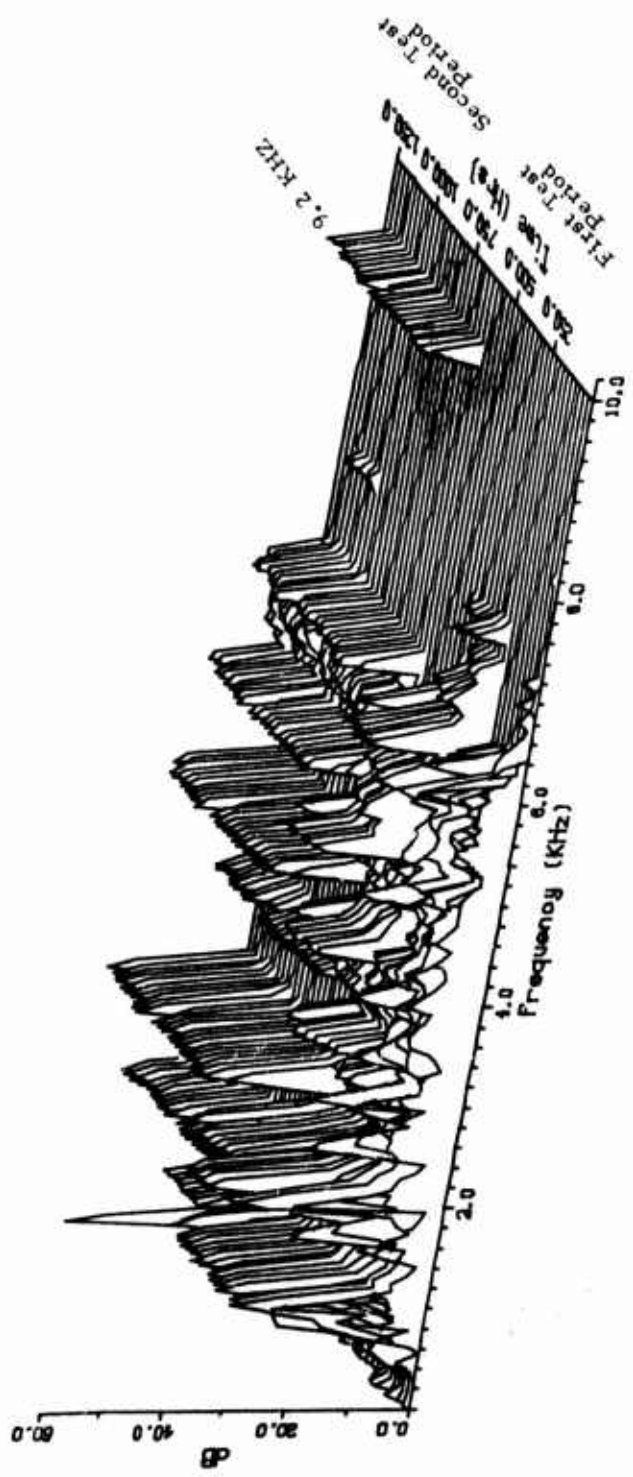


Figure 46. Overall View of HT Vibration Data Base,
Output Lateral Accelerometer.

parameters which may or may not indicate changes in the mechanical condition of the gearbox. An example of an unexplained change in the vibration spectrum is shown in Figure 46 for the HT gearbox. At hour 525 a vibration component at 9.2 kHz appeared in the output of the output lateral accelerometer. As seen in the figure, this frequency was recorded for the rest of the HT gearbox tests even though the gearbox was disassembled for inspection at test hour 861.

Figure 47 is an example of an attempt to curve-fit the entire time history of the vibration signals at 3202 Hz obtained from the input lateral accelerometer of the HT gearbox. Our statistical analysis gave this frequency bin a Z-score of 3.8. This frequency is close to the third harmonic of the gear mesh frequency. It is obvious from the figure that polynomial and exponential curve fitting could not account for the abnormal increase in amplitude of this frequency at the 500-hour point.

Although a large number of what appeared to be statistically significant frequency bins of the HT gearbox were trended using polynomial and exponential curve fitting, they are not reported here because they provided no new insight into the mechanical condition of this gearbox.

The least-mean-square (LMS) prediction technique was also applied to a selected number of frequency bins from the HT gearbox which were shown to be statistically significant. As shown in Figure 48, the LMS technique was used on the vibration frequency of 3202 Hz to predict the PSD time history of this signal from 479 to 606 hours of testing based on the actual data obtained between test hours 350 and 478. The presence of the step increase in vibration level at hour 470 caused the LMS technique to significantly underestimate the actual data during the predicted period.

Since the LMS prediction technique is limited in the range over which the prediction can be made, only the data relevant to the prediction is shown in Figure 48. Due to lack of funds, the LMS technique was not applied to any other test intervals at 3202 Hz.

If a larger prediction range were used, a better fit to the data might have been obtained.

The vibration data from the HT gearbox was characterized by many abrupt changes in amplitude at certain frequency bins. These are considered to be abnormal and could have been caused by instrumentation problems experienced early in the testing program. For this

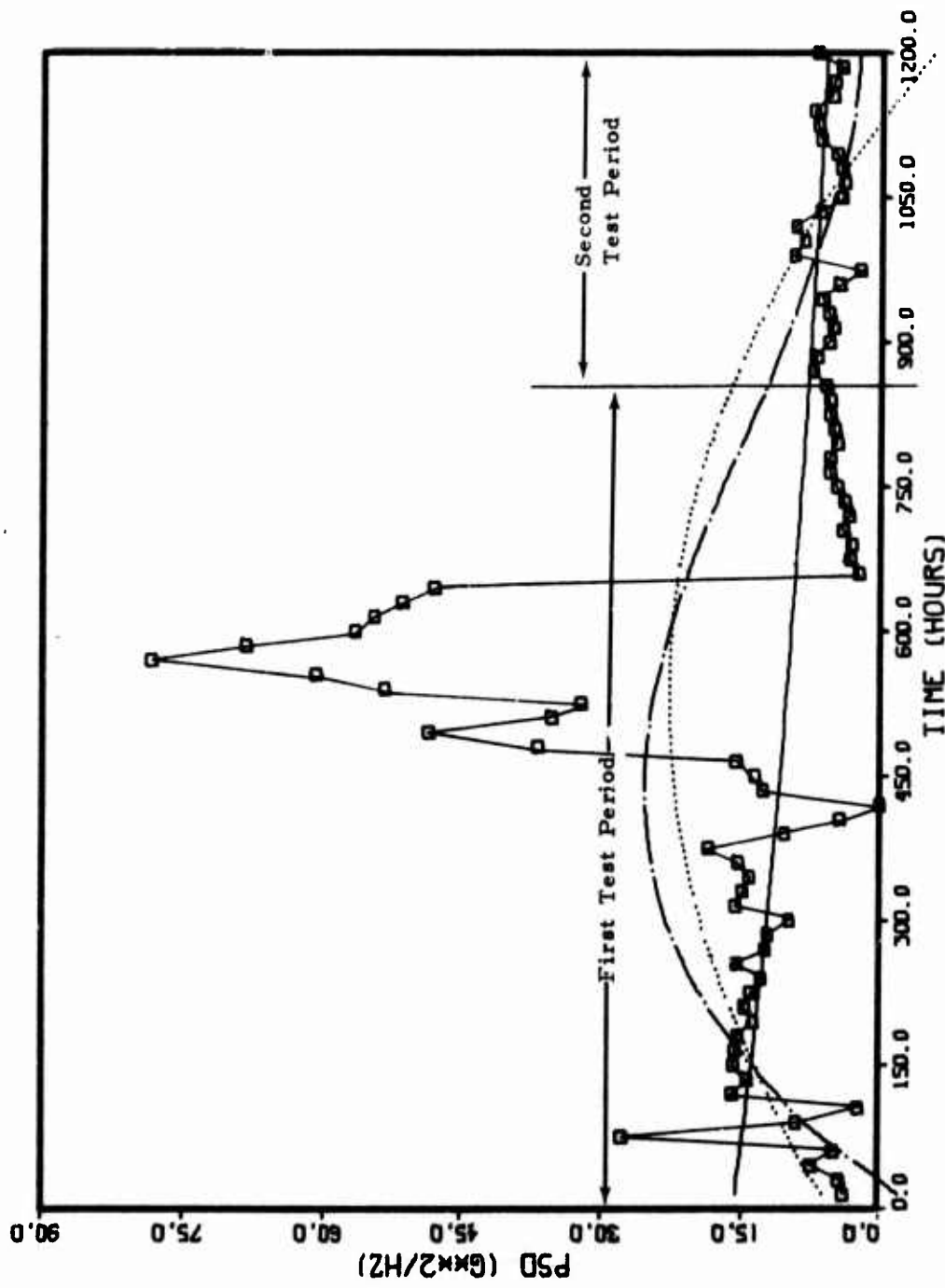


Figure 47. PSD Vibration Path, HT Vibration Data, Input Lateral Accelerometer, 3202 Hz.
 Data Point \square Quadratic Fit... Cubic Fit - - - - - Exponential Fit — $Z=3.8$

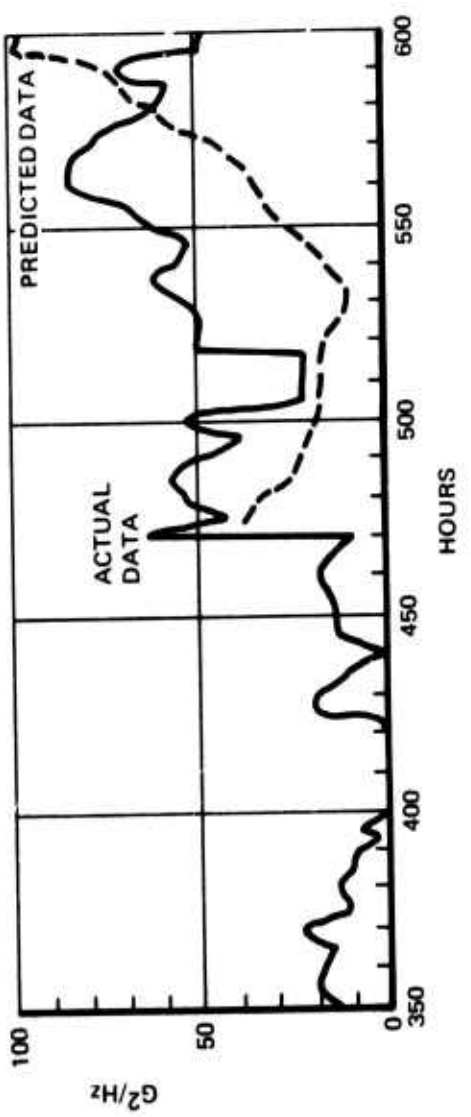


Figure 48. Prognostic Trend of HT Vibration Data,
Input Lateral Accelerometer, 3292 Hz.

reason, no attempt has been made to try to explain the sometimes unusual behavior of the vibration spectrum from this gearbox.

The LMS prediction technique looks promising as a prognostic tool for predicting future trends in vibration signals based on actual data obtained in previous periods of time.

Correlation of Sensor Outputs With Mechanical Condition

The data collected from the HT gearbox was sufficient to show a correlation between the observed mechanical bearing wear, the signals received from the shock pulse analyzer, and the iron content of the gearbox oil as measured by spectroscopic oil analysis. Although several vibration signals were found to deviate from the initial vibration spectrum in a statistically significant sense, no absolute correlation to gearbox wear could be made. The oil debris monitors and the temperature sensors did not yield useful data, but the ultrasonic sensors did detect a long-term warmup transient.

Summary of HT Gearbox Test Results

Of the 1450 test hours accrued on the HT gearbox, useful data was obtained from 1277 hours. The gearbox started the first test period in good condition, and deteriorated to fair condition by the end of the first period (861 hours). During the second test period the gearbox further deteriorated from a fair to a poor condition. By the end of the second test period the gearbox components were sufficiently worn that this gearbox could no longer be classified as being in a serviceable condition. In fact, it was our conclusion that the operational condition of this gearbox was close to the onset of failure. There were no trends in the vibration signals which suggested that the bearings were heavily worn, although SOA and shock pulse data did indicate that periods of heavy wear had occurred.

The wear process exhibited by the HT gearbox is of great importance to prognostics, since this gradual noncatastrophic wear process represents the type of wear pattern one would expect to occur in normal helicopter operation. This gradual, well-behaved wear is also the most difficult to determine since it is not easily detectable by current diagnostic sensors and analysis techniques. This is not to say that it is impossible to determine this type of wear, but only that a sufficient analysis has not been done to isolate wear indications which might be present in the vibration data.

BAD BEARING (BB) GEARBOX TESTS

Gearbox BB was selected for testing as an example of an incipient failed bearing. This gearbox was tested immediately following the first test period of gearbox HT. As in the case of gearbox HT, accelerometer monitoring pads attached with epoxy to the appropriate sensor locations and the accelerometers were firmly screwed into place. The test cell was operated at 40 hp at the gearbox output shaft, and the input rpm was 4150. This gearbox failed catastrophically in 166 hours of testing, and much of the data collected was useless to the prognostic effort due to instrumentation difficulties.

Mechanical Condition of BB Gearbox

Visual inspection of the ball and roller bearings before testing showed the input duplex pair to be in fair condition, with moderate wear on the races and small dents and cuts on the balls. The output duplex pair was in fair to poor condition, with moderate to heavy denting in the races and heavy wear and denting on the balls. The input roller bearing was in fair condition, with small to large particle denting and light electrical pitting. The output roller was in fair to good condition, with moderate inner race abrasive wear and overall electrical pitting and denting.

Noise testing of the ball bearings verified the visual examination by showing the input duplex pair to have extreme local damage but only light to moderate wear, while the output duplex pair was classified as extremely worn with light to negligible local damage.

Visual examination after the 166-hour test period revealed that one-half of the input duplex pair was in fair condition. The other half was in poor condition, with wide circumferential heat coloration bands. This condition was confirmed by noise tests which indicated extreme wear. The raceway wear depth had increased from the nominal 20 μ in to 216 μ in, indicating that catastrophic failure was imminent.

The dynamic noise test level also increased over the test interval from 6.5 to 20.5 db.

The raceway wear measurements on the output duplex pair (BB-3 and BB-4) prior to testing showed respective wear depths of 160 and 136 μ in and noise levels of 20.5 and 18.5 db. These bearings failed catastrophically during the 166-hour test period and furnish rather convincing evidence that bearings with these dynamic noise test levels

are in an advanced state of wear and could be approaching the onset of catastrophic failure. The post-test inspection of the failed components revealed that the balls of the raceways were heavily fatigued, with the raceways exhibiting extreme heat coloration. The ball retainer in one of the bearings (BB4) was just short of total separation into two halves due to thru-wear between the ball pockets. Noise testing was not possible due to the catastrophic nature of the failures.

The input roller bearing deteriorated from a fair to a poor condition with small to large particle denting and light electrical pitting. The output roller deteriorated from a fair to a poor condition over the test interval, with abrasive wear, particle scoring and denting.

The SEM photomicrographs clearly show the particle scoring and the pitting. The failure modes of the BB gearbox are rather dramatic and are readily apparent in most of the observations made and documented in Appendix B.

Spectroscopic Oil Analysis (SOA)

Oil data was collected at regular intervals during the testing of the BB gearbox. Duplicate samples were taken and supplied to the Eustis Directorate for future in-house testing of other types of oil debris sensors. Figure 49 summarizes the results of the SOA on the BB gearbox.

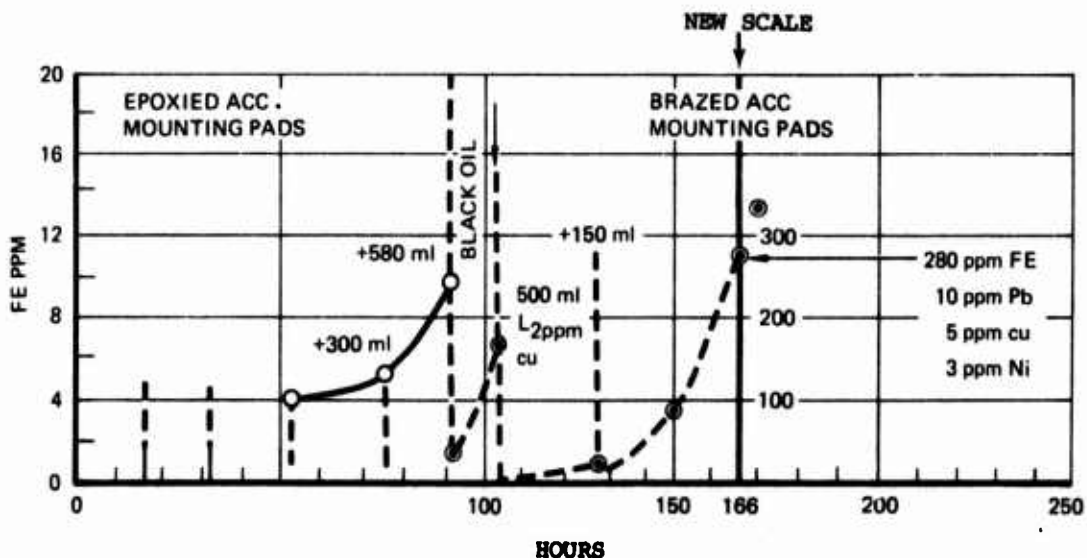


Figure 49. Summary of BB Gearbox SOA.

At test hour 92, the oil was observed to be a very dark color, which probably was due to the rapid wear of the ball retainer of the output duplex pair. The downward arrow (↓) marks the test hour where 500 ml of oil was added due to an oil line break in the oil circulation system.

At hour 130, 150 ml was added to compensate for what was initially believed to be a leak in one of the gearbox seals. However, it was later discovered that the oil had been lost due to a catastrophic failure in the sensor head of the X-ray fluorescence type oil debris monitor.

By the end of test hour 166, large concentrations of lead, copper, and nickel were observed in the SOA. These metals probably came from the bronze retainer, which was very badly worn. Some of the copper concentration may have been due to gear wear since during manufacture, gear is copper coated before it is anodized.

Oil Debris Monitors (ODM)

Both the X-ray fluorescence and the capacitance type oil debris monitors were in use during the entire BB test period. As stated before, neither sensor yielded reliable data. The X-ray fluorescence type sensor did have an abrupt step-like change in output at test hour 75 as shown in Figure 50.

This abrupt change in sensor level occurred within a 4-minute sampling interval and correlates with a corresponding step-like change in signal from the output ultrasonic accelerometer. We now know that the X-ray fluorescence ODM was probably not functioning properly during the testing of gearbox BB, but it appears that it did detect the sudden increase in iron concentration which occurred at test hour 75. The ODM failure occurred when the molybdenum window fractured. The exact time of failure is not known, but we suspect that it occurred when the step-like increase in its output occurred at test hour 75 or shortly after. After the oil was changed at 100 hours, this ODM still registered full scale, which indicated that the sensor had failed. When the capacitance ODM did not detect the high concentration of metals observed in the SOA, we assumed that it was either defective or had a sensitivity far below the manufacturer's specifications. Figure 51 shows an SEM picture of some of the metallic debris removed from the measurement capacitor in the capacitance type ODM.

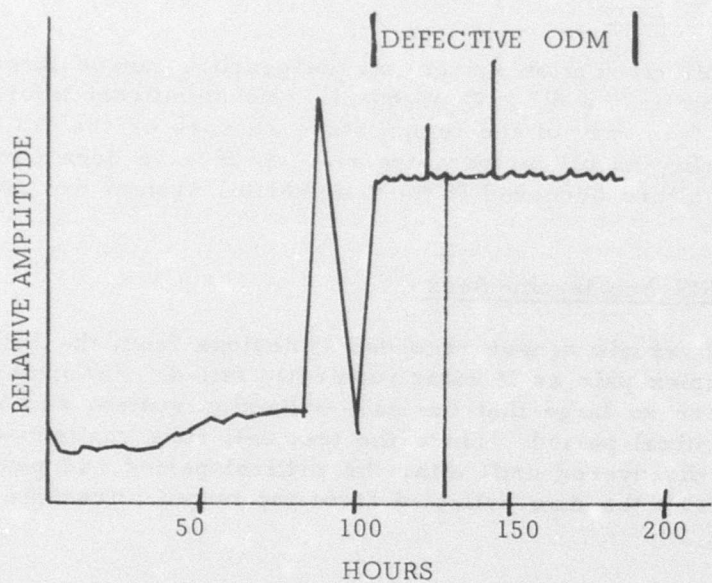


Figure 50. Output of X-ray Fluorescence ODM.

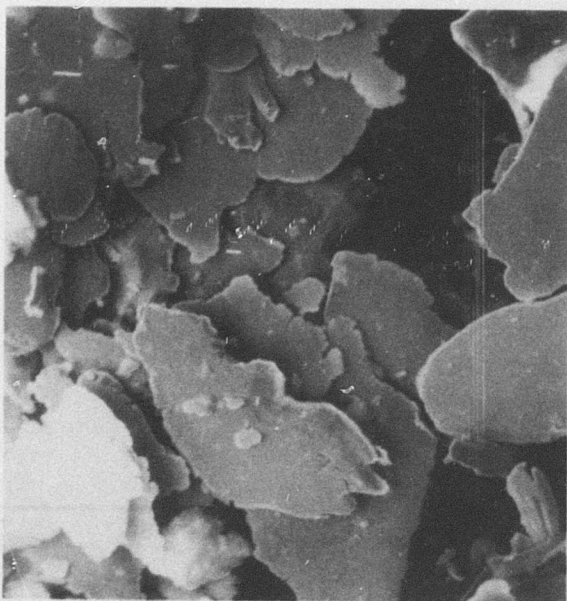


Figure 51. Oil Debris Found in Measurement Capacitor of Capacitance Type ODM.

Temperature Sensors

The 800-ml oil circulation system on the gearbox caused large heat losses to occur in the oil. Consequently, no significant information was obtained from any of the temperature sensors on the BB gearbox. In all probability an oil temperature rise would have been observed as catastrophic failure occurred if the original oil system had not included the ODMs.

Ultrasonic RMS Accelerometers

The output ultrasonic sensor recorded emissions from the BB gearbox output duplex pair as it catastrophically failed. Unfortunately, the emissions were so large that the data collection system was saturated during the critical period. Since the test cell runs unattended, this fact was not discovered until after the critical period had passed. Figure 52 shows the data collected from the output ultrasonic sensor.

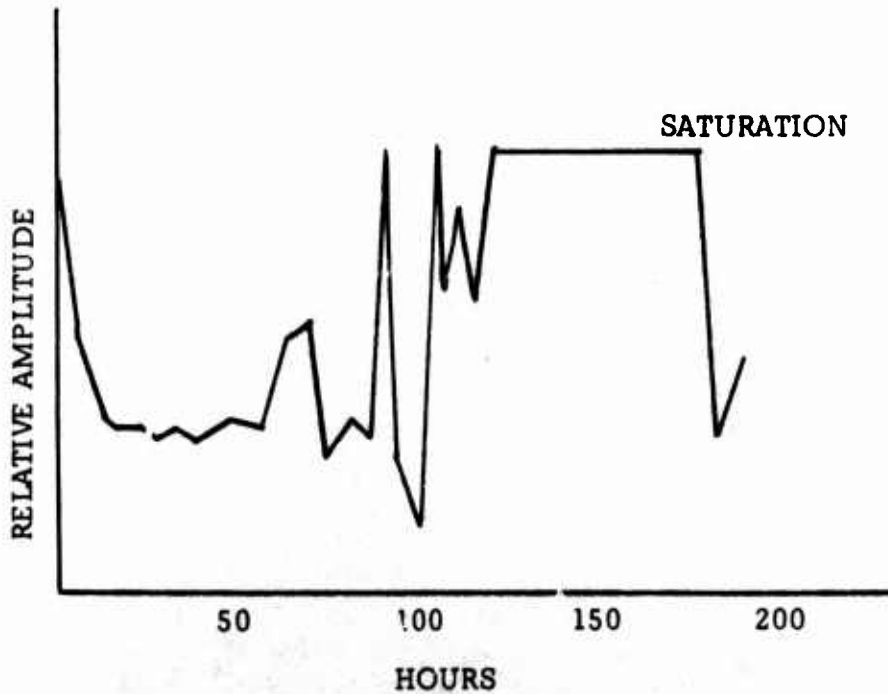


Figure 52. Ultrasonic Data From Output Ultrasonic Accelerometer.

Shock Pulse Analyzer

The shock pulse analyzer was not available during the testing of the BB gearbox.

Low-Frequency Vibration Data

In accordance with our test program, the BB gearbox was disassembled prior to testing to inspect the components and document their initial condition. In order to expedite the test program, this gearbox was reassembled and placed in operational test before we had received the results of the wear measurements from our vendor. We had no indication that this gearbox was on the verge of failure in its initial condition, and it failed catastrophically before we received the data on the initial inspection. However, considering our level of experience at that time in the test program, even if the data had been available prior to testing, we are not sure that we would have been able to determine that the BB gearbox was on the verge of catastrophic failure by analyzing the data obtained from the initial inspection. Another unfortunate circumstance that occurred at the same time was that our principal investigator took his scheduled vacation during the first part of the BB gearbox testing, and the responsibility for conducting the test program was assigned to a less experienced engineer. For this reason the saturation of the electronic data collection system by the output of the ultrasonic sensor went undetected. As the gearbox approached catastrophic failure, the overall vibration level increased significantly, and the torque created by the moment arm of the accelerometer broke the mounting pads loose from the gearbox housing. This happened several times before the mounting pads were finally brazed in place. At the 94-hour point, the computer shut down the test cell after 14 hours of testing due to exceedance of vibration limits. The oil taken at this point was a very dark color, probably due to excessive heating and deterioration of the output bearing. Since we were not aware of the poor initial condition of this gearbox, these events were not recognized as indicators of catastrophic failure, and testing of the gearbox was continued for another 70 additional hours. Testing was finally terminated when it was found that the brazed accelerometer pads were beginning to separate from the housing.

Figures 53, 54, and 55 show an overall view of the vibration data collected from the three low-frequency accelerometers on the BB gearbox. Note the significant increase in energy in the high-frequency components and the total absence of a recognizable garmesh harmonic structure (see HT data base for comparison, Figures 44,

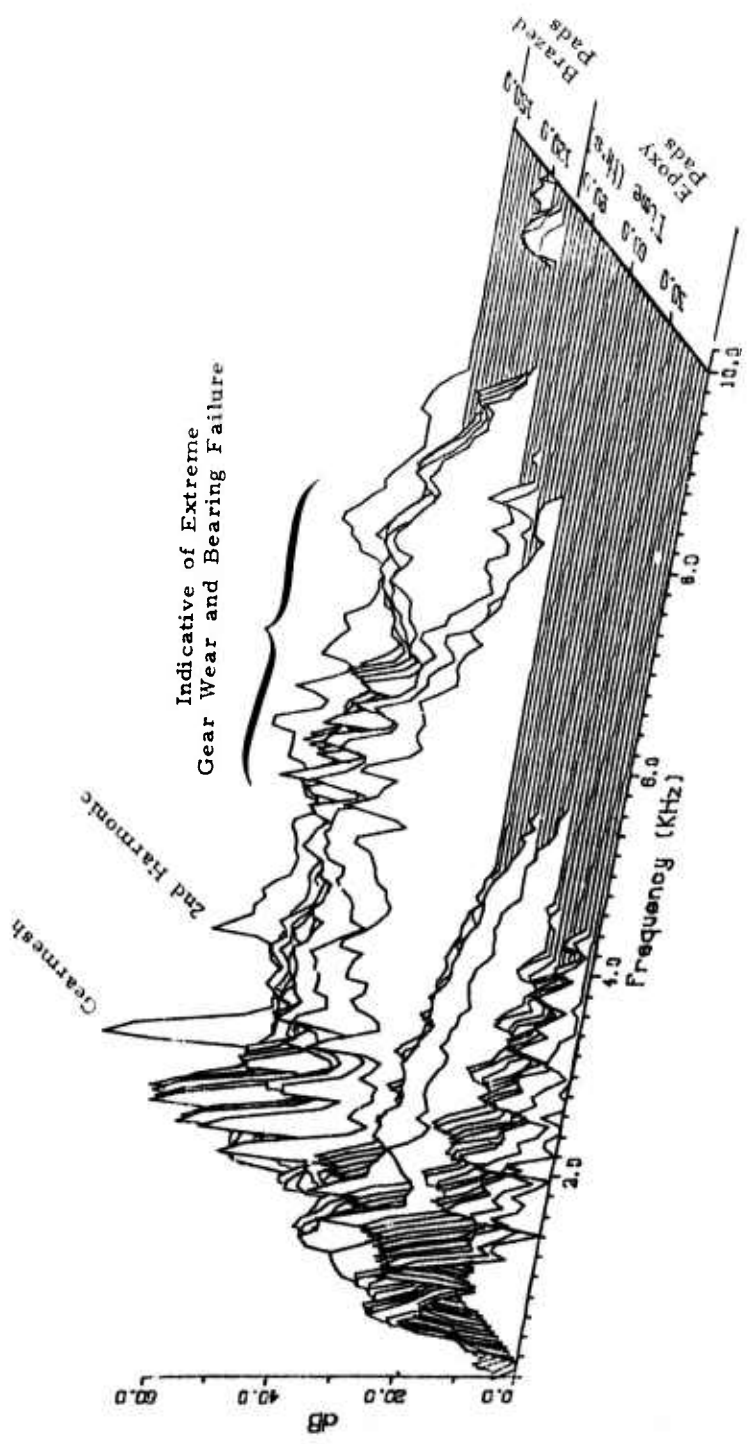
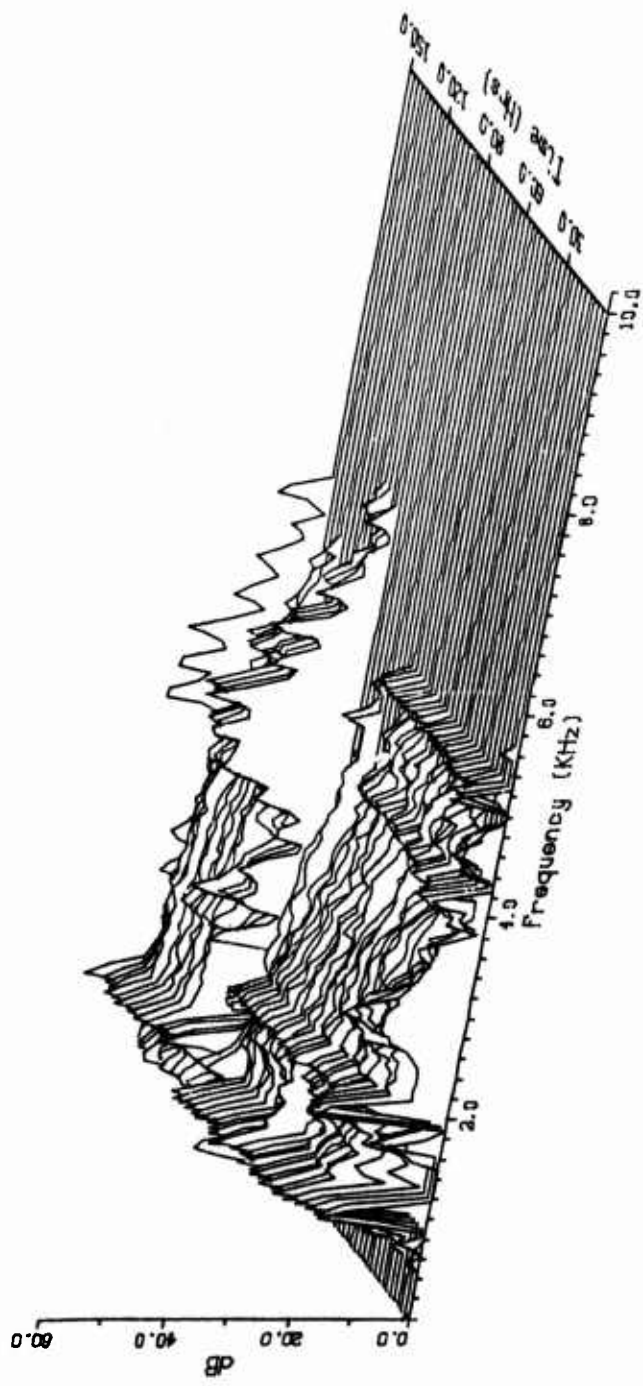


Figure 53. Overall View of BB Vibration Data Base, Input Lateral Accelerometer.

Figure 54. Overall View of BB Vibration Data Base, Skew Accelerometer.



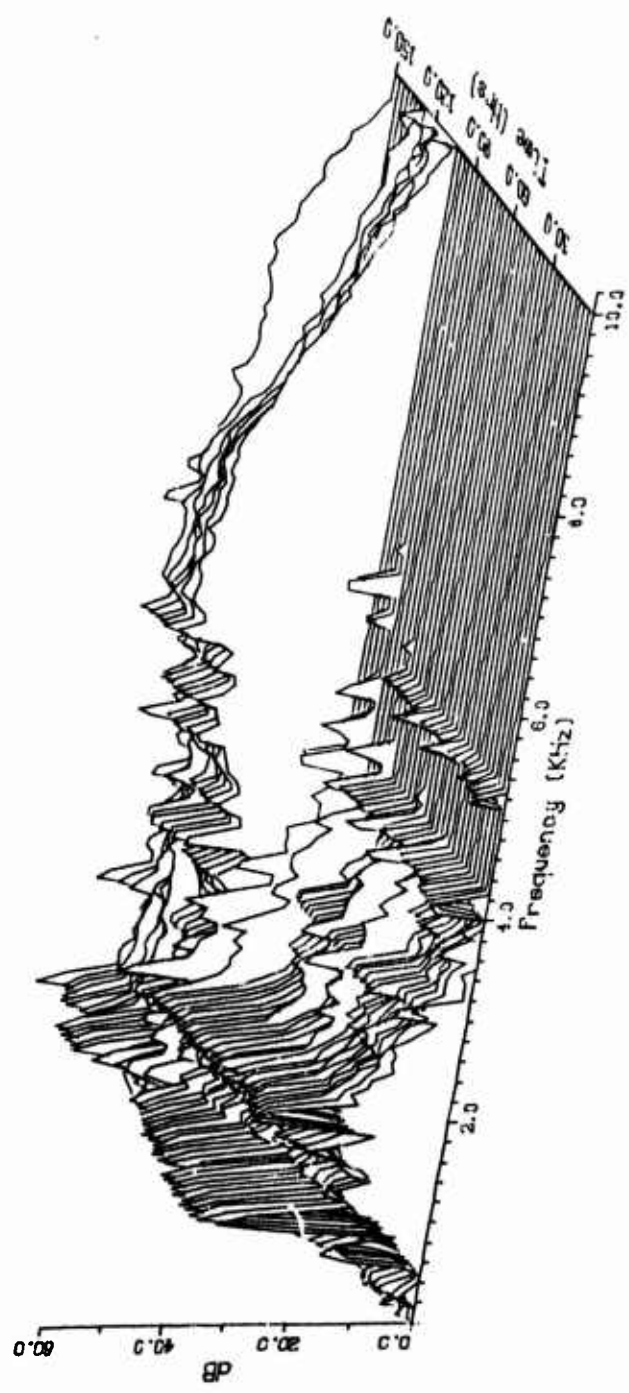


Figure 55. Overall View of BB Vibration Data Base, Output Lateral Accelerometer.

45 and 46). In comparing these spectra with the vibration spectrum obtained from gearbox BG in the next section (Figures 57, 58 and 59), it can be seen that a full spectrum of high-frequency components is also a characteristic of bad gears. We know from visual inspection that the BB gears were in poor condition at the end of the test period; therefore, the lack of a garmesh harmonic structure in the vibration spectra must be due to intermixing of the vibration energy generated by the failed output bearing and the garmesh. This is not an unreasonable assumption to make since it was noted that by the end of the test program on this gearbox, the wobble in the output shaft was on the order of tenths of an inch, and such a large wobble would cause the garmesh frequency to oscillate violently about its mean value (1070 Hz). This oscillation would probably be somewhat random in nature, and its vibration spectrum could be interpreted as resulting from frequency modulation (FM) of the garmesh structure by broadband noise. The resulting complex FM sideband structure would suppress the FM carrier (garmesh frequencies) as carrier energy was diverted into sideband energy.

It is unfortunate that the numerous accelerometer attachment problems encountered in testing this gearbox precluded us from obtaining a data base that was usable for trending or reliable for diagnostics. A good data base would have provided the signal structure associated with a catastrophic failure and at least, for diagnostic purposes, would have given the analyst an excellent opportunity to study the vibration spectra associated with this type of failure.

Correlation of Sensor Outputs With Mechanical Condition

The BB gearbox was on the verge of catastrophic failure prior to testing. Its condition was deteriorating so rapidly from the start of the test program that indications of wear were given by all sensors except the temperature sensors and the ODM's.

The oil temperature sensor did not detect the catastrophic failure because of heat transfer to the oil circulation system for the ODM's, and the X-ray fluorescence ODM did produce a step-like output just prior to the failure of the gearbox and its own subsequent failure. The ambient temperature sensor might have detected the approaching failure if it had been located on the output duplex bearing pair. The output of the ultrasonic accelerometers saturated the data processing electronics. The low-frequency vibration data showed gross changes in structure with an increase in energy content of most of the frequencies within the measured frequency range. This dramatic

change in structure was observed in the data collected from both lateral accelerometers. This is to be expected since both the input and output duplex bearing pairs were in a severe state of wear during most of the 166 test hours.

Though the metallic particle concentration was diluted by the oil circulation system for the ODM's, the appearance of copper shortly after 100 hours was an indication that abnormal wear was occurring. The dilution of the particle concentration due to the addition of oil to compensate for the leak in the oil line and failure of the X-ray fluorescence ODM further reduced the sensitivity of the SOA over much of the test period. However, analysis of the diluted oil taken from the failed gearbox clearly shows that the gearbox had undergone catastrophic failure.

Summary of BB Gearbox Test Results

Because of the failed state of this gearbox prior to testing and its short lifetime of 166 hours, none of the data obtained from the sensors was usable for prognostic trending. The problems encountered with the low-frequency accelerometer mounting pads and uncertainties introduced into the SOA due to diluting the metallic particle concentration with the oil circulation system for the ODM's make these measurements of limited value as useful diagnostic indicators of the catastrophic failure which occurred in the BB gearbox. The growth of the high-frequency components in the low-frequency accelerometer output data gives a qualitative indication of how the vibration signal structure is modified as bearings begin to fail.

BAD GEAR (BG) GEARBOX TESTS

The bad gear, BG, followed the bad bearing, BB, gearbox in the overall testing sequence. A total of 1031 test hours at 40 hp load to the output shaft was accumulated on this gearbox, of which 951 hours were trendable. The accelerometer mounting pads were welded to the gearbox housing to ensure proper sensor contact.

At test hour 326, a catastrophic failure of the test cell occurred. One of the spherical roller bearings which support the high-speed jack shaft which supplies input power to the gearbox failed due to excessive end loading. Support bearings are shown as the two sets of four square blocks in Figure 2 in the discussion of the "Test Stand." They also support the pulley arrangement between the electric motor and the gearbox shaft. The improper loading of the

bearing nearest the gearbox resulted in excessive heating, loss of lubricant and finally loss of rpm. The rpm sensor detected the malfunction and shut down the test cell. The load was adjusted to correct the problem and a new bearing was installed. Though no further problems were encountered with this bearing, precautionary measures were taken to prevent a reoccurrence of this type of failure. Thermal circuit breakers to limit the temperature rise to 100°C were installed on each of these spherical bearings. It was worth noticing that this was the only failure which occurred in the test cell itself in almost 5000 hours of testing.

Mechanical Condition Summary for Gearbox BG

Visual inspection of the bearings before testing revealed moderate to heavy race wear in the input duplex pair and an overall fair to poor condition. The condition of the output duplex pair was slightly worse, with heavy denting and pitting and heavy abrasive raceway wear. Noise testing indicated that the input duplex pair had light local damage with overall moderate wear. Noise testing of the output duplex pair indicated heavy to extreme wear with negligible local damage. Dynamic noise tests on the input BG bearings, after tests on the BG gearbox were concluded, showed that the BG bearings were almost in the same stage of wear as the BB input bearings prior to testing the BB gearbox. See Appendix B for more details.

The input roller bearing was in fair to poor condition, with heavy denting and fine abrasive wear. The output roller was in fair to good condition, with only slight denting and slight abrasive wear. After 1031 hours of testing, visual inspection of the input duplex pair indicated moderate to heavy wear, with many small dents on the raceways. The balls were heavily dented and pitted. Noise testing revealed that both bearings in the duplex pair had deteriorated from a moderate to a heavy general wear condition.

Visual inspection of the output duplex pair indicated an overall poor condition, with heavy abrasive wear, many small dents, and high contact angle. Dynamic noise tests on the output duplex pair revealed extreme general wear and a noise level of 18.5 db. Final receiving measurements of BG's output duplex pair of 93 and 150 μ in are comparable to initial raceway measurements of 160 and 136 μ in measured on the output duplex pair of the BB gearbox prior to test. Since the BB gearbox failed after 166 hours of testing, it is probable that the BG gearbox would have experienced a catastrophic failure of the output bearing rather than a gear failure if the testing of the BG gearbox had been continued for another 100 or so hours.

Visual inspection of the roller bearings after the 1031-hour test period revealed many small dents and fatigue pitting with an overall deterioration in condition as a result of the testing.

Spectrochemical Oil Analysis

Oil samples were periodically taken during the testing of gearbox BG, and the SOA data is summarized in Figure 56. The data indicates the presence of a high concentration of iron in the oil at the start of testing. This condition persisted throughout the BG test period and is probably associated with gear wear. We know from the mechanical measurements performed before and after testing that the wear in the output duplex bearing was in an advanced stage and the gearbox was in the initial phase leading to catastrophic failure.

The SOA detected 2 to 3 ppm of nickel and 8 ppm of tin between test hours 358 and 449. The presence of these metals in the oil was confirming evidence that the stainless steel balls and raceways in the output duplex bearing were experiencing excessive wear. The re-appearance of a high concentration (8 ppm) of lead at test hour 527 could be attributed to excessive wear in the bronze ball retainer.

In attempting to interpret this data, it must be remembered that the oil circulation system was attached to the BG gearbox throughout the test period. Therefore, the metallic particle concentrations produced by the gearbox could have been diluted by as much as 10:1 in the oil samples taken for the SOA.

Oil Debris Monitors (ODM)

No data was collected from the oil debris monitors since both devices had been returned to their vendor for repairs. The circulating oil system was connected during the complete test period of the BG gearbox as prescribed by our original test program plan.

Temperature Sensors

Analysis of the gearbox temperature sensor outputs revealed no useful data from either the ambient sensor or the oil temperature sensor.

Ultrasonic RMS Accelerometers

An analysis of the data taken from the input and output lateral ultrasonic accelerometers provided no information which could be

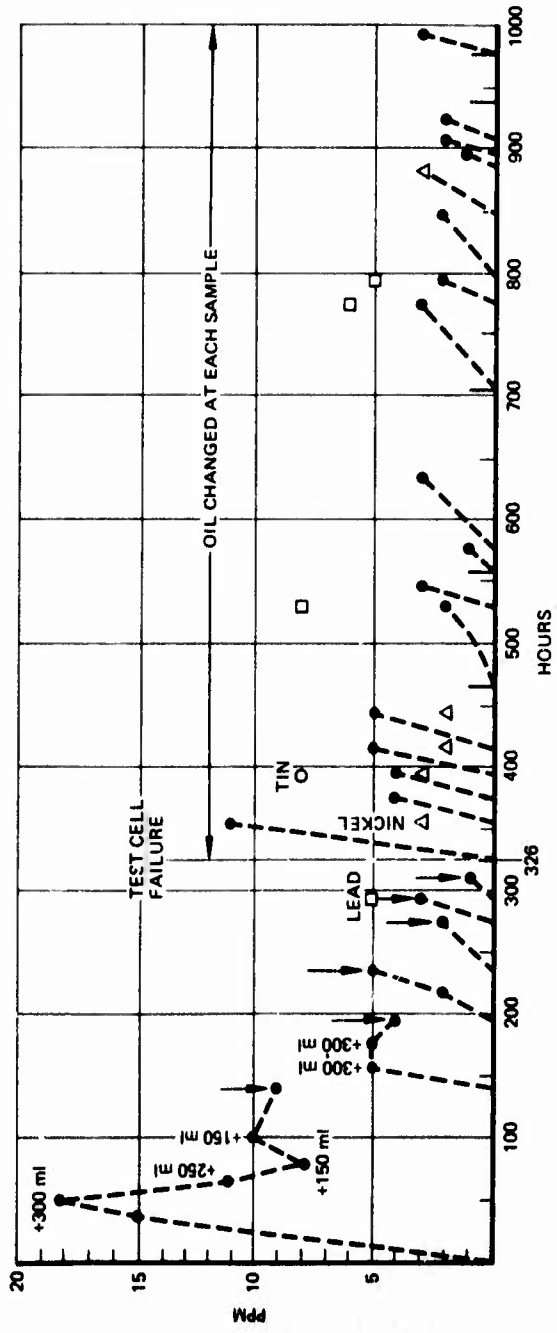


Figure 56. Summary of BG Gearbox SOA.

- Iron
- Tin
- Lead
- △ Nickel
- ↑ Oil Change

Note: All data taken with 800 ml oil circulation system attached.

related to the mechanical condition of the BG gearbox. Even though the post-test measurements showed that the output duplex bearing was in an advanced stage of wear, this wear process was not reflected in the output of the ultrasonic sensors. It appears that the wear must approach the onset of catastrophic failure before it causes significant changes in the output level of the ultrasonic accelerometers. This conclusion is supported by the test results obtained from the BB gearbox. The ultrasonic sensor outputs showed no abnormal changes until immediately prior to the catastrophic failure of the gearbox.

Though these results are not very encouraging, we cannot categorically eliminate ultrasonic sensors from further consideration as a useful prognostic tool. As discussed in other sections, the shock pulse analyzer (an ultrasonic sensor) appears to provide information which can be of value to prognostic efforts. It was also mentioned in the section on "Test Instrumentation and Procedure", that because of the unavailability of broadband ultrasonic accelerometers, low-frequency accelerometers with narrowband filtering were used as "ultrasonic accelerometers" in this test program, and for this reason the ultrasonic signal processing was far from optimum.

Shock Pulse Analyzer

The shock pulse analyzer was not available during the testing of gearbox BG, so no shock pulse data was collected.

Low-Frequency Vibration Data

The vibration data collected during the BG test period is characterized by a strong harmonic structure with much of the high frequencies filled in by broadband noise as shown in the overall view of the BG vibration data base given in Figures 57, 58 and 59.

Attempts at long-term trending were not particularly successful due to erratic short-term fluctuations of the data. Figures 60 and 61 show two examples of the application of the LMS technique to the BG vibration data. The frequency bin (2031 Hz) shown in Figure 60 is slightly below the second garmesh harmonic of the frequency. This energy may be due either to "spillover" of second harmonic energy into this bin (due to finite sidelobe suppression) or to a growth in the sideband structure of the garmesh. Our processing resolutions of 78.125 Hz is insufficient to distinguish how much of each process is occurring. That frequency bin was selected for trending because its Z-score of 4.7 at test hour 375 exceeded the Z-score criterion of 4.3. The LMS trend prediction for the test interval between 146

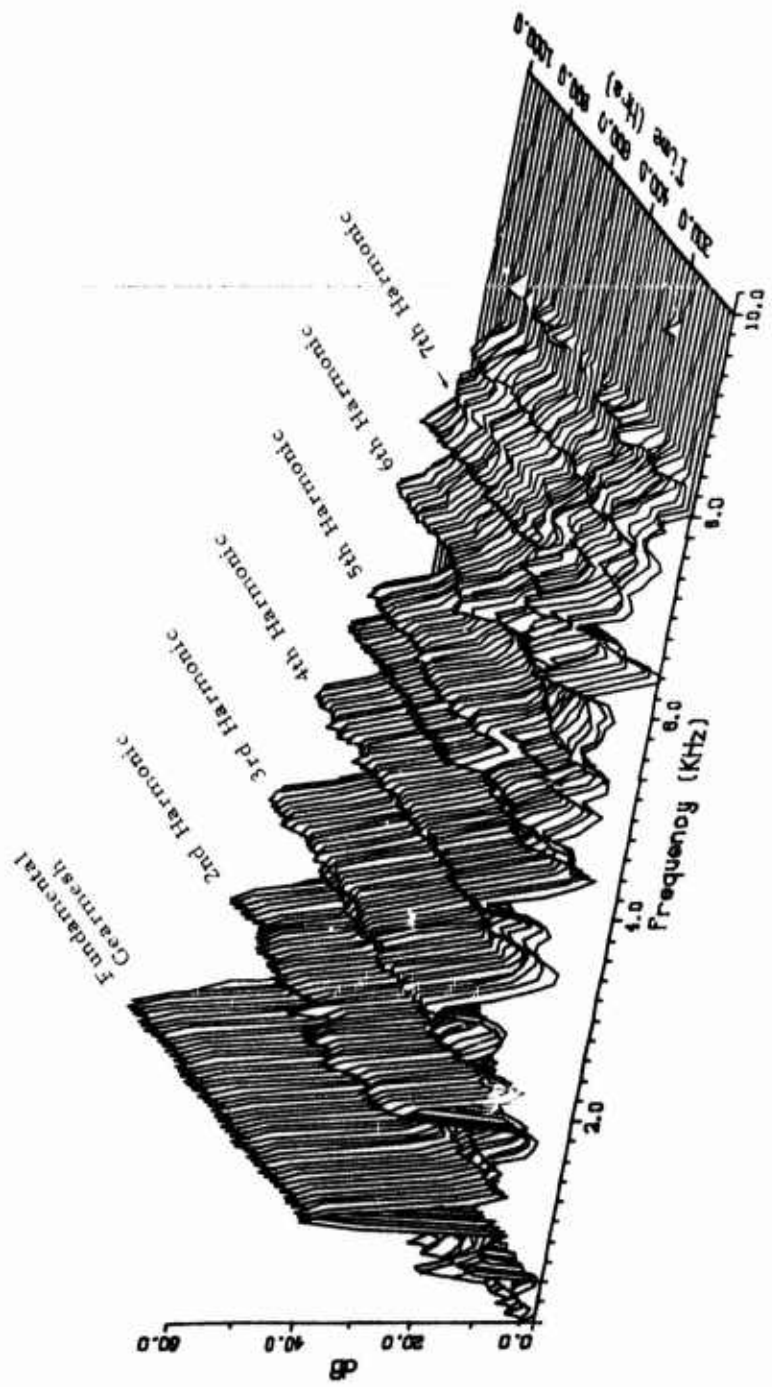


Figure 57. Overall View of BG Vibration Data Base,
Input Lateral Accelerometer.

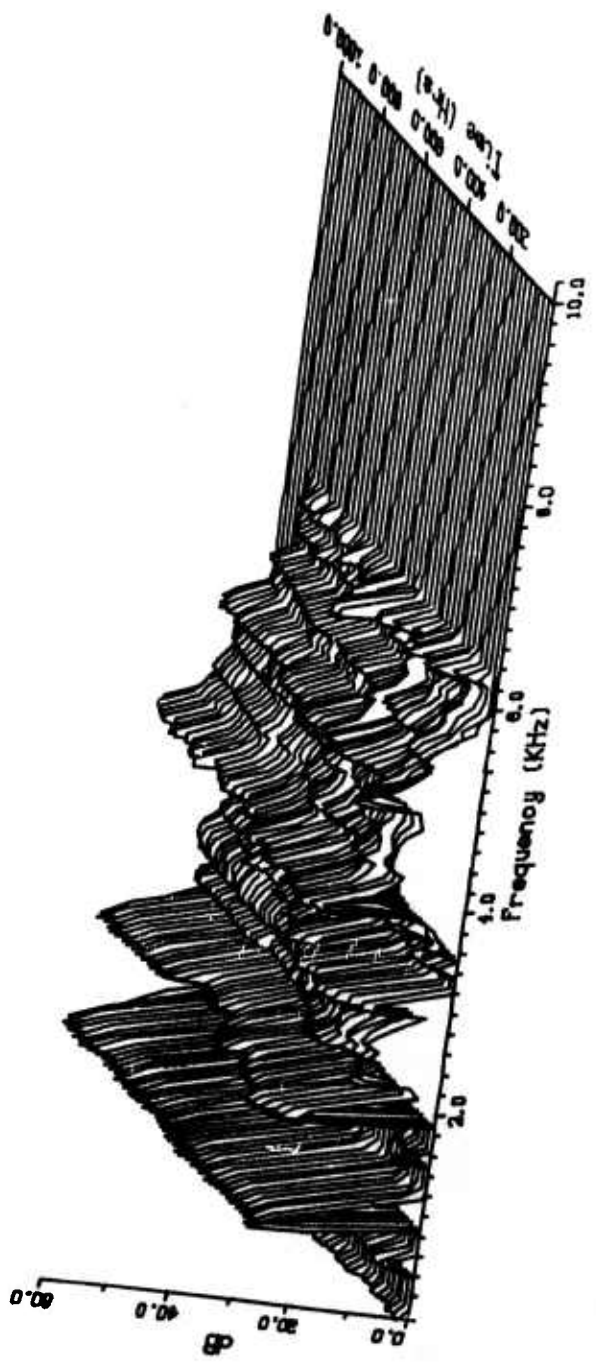


Figure 58. Overall View of BG Vibration Data Base, Skew Accelerometer.

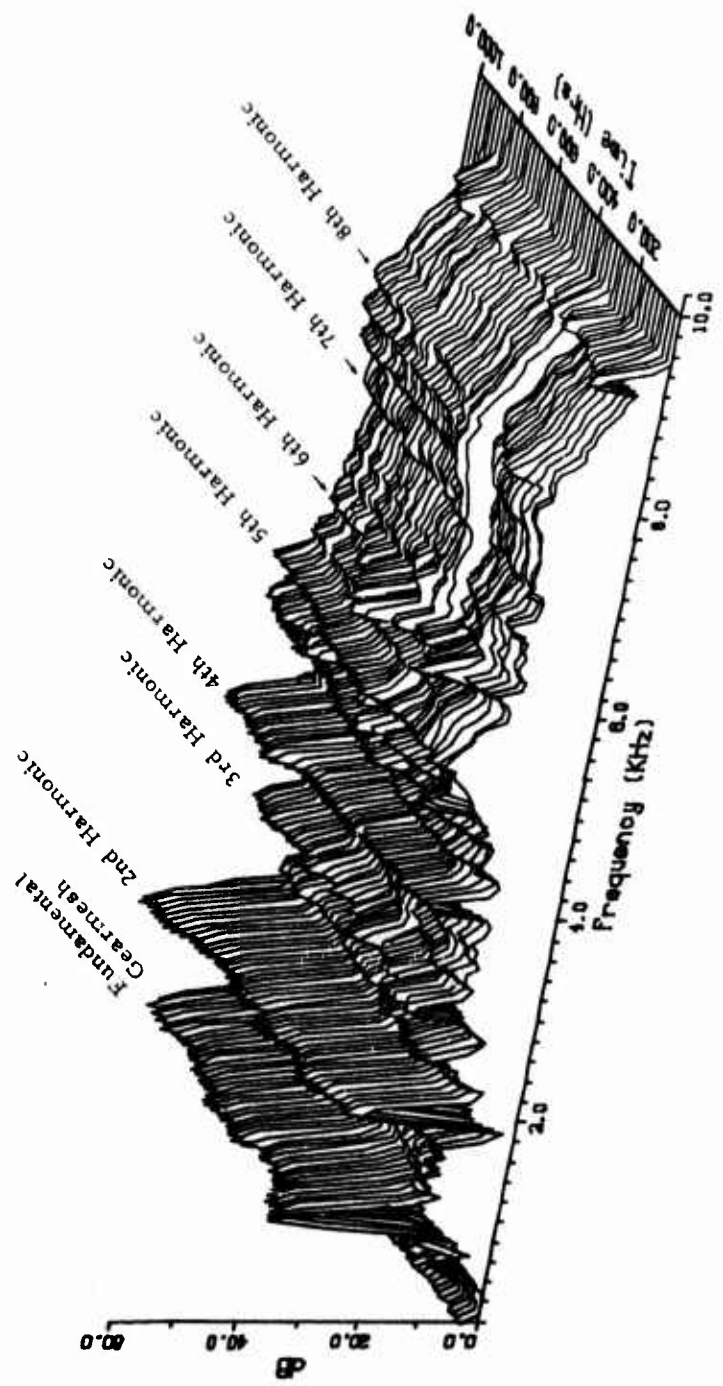


Figure 59. Overall View of BG Vibration Data Base,
Output Lateral Accelerometer.

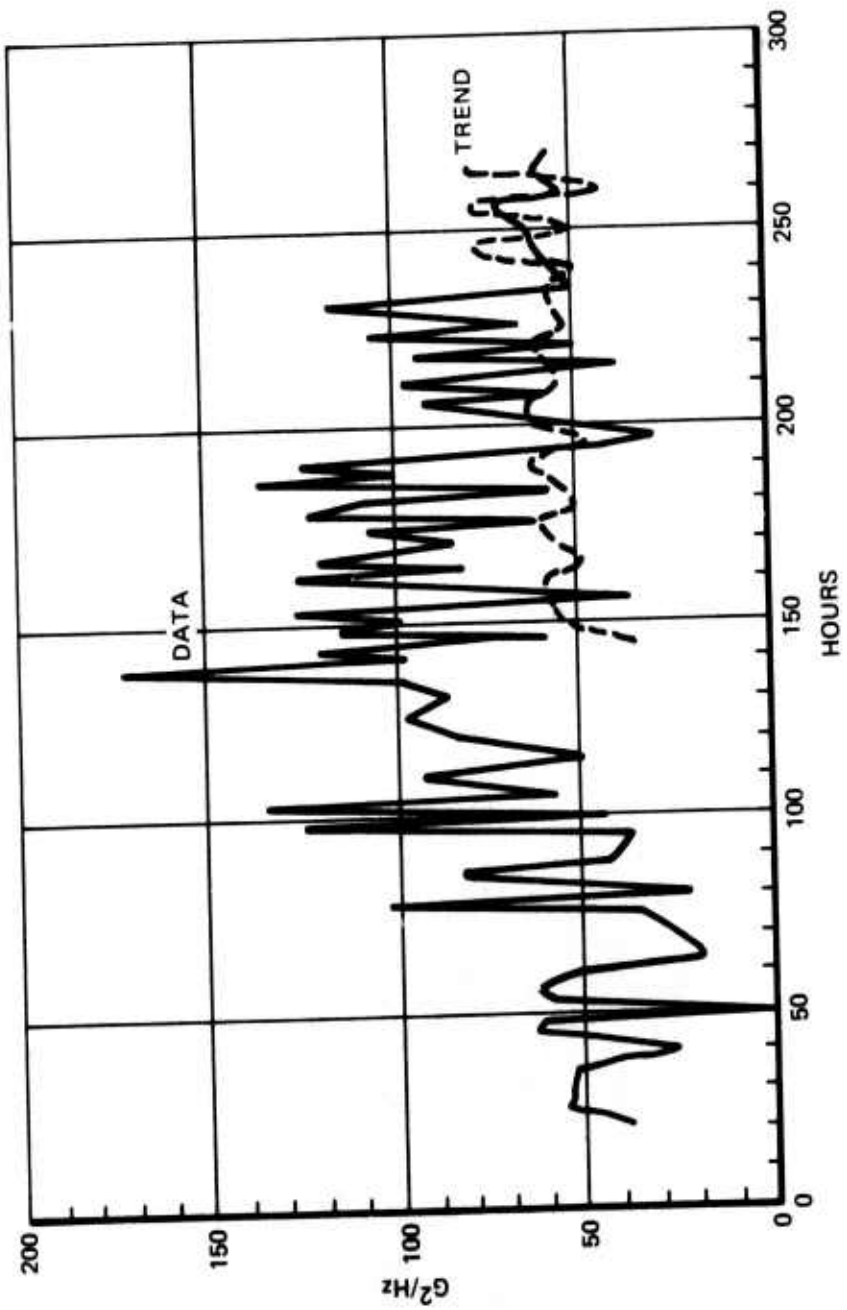


Figure 60. Prognostic Trend of BG Gearbox, Output
Lateral Accelerometer, 2031 Hz.

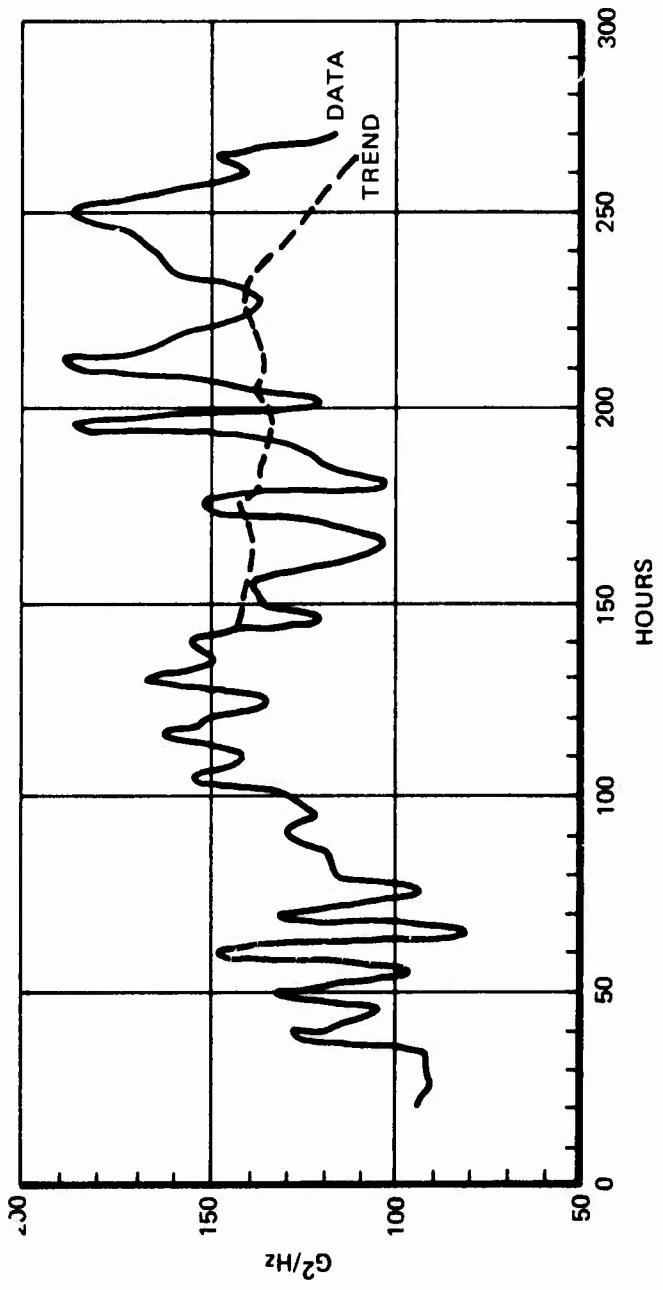


Figure 61. Prognostic Trend of BG Vibration Data,
Output Lateral Accelerometer, 4140 Hz.

and 270 hours was based on data during the test interval between 20 and 148 hours.

Figure 61 is a plot of the time history of the signal for the frequency bin at 4140 Hz. Though this frequency bin had a Z-score of only 1.8 at test hour 275, its Z-score increased to 4.7 at hour 450. For the most part the LMS prediction of future data trends based upon the data obtained during hours 20 to 140 was within 3 dB of the actual data.

Since the BG gearbox was on the verge of catastrophic failure prior to testing, the sensor data collected during the tests was of little value to this prognostic effort.

Correlation of Sensor Outputs With Mechanical Condition

The oil debris monitors were not used and the shock pulse analyzer was not available during the BG gearbox tests. The oil temperature sensor and ultrasonic RMS accelerometer showed no significant changes in output over the test interval. The output duplex bearing (BG-4) had an initial dynamic noise level of 16.5 db and raceway wear of 140 μ in. This was an extreme wear condition prior to test. The SOA showed a relatively high concentration of iron throughout the test period. The presence of tin, lead and nickel partway through the test period indicated that unusual wear was occurring, probably in the bronze ball retainer and stainless steel balls and raceways of the output duplex bearing. The final test inspection showed a 2 db increase in noiseband level for the output duplex bearing (BG-4) and 150 μ in of raceway wear. The low-frequency vibration data from the input and output duplex pairs exhibited the same structure as the data from the BB gearbox, in that the energy in the high-frequency components increased with time and new high-frequency components appeared with time. The greatest energy shift in the vibration spectra was observed in the output of the accelerometer on the output duplex pair which was the bearing with the worst initial and final wear.

Summary of BG Gearbox Test Results

Though the ODM's were removed for the BG gearbox tests, the oil circulation system was attached to the gearbox and contributed to the dilution of the metallic particle concentration. Because of this, the SOA produced no trendable data. The low-frequency vibration data from the input and output duplex pairs did undergo some rather dramatic changes during the test period. However, the trending

techniques developed for this program could not be fitted to any of the frequency bins selected, because of the short-term fluctuations which occurred throughout the test period. This gearbox was in an advanced stage of wear at the beginning of the tests and was not expected to yield good prognostic data.

However, the vibration data obtained from this gearbox should be trendable. Future efforts should be devoted to developing new analytical techniques for determining the relationship between the mechanical condition of the BG gearbox and the change in structure observed in the vibration spectra.

Because the output duplex bearing (BG-4) exhibited extreme wear in its initial condition, it was impossible to determine the contribution of the bad gear (which was the subject of this test) to the metal found in the SOA and to the changes observed in the low-frequency vibration data.

BAD BEARING TWO (BBT) GEARBOX TESTS

Gearbox BBT was tested after the second HT test period. This gearbox had 1200 hours of prior operational use and was selected for testing because of indications that it had an incipient failed output duplex bearing pair. The total cumulative test time of 1023 hours was divided into two test intervals. The first test interval lasted 407 hours and produced 407 hours of trendable data. The second test period lasted 616 hours and yielded 615 hours of trendable data. One hour of data was lost when the test cell did not shut down on command because of a failed logic gate.

Mechanical Condition of BBT Gearbox

The BBT gearbox was inspected three times during the test program. A detailed account of the inspection results is given in Appendix II.

The first inspection was conducted prior to testing and served to document the initial condition of the gearbox. Visual examination of the ball and roller bearings indicated that they were in fair condition, with wide ball tracks, electrical pitting and denting, and light to moderate wear. Dynamic noise tests indicated heavy wear for both input and output duplex bearings, with extreme local damage in the input duplex pair and light to negligible local damage in the output duplex pair.

At the end of the first test interval (407 hours), another gearbox

inspection was performed. Visual inspection of ball and roller bearings indicated an overall fair to poor general condition, with scoring, heat coloration, pitting and denting. Dynamic noise tests indicated an overall improvement in the condition of the input duplex pair. This was probably due to the removal of the extreme local damage which may have been caused by a particular rough spot which was smoothed out during testing. The output duplex pair continued to deteriorate, going from a heavy general wear condition to a condition of extreme wear. The roller bearings showed increased signs of wear, evidenced by circumferential wear lines, moderate to heavy wear, and pitting and denting.

The final gearbox examinations occurred at the end of the second test period (an additional 616 hours). By this time the gearbox had been subjected to over 1000 hours of testing at a 40-hp load. Visual examination of the ball and roller bearings indicated a poor condition, with moderate to heavy wear, transverse vibratory markings, and corrosive stains. Dynamic noise testing indicated continued bearing deterioration, especially in the output duplex pair, where the general wear was classified extreme and the local damage moderate (increasing from negligible).

At test hour 246 of the second test period, the input coupling of the gearbox failed. This is a gear-type coupling designed to accommodate shaft expansion and misalignment. The splines in the outer portion of the input coupling (the portion supplying power to the gearbox) fractured, allowing the high-speed test cell jack shaft to spin freely. Figure 62 illustrates a cutaway section of the outer part of the coupling, detailing the nature of the failure. This coupling is part of the gearbox and not a part of the test cell.

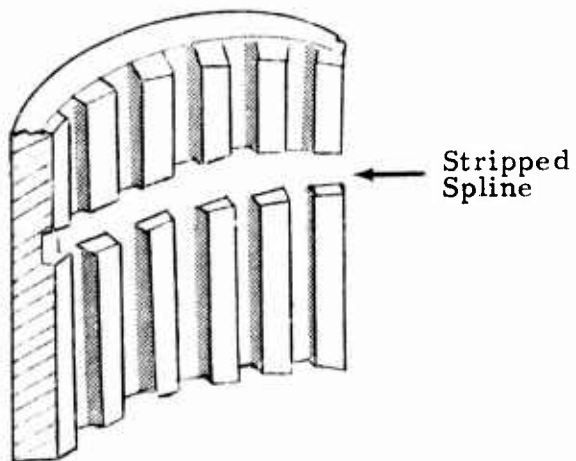


Figure 62. Cutaway Sectional Illustration of Failed Input Coupling.

Figure 63 shows the failed coupling alongside a good coupling for comparison purposes. Note the stripped spline halfway down the coupling. The defective coupling was replaced with a good one from another gearbox, and testing resumed.

At the 550-hour point of the second test interval, snapping sounds occurring at 1-minute intervals were detected as emanations from the gearbox drive train. Though we were unable to locate the source of the sounds, we suspected they were originating in the chain coupling between the gearbox output shaft and the hydraulic pump. During the gearbox teardown at the end of the second test period, two small pieces of steel wire were found in the area of the pinion gear and the input bearing assembly. Elemental analysis of the wire in the scanning electron microscope identified the wire as type 302 to 304 stainless steel. This conclusion was based on measurements of the proportions of iron, chromium and nickel content of the wire. How the wire found its way into the gearbox is unknown, but we suspect it to be part of the safety wire used to secure the oil filler tube to the gearbox, (see Figure 11 for details).

The ring gear had a fair wear pattern, but the teeth were badly galled. Traces of steel splinters were found inside the box. The pinion gear (which rotates 2-1/2 times as fast as the ring gear) was very badly galled - approximately twice as bad as the ring gear.

Spectroscopic Oil Analysis (SOA)

The circulating oil system and the oil debris monitors used during tests conducted on previous gearboxes were not used on the BBT gearbox due to repeated malfunctions of the ODM's. As a result, the total volume of oil used to lubricate the gearbox dropped from 800 ml to 100 ml. The extra 20 ml above the 80 ml required by the gearbox was used to fill a small drain line which was connected to a drain valve at the bottom of the gearbox. The drain line and valve enabled us to change the gearbox oil without removing the protective explosion cage which was placed around the gearbox as a safety precaution.

Due to a misunderstanding between the contracting agency and the principal investigator, the procedures for taking the oil samples were not in accordance with the Army practice of taking a small oil sample every 25 hours and performing an oil change every 100 hours. The oil analysis data gathered during the testing of the BBT gearbox is shown in Figure 64. The oil samples were not taken at regular intervals, but the oil was changed at the time corresponding to each

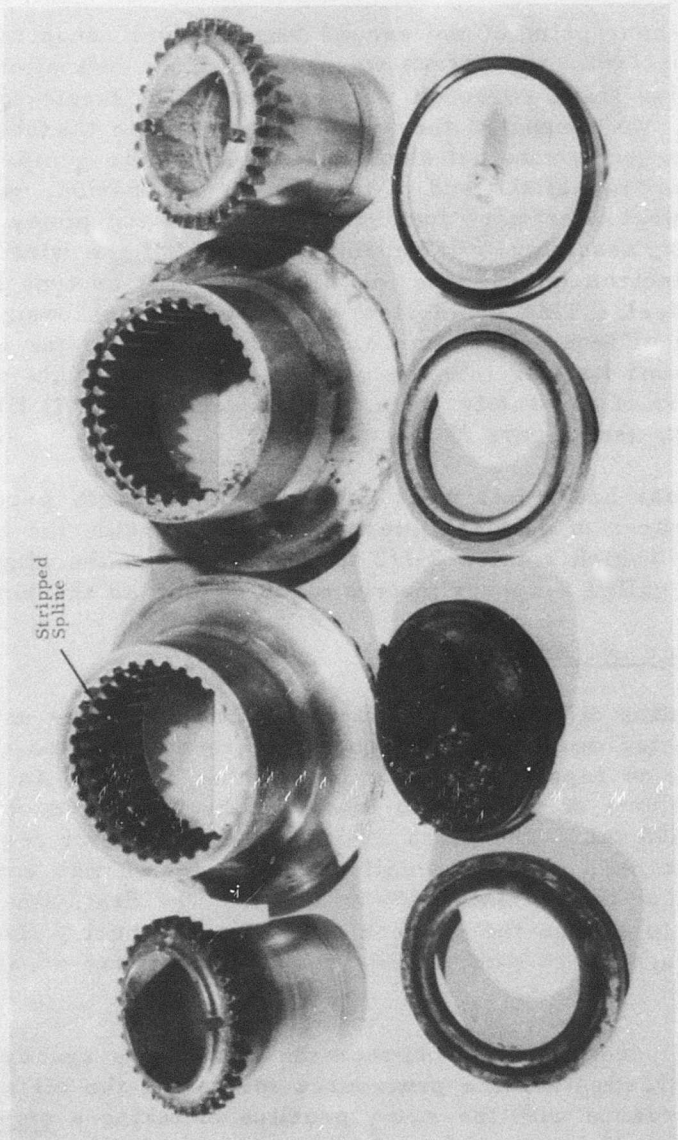


Figure 63. Comparison of Failed Input Coupling With Good Coupling.

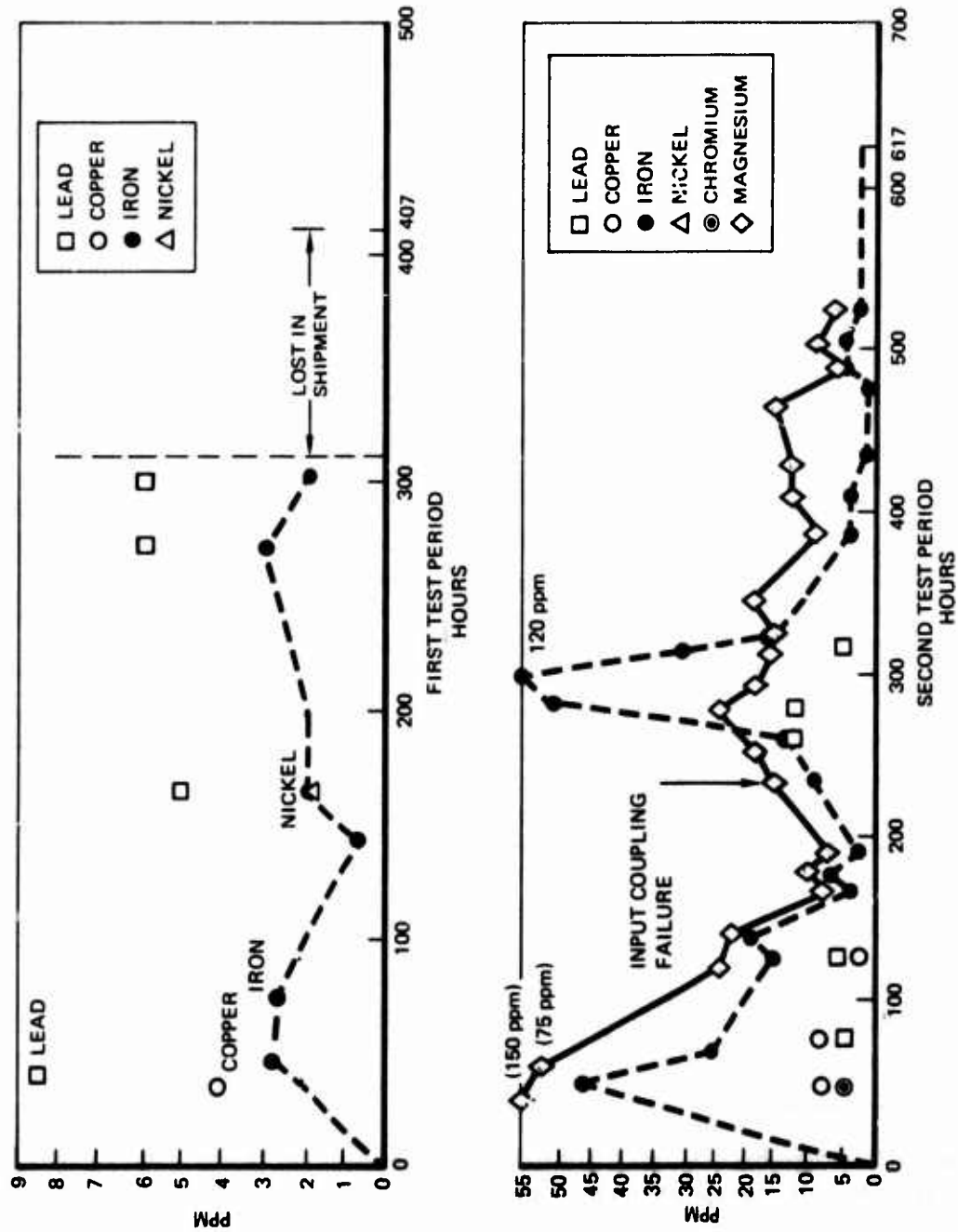


Figure 64. Summary of BBT Gearbox SOA.

data point in Figure 64. These frequent oil changes prevented the normal buildup of metallic particle concentrations with time and resulted in concentration levels which were near or below the threshold of detection of the SOA during the first test period of the BBT gearbox.

The SOA did detect two periods of extreme wear during the second test period. The iron and magnesium contents for the first 150 hours of this test period are well above the levels observed during the first test period. The appearance of traces of copper, chromium, and lead during this same test interval is indicative of bearing raceway and retainer wear, probably in the output duplex bearing. The gearbox housing is the only part of the gearbox fabricated from magnesium. The high concentration of magnesium measured by the SOA in the first 150 hours and persisting at a lower level throughout the remainder of the second test period could have been caused by scratching of the inner housing during reassembly or the continuous rubbing of the loose piece of wire in the gearbox against the housing. Since in most cases the magnesium concentration did decrease with each oil change, the wire was probably the problem. The second period of excessive wear occurred at around test hour 300. The iron content increased to over 120 ppm in just 15 hours of testing. We can only speculate that the wire had lodged in the gear teeth and, because of its hardness, it eroded the teeth. As noted earlier, the post-test inspection found excessive galling of the teeth, and the broken ends of the wire had been flattened. At the end of this interval, the gears probably broke the wire and either part or all of the wire was dislodged from the gear. From an operational standpoint, this gearbox would have been removed from further service when the presence of this high concentration of iron was detected.

Oil Debris Monitors (ODM)

The oil debris monitors and the circulating oil system were not connected during the testing of gearbox BBT.

Temperature Sensors

Gearbox oil temperature was monitored throughout both test periods, but no significant temperature changes were observed.

Ultrasonic RMS Accelerometers

Ultrasonic data was collected from the accelerometers on the input and output lateral locations on the BBT gearbox. No significant

changes were observed in the output of either sensor during either of the test periods.

Shock Pulse Analyzer

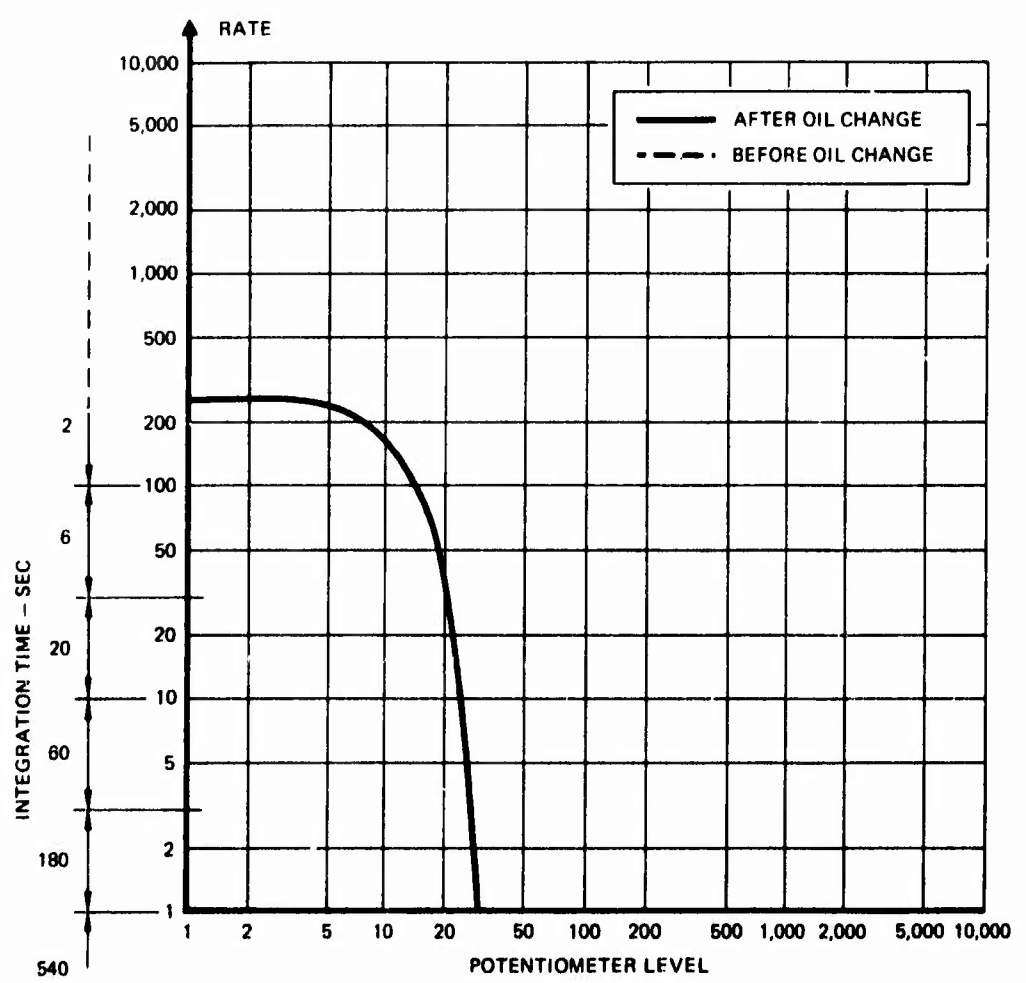
During the first test period, shock pulse data was taken just prior to taking an oil sample. In our original discussions with the manufacturer concerning the proper usage of the analyzer, we were not informed that as the oil condition degrades, the shock pulse levels usually increase and mask the information related to the true condition of the mechanical components. We observed this effect during the second test period of the BBT gearbox when we took shock pulse data before and after an oil change. The differences between a good shock profile and a used oil dominated profile are usually significant. The profile obtained with used oil usually indicates a bearing wear condition much worse than it actually is.

Figure 65 is the shock emission profile obtained from the output duplex bearing of the BBT gearbox. This data was taken at the start of the first test period with new oil in the gearbox. This curve indicates that the bearing is moderately worn but is still in good condition. Figure 66 shows the shock emission profile for the same bearing at the start of the second test period. When compared with Figure 65, we see that the maximum shock rate (related to general wear) has increased slightly, but the peak shock pulse amplitude has risen substantially, which correlates well with the results obtained from the dynamic noise tests.

Figure 67 shows the shock emission profile taken on used and new oil at test hour 75 of the second test period. A large increase in shock pulse rate normally indicates abnormal wear in the bearing. This profile was taken during the first period of excessive wear as verified by the SOA.

Figure 68 shows the shock emission profiles taken before and after an oil change during the second period of excessive wear at around test hour 300 of the second test interval. Here, again, we see large fluctuations in the profile. The gearbox produced a "high scream for a period of 30 or 40 seconds," during which time the shock pulse rate exceeded a value of 1000 and then immediately returned to normal.

Figure 69 shows the shock emission profile taken at the peak of the second period of excessive wear at slightly later than 300 hours. Note the reduction in the peak values after the oil change.



**Figure 65. Shock Emission Profile - BBT Startup,
First Test Period**

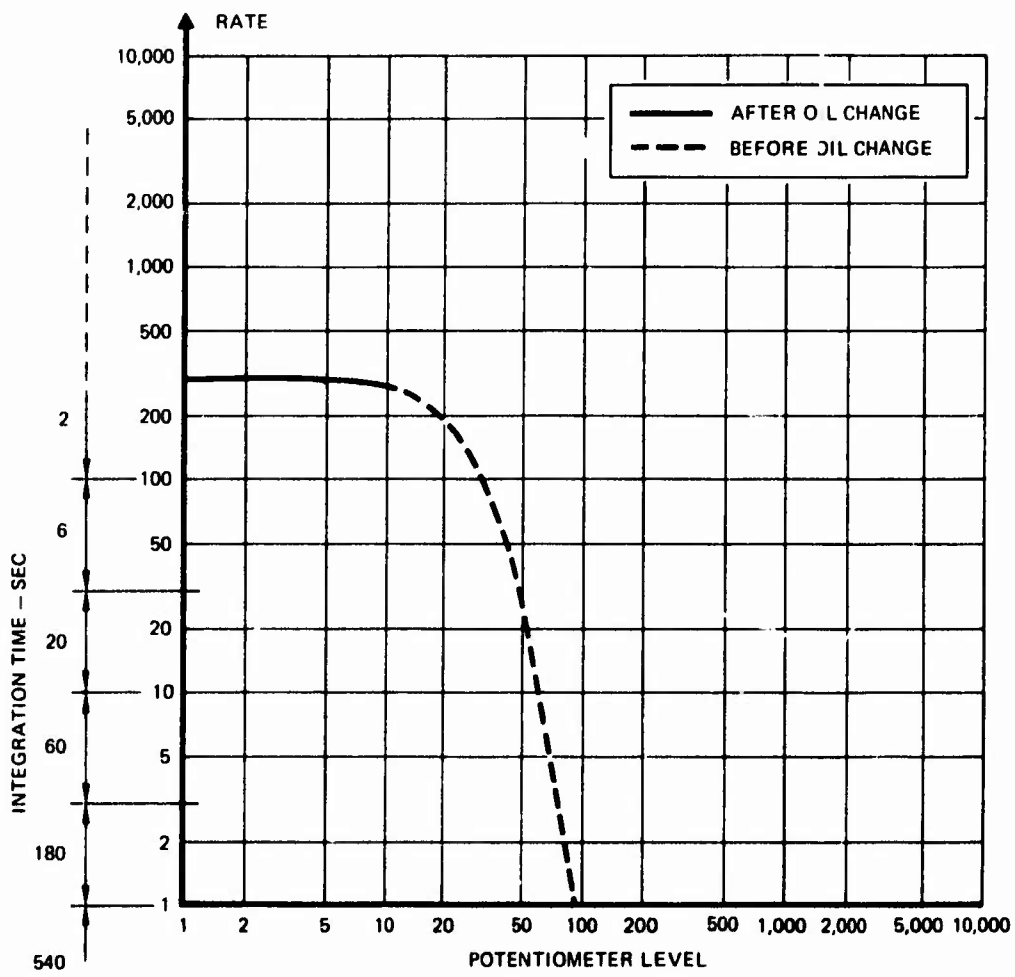


Figure 66. Shock Emission Profile - BBT Startup,
Second Test Period.

SPV = 15° After 30 minutes of test.

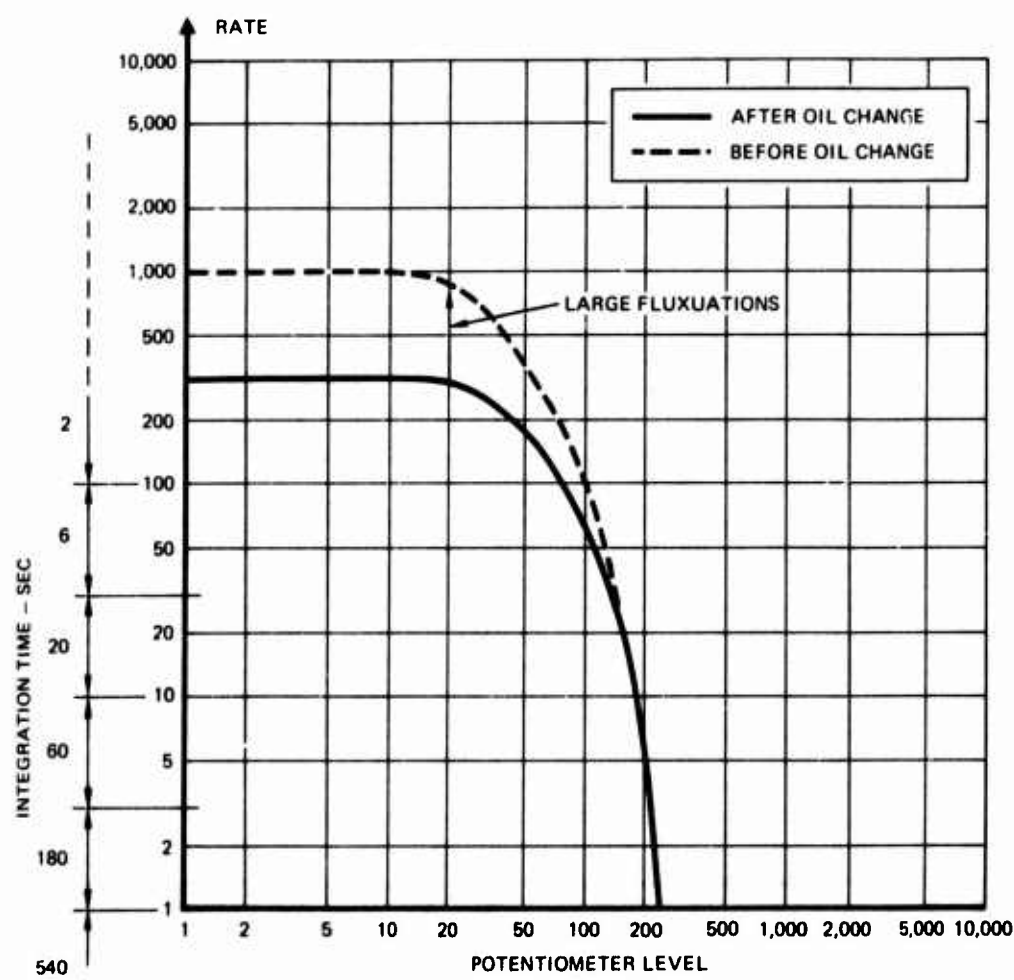


Figure 67. Shock Emission Profile - BBT 75 Hours Into Second Test Period.

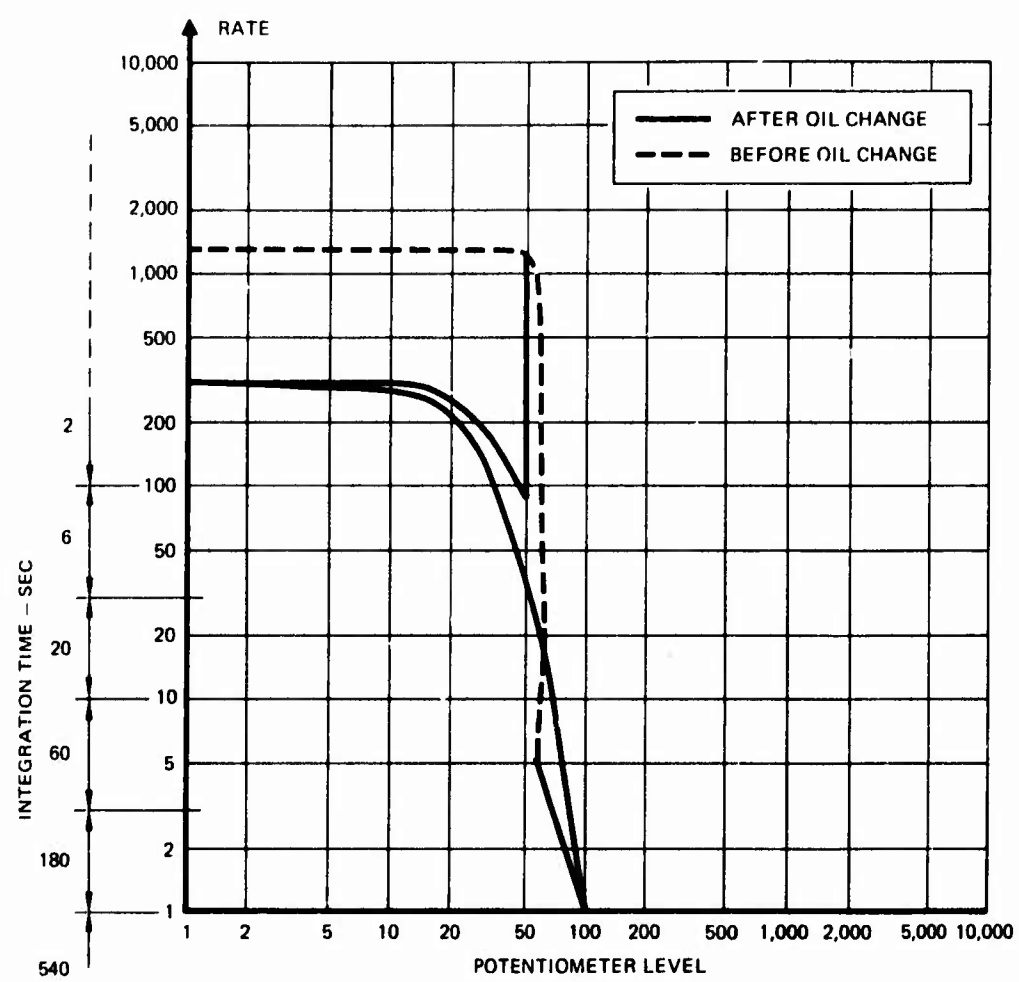


Figure 68. Shock Emission Profile - BBT, 300 Hours Into Second Test Period.

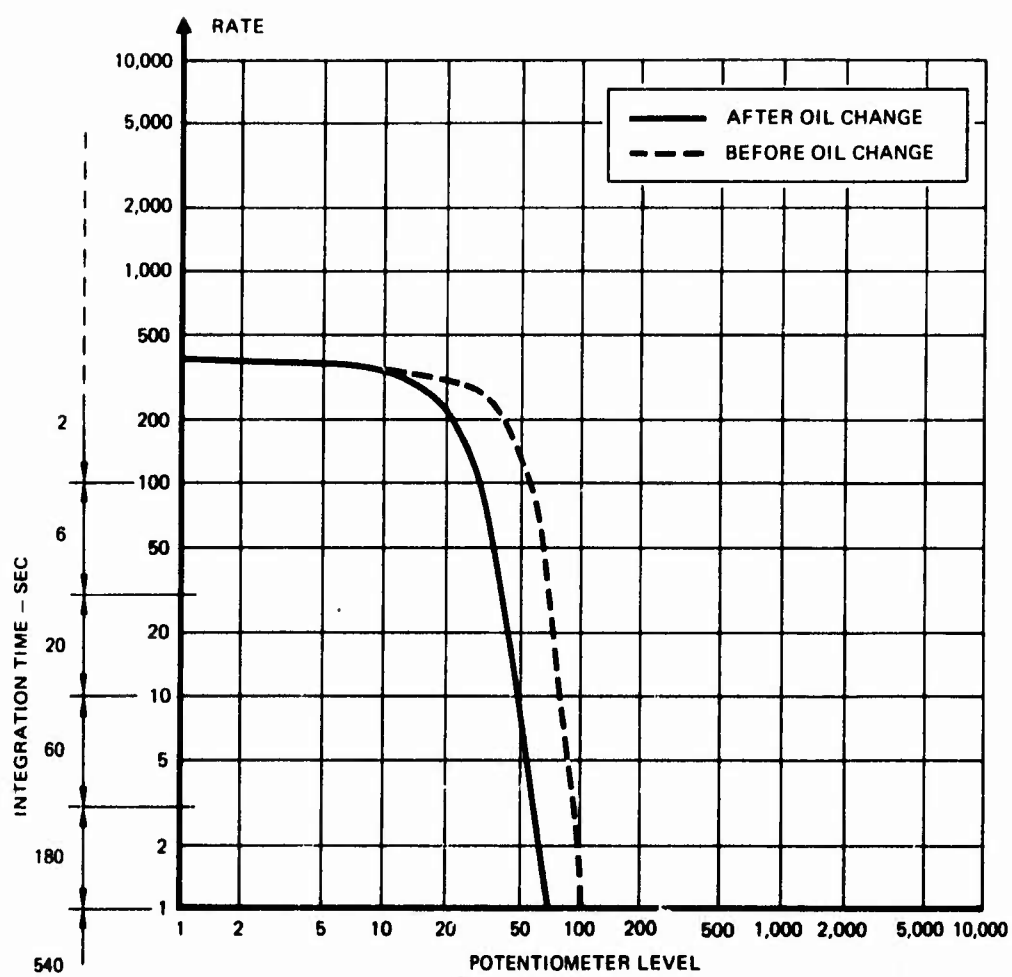


Figure 69. Shock Emission Profile - BBT, Peak of Wear Period.

Figure 70 shows the final shock emission profile taken at test hour 599. In comparing this final profile with the starting profile shown in Figure 66, we can find only minor differences. We know from the mechanical measurement made during and after testing that the output duplex bearing which was being monitored by the shock pulse analyzer was in an extremely worn condition. The shock emission profile taken near the end of the test does not indicate excessive wear of this bearing. However, the dynamic noise levels of this bearing were relatively high at the start of testing and showed a relatively small increase also at the end of the test program.

If we plot the shock pulse value (SPV) for the BBT data as manually taken with the shock emission profile, Figure 71, we observe a well-defined exponential growth in the SPV for almost 700 hours. Furthermore, this trend appears smooth and continuous irrespective of the condition of the oil or the number of times it was changed, and in spite of the fact that the gearbox was completely disassembled during the test interval.

The initial long-term SPV growth is abruptly terminated for some unknown reason after about 300 hours into the second test period. The SPV drops to some value which is higher than the initial value and begins to increase again with testing time. Apparently, the SPV builds up until the gearbox components can no longer operate in the mode which causes this large-amplitude shock, and it abruptly changes its operating mode. The frequency of these SPV growth periods appears to increase as the bearing deteriorates.

The data plotted in Figure 71 was taken manually, and the true shape of the curves and frequency of occurrence of the repetitive exponential behavior of the SPV cannot be determined. Though the SPV data was collected continuously throughout the BBT tests by the automatic data collection system and stored on magnetic tape, there was not sufficient time or funds available to analyze this data base on this contract.

As will be shown in the next section, this short-term repetitive exponential behavior can also be seen in the low-frequency vibration data.

Low-Frequency Vibration Data

Low-frequency vibration data was collected from accelerometers placed in the input lateral, skew, and output lateral positions of the BBT gearbox. Figures 72, 73 and 74 show the overall time histories

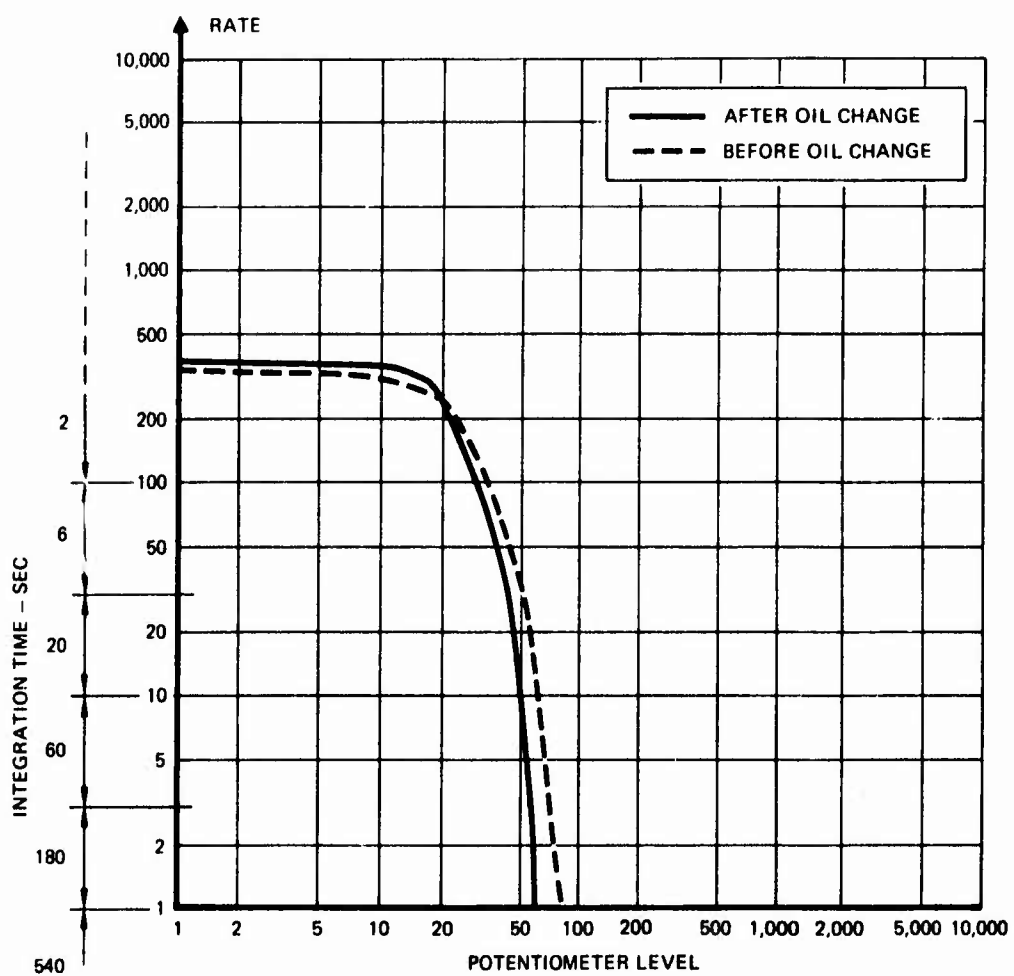


Figure 70. Shock Emission Profile - BBT, 599 Hours Into Second Test Period.

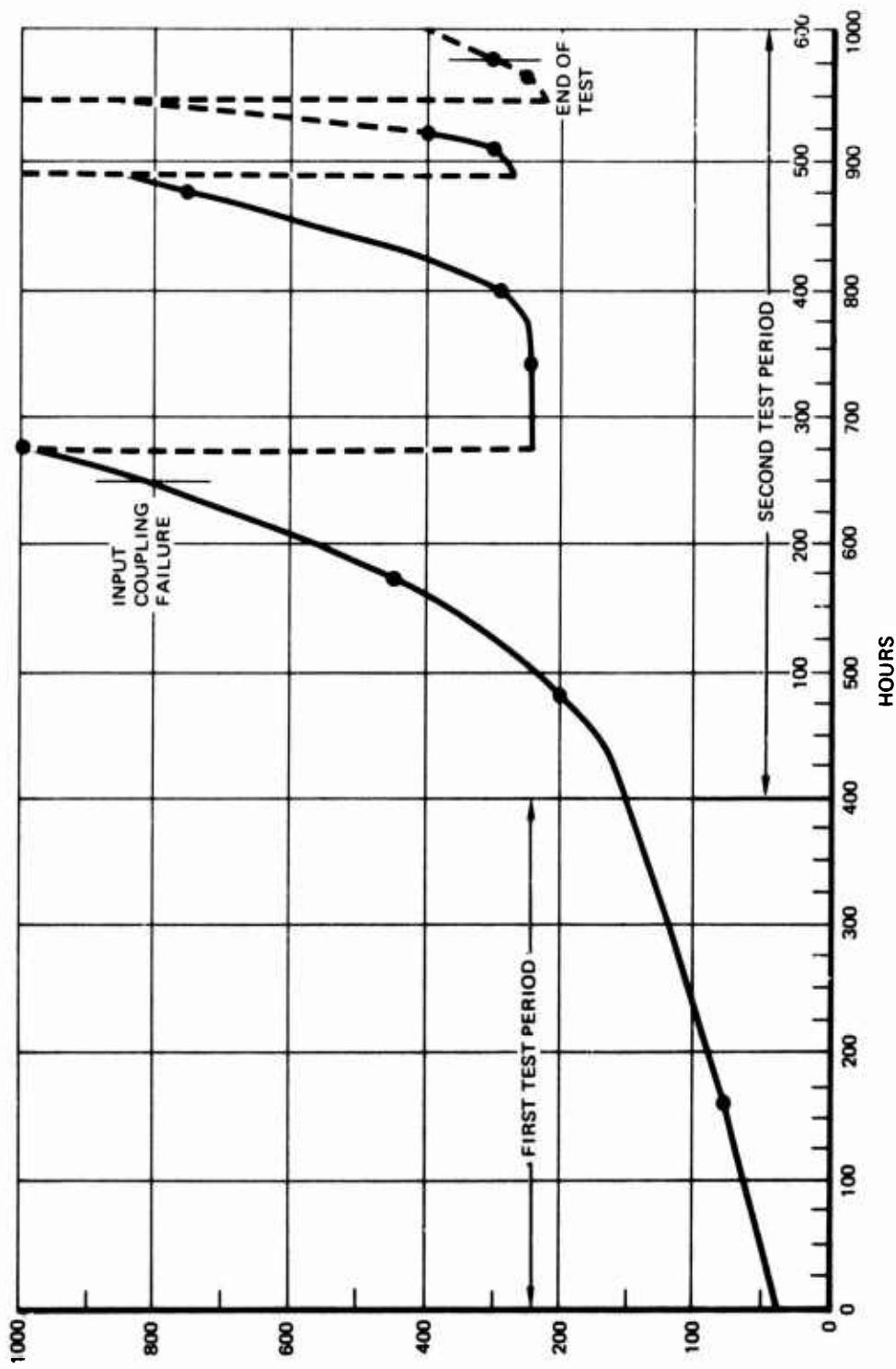


Figure 71. Shock Pulse Value for BBT.

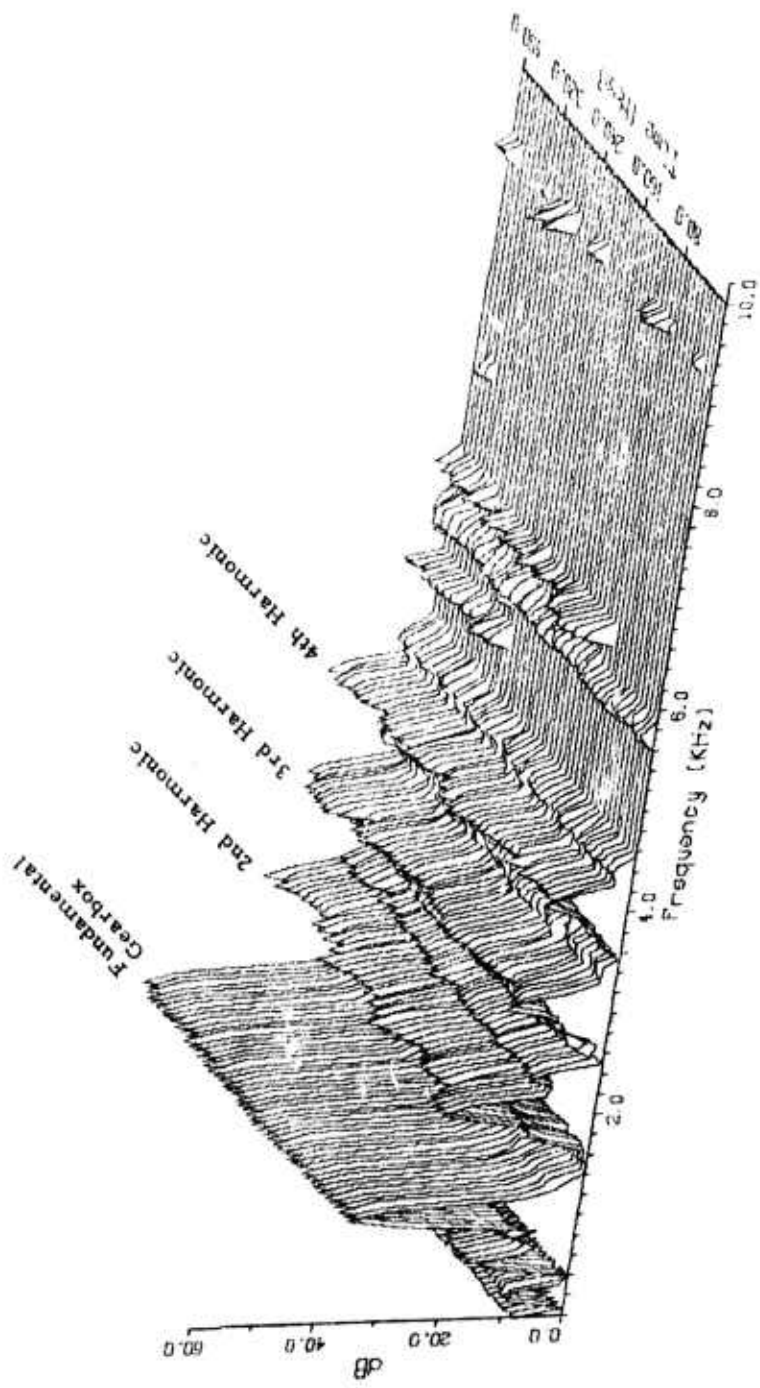


Figure 72. Overall View of BBT Vibration Data Base,
Input Lateral Accelerometer.

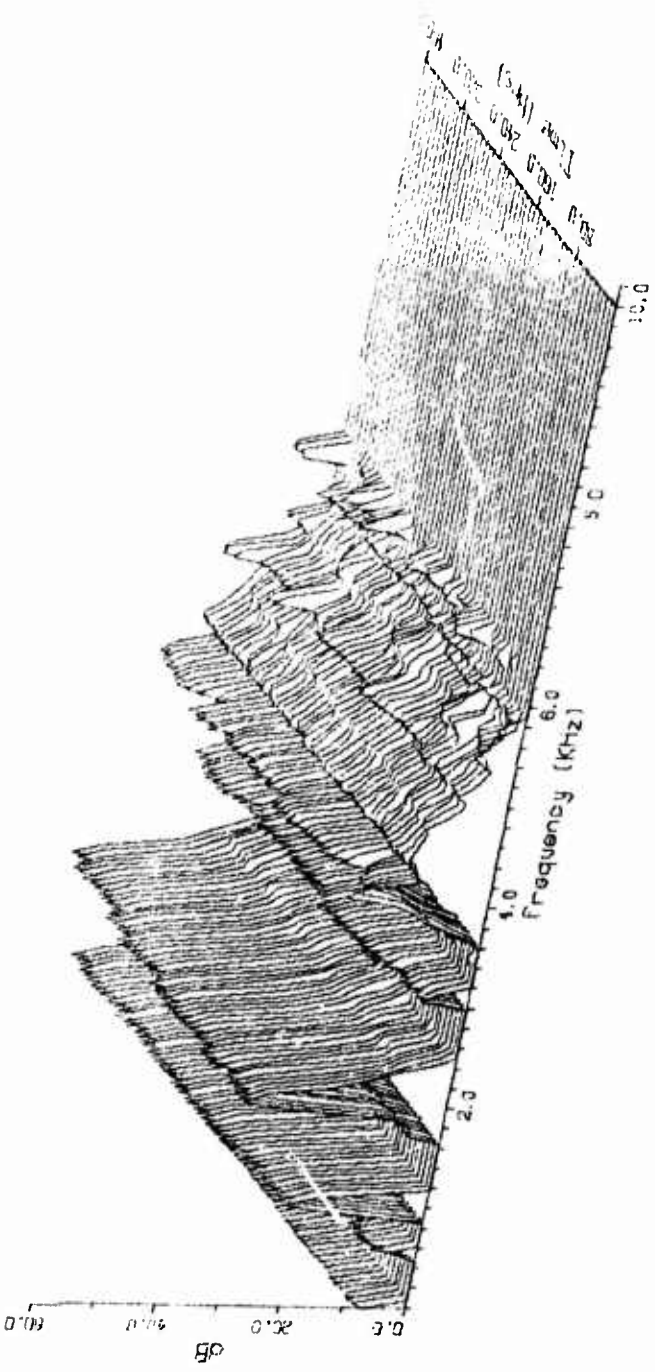


Figure 73. Overall View of BBT Vibration Data Base, Skew Accelerometer.

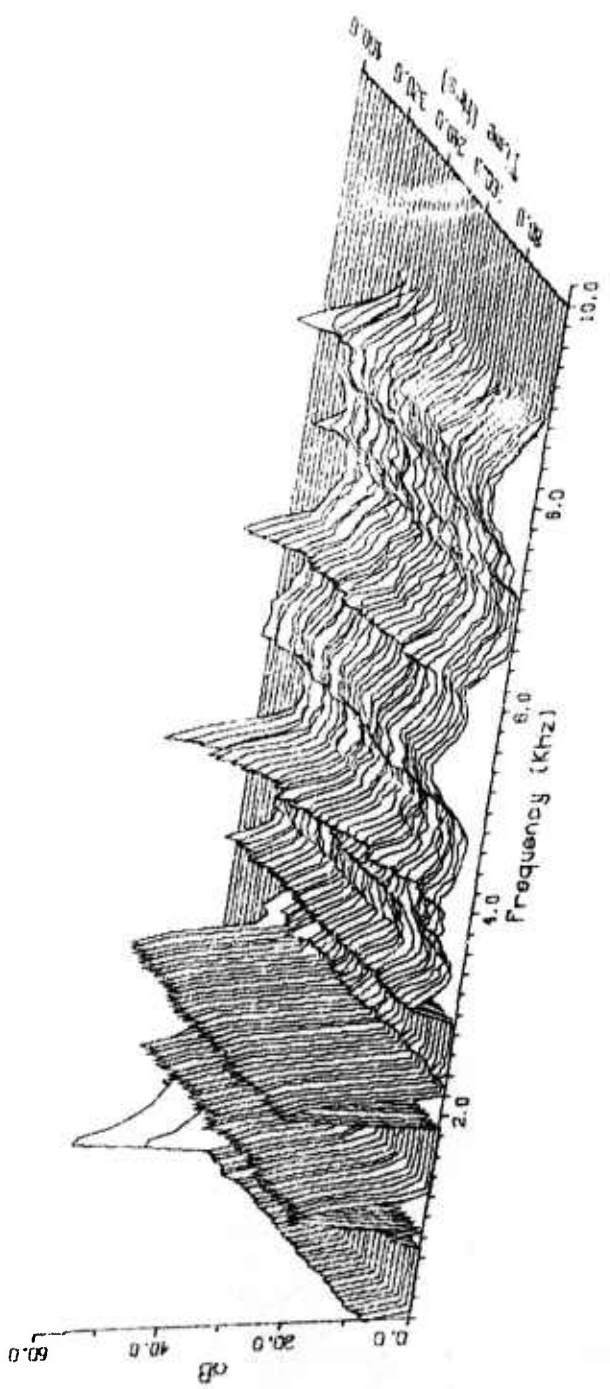


Figure 74. Overall View of BBT Vibration Data Base,
Output Lateral Accelerometer.

of the vibration signals from these sensors. Though the vibration data base does include vibration spectra for the entire BBT test period, analysis time was not available to process the data obtained after 400 hours of testing.

As mentioned in the previous section on the shock pulse analyzer, repetitive exponential signal buildups followed by rapid decay have been observed in the BBT gearbox vibration data. This similar behavior can be seen in Figure 75, which is a plot of the time history of the energy in frequency bin 4219 Hz of the vibration spectrum obtained from the output lateral accelerometer during the first test period of the BBT gearbox. As in the case of the shock pulse value, the vibration energy reaches its maximum value in a shorter period of time in each successive interval. At least for this frequency bin, the time difference between peaks seems to follow an exponential relationship, with each successive peak substantially larger than the previous peak. How this repetitive exponential behavior of the energy in the vibration signals relates to the mechanical condition or wear pattern of the gearbox components is currently not understood. However, if further analysis of the vibration data does verify the existence of a relationship, this phenomenon might prove to be a very useful prognostic tool.

When this frequency bin was first plotted and curve fitted with exponential and polynomial functions, as shown in Figure 76, the true structure of this signal was destroyed due to aliasing errors in the plotted data. The data points were represented by small boxes (\square), each box being the average of five consecutive hourly data points. The actual time history had significant short-term fluctuations which weighted the averages used in the plotting process in such a manner that the plots are not a true representation of the time history of the signal. The repetitive exponential structure of the original data can be easily destroyed by improper sampling and processing of the vibration signals. It must be strongly emphasized that proper sampling techniques must be used when data is being collected for trending purposes. It now appears that in order to obtain trendable vibration data from 90° gearboxes in advanced stages of wear, time samples must be taken at intervals of an hour or less.

Figure 75 (discussed earlier) also shows how the time history of frequency bin 4219 Hz from test hour 150 to 278 of the first test period was used to predict the future test data between hours 279 and 406 using the LMS prediction technique. The predicted trend is not a good approximation to the actual data obtained for that period due

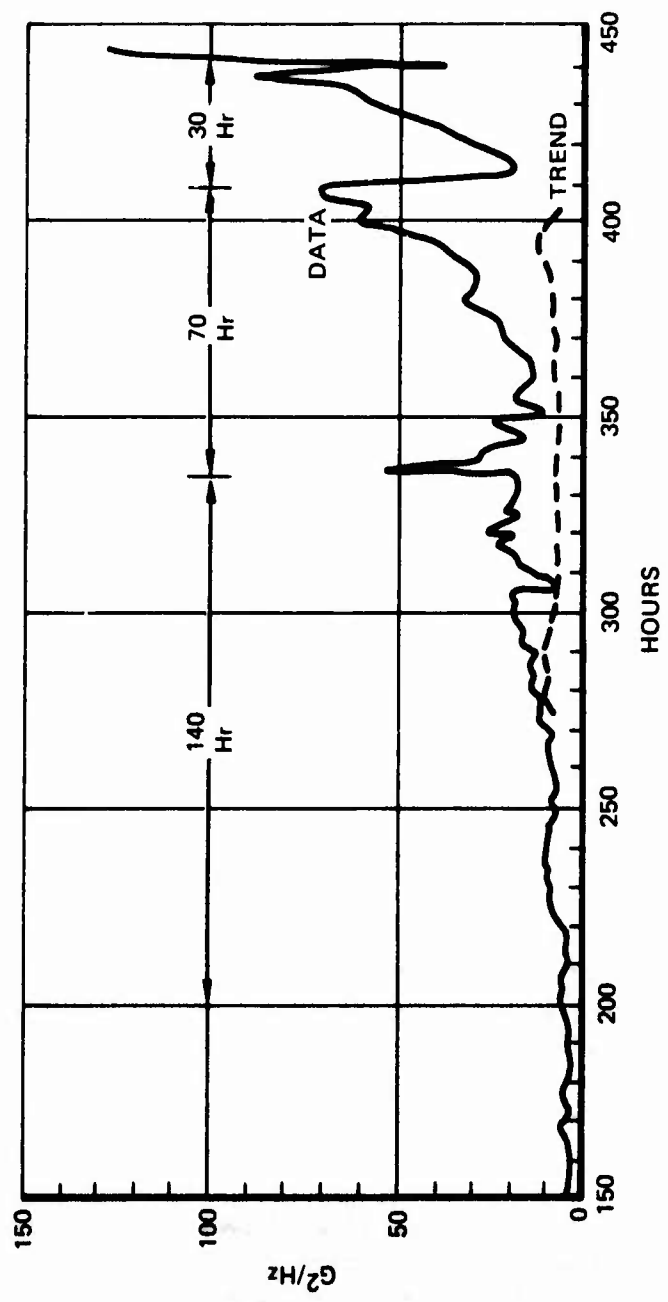


Figure 75. Prognostic Trend of BB7 Gearbox, Output Lateral Accelerometer, 4219 Hz.

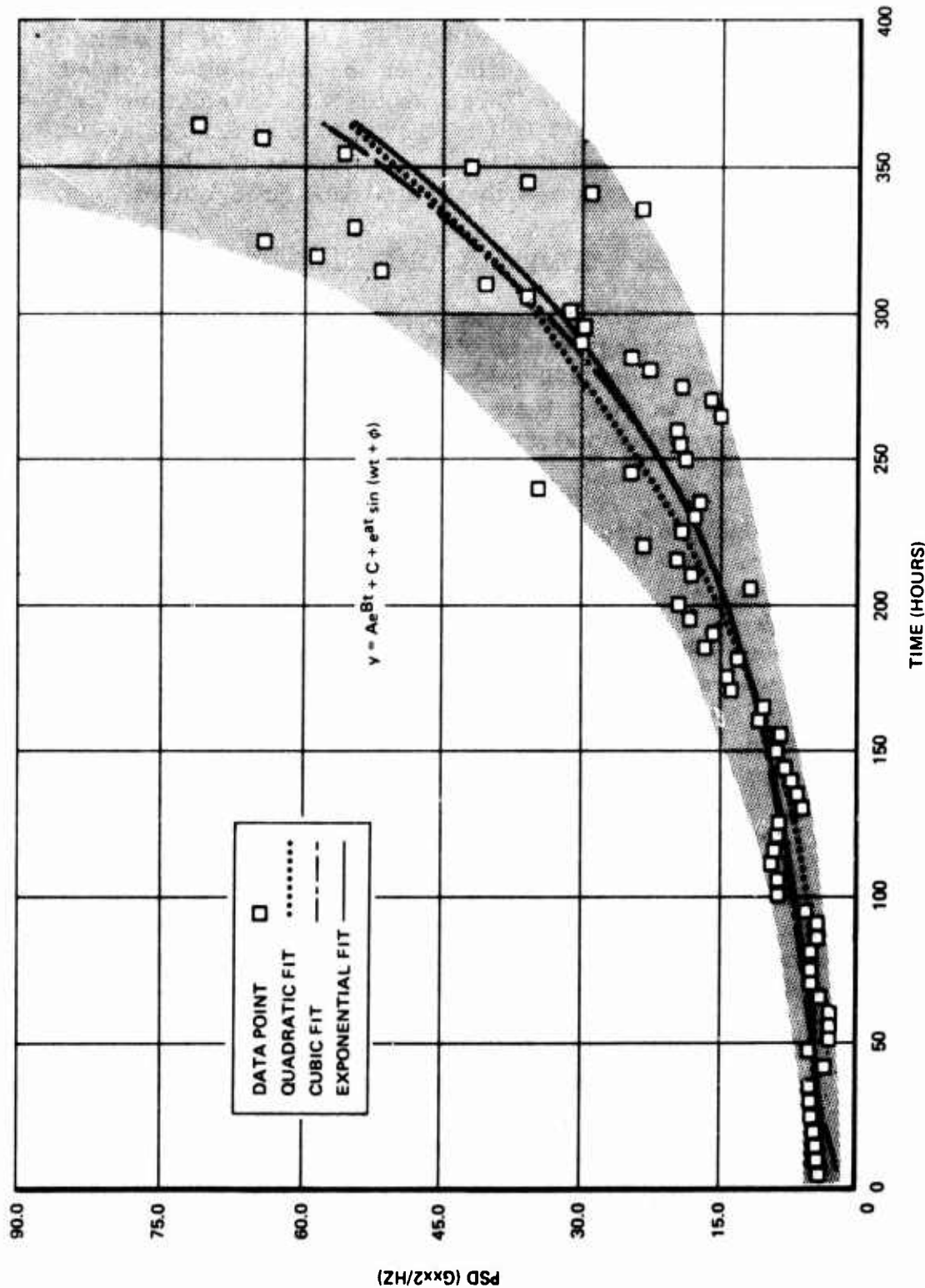


Figure 76. Aliasing Errors in Plot of BBT Vibration Data, 4219 Hz.

Note: Aliasing errors in plotted data values mask true nature of data (Figure 75) and lead to wrong formulation of trending equation.

mainly to the fact that the statistics for this data sample are non-stationary.

Figures 77 and 78 are additional examples of LMS trending of BBT vibration data. Figure 77 was included as an example of how effective the LMS trending technique can be when the data being trended is reasonably stationary. Figure 78 shows the LMS prediction for nonstationary frequency bin (1172 Hz) of the input lateral accelerometer. With the exception of the large transient at the 150-hour point, the predicted trend followed the actual data quite closely.

Correlation of Sensor Outputs With Mechanical Condition

The oil debris monitors (ODM) and the supporting oil circulation system were removed during testing of the BBT gearbox. This reduced the oil reservoir from 800 ml to 100 ml, resulting in only a 25% dilution of the oil in these tests. The oil temperature sensor and ultrasonic RMS accelerometers showed no significant changes during the test period.

The bearings in this gearbox were less worn than those in the BB and BG gearboxes, but all showed heavy to extreme wear, with the most advanced wear observed in the output duplex pair (BBT-3, BBT-4). Though the metallic particle concentration in these tests was diluted by only 25%, the usefulness of the SOA data for prognostic trending was severely reduced because the oil was changed every time an oil sample was taken. The SOA did detect large concentrations of lead, iron, nickel and copper during the first test period, but these could not be related to excessive wear in the gearbox. The SOA data from the second test period showed large concentrations of magnesium and iron, and smaller concentrations of lead, copper, nickel and aluminum. The two stainless steel wires found in the gearbox when it was inspected after the tests probably was the cause of the abnormal iron and magnesium concentrations and made it impossible to trend the iron concentration caused by normal gear and bearing wear. This was the first test in which good shock pulse analyzer data was obtained.

However, after discovering the effect of used oil on the shock pulse rate data, the normalized shock pulse curves showed no change from the beginning of the first test period to the end of the second test period. It appears that the 3-db increase in noise level of the output duplex bearing, as measured in the post-test inspection, was below the sensitivity of the shock pulse analyzer. The shock pulse values, however, seem to show a repetitive exponential structure in which the shock pulse level rises exponentially with time to a

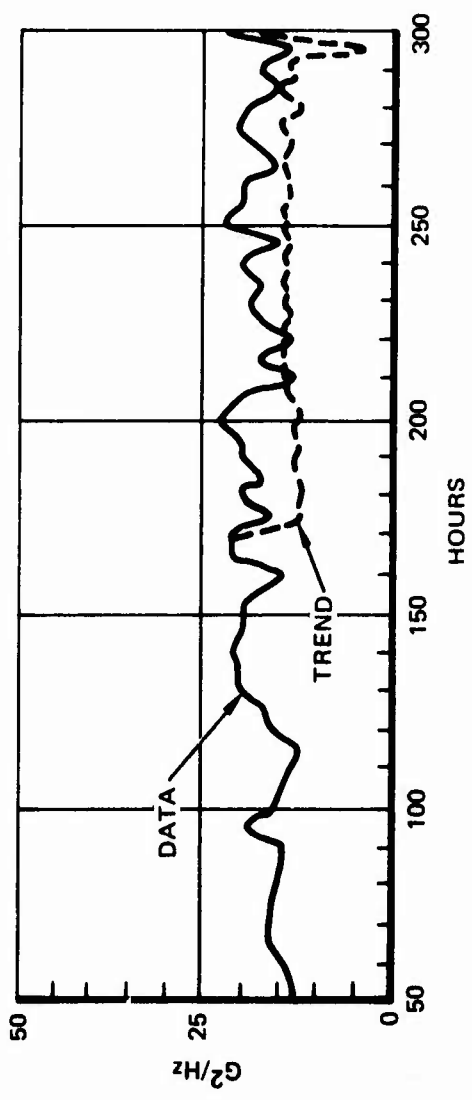


Figure 77. Prognostic Trend of BBT Gearbox, Skew Accelerometer, 4297 Hz.

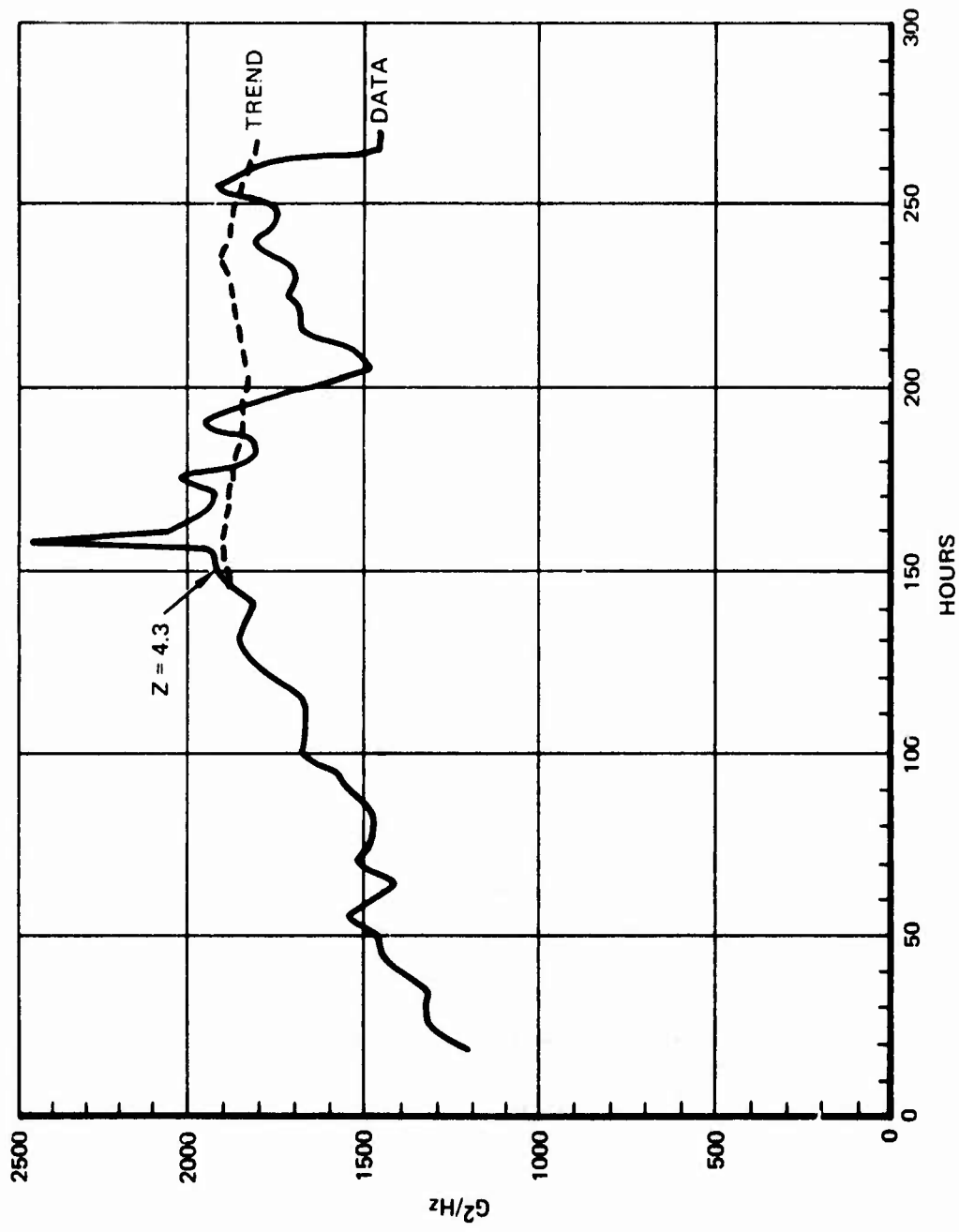


Figure 78. Prognostic Trend of BBT Gearbox, Input Lateral Accelerometer, 1172 Hz.

maximum, drops to some higher minimum initial value, and rises again. The time intervals for the exponential rise and fall decrease with time. This phenomenon can also be observed in the low-frequency vibration data. However, it was not possible to correlate this repetitive increase and decrease in vibration energy with any other sensor outputs or with the actual wear patterns of the gearbox components.

Summary of BBT Gearbox Test Results

The SOA data cannot be used for trending because of the wire which inadvertently found its way into the gearbox prior to the second test period and the fact that the oil was replaced every time a sample was taken for the SOA.

This gearbox provided more shock pulse analyzer data than any of the others. However, when the shock pulse profiles were corrected to account for the presence of used oil, the profiles taken at the beginning and end of the tests were essentially the same. The shock pulse analyzer appears to be an excellent oil debris monitor, at least for a gearbox in the same advanced wear condition as BBT. Metal particles in the oil can cause a dramatic increase in the shock pulse rate and give a good indication that wear is occurring at that particular moment. In this respect the shock pulse analyzer might be a potentially valuable diagnostic tool. The entire shock pulse value and low-frequency accelerometer data bases were not completely processed because of a lack of time. However, a cursory analysis of the parts that were processed shows that both signal structures exhibit a repetitive exponential increase and sharp decrease in vibration energy with time, with a decreasing time interval between the start and termination of the successive exponential curves. Though this phenomenon could not be correlated with the mechanical condition of the gearbox at any particular point in time, it could provide an insight into the nonstationary characteristics of gearbox vibration signals. The limited data analyzed does appear to have some type of trend, and if appropriate analysis techniques are developed, this behavior might prove to have some prognostic value. There is no question that the rest of the shock pulse data and vibration data bases should be processed and analyzed in any future analytical effort.

BAD BEARING THREE (BB3) GEARBOX TESTS

Gearbox BB3 (Bad Bearing 3) was the last gearbox tested under this contract. A total of 1100 test hours were accumulated on BB3 which

yielded 1086 hours of usable data. Fourteen hours of data were lost when the test cell failed to shut down properly due to a sticking control relay. The gearbox was loaded to 40 hp on the output shaft, and the gearbox input rpm was 4150.

Mechanical Condition of BB3 Gearbox

Initial visual inspection of the input duplex pair revealed it to be in fair condition, with light scratches, pits and dents and overall moderate wear. Dynamic noise testing verified the visual examination by indicating a moderate general wear condition with light local damage.

Initial visual inspection of the output duplex pair revealed an overall poor bearing condition, with moderate to heavy wear and considerable pitting and denting. Dynamic noise testing indicated heavy to extreme wear, with only light local damage.

Initial visual inspection of the input and output roller bearings showed them to be in fair to poor condition, with light to moderate wear and evidence of fatigue spots on some of the rollers.

After gearbox BB3 was inspected again to determine how the wear had progressed, half of the input duplex pair, BB3-1, had degraded slightly, with an increase in local damage from light to moderate. The other half of the input duplex pair, BB3-2, degraded from moderate wear to heavy wear, with evidence of heat coloration in balls and inner race, and considerable pitting and denting of the balls with visibly out-of-round ball retainers. Dynamic noise testing indicated heavy wear with light local damage. The output duplex pair showed heavy to extreme wear at the start of the tests and showed extreme wear at the end of the test period. The roller bearings were in poor condition, with moderate to heavy wear, a few fatigue spots, and some heat discoloration.

Detailed information concerning the mechanical condition of the BB3 gearbox is given in Appendix B.

Spectroscopic Oil Analysis (SOA)

The circulating oil system was not used during the test of BB3. The filler tube and drain pipe arrangement discussed in the SOA section of the BBT gearbox test results was utilized to supply lubricant to the gearbox under test. The same oil sampling procedures described for BBT were used with BB3 (i.e., oil samples were taken at

regular intervals, and the oil was changed every time a sample was taken).

Figure 79 summarizes the results of the SOA. The presence of small amounts of copper in the first two oil samples probably does not constitute a significant wear problem. The very high level of magnesium is probably due to contamination of the gearbox at assembly time, since the magnesium concentration decreases after several oil changes. The SOA indicates excessive gear wear between test hours 650 and 850, since there was no indication of copper or chromium in the oil after the first 100 hours. These metals are normally present when there is excessive wear in the bearings.

Oil Debris Monitors (ODM)

The oil debris monitors and the circulating oil system were not connected during the testing of the BB3 gearbox.

Temperature Sensors

Due to lack of time and funding, the output from the oil temperature sensor was not analyzed.

Ultrasonic RMS Vibration Data

This data was collected and stored on magnetic tape but was not analyzed.

Shock Pulse Analyzer

Shock emission profiles were collected before and after each oil sample that was taken for the SOA. Representative examples of this data are shown in Figures 80, 81, 82 and 83. Figure 80 shows the shock pulse data after the first 62 hours of running. The large change between dirty and clean oil is due mainly to the "green run" condition, i.e., the newly assembled gearbox is undergoing accelerated wear due to microscopic misalignments. As shown in the previous section on spectroscopic oil analysis, the iron content at this time is 8 ppm, but the magnesium concentration is extremely high. The shock emission profiles remained relatively unchanged until test hour 725, when the iron content jumped to 27 ppm, apparently indicating the onset of a heavy wear period. At the 800-hour point, the shock emission profile, Figure 81, does not show the earlier observed effects of used oil, despite the fact that the used oil was a dark grayish brown after only 17 hours of running between oil changes. The iron concentration at this time was 21 ppm. For the next 165

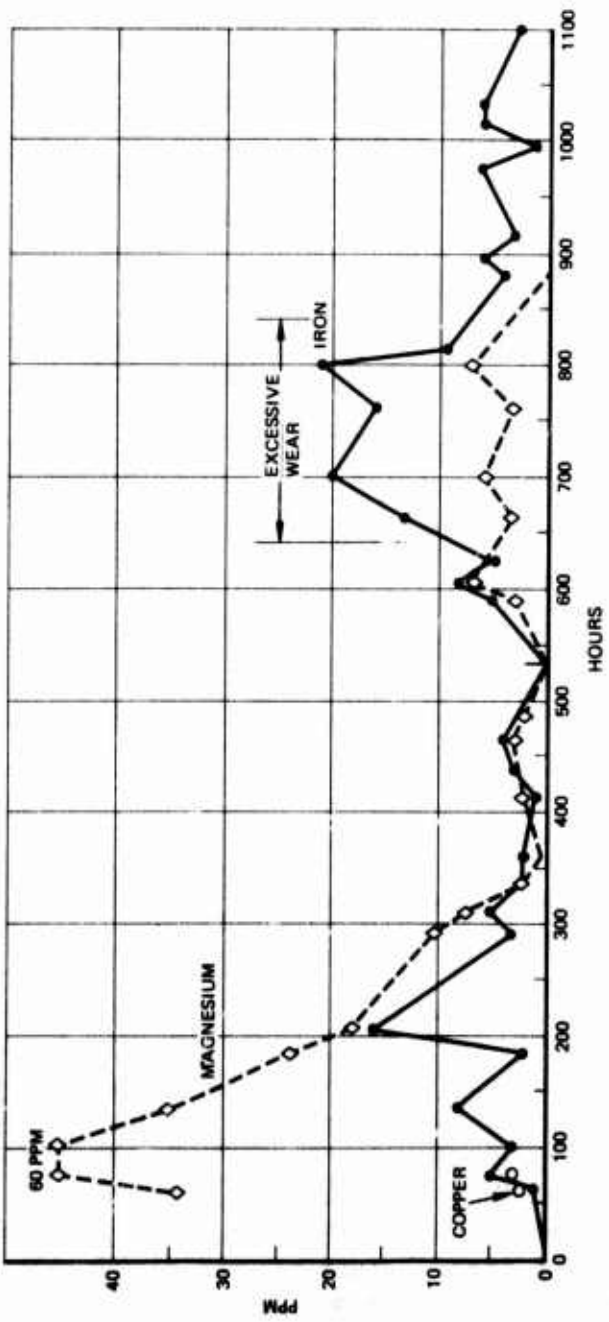


Figure 79. Spectroscopic Oil Analysis Summary, BB3.

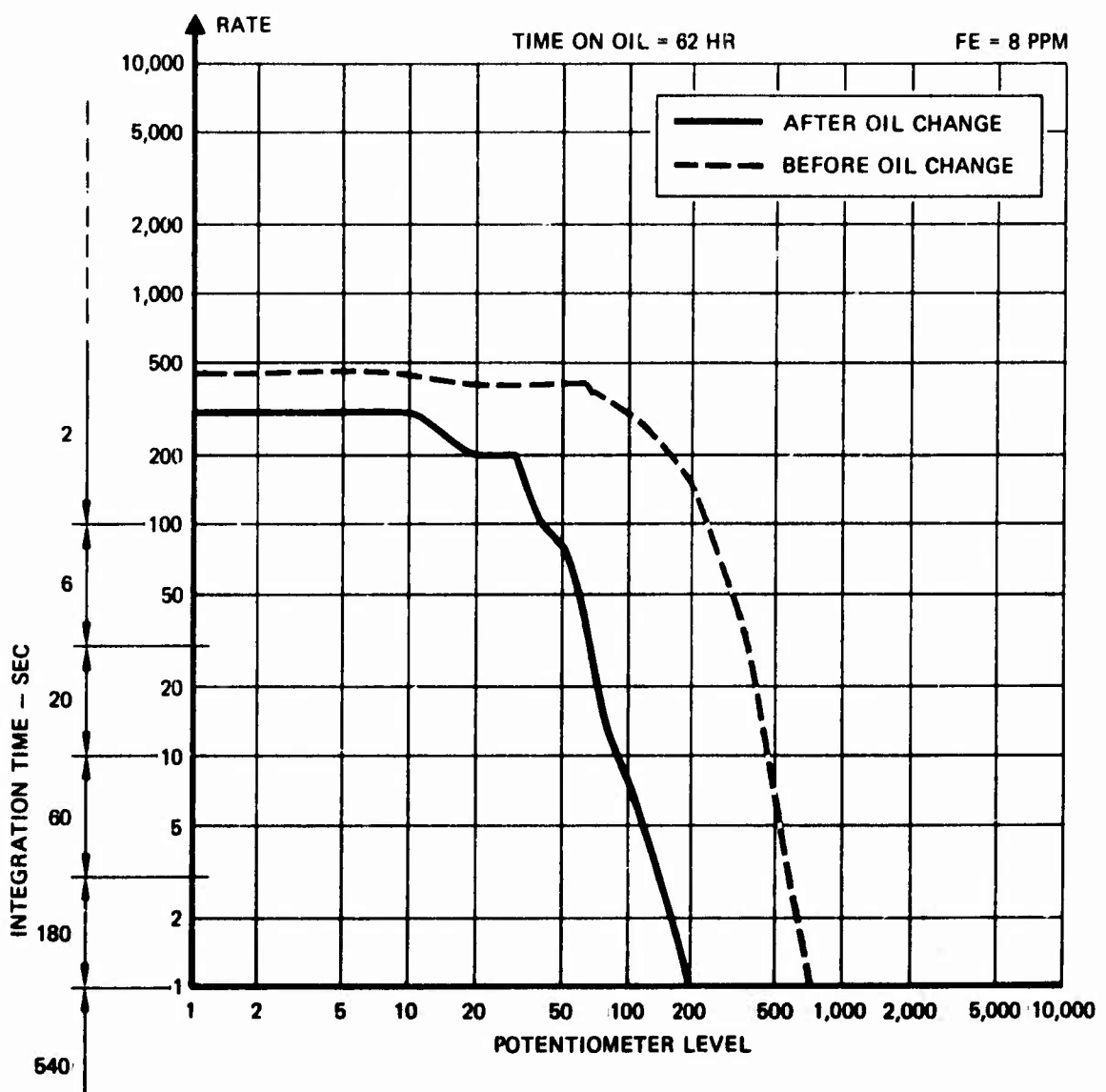


Figure 80. Shock Pulse Data for BB3 at the 62-Hour Point.

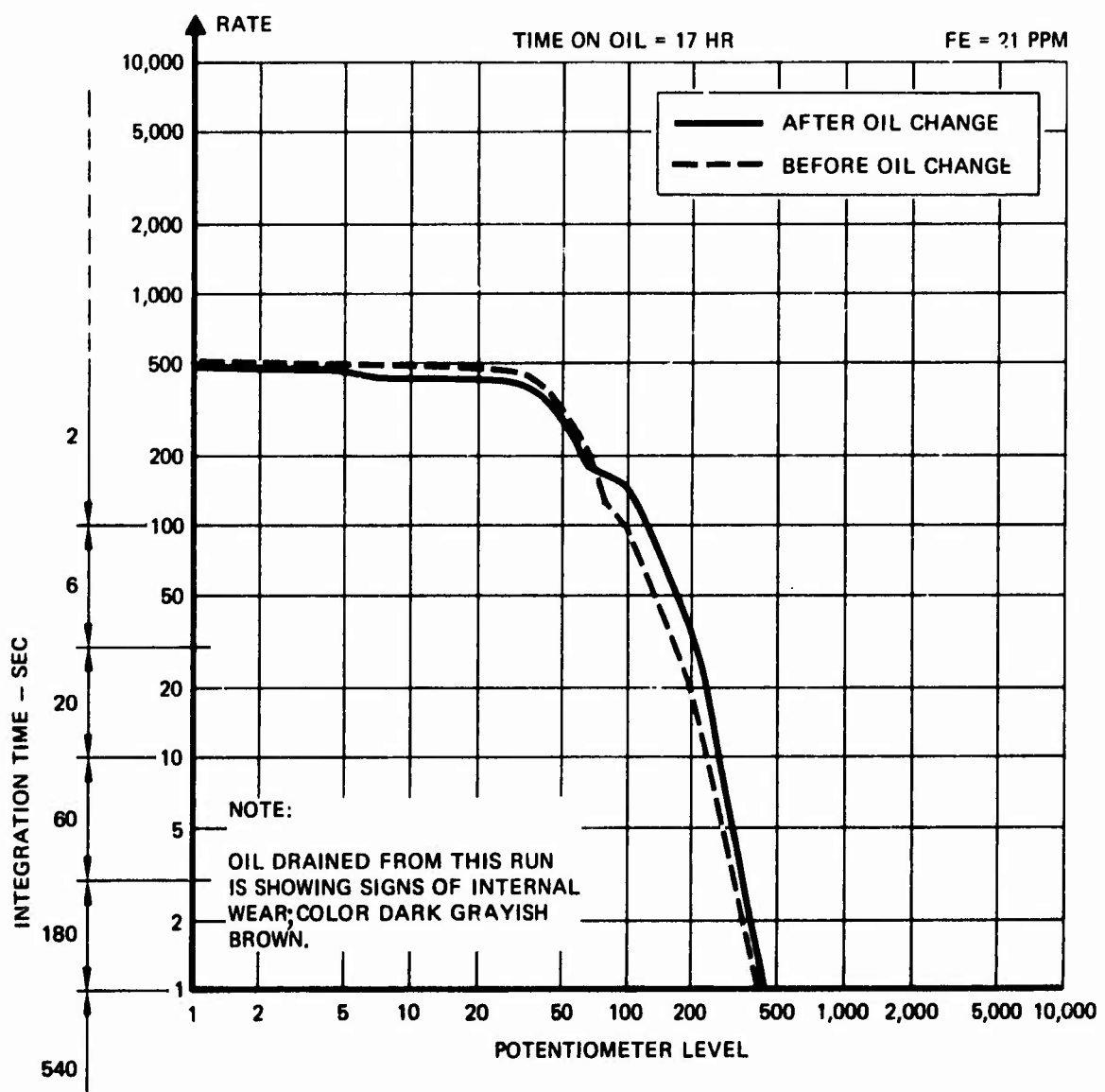


Figure 81. Shock Pulse Data for BB3 at the 800-Hour Point.

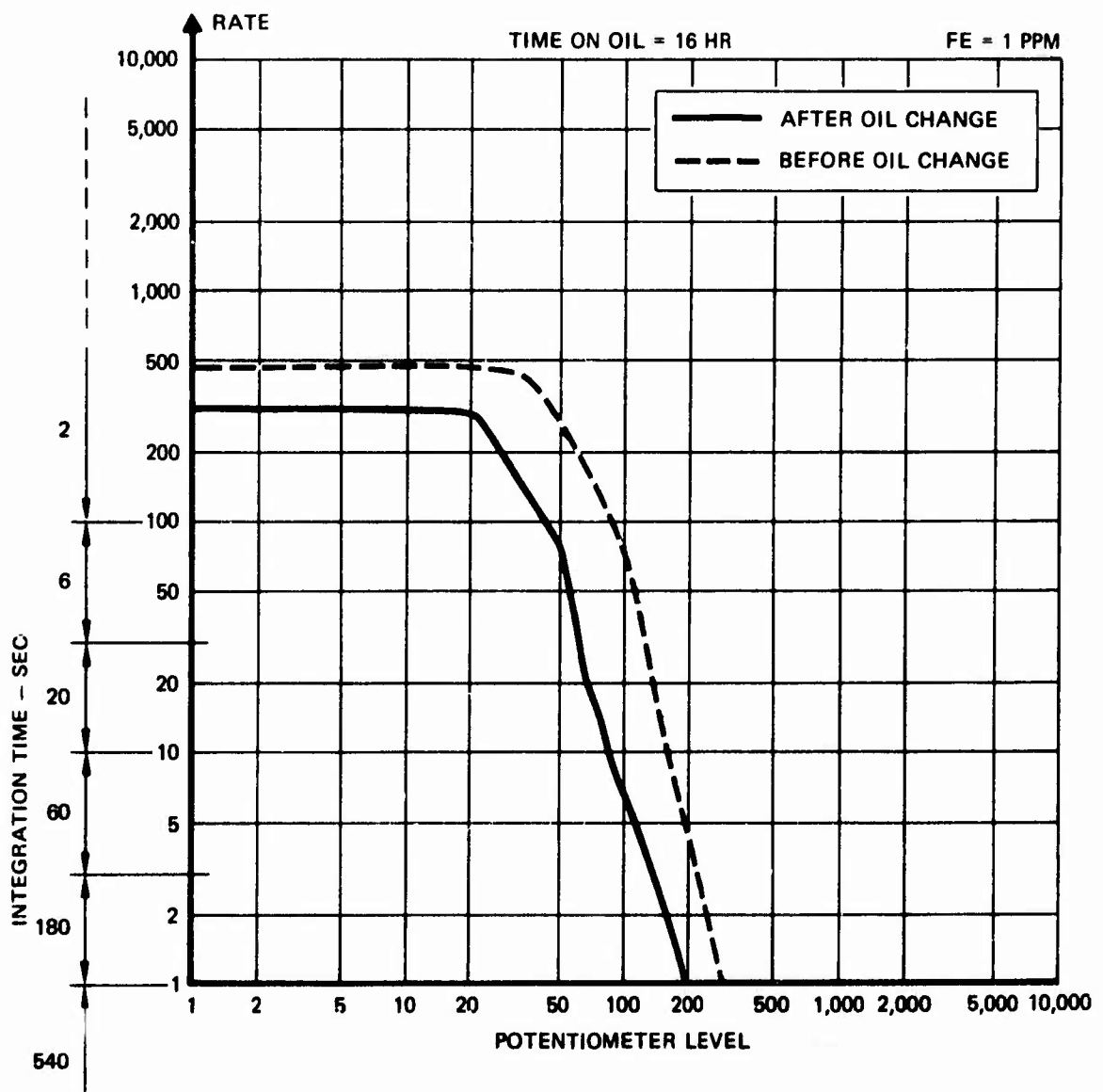


Figure 82. Shock Pulse Data for BB3 at the 980-Hour Point.

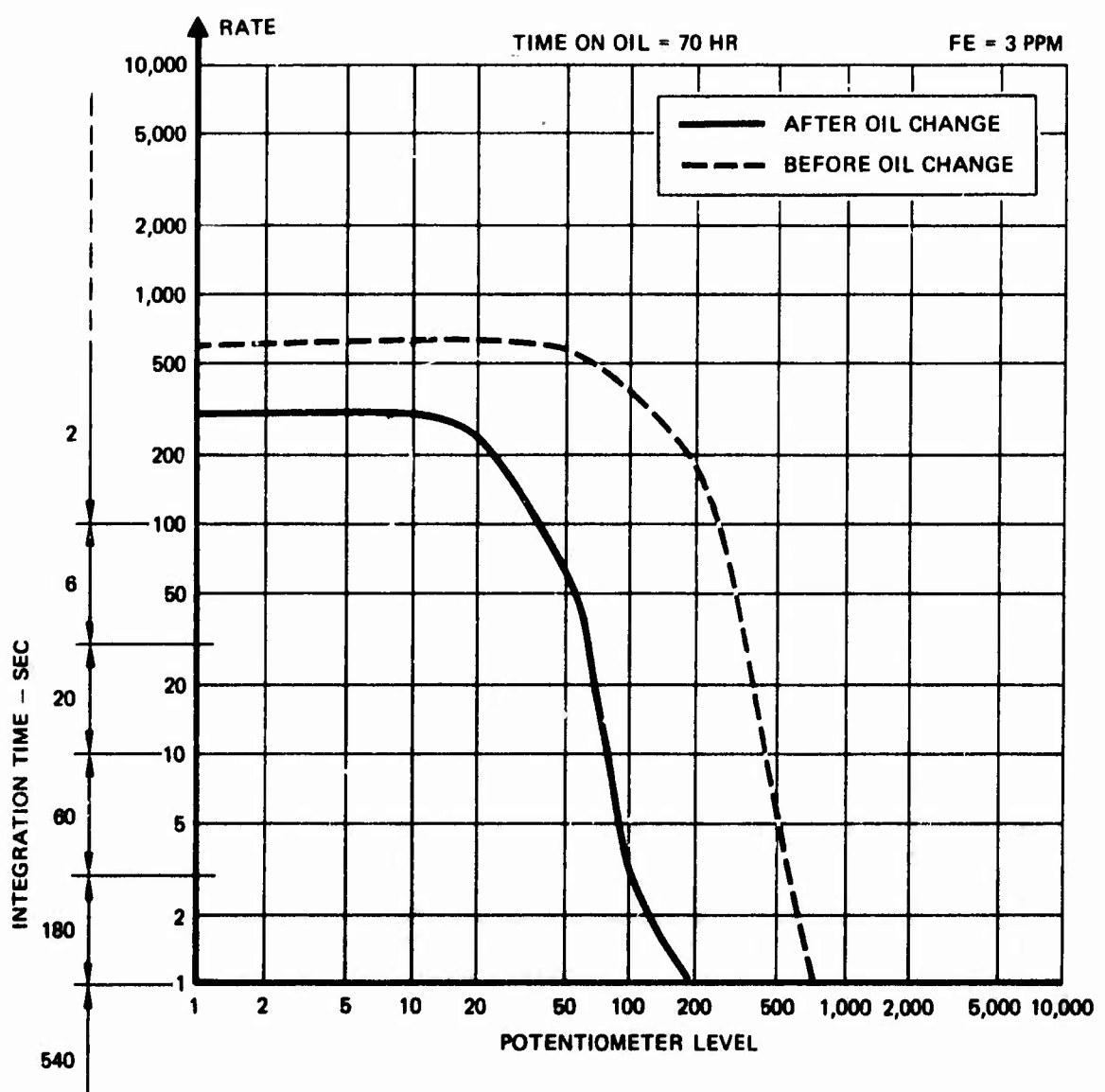


Figure 83. Shock Pulse Data for BB3 at the 1100-Hour Point.

hours, the data did not change significantly except that the iron content dropped to less than 9 ppm. During the next 16 hours of testing, the bearing seemed to recover considerably, as shown in Figure 82, and the iron content dropped to 1 ppm.

The shock emission profile, for the final 70 hours of testing, is shown in Figure 83. The iron content is 3 ppm, indicating normal wear. The profile taken with new oil does not differ significantly from the new oil profile taken at the start of testing (Figure 80) a thousand hours earlier. Although the bearings have deteriorated significantly over the course of the test period, evidence of this wear cannot be determined by comparing the final shock emission profile with the initial profile. Shock pulse value (SPV) data is plotted in Figure 84. The characteristics of this data near the end of testing are similar to those observed in the SPV curves obtained from the BBT gearbox. The shock pulse values remained at a relatively constant low value for more than half of the test hours. Shortly after the 600-hour point a noticeable increase in the SPV occurred. The shock pulse value started to rise very rapidly, this rise occurring during the period of excessive wear, as verified by the SOA. After this rise, an abrupt decrease in the shock pulse value was observed. This first exponential growth and rapid decay of the SPV were followed by successive periods of growth and decay. Although catastrophic failure of this gearbox would probably not occur, if testing continued for several hundred additional hours, the excessive wear detected at the 800-hour point would have been sufficient justification for requiring removal of this gearbox from service.

Low-Frequency Vibration Data

Of the 1100 hours of testing performed on gearbox BB3, 1086 hours of useful data was collected. Figures 85, 86 and 87 summarize the time history of the vibration data collected from each low-frequency accelerometer. Note the well-defined gearmesh harmonic structure and an almost total absence of the previously observed high-frequency components associated with excessive gear wear. Most of the weak vibration signals which lie between the dominant gearmesh harmonic structure are below the dynamic range of the data collection system, and as a result only a few frequency bins met the Z-score test as potentially trendable signals.

Figure 88 is a plot of data obtained from the input lateral accelerometer, frequency bin 4140 Hz, over the time period of 50 to 300 hours. The LMS trend line is also shown, which is the prediction of the future data (hours 178 to 300) based upon the past data (hours

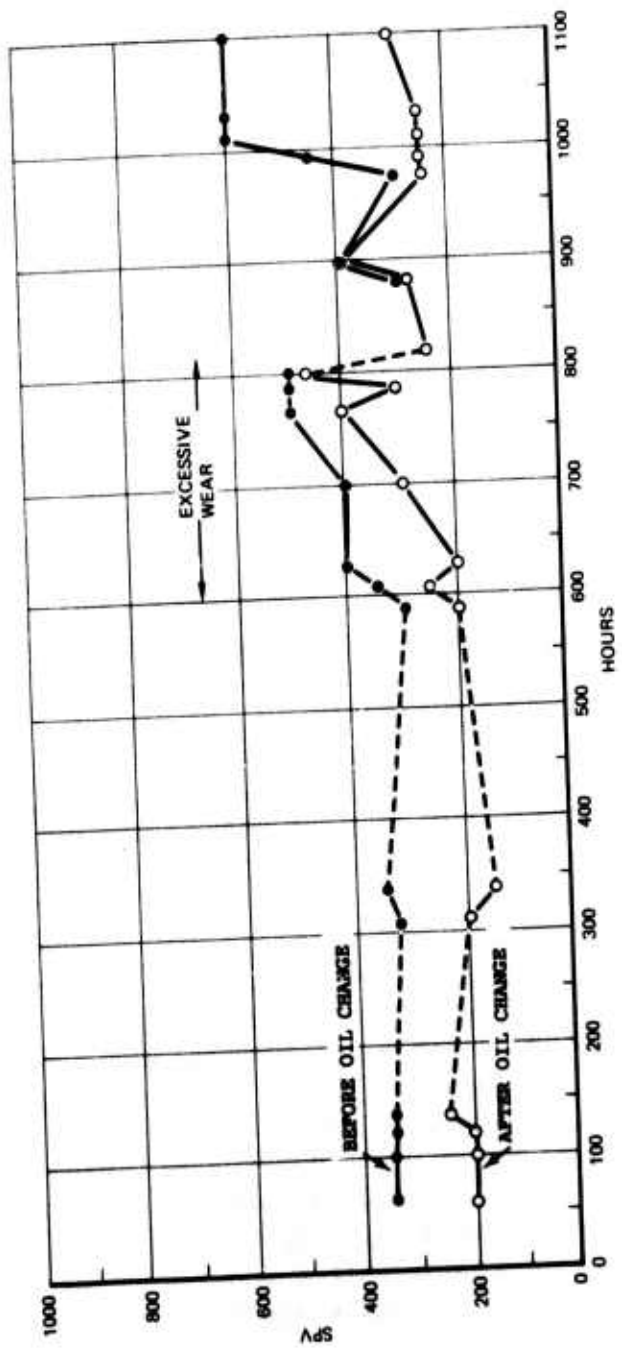


Figure 84. Shock Pulse Value Data, BB3.

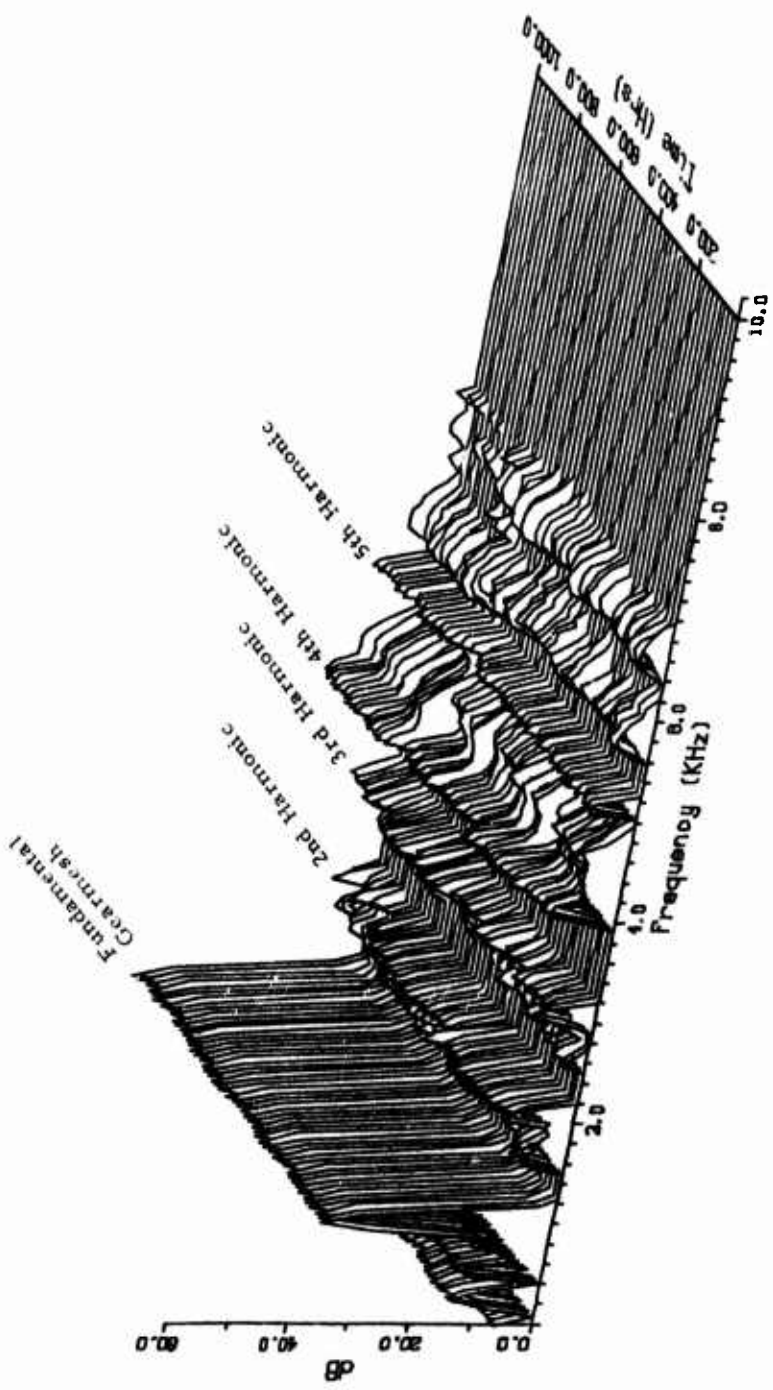


Figure 85. Overall View of BB3 Vibration Data Base,
Input Lateral Accelerometer.

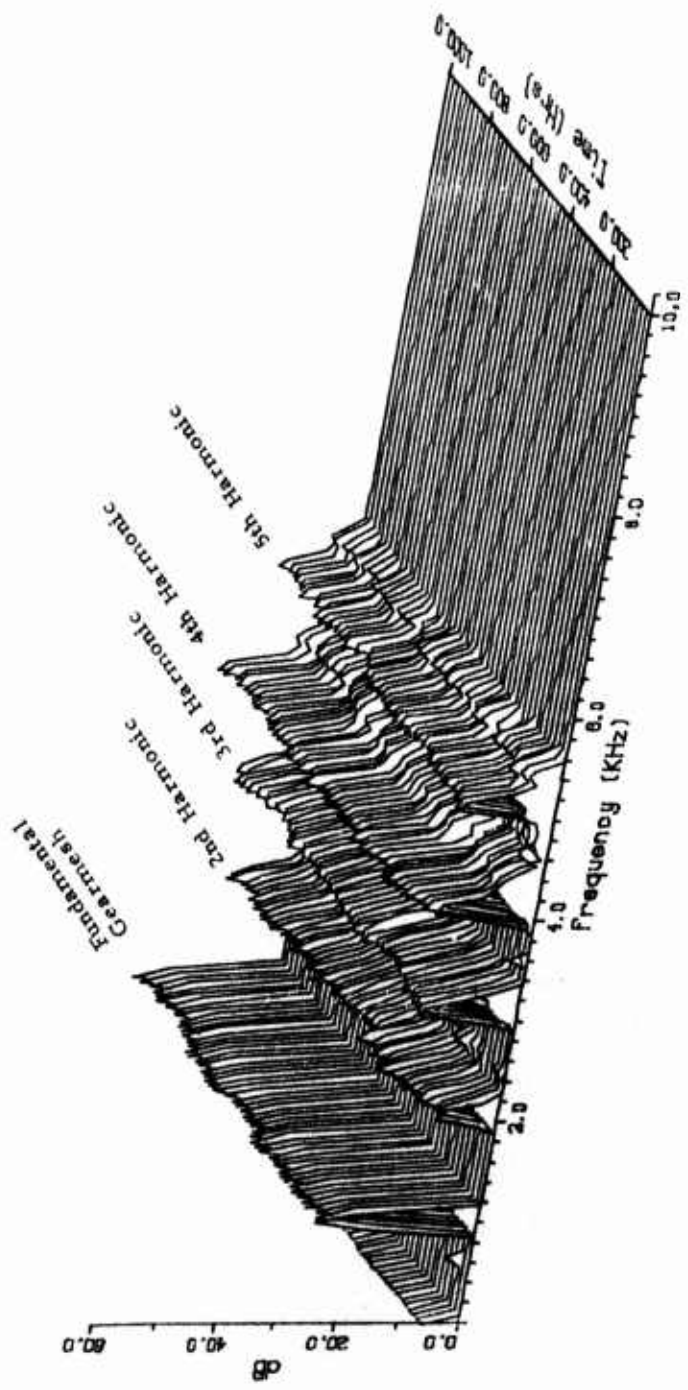


Figure 86. Overall View of BB3 Vibration Data Base, Skew Accelerometer.

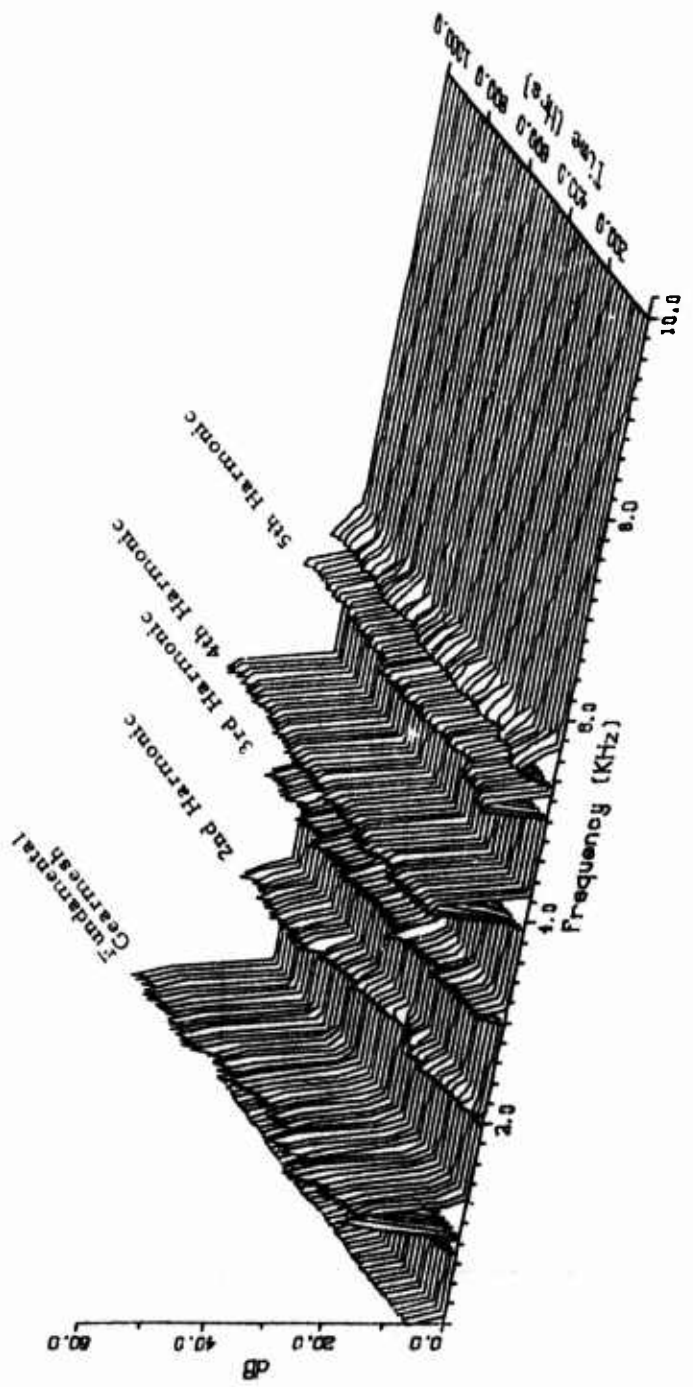


Figure 87. Overall View of BB3 Vibration Data Base,
Output Lateral Accelerometer.

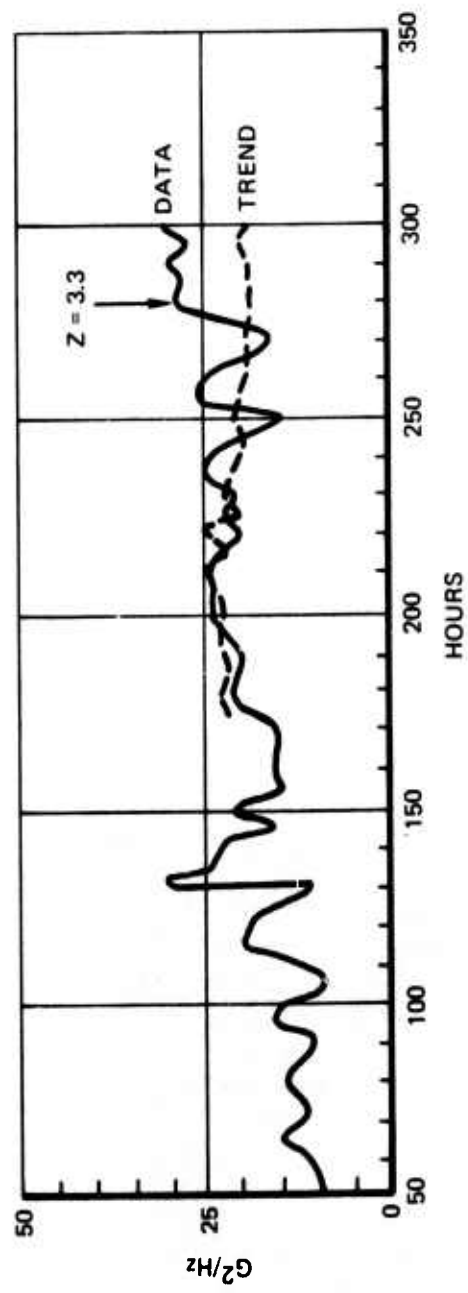


Figure 88. Prognostic Trend of BB3 Gearbox, Input Lateral Accelerometer, 4140 Hz.

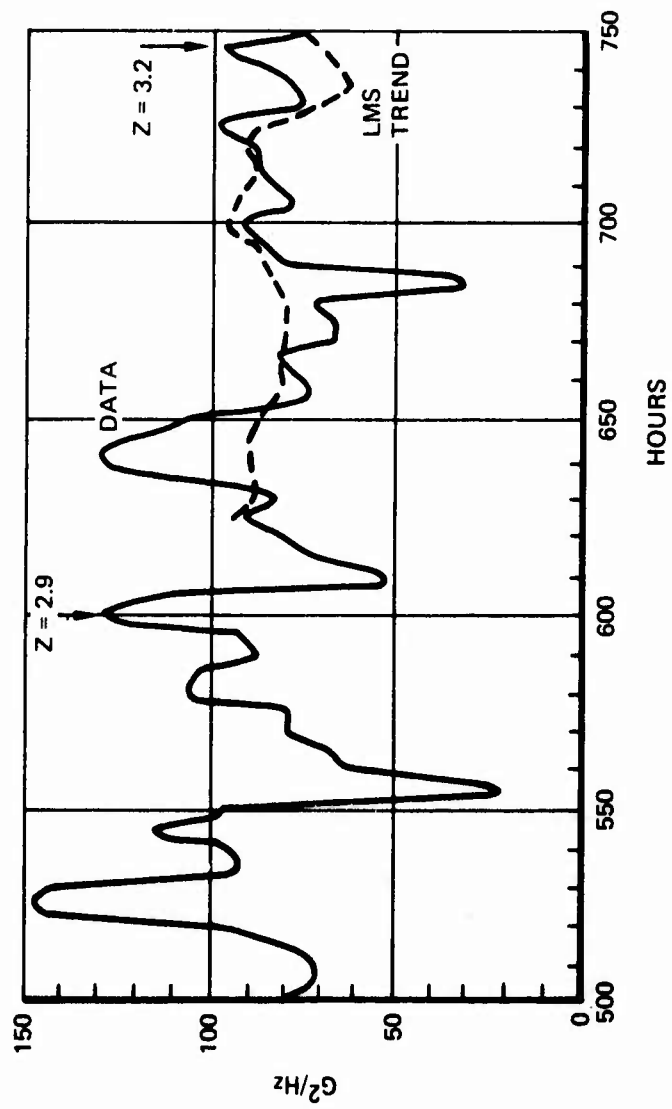


Figure 89. Prognostic Trend of BB3 Gearbox, S'ew Accelerometer 4140 Hz.

50 to 177). The predicted trend is quite good over the first 60 hours, but it tends to underestimate the actual data for the last 60 hours. We can also see that extrapolations of a linear curve fit over hours 50 to 170 would have also been a fairly accurate prediction of the actual values obtained during test hours 178 to 300. Figure 89 is a plot of vibration data from the skew accelerometer for frequency bin 4140 Hz, from test hour 500 to test hour 750. This data is characterized by large oscillations which account for the lower Z-score calculated at test hour 600 than at test hour 750, despite the fact that the group PSD mean is higher at hour 600 than at hour 750. The example given in Appendix A, following Table V, illustrates this point more fully. The LMS prediction of future vibration data values between test hours 529 and 750 is based upon the test data available during test hours 500 to 628. Although the data continued to oscillate, the LMS trend provided a good quantitative estimate of actual vibration levels observed during that period of time.

Correlation of Sensor Outputs With Mechanical Condition

Correlation between the iron content found by the spectroscopic oil analysis and the shock pulse value was seen to occur during test hours 600 and 800. We know from visual inspections that the output duplex bearing did undergo substantial wear, but we can only speculate at what point during the testing this wear occurred. Due to dynamic range limitations of the vibration data, not many frequency bins were trended. It is worthy of note that the Z-score detected statistically significant increases in frequency bin 4140 Hz for the skew accelerometer during the period of excessive wear noted from SOA and the shock pulse value.

Summary of BB3 Gearbox Test Results

In summary, shock pulse data and spectroscopic oil data yielded most of the useful information regarding the condition of BB3. BB3 was tested for 1100 hours, and the bearings, particularly the output duplex pair, deteriorated from moderately worn to extremely worn. Insufficient data analysis has been performed on BB3 to fully evaluate the data collected.

VIBRATION DATA - BEARING FREQUENCIES

The linear discriminant method for determining which bins to trend does so without reference to any mechanical model for the gearbox. As such, bearing frequencies are not given any special significance, and indeed were seldom statistically significant. The bearing

frequencies are well-defined spectrum lines between 200 and 1100 Hz for the 90-degree gearbox. For the HT gearbox, the amplitude of bearing frequencies increased to a Z-score of 3.2 at the 725-hour point but were completely absent at the 1200-hour point. The BG gearbox had an increasing level of bearing frequencies, and by hour 675 the Z-score was 3.1, rising to 3.7 at the 700-hour point, but falling to 2.4 at the 850-hour point. BB2 and BB3 generally saw a decreasing level at bearing frequencies, with a Z-score between -3.1 to -3.4.

Most of the bearing frequencies observed were those clustered around 300 Hz, which corresponds to the output roller bearing. Because of the coarseness of the PSD (78.125 Hz), it was not possible to be more specific than to indicate which bearing was at fault. The dynamic range limitation of the PSD often caused the bearing frequencies to be unmeasurable. All things considered, it is not too surprising that significant bearing frequencies were not generated since visual inspection of the balls and raceway does not show macro-pits and spalls. The bearings do wear, however, but their wear seems to be more uniform than local, and uniform wear does not lead to large-amplitude bearing frequencies.

CONCLUSIONS

The results of this program are not easily summarized. This was an ambitious program, which attempted to solve many problems in a field where little previous work has been done. Problems were encountered in learning how to locate and operate new sensors and how to interpret their output signals. Modification of the test cell to accomodate the oil debris monitors (ODM) made the SOA and shock pulse analyzer data of limited value to this prognostic effort. Though there were problems encountered that were not anticipated at the beginning of this program, except for schedule difficulties, the program ran as smoothly as one could expect.

In this section we will summarize the overall conclusions reached on this program. The reasoning behind these conclusions is discussed in the discussion of the gearbox test results in the report.

1. Documentation of Gearbox Wear. Visual inspection by an expert, dynamic noise testing, mechanical measurements and SEM photographs of bearings were the techniques used to document the pre- and post-test wear condition of each gearbox. Dynamic noise tests proved to be the most consistent and reliable indicator of bearing wear and should be a required part of any future experimental program. It was not possible to obtain any quantitative information on gear wear.
2. Temperature Sensors. Ambient air and gearbox oil temperature sensors provided no useful information to this program. The external oil circulating system used in conjunction with the two ODM's provided sufficient cooling of the oil to allow the BB gearbox to fail catastrophically without a detectable rise in the oil temperature.
3. Spectroscopic Oil Analysis. Spectroscopic oil analysis was a useful technique for determining periods of excessive wear and provided some insight as to which mechanical component was the probable cause of the metallic concentrations detected. Improper sampling procedures and the external oil circulating system greatly reduced the effectiveness of the SOA for determining prognostic trends.
4. Oil Debris Monitors. The capacitive type and the X-ray fluorescence type ODM's did not produce any significant data due to repeated sensor failures. A great deal of effort

was expended trying to determine if they were functioning properly and in removing and repairing them. The circulating oil system which was required by these sensors diluted the SOA particle concentrations and nullified the potential usefulness of the oil temperature sensor.

5. Gearbox Load. The gearbox was loaded to 40 hp, which represents 66% of the nominal running torque. This low torque load was probably insufficient to produce normal gear wear patterns, although significant bearing wear was observed during the tests.
6. Ultrasonic RMS. The ultrasonic RMS accelerometers produced little significant data, due mainly to the utilization of narrow band accelerometers. The peak detector should have had a very fast attack time since the occasional fast transients that it was designed to ignore may be extremely important in analyzing short-term fluctuations in the gearbox operating condition.
7. Shock Pulse Analyzer. A significant amount of data was obtained from the shock pulse analyzer on the final two gearboxes tested. The preliminary results look very encouraging. We observed repeated buildups of the shock pulse value (SPV) followed by a rapid decline in level, and these buildups have been associated with increased wear as measured by SOA. This repeated exponential buildup and decay may very well be a fundamental property of the 90° gearbox as it passes from incipient failure to failure, and it may even be a fundamental characteristic of most gearboxes and transmissions. It will take further study of the shock pulse value data which was not reduced to determine if this speculation can be confirmed for the 90° gearbox. The shock emission profiles were not very useful for prognostic purposes. There was no noticeable difference between profiles taken at the beginning and end of the test periods. Though the shock pulse profile seemed to be sensitive to wear contaminants in the oil, there were times when the oil was dirty, and this fact was not evidenced in the shock pulse profiles.
8. Low-Frequency Accelerometers. Vibration signals constitute the largest data base obtained on this program. It is the only data that provided enough continuous information that was usable for trending. Though it appears certain that information relating to bearing and possibly gear wear

is embedded in the vibration signal structure, our attempts to extract this information were unsuccessful. The exponential buildup and decay observed in the shock pulse value (SPV) of the shock pulse analyzer can also be seen in the structure in the vibration signals. This vibration data base should be extensively analyzed, and future experimental programs should include the use of low-frequency accelerometers.

9. Analysis. The least-mean-square (LMS) trending technique is most useful on stationary or slowly changing data. The LMS technique can accommodate oscillating data values, but because it requires the computation of derivatives, it is subject to numerical computation errors. Work needs to be performed to develop advanced trending techniques which can handle non-stationary data.
10. Gearbox Selection. The technique used to select the gearboxes for this test program was certainly not optimum, since only a qualitative assessment of their mechanical condition could be made. Due to the lack of quantitative or even good quality methods for determining the initial condition of the gearboxes, Bad Bearing (BB) and Bad Gear (BG) gearboxes were already failed at the start of testing. Neither gearbox provided information of any significant value to this prognostic effort.

The objective of this program was to test five different UH-1 90° gearboxes which were in different stages of mechanical wear and to determine which of the sensors used to monitor the mechanical condition of the gearbox components provided data which might contain the information necessary to determine the remaining useful life of these components.

In reviewing the effort conducted on this program, we feel that a great deal was accomplished in attempting to meet these objectives. This was an ambitious program which involved building a unique test cell and automatic data collection and reduction system which, except for some minor problems, performed in exemplary fashion. However, there were many unknowns involved in how to reduce the various types of data, how to process it, and how to interpret the results. Considering all the unknowns faced at the start of this program, we feel the results represent a significant contribution to the state of the art of prognostics and provide a sound basis for further work in this interesting and important field.

RECOMMENDATIONS

Although DOD has funded many programs to study techniques for diagnosing machines, relatively little effort has been devoted to studies whose objective is to attempt to relate the time-changing signal structure of the output of various sensors to the mechanical condition of machines in order to develop techniques for predicting the useful remaining mechanical life of those machines. In this respect the work accomplished under this program is relatively unique and represents one of the most comprehensive data bases ever collected for prognostic studies. However, the prognostic problem has not been solved. The insights gained on this program into the wear characteristics of 90° gearboxes and the lessons learned on how to collect and interpret the sensor data are the basis for the following recommendations for future prognostic studies.

1. Data Quality. Since prognostics deals with the time rate of change of sensor signals as a function of component wear, it is essential that some relationship exists between the actual wear occurring in the mechanical components and the signal structure at the output of one or more sensors. It is also essential that the data processing system be capable of detecting the required signals in the presence of the large-amplitude signals which are characteristic of the mechanical system. In the case of vibration data, the wear process appears to produce frequency components whose amplitudes are many decibels less than the amplitudes of the fundamental garmesh frequencies. A successful prognostics technique must be capable of detecting these new frequency components as soon as they appear and tracking them as the wear progresses. In order to locate these low-amplitude signals, a high-precision ADC is needed.
 - (a) It is recommended that the precision of the ADC in the data collection system be increased from the present 10 bits to 12 bits at the minimum, and to 13 or 14 bits if funds are available. A 14-bit ADC will provide a dynamic range of nearly 80 dB, which should be sufficient to detect low-amplitude vibration components with sufficient precision to allow accurate trending.
 - (b) In addition to improved dynamic range, the frequency resolution of the vibration data should be increased from 78 Hz/bin to at least 20 Hz/bin, and the upper range of the PSD calculation should continue to be at least 10 kHz. This means that the fast Fourier

transform dimensions should be increased from 265 data points/transform (128 frequency bins) to at least 1024 data points/transform (512 frequency bins).

- (c) Low mass accelerometers (e.g., B&K 4322) should be used to collect vibration data in order to minimize the mounting problems, and the accelerometer mounting pads should be welded to the gearbox at the appropriate sensor location.
- (d) The skew accelerometer location can be deleted in future work since the input lateral and output lateral locations, which are much closer to the bearings, yield better and more consistent data. This data channel can then be used for other sensors.

2. Ultrasonic Sensors. The results of our limited data analysis efforts on this program indicate that ultrasonic signals may contain information relating to component wear, and the development of techniques to extract this information could provide us with a useful prognostic tool. Though the ultrasonic accelerometers did not provide useful information on this program, they cannot be eliminated from consideration as a potential prognostic tool. The results obtained from this program suggest that the shock pulse analyzer may be a sensitive indicator of component wear.

- (a) It is recommended that shock emission profiles be taken for every bearing location, instead of the one location used in this program. The shock pulse value (SPV) for each location should be monitored so that the repetitive exponential behavior of this data, as observed in BBT and BB3, can be analyzed in detail.
- (b) Broadband accelerometers have been developed for acoustic emission applications, and their applicability as an effective ultrasonic sensor should be studied in any future diagnostic effort.
- (c) A considerable amount of research is now being devoted to ultrasonics. New techniques for analyzing ultrasonic signals and new concepts for ultrasonic sensors are being developed. A survey of the new developments in the field of ultrasonics should be made, and the most promising analysis

techniques and sensors should be incorporated into future studies aimed at solving the prognostics problem.

3. **Oil Analysis:** There is little doubt that spectroscopic oil analysis (SOA) is an important diagnostic tool with considerable prognostic potential. To determine its value as a prognostic tool for predicting wear in helicopter mechanical components, the standard Army procedures for taking SOA oil samples should be followed.
 - (a) Deviations from established Army SOA procedures should be minimized. Oil samples should be taken at regular intervals, and the volume of the sample should be limited to a small percentage of the gearbox oil. The Army schedule for oil changes should be strictly adhered to.
 - (b) External oil debris monitors (ODM) which require a circulating oil system should not be used in tests conducted on mechanical systems which are not specifically designed to operate with such a large oil reserve. The possibility of developing useful prognostic techniques for predicting the future condition of operating machines is sufficiently intriguing to attempt to try every reasonable monitoring concept available which might provide a successful solution to the prognostic problem. However, new sensors should be selected with caution. The testing of a sensor which is still in the early stages of development can constitute a test upon a test, and the real objective of studying the wear process of mechanical components may be lost due to the problems encountered in trying to interpret the sensor output and make the sensor perform properly.

It is recommended that in future efforts, prototype sensors such as the ODM's be used only on a non-interference basis so that meaningful SOA and shock pulse analyzer data can be obtained.

4. **Test Parameters and Procedures:** The experience gained from long-term testing has resulted in the following recommendations.

- (a) The results of the detailed visual examination and dynamic noise testing should be available before testing. This will allow the investigator to make some estimate of the seriousness of the incipient failure and, with experience, gauge the amount of life expected from the gearbox. With this insight into its mechanical condition, he can more readily determine whether abnormal signals are caused by the gearbox or by test cell malfunctions.
- (b) If further tests are conducted on 90° gearboxes, running torque should be increased from 40 hp to the nominal operational level of 70 hp to more nearly reflect the actual gear and bearing wear to be expected in the field.
- (c) Gearbox input torque and output torque should be directly monitored with torque sensors to ensure accurate loading levels.
- (d) A factory new or green run gearbox should be tested to establish baseline values for the visual examinations of wear and dynamic noise and to provide initial condition sensor signals for long-term trend analysis.
- (e) If further prognostic work utilizes the UH-1 90° gearbox as a test vehicle, the 42° gearbox, which feeds the 90° gearbox in the helicopter, should also be tested. If a new, higher torque test cell is constructed, the 42° gearbox could be included at little cost. In actual operation, the characteristics of rotating components in the 42° gearbox can be observed in the output of sensors located on the 90° gearbox due to mechanical coupling. Tests of the 42° gearbox would provide an extensive data base on a different type of machine and should also provide information on whether or not the prognostic information and the sensors from which it was obtained are common to both gearboxes. It will also enable us to more readily determine the unique characteristics of each gearbox so that in actual operation these characteristics can be identified in the output signals from the sensors.

5. Analysis Effort. The mechanics of designing and building a test cell, writing the necessary software to run it, and collecting nearly 5000 hours of data from five gearboxes constituted a significant portion of the effort expended on this program. The logistics problem in collecting, reducing, processing and storing the massive amount of data collected was grossly underestimated.

- (a) We strongly recommend that in future efforts, greater recognition be given to the tremendous amount of data which must be processed and an adequate analytical effort be funded in conjunction with the test program. The magnitude of this task should not be underestimated. A well-rounded program should include studies of the entire data base, not just "quick looks."
- (b) The analytical effort should investigate the relationship between sensor outputs as a function of wear.
- (c) A significant effort should be devoted to developing new techniques for analyzing vibration data. It is apparent from the results obtained on this program that component wear is reflected in the vibration signal structure, but the techniques applied were inadequate to make it readily apparent.
- (d) The LMS trend technique has yielded some encouraging results, but the fact that it requires the data to be statistically stationary might be a limitation on its usefulness. However, if the wear in a gearbox progresses at a slow rate, with abnormal wear occurring only near the end of its useful life, the LMS technique might produce valuable trending information over a large portion of the gearbox life, with large deviations from the predicted trend signaling the onset of abnormal operating conditions.

Additional effort should be expended to modify the LMS technique or to develop new analytical techniques which could take into account the non-stationary characteristics of the data.

LITERATURE CITED

1. "Advanced Capacitative Oil Debris Monitor," Franklin Institute Research Laboratories, USAAMRDL Technical Report 73-53, Eustis Directorate, U.S. Army Air Mobility Research and Development Laboratory, Fort Eustis, Virginia, August 1973.
2. "A Nucleonic Oil Debris Monitor for Detecting Metal in Recirculating Systems," Nucleonics Data Systems; USAAMRDL-TR-74-28, Eustis Directorate, U.S. Army Air Mobility Research and Development Laboratory, Fort Eustis, Virginia, June 1974.
3. SKF Industries, Inc., SKF MEPA-10A SHOCK PULSE METER, Research Laboratory, SKF Industries, Inc., Engineering and Research Center, King of Prussia, Pennsylvania.
4. SKF Industries, Inc. USER'S MANUAL SHOCK PULSE METER TYPE M MEPA-10A, Research Laboratory, SKF Industries, Inc., King of Prussia, Pennsylvania.
5. Otnes, R. K. and Enochson, L., "Digital Time Series Analysis," J. Wiley and Sons, New York, 1972, Ch. 11.
6. Spiegel, Murray R., "Theory and Problems of Statistics (Schaum's Outline)," Schaum Publishing Company, 1961, Ch. 10.
7. Popoulis, Athanasios, "Probability, Random Variables, and Stochastic Processes," McGraw Hill Book Company, 1965, Ch. 11-2 and Example 11-4.
8. Lee, Y. W., "Statistical Theory of Communications," Wiley, 1960.
9. Otnes, Robert K. and Enochson, Loren, "Digital Time Series Analysis," John Wiley and Sons, pg. 399, 1972.

APPENDIX A
DEVELOPMENT OF Z-SCORE TEST AND
LMS PREDICTION TECHNIQUES

In this appendix the theory used to develop the Z-score (linear discriminant) test for statistically significant changes in the PSD's of the vibration data obtained on this gearbox test program is discussed. The development of the least-mean-square (LMS) prediction technique which was applied to a limited amount of the vibration data is also discussed.

DEVELOPMENT OF Z-SCORE TEST⁽⁶⁾

The Z-score is defined as

$$Z_l(k) = \frac{M_l(k) - M_{25}(k)}{\sqrt{S_l^2(k) + S_{25}^2(k)}} , \quad l = 50, 100, \dots \quad (19)$$

where

$Z_l(k)$ = l th Z-score for k th frequency bin

l = reference time index

k = frequency bin index

$M_l(k)$ = l th mean of $P_t(k)$ over T hours* at frequency k .

$S_l(k)$ = l th standard deviation of $P_t(k)$ over T hours*

$M_{25}(k)$ = baseline group PSD mean (at 25 hours) against which all $M_l(k)$ are compared

For large sample sets (when the number of samples is greater than 30), the sampling distribution of the differences of sample statistics for two populations (within the sample set) is very closely normally distributed. Such sampling methods are known as large sampling methods. The samples which were used in the Z-score test were the 50 averaged PSD's belonging to PSD groups $l = 50, 100, 150, \dots$,

*Determine equations (5) and (6) in the section on "Data Analysis - Theory and Procedures."

from the population of all PSD's taken from the gearbox under test. The sampling distribution for the differences between the average of PSD samples in group 25, $M_{25}(k)$, and the average of PSD samples in each of the other groups, $M_l(k)$ will then be normally distributed, since the sample size of 50 is greater than 30.

Therefore, we can expect to find the actual sample difference of a frequency bin (k) to lie within the interval

$$(M_l - M_{25}) \pm Z_C \sqrt{S_{25}^2 + S_l^2} \quad (20)$$

β percent of the time, where Z_C is the confidence coefficient and β is the confidence level (percentage confidence). Values of β corresponding to several values of Z_C are listed in Table IV below.

TABLE IV. LEVEL OF CONFIDENCE, β , VERSUS CONFIDENCE COEFFICIENT, Z_C				
Confidence Level, β	99%	95%	90%	80%
Confidence Coefficient, Z_C	2.58	1.96	1.645	1.28

In a similar manner, confidence limits for the sample difference standard deviation are given by

$$\sqrt{S_{25}^2 + S_l^2} \left[1 \pm Z_C / \sqrt{2N} \right] \quad (21)$$

where the sample standard deviation has been used as an estimate for the population standard deviation, and N (=50) is the number of PSD's in each group.

The normal Z-score distribution provides a statistically meaningful test of the basic assumption that there exists a significant difference between group PSD means. It is desired to determine those frequency bins, k , for which one would accept the basic assumption that there is a significant difference between group PSD means at a given level of significance, α ; i.e., the probability is α that one would reject the basic assumption when it should be accepted.

The Z-scores for given levels of significance, α , are listed in Table V. These scores are derived from the standard normal Z-score distribution.

TABLE V. LEVEL OF SIGNIFICANCE, α , VERSUS REQUIRED Z-SCORE, Z				
Level of Significance, α	0.1	0.05	0.01	0.005
Minimum Required Z-score, Z	± 1.645	± 1.96	± 2.58	± 2.81

The following is an example of how the Z-score test is used to determine if there is a significant difference between two classes of data at a given level of significance.

Example: Let the means and standard deviations for two PSD groups at a particular frequency index k be given as

$$M_{25} = 70 \quad S_{25} = 7$$

$$M_{250} = 96 \quad S_{250} = 5$$

Is there a statistically significant difference between the two groups of data at a level of significance of 0.05; i.e., can we be 100 (1 - .05) = 95% confident that the two groups are significantly different?

The Z-score is

$$Z_{250} = (M_{250} - M_{25}) / \sqrt{S_{25}^2 + S_{250}^2} = 3.02$$

From Table V, the PSD differences are significant if Z lies outside the range -1.96 to +1.96; hence, at a 0.05 level of significance, there is a statistically significant difference between the two PSD groups.

Suppose, however, that $S_{250} = 15$ instead of 5. Then Z_{250} would be 1.57 and there would not be a significant difference between the groups at the 0.05 level of significance.

CORRECTED Z-SCORE

The Z-score as formulated above allows one to correctly determine 100 $(1 - \alpha)\%$ of the time those frequency bins for which there are statistically significant differences between group PSD means. The Z-scores as defined in equation 19 will now be modified so that the determination of the statistically significant differences in PSD groups is 100 $(1 - \alpha)\%$ correct at a given confidence level β (percentage confidence).

In modifying the Z-score test, one must specify confidence limits for the sample difference means and standard deviations of the PSD groups. The means and standard deviations are given by equations (5) and (6) which can be found in the body of this report in the section on "Statistical Analysis of Vibration Data." Substituting these expressions into equation (21) results in the corrected Z-score given by

$$\hat{Z}_\ell(k) = \left[\frac{1}{1 \pm Z_C / \sqrt{2N}} \right] \left[Z_\ell(k) \pm Z_C \right] \quad (22)$$

where

$\hat{Z}_\ell(k)$ = ℓ th corrected Z-score for k th frequency bin

$Z_\ell(k)$ = ℓ th Z-score (equation 1)

ℓ = reference time index

Z_C = confidence coefficient (Table IV)

N = sample size = 50

k = frequency bin index

The significance of the corrected Z-score, \hat{Z}_ℓ , is that it tells how much the magnitude of the measured Z-score, Z_ℓ , must be decreased (due to the uncertainties imposed by the confidence level specifications, Z_C , on the PSD sample data) in order to show significant statistical differences between PSD groups at a given level of significance. The worst-case (smallest magnitude) \hat{Z}_ℓ is then given as

$$\hat{Z}_\ell(k) \Big|_{w.c.} = \xi \left\{ Z_\ell(k) - Z_C \operatorname{sgn} [Z_\ell(k)] \right\} \quad (23)$$

subject to

$$|Z_\ell(k)| > Z_C$$

where

$\hat{Z}_\ell(k) \Big|_{w.c.}$ = ℓ th worst-case corrected Z-score
at frequency bin k

$\xi = 1/(1 + Z_C/\sqrt{2N})$ = confidence correction factor

$$\operatorname{sgn}[X] = \begin{cases} +1, & X \geq 0 \\ -1, & X < 0 \end{cases}$$

Z_C = confidence coefficient (Table IV)

Z_ℓ = ℓ th Z-score (equation 17)

N = sample size (=50)

The restriction on equation (23), $|Z_\ell(k)| > Z_C$, implies that when the Z-score is less than the confidence coefficient, Z_C , there is no statistically significant difference between the PSD groups being compared.

For a confidence level of 95%, $Z_C = 1.96$ from Table III, and the worst-case Z-score at a level of significance of 0.05 for $N = 50$ becomes

$$\hat{Z}_\ell(k) \Big|_{w.c.} = .836 \left\{ Z_\ell(k) - 1.96 \operatorname{sgn}[Z_\ell(k)] \right\} \quad (24)$$

Table VI lists the values for the confidence correction factor, ξ , for various confidence levels, β , for a sample size, N , of 50.

Following is an example of how to determine whether or not there is a statistically significant difference between two classes of data at a given confidence level and a given level of significance.

TABLE VI. CONFIDENCE LEVEL, β , VERSUS
CORRECTION FACTOR, ζ

Confidence Level, β ,	99%	95%	90%	80%
Confidence Correction Factor, ζ	0.795	0.836	0.859	0.887

Example: Let the sample means and standard deviations for two PSD groups at a particular frequency index, k , be given as follows:

$$M_{25} = 96 \quad S_{25} = 3$$

$$M_{250} = 70 \quad S_{250} = 4$$

Assume that each group contains 50 PSD samples. Is there a significant difference between the two groups at a 95% confidence level for a level of significance of 0.05; i.e., can we be 95% sure that $100(1 - .05)\% = 95\%$ of the time there will be a significant difference between random samples taken from two populations (groups)?

The Z-score, equation (23), is $Z_{250} = (70 - 96)/\sqrt{9 + 16} = -5.20$. Equation (24) contains the necessary correlation factors to compute the worst-case corrected Z-score, $\hat{Z}_{w.c.}$. By substitution into equation (24), we get

$$\hat{Z}_{250} \mid_{w.c.} = 0.836(-5.20 - 1.96 \operatorname{sgn}(-5.20)) = -2.71$$

Since $\hat{Z}_{250} \mid_{w.c.}$ lies outside the range -1.96 to +1.96 (see Table VI), there is a significant difference between the two groups at a 95% confidence level for a level of significance of 0.05.

Suppose, however, that $M_{25} = 75$ instead of 96. Then Z_{250} would be -1.0. Since $|Z_{250}| < Z_C$, we cannot be 95% confident that 95% of the time a random sample in group 25 will differ significantly from a random sample in group 250.

On this contract, those frequency bins which showed a statistically significant difference at a 95% confidence level for a level of

significance of 0.05 were selected for trending. To find the Z-score threshold value, we solve equation (24) for Z as shown below:

$$\hat{Z}|_{w.c.} = .836 [Z - 1.96 \operatorname{sgn} Z] \geq 1.96$$

$$\begin{aligned} |[Z - 1.96 \operatorname{sgn} Z]| &\geq 2.34 \\ |Z| &\geq 4.3 \end{aligned}$$

Whenever the Z-score for a particular frequency bin equaled or exceeded 4.3, that frequency bin was selected for trending.

Whenever the above criterion was not met, trending requirements were relaxed to include frequency bin differences at the 90% confidence level to 0.10 level of significance, which, by equation (23), required $|Z| > 3.56$.

DERIVATION OF LMS PREDICTION TECHNIQUE⁽⁷⁾

In this section we discuss the theory used in developing the least-mean-square (LMS) error prediction technique and its applicability to trending of gearbox vibration signals.

The specific prediction problem to be solved can be stated as follows: given a PSD time signal $s(t)$ known from $t = 0$ to $t = T$; for a given t , predict $s(t)$ some time λ in the future in terms of a linear combination of $s(t)$, $s'(t)$, and $s''(t)$ with minimum mean square error.* In other words, our task is to determine constants a_0 , a_1 , and a_2 such that

$$s(t+\lambda) \sim a_0 s(t) + a_1 s'(t) + a_2 s''(t), \quad 0 \leq t \leq T \quad (25)$$

and for which the mean square error

$$E \left\{ [s(t+\lambda) - a_0 s(t) - a_1 s'(t) - a_2 s''(t)]^2 \right\} \quad (26)$$

is minimum, where $E \{ \}$ is the expectation operator.

* Note: $s'(t) \triangleq \frac{d}{dt} s(t)$, $s''(t) \triangleq \frac{d^2}{dt^2} s(t)$

The above problem is a special case of the following (linear) least-mean-square (LMS) prediction problem. Find the impulse response $h(t)$ of a linear filter operating on $s(t)$ such that

$$s(t+\lambda) \sim \int_{-\infty}^t s(\alpha) h(t-\alpha) d\alpha \quad (27)$$

with minimum mean square error

$$E \left\{ [s(t+\lambda) - s(t)]^2 \right\} \quad (28)$$

The impulse response, $h(t)$, is found by solving a Wiener-Hopf type of integral equation. The solution of this integral equation requires a considerable programming and computational effort, which was not felt to be justified for the small additional prediction accuracy gained over using the approximations given in equations (25) and (26).

The solution of any linear mean square estimation problem requires that the error be orthogonal to the approximating signal over the time interval of interest. For the specific problem given above, this means that

$$E \left\{ [s(t+\lambda) - a_0 s(t) - a_1 s'(t) - a_2 s''(t)] \begin{bmatrix} s(t) \\ s'(t) \\ s''(t) \end{bmatrix} \right\} = 0 \quad (29)$$

for $0 \leq t \leq T$, where

$$E \left\{ \begin{bmatrix} s(t) \\ s'(t) \\ s''(t) \end{bmatrix} \right\} = 0 \quad \text{means} \quad \begin{aligned} E \left\{ \begin{bmatrix} s(t) \\ s'(t) \\ s''(t) \end{bmatrix} \right\} &= 0 \\ E \left\{ \begin{bmatrix} s(t) \\ s'(t) \\ s''(t) \end{bmatrix} \right\} &= 0 \end{aligned}$$

The orthogonality equations given by (29) can be approximately represented by the following set of simultaneous equations:

$$\begin{aligned} R(\lambda) - a_0 R(0) - a_1 R'(0) - a_2 R''(0) &= 0 \\ R'(\lambda) - a_0 R'(0) - a_1 R''(0) - a_2 R'''(0) &= 0 \\ R''(\lambda) - a_0 R''(0) - a_1 R'''(0) - a_2 R^{IV}(0) &= 0 \end{aligned} \quad (30)$$

where

$R(\lambda)$ = autocorrelation function of $s(t)$

$R^{(n)}(\lambda) = d^n/d\lambda^n R(\lambda)$.

Because we are using a finite interval of data, the autocorrelation function $R(\lambda)$ is defined here to be

$$R(\lambda) = E \{ s(t + \lambda) \} \triangleq \frac{1}{T - \lambda} \int_0^{T - \lambda} s(t + \lambda) s(t) dt \quad (31)$$

for $0 \leq t \leq T, 0 < \lambda < T$

The autocorrelation function, $R(\lambda)$, is symmetrical about the origin, i.e., $R(-\lambda) = R(\lambda)$ and consequently $R'(0) \triangleq 0$. Equations (30) can be solved for a_0 , a_1 , and a_2 by the usual algebraic methods; the results are

$$a_0 = \frac{R(\lambda) - a_2 R''(0)}{R(0)} \quad (32)$$

$$a_1 = \frac{R'(\lambda) - a_2 R''(0)}{R'''(0)} \quad (33)$$

$$a_2 = \frac{R(\lambda)R''(0)^2 - R'(\lambda)R(0)'''(0) + R''(\lambda)R(0)R''(0)}{R(0)R''(0)R^{IV}(0) - R(0)R'''(0)^2 - R''(0)^3} \quad (34)$$

Numerical differentiation of a function in tabular form is subject to large numerical errors. Therefore, it was felt that it would be unreasonable to expect that higher order derivatives (third and fourth) of the autocorrelation function could be accurately computed, and for this reason the a_2 coefficient in equation (34) was set to zero. The resulting equation which was actually programmed and used in trending the vibration data is as follows:

$$s(T + \lambda) = a_0 s(T) + a_1 s'(T) \quad (35)$$

where

$$a_0 = R(\lambda)/R(0)$$

$$a_1 = R'(\lambda)/R''(0)$$

$$R(\lambda) = \frac{1}{T - \lambda} \int_0^{T - \lambda} s(t + \lambda) s(t) dt$$

λ = number of hours (past T) for which the prediction is being made ($0 < \lambda < T$).

In general, the coefficients a_0 and a_1 are functions of λ ; therefore, unlike a polynomial, these coefficients change with λ . However, for $\lambda \ll 1$, by equations (30), $R(\lambda) \approx R(0)$ and $R'(\lambda) \approx \lambda R''(0)$. Substituting these approximations into equation (35) yields

$$\begin{aligned} s(T + \lambda) &= a_0 s(T) + a_1 s'(T) \\ a_0 &= R(\lambda)/R(0) \approx R(0)/R(0) = 1 \\ a_1 &= R'(\lambda)/R''(0) \approx \lambda R''(0)/R''(0) = \lambda \\ s(T + \lambda) &= s(T) + \lambda s'(t) \end{aligned} \tag{36}$$

which agrees with the first two terms of a Taylor expansion of $s(t)$ about point $s(T)$.

Example: Suppose a stationary random process is described by the autocorrelation function

$$R(\lambda) = A \cos(\alpha\lambda), |\lambda| < T$$

If $s(t)$, $0 \leq t \leq T$, is a sample function from this process, predict $s(t + \lambda)$ in terms of $a_0 s(t) + a_1 s'(t)$ with minimum error

$$E \left\{ [s(t + \lambda) - a_0 s(t) - a_1 s'(t)]^2 \right\}$$

Solution: We know from the LMS prediction technique that

$$a_0 = R(\lambda)/R(0) \text{ and } a_1 = R'(\lambda)/R''(0)$$

Substituting, we find

$$a_0 = \cos(\alpha\lambda) \text{ and } a_1 = \sin(\alpha\lambda)/\alpha$$

Therefore,

$$s(t + \lambda) \approx \cos(\alpha\lambda)s(t) + \sin(\alpha\lambda)s'(t)/\alpha$$

The mean square prediction error turns out to be

$$\begin{aligned}
 & E \left\{ [s(t+\lambda) - a_0 s(t) - a_1 s'(t)]^2 \right\} \\
 &= R(0) - a_0 R(\lambda) + a_1 R'(\lambda) \\
 &= A - A \cos^2(\alpha\lambda) - A \sin^2 \alpha\lambda = 0
 \end{aligned}$$

Given this stationary process described by its autocorrelation function, the LMS technique predicts future signal values with no error (perfect prediction) for any allowed prediction time.

The above results do not hold for nonstationary processes.

We have yet to comment on the condition under which the preceding prediction analysis is valid. The condition which must be satisfied is that the vibration data be ergodic and stationary. Ergodic means that time averages can be used in place of ensemble averages in obtaining vibration statistics, e.g., correlation functions. Stationary* means that the various expectations of the random variable data (e.g., mean, variance, correlation function, etc.) are invariant with translations in time. This implies that these statistics can depend only on the time differences of the variables involved. There are several definitions of stationarity. The definition we are interested in is called wide sense stationary.

If

$$E \left\{ s(t) \right\} \stackrel{\Delta}{=} 1/T \int_{t_0}^{t_0+T} s(t) dt = m_s(t_0) = \text{constant}$$

and

$$\begin{aligned}
 E \left\{ s(t+\lambda) s(t) \right\} & \stackrel{\Delta}{=} 1/T \int_{t_0}^{t_0+T} s(t+\lambda) s(t) dt \\
 &= R_{ss}(t_0, t_0 + \lambda) = R_{ss}(\lambda)
 \end{aligned}$$

for any t_0 , then the data is said to be wide sense stationary.

*In general, a physical random process, such as an operating gearbox, is considered to be stationary when the physical condition and operating environment (load, temperature, mechanical drive system, etc.) remain essentially unchanged over time.

The wide sense stationarity assumption allows us to reduce the orthogonality equations which involve averages of unknown data in terms of averages computed from known data (i. e., the correlation function $R(\lambda)$, $0 < \lambda < T$, from known data $R(t)$, $0 \leq t \leq T$). Assuming that the operating gearbox is a stationary process, then the LMS prediction technique developed above will predict future values of the data with minimum error in a least-mean-square error sense using the actual vibration data obtained in a previous time interval.

In summary, although it appears that the LMS prediction technique does provide a fairly accurate prediction of the future vibration levels as based on previously measured values for a stationary process, the vibration signals which are associated with gearbox wear are not stationary in the long-term sense. However, the value of the LMS technique may lie in the fact that it is not a good predictor of a non-stationary process such as accelerating wear in the gearbox. If the LMS prediction is valid only for subtle changes in the vibration signal statistics, then large deviations from the LMS predicted values would indicate the presence of a nonstationary process which in turn might be relatable to accelerating wear. Since deviations from the predicted values may be the indicators of wear and not the prediction itself, the LMS technique for a stationary process is probably of more value as a diagnostic rather than a prognostic tool. The LMS technique can be extended to the nonstationary process⁹ and might have potential as a prognostic tool. At this point in time there has not been sufficient work done on the application of the stationary process LMS technique to the gearbox vibration data base to obtain any firm conclusions on the value of this prediction technique to the current contractual effort. LMS techniques for both stationary and nonstationary processes should be studied in greater depth in future prognostic efforts.

APPENDIX B
DETAILED DOCUMENTATION OF GEARBOX TESTS

This appendix contains detailed documentation for the gearboxes tested under this contract. The various testing procedures used to document the mechanical condition of each component are discussed in the text of this report in the section on "Test Instrumentation and Procedures."

An alphanumeric labeling system was used to identify each gearbox:

HT	=	High Time Unit	=	ABC-1329
BB	=	Bad Bearing #1	=	ABC-3398
BG	=	Bad Gear	=	B13-6884
BBT	=	Bad Bearing #2	=	B13-3395
BB3	=	Bad Bearing #3	=	B13-9974

Bearings were identified by a dash number:

-1	=	Input Duplex pair, bearing A
-2	=	Input Duplex pair, bearing B
-3	=	Output Duplex pair, bearing A
-4	=	Output Duplex pair, bearing B
-5	=	Input Roller
-6	=	Output Roller

Figure 90 shows the locations for each of these components. Figure 91 shows a partial disassembly of a gearbox to show its overall complexity.

HIGH TIME (HT) GEARBOX (ABC-1329)

This gearbox had reached TBO* (1200 hours) and did not show signs of significant internal damage. The manufacturer and serial number for each bearing are listed below:

HT-1	:	Fafnir 7207PW2	S/N 30638-1
HT-2	:	Fafnir 7207PW2	S/N 30638-2
HT-3	:	Fafnir 9108W1-3	S/N 34673-1
HT-4	:	Fafnir 9108W1-3	S/N 34673-2
HT-5	:	MRC R11OKD	S/N 32311
HT-6	:	— (not available)	

*Time Between Overhauls

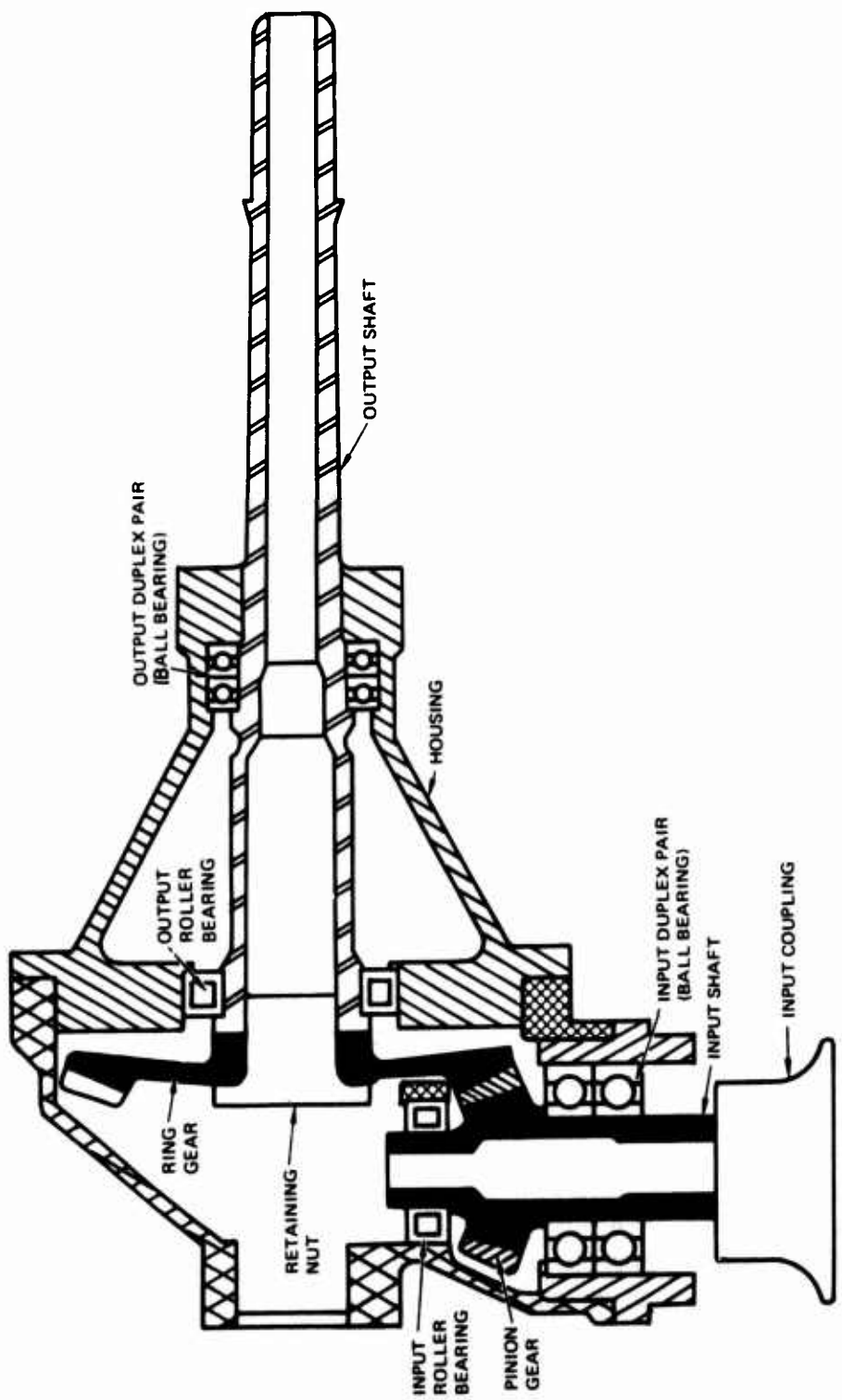


Figure 90. Cross-Sectional View of 90° Gearbox.

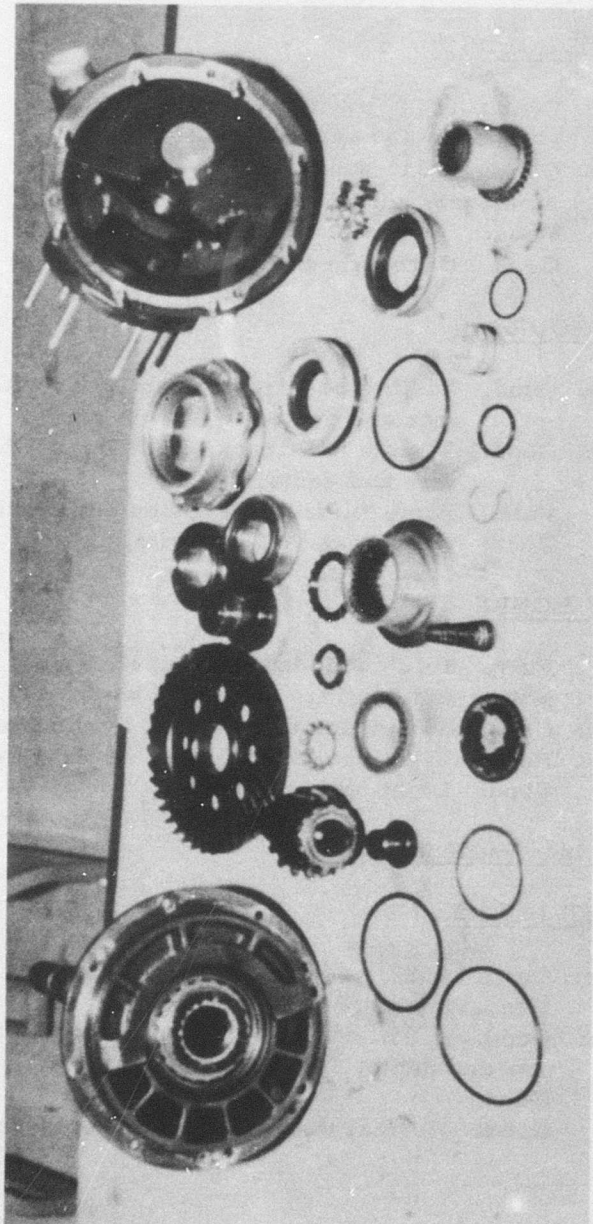


Figure 91. Partial Disassembly of a 90° Gearbox.

Visual Inspections of HT Gearbox Bearings

HT-1 Ball Bearing Visual Inspection

ZERO TEST HOURS

Outer Race: Good. 0.11" wide ball track, light wear with small pits and dents.
Inner Race: Good. 0.11" wide ball track, light wear with small pits and dents, oil deposit over 75% of raceway.
Balls: Good.
Retainer: Good. Carbonized oil deposits.

877 TEST HOURS

Outer Race: Good. Visible ball track, light wear with small pits and dents.
Inner Race: Good. Visible ball track, light wear with small pits and dents.
Balls: Fair. Some surface corrosion and denting.
Retainer: Good. Carbonized oil deposits.

1454 TEST HOURS

Inner Race: Fair. 0.12" wide ball track, electrical damage-pitting and denting, moderate wear.
Outer Race: Generally similar to inner, 0.1" wide ball track.
Balls: Poor. Light scratches, pits, several large dents.
Retainer: Good. Light pocket wear.

HT-2 Ball Bearing Visual Inspection

ZERO TEST HOURS

Outer Race: Good. 0.09" wide ball track, light wear with small pits and dents.
Inner Race: Good. 0.09" wide ball track, light wear with small pits and dents.
Balls: Good.
Retainer: Good. Normal wear, heavy carbon deposits.

877 TEST HOURS

Outer Race: Good. Visible ball track, light wear with small pits and dents.
Inner Race: Good. Visible ball track, light wear with small pits and dents.
Balls: Good. Some light denting.
Retainer: Good. Normal wear, heavy carbon deposits.

1454 TEST HOURS

Inner Race: Fair. 0.1" wide ball track, electrical damage - pitting and denting, moderate wear.
Outer Race: Generally similar to inner. 0.12" wide ball track. Rather coarse, liney original finish.
Balls: Fair. Light pitting and denting. Considerable surface frosting due to fine electrical pitting. Some circumferential banding.
Retainer: Good. Light pocket wear.

HT-3 Ball Bearing Visual Inspection

ZERO TEST HOURS

Outer Race: Good. 0.08" wide ball track, light abrasive wear with light denting.
Inner Race: Good. 0.08" wide ball track, light abrasive wear with light denting.
Balls: Good.
Retainer: Good. Normal wear.

877 TEST HOURS

Outer Race: Good. 0.093" wide ball track, light pitting and denting.
Inner Race: Fair. Visible ball track, some pitting and heavy denting.
Balls: Good.
Retainer: Good. Normal wear.

1454 TEST HOURS

Inner Race: Fair. 0.09" wide ball track, electrical damage - pitting and denting, moderate wear.

Outer Race. Generally similar to inner; 0.09" wide ball track.
Balls: Poor. Pitting and denting; several large dents.
Retainer: Fair. Light pocket wear. Visibly out-of-round.

HT-4 Ball Bearing Visual Inspection

ZERO TEST HOURS

Outer Race: Good. 0.06" wide ball track, light abrasive wear with light denting and pitting.
Inner Race: Good. 0.06" wide ball track, light abrasive wear with slight pitting.
Balls: Good.
Retainer: Good. Normal wear.

877 TEST HOURS

Outer Race: Fair. .078" wide ball track, light wear with moderate denting and pitting.
Inner Race: Good. 0.06" wide ball track, light abrasive wear with slight pitting.
Balls: Poor. Some corrosion and moderate denting.
Retainer: Good. Normal wear.

1454 TEST HOURS

Inner Race: Fair. 0.09" wide ball track, electrical damage - pitting and denting, light-to-moderate wear.
Outer Race: Generally similar to inner; 0.09" wide ball track.
Balls: Fair. Pitting and denting.
Retainer: Fair. Visibly out-of-round, light pocket wear.

HT-5 Roller Bearing Visual Inspection

ZERO TEST HOURS

Outer Race: Good. Light abrasive wear with slight brinelling.
Inner Race: Good. Light wear, light denting.
Rollers: Good. Light wear, light denting, some circumferential bands.
Retainer: Good. Normal wear.

877 TEST HOURS

Outer Race: Fair. Light wear, some scoring, small-to-large particle denting.
Inner Race: Fair. Light wear, some scoring, small-to-large particle denting.
Rollers: Fair. Light wear, small-to-large particle dents, scoring.
Retainer: Fair. Normal wear, some damage at #10 pocket (CW from 'X').

1454 TEST HOURS

Inner Race: Fair. Electrical damage - pitting and denting, light-to-moderate wear.
Outer Race: Fair. Similar to inner.
Roller: Fair. Similar to inner raceway. Some banding and light end wear.
Retainer: Good.

HT-6 Roller Bearing Visual Inspection

ZERO TEST HOURS

Outer Race: Good. Slight abrasive wear, slight denting.
Inner Race: Good. Light abrasive wear, small-particle dents.
Rollers: Good. Light abrasive wear, small-particle dents.
Retainer: Good.

877 TEST HOURS

Outer Race: Good. Slight wear and denting.
Inner Race: Good. Light abrasive wear, small-particle dents.
Rollers: Fair. Some scoring and corrosion, small-to-large particle dents.
Retainer: Good.

1454 TEST HOURS

Inner Race: Unable to examine; disassembly unauthorized.
Outer Race: Fair. Light-to-moderate wear.
Rollers: Light-to-moderate wear, pitting and denting, light end wear.
Retainer: Good.

HT Gearbox Mechanical Condition Summary

Table VII summarizes the results of the mechanical measurements made on the ball bearings in the HT gearbox. Table VIII summarizes the mechanical measurements for the roller bearings.

HT Gearbox Bearing Photographs and Cross-Groove Profiles

Figures 92 through 103 show the polar representation of the cross-groove profile for the HT bearings. Figures 104 through 113 show the scanning electron photomicrographs for the bearings taken at various test times. SEM pictures are taken in the secondary emission (SEC) mode unless specifically marked backscatter emission (BSE) mode.

A more detailed discussion of the cross-groove profile measurement technique and the difference in SEM modes of operation can be found in the text of this report in the section on "Test Instrumentation and Procedures."

TABLE VII. MECHANICAL MEASUREMENTS FOR HT BALL BEARINGS

Bearing	Test Time (hr)	Noise Level (dB)	Peak Rise (dB)	General Condition (Wear)	Local Damage	Raceway Wear Depth (μ in.)	Radial Play (in.)
HT-1	0	-0.5	3	negligible	light	85	.0074
	877	3	3	moderate	light	88	.0074
	1454	7	-1	heavy	negligible	negligible	.0078
HT-2	0	3.5	2.5	moderate	light	55	.0073
	877	4	2	moderate	light	57	.0072
	1454	9.5	2.5	heavy	light	75	.0077
HT-3	0	2.0	2.5	light	light	146	.0032
	877	4.5	1.5	moderate	light	170	.0035
	1454	10.0	4	heavy	negligible	60	.0032
HT-4	0	0.5	2	light	light	124	.0030
	877	2.5	6	light	moderate	150	.0032
	1454	8.5	-1	heavy	negligible	negligible	.0033

TABLE VIII. MECHANICAL MEASUREMENTS FOR HT ROLLER BEARINGS

Bearing	Time (hr.)	Axial Clearance of Roller in Inner Race (in.)	Roller Contour (μ in.)	Roller Crown	
				Drop (μ in.)	Length (in.)
HT-5	0	.0023	20 concave	50	.057
	877	—	—	—	—
	1454	.0025	10 concave	48	.070
HT-6	0	.0032	20 convex	335	.037
	877	—	—	—	—
	1454	.0025	30 convex	—	full*

* A Full Roller Crown Is Indicative of Severe Wear.

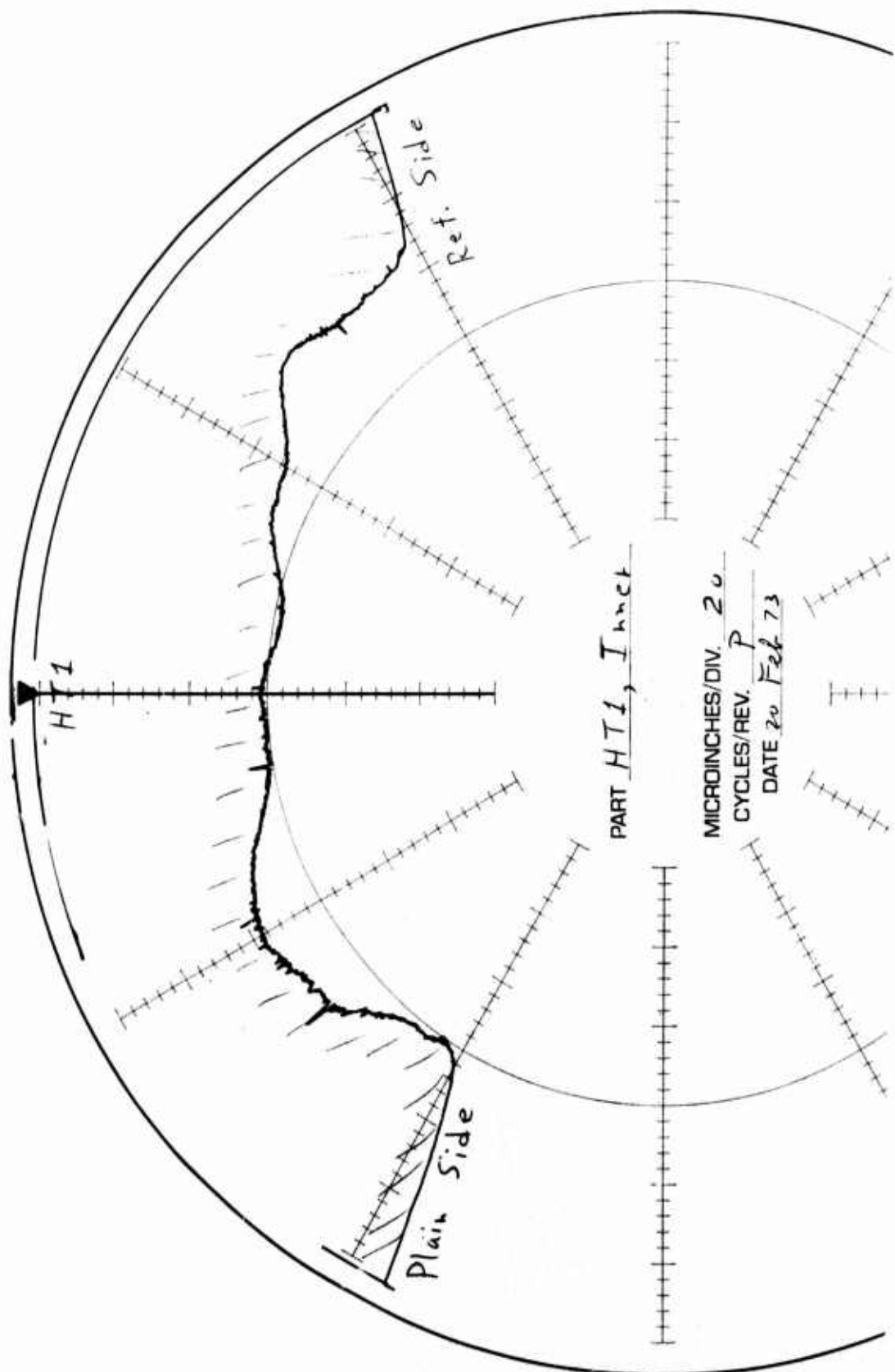


Figure 92. HT-1 Cross-Groove Profile at Zero Test Hours.

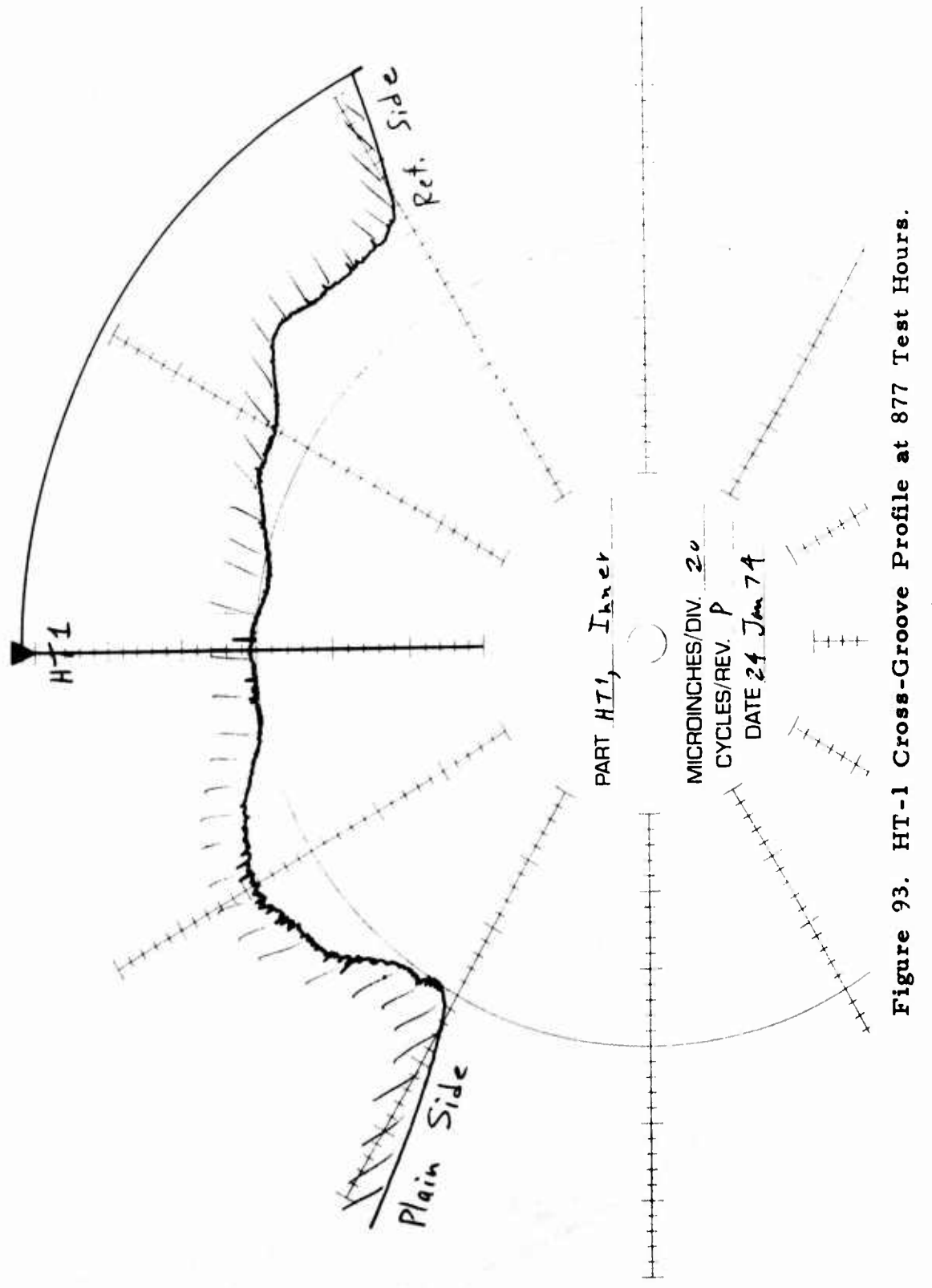
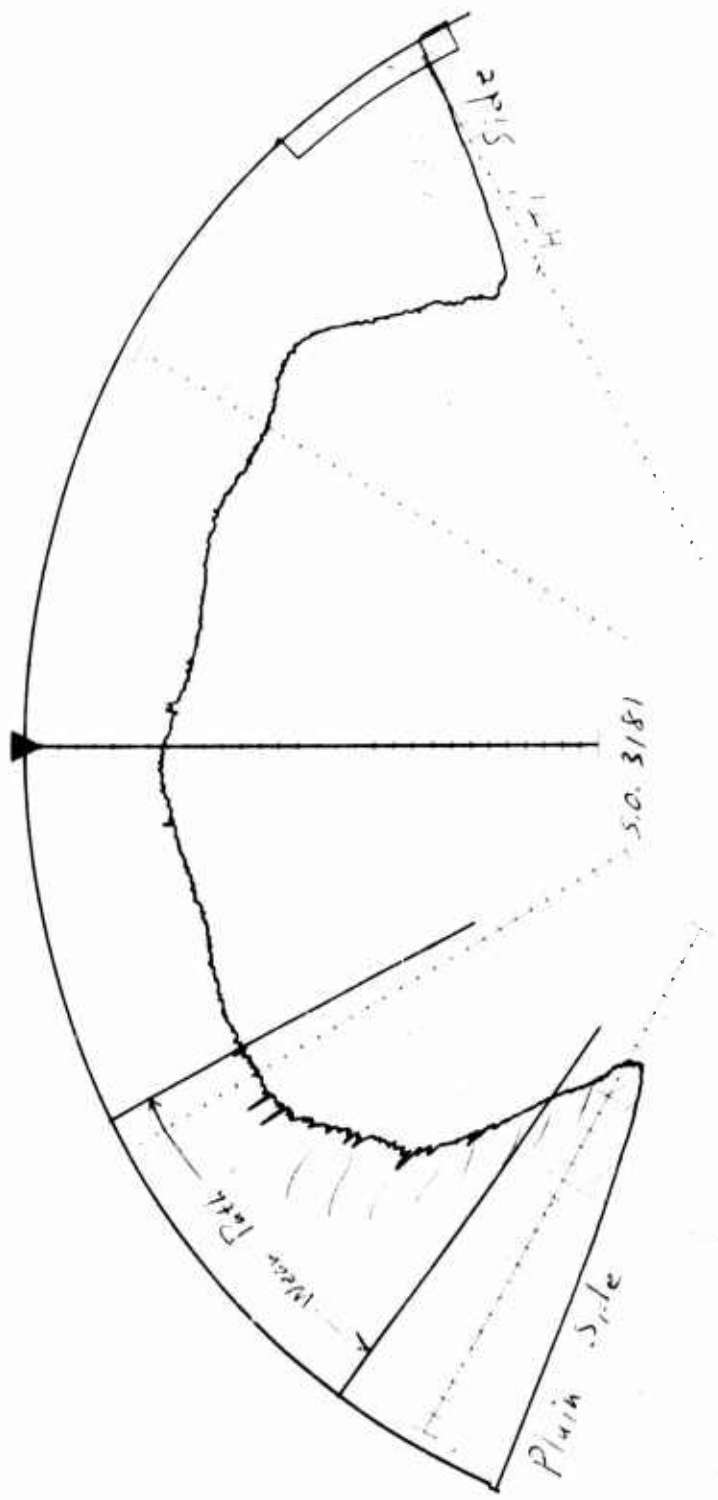


Figure 93. HT-1 Cross-Groove Profile at 877 Test Hours.



PART HT1, Liner

MICROINCHES/DIV. 20
CYCLES/REV. P
DATE 7 May 74

Figure 94. HT-1 Cross-Groove Profile at 1454 Test Hours.

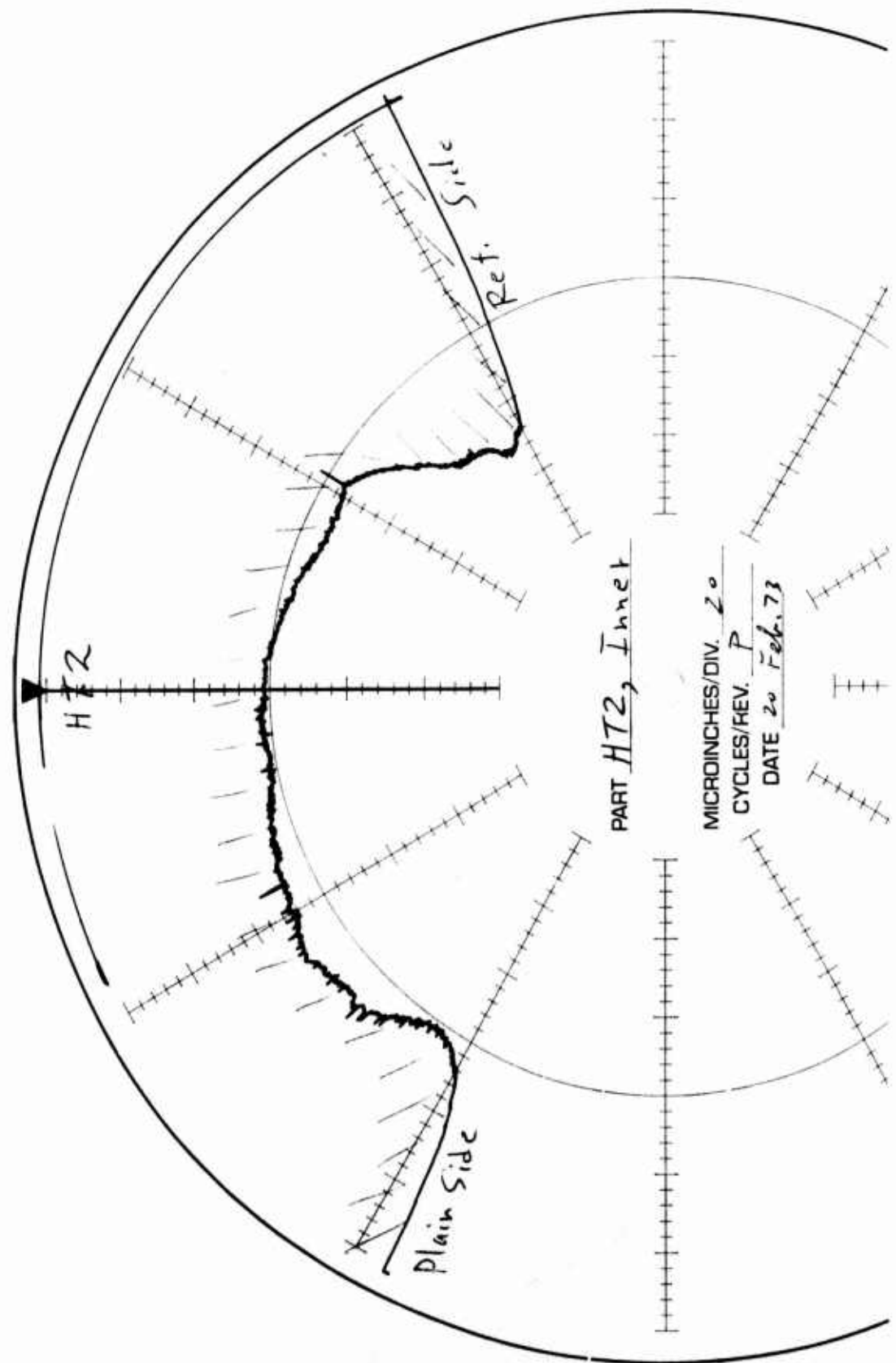


Figure 95. HT-2 Cross-Groove Profile at Zero Test Hours.

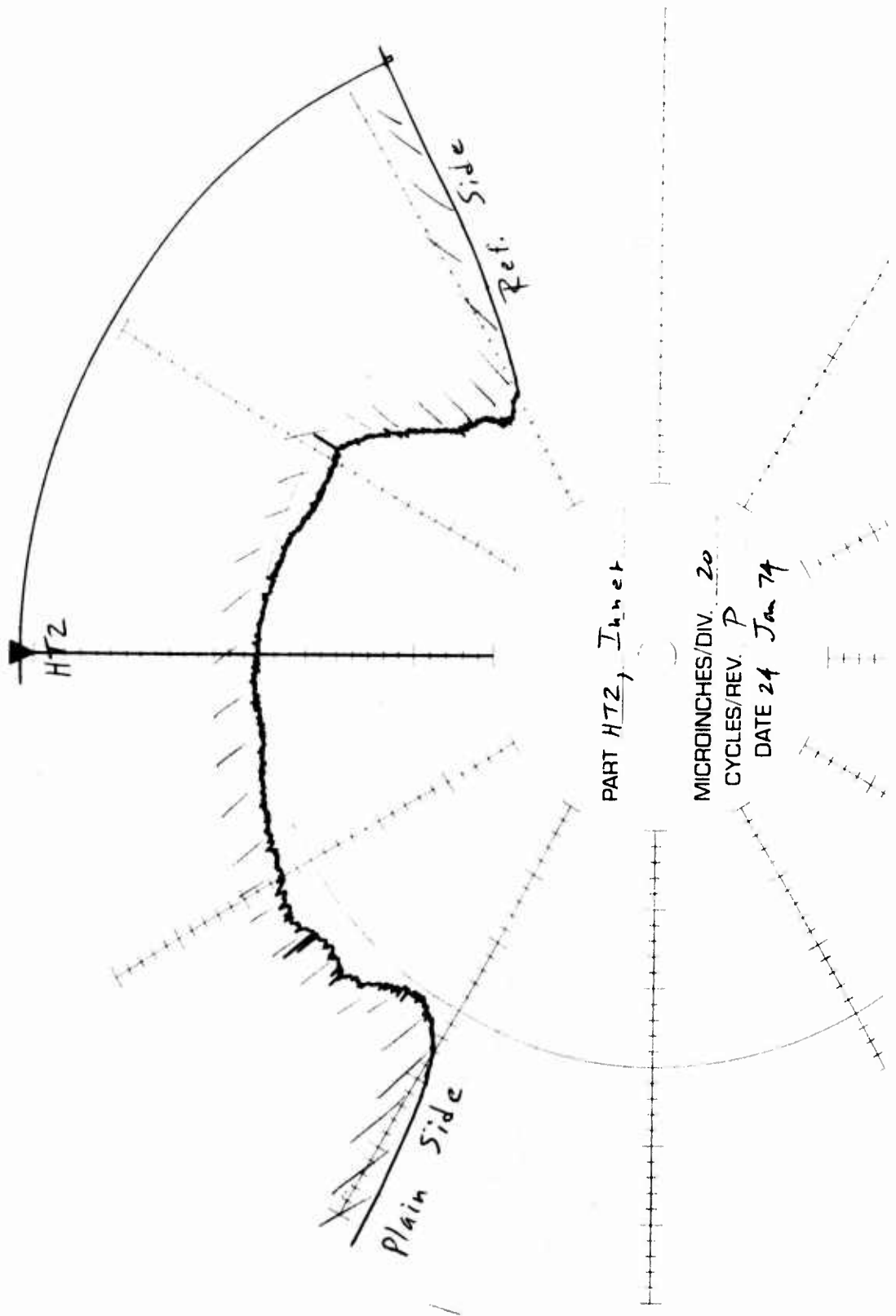


Figure 96. HT-2 Cross-Groove Profile at 877 Test Hours.

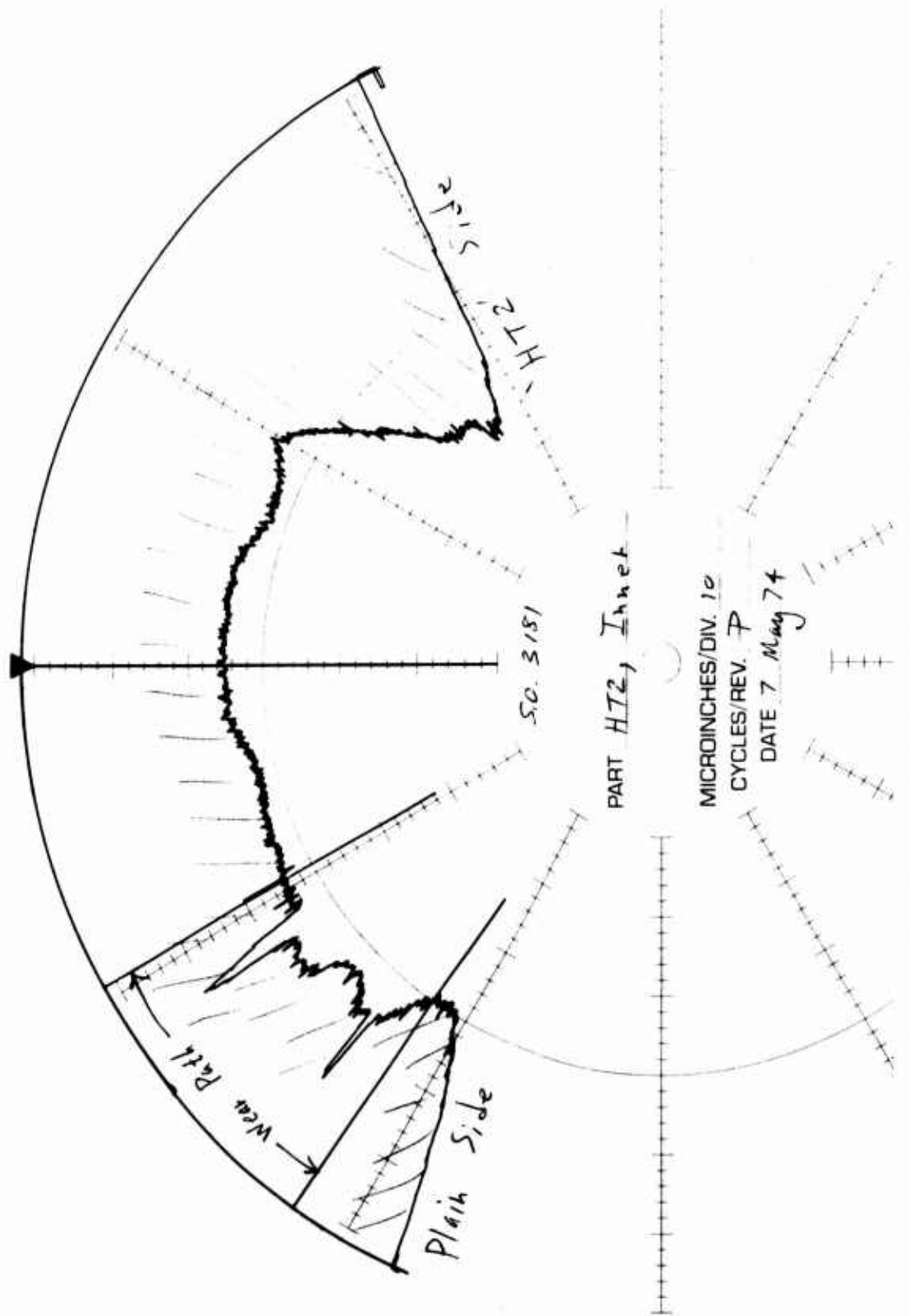


Figure 97. HT-2 Cross-Groove Profile at 1454 Test Hours.

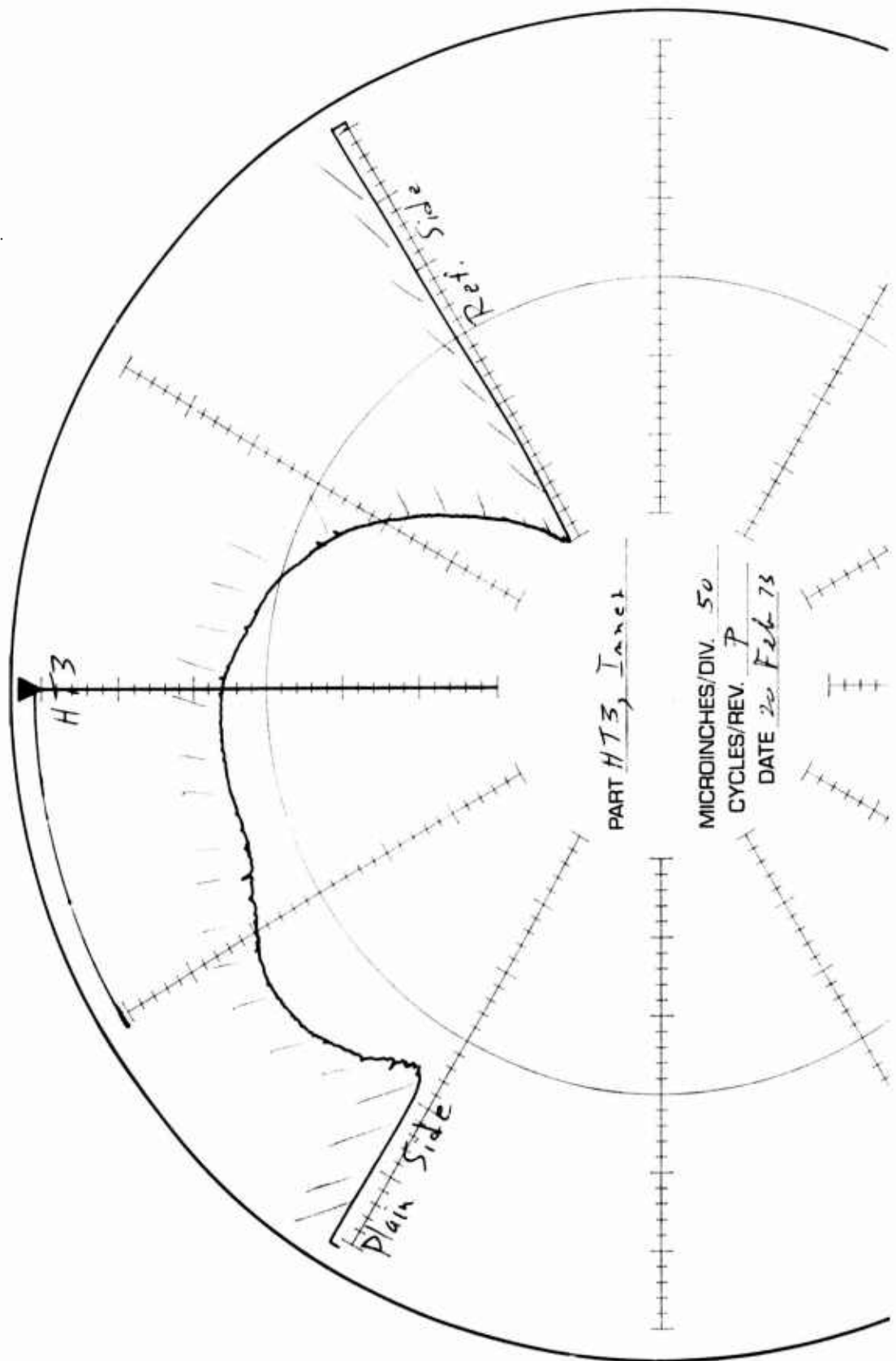


Figure 98. HT-3 Cross-Groove Profile at Zero Test Hours.

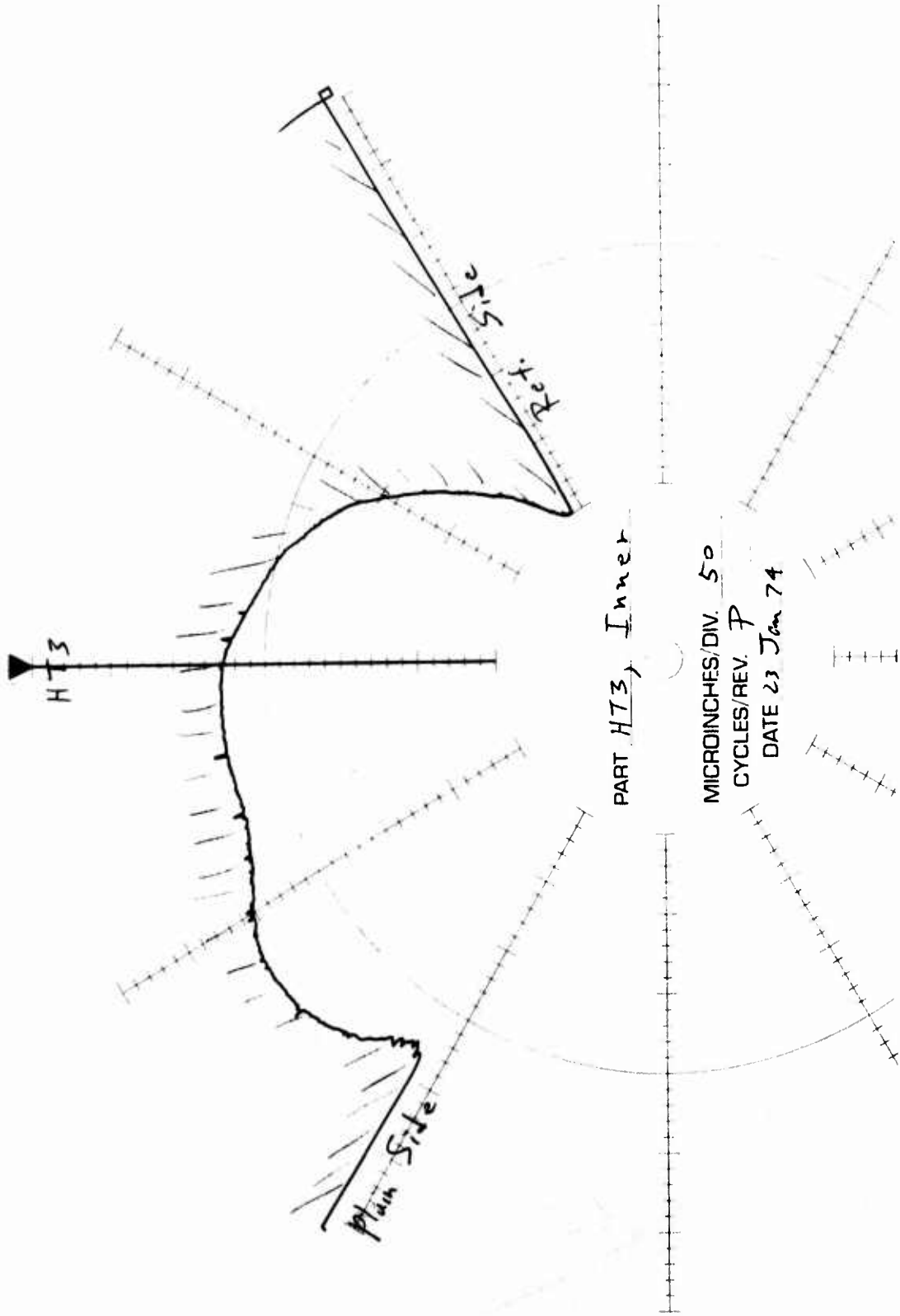


Figure 99. HT-3 Cross-Groove Profile at 877 Test Hours.

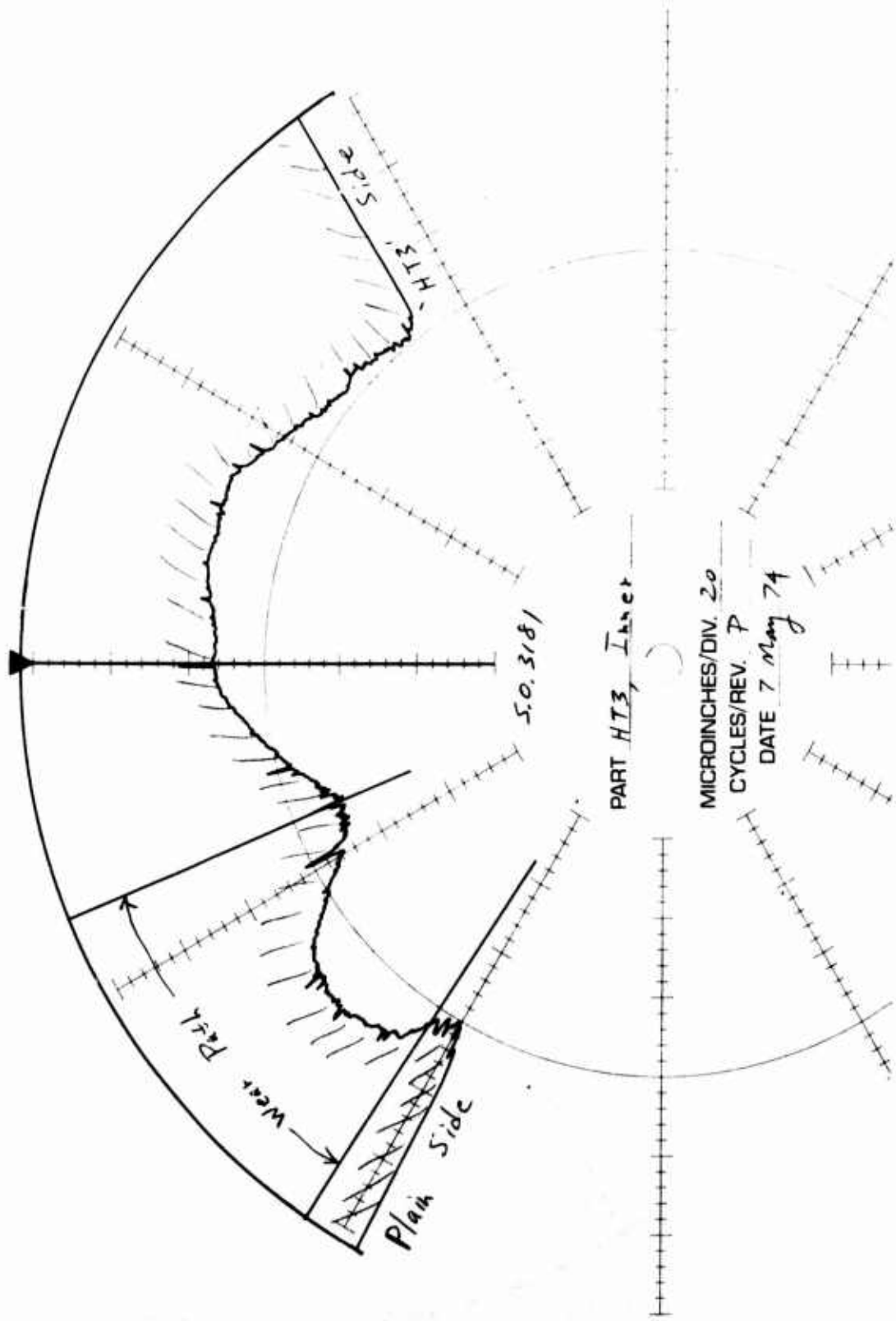


Figure 100. HT-3 Cross-Groove Profile at 1454 Test Hours.

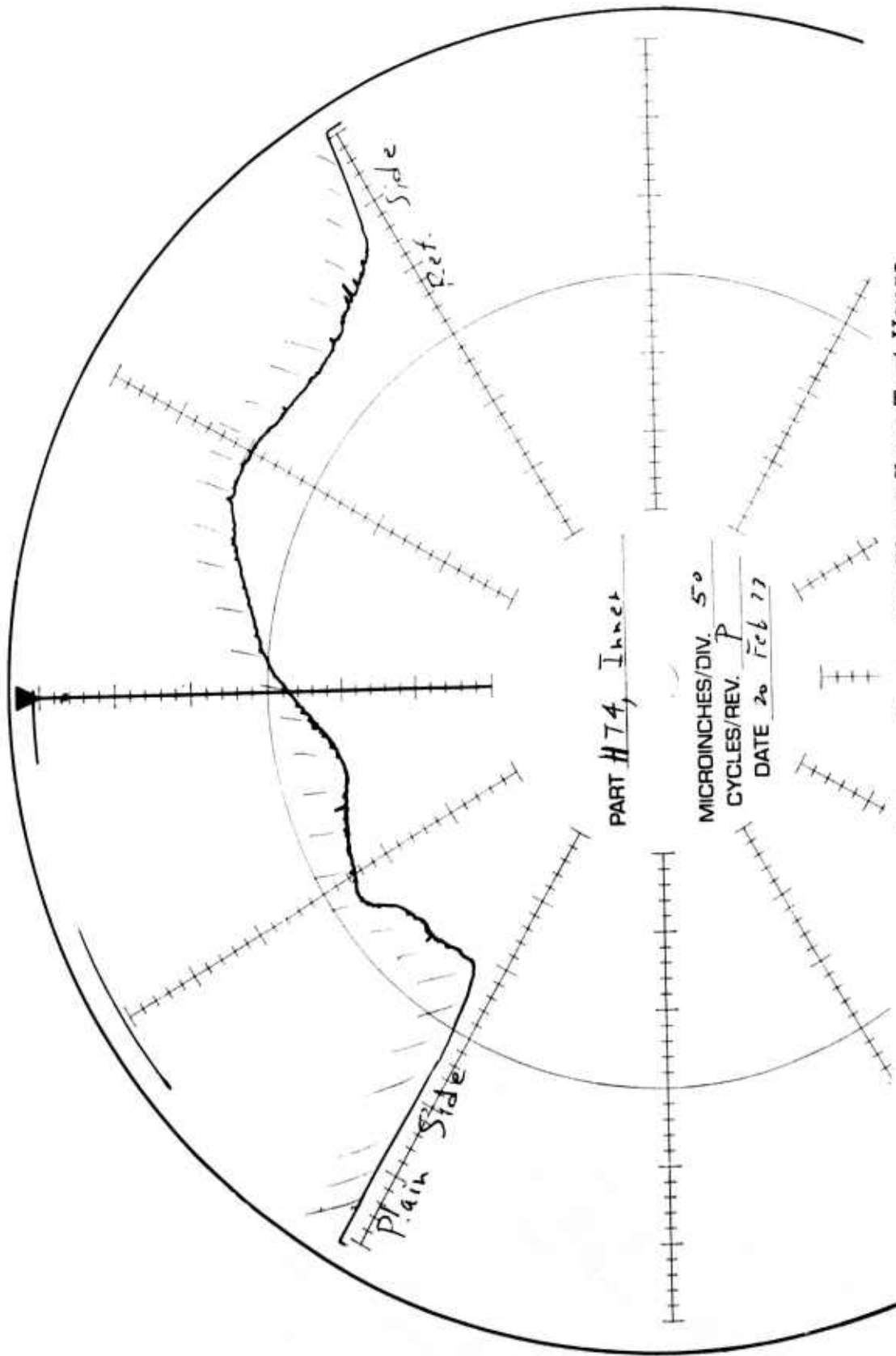


Figure 101. HT-4 Cross-Groove Profile at Zero Test Hours.

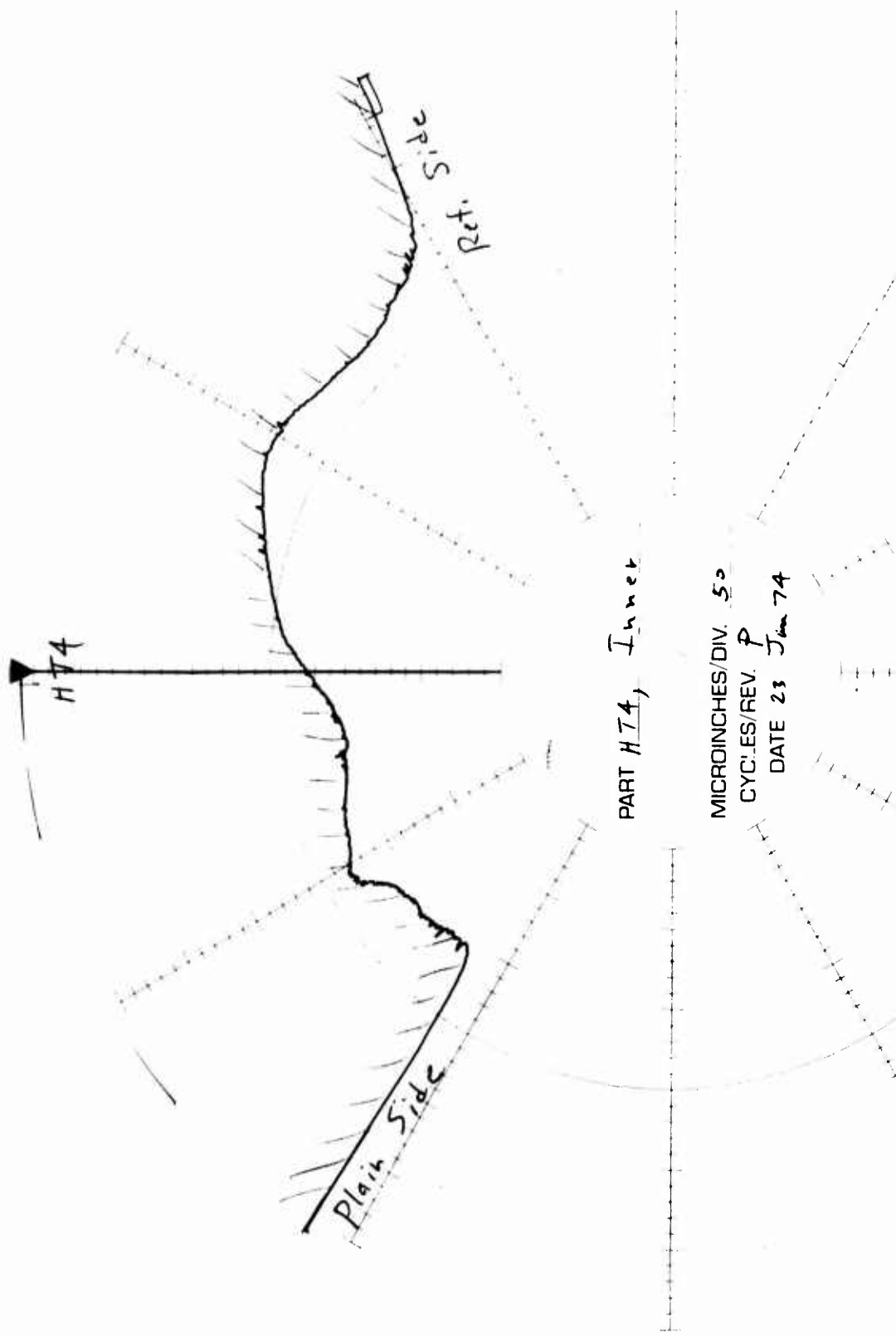


Figure 102. HT-4 Cross-Groove Profile at 877 Test Hours.

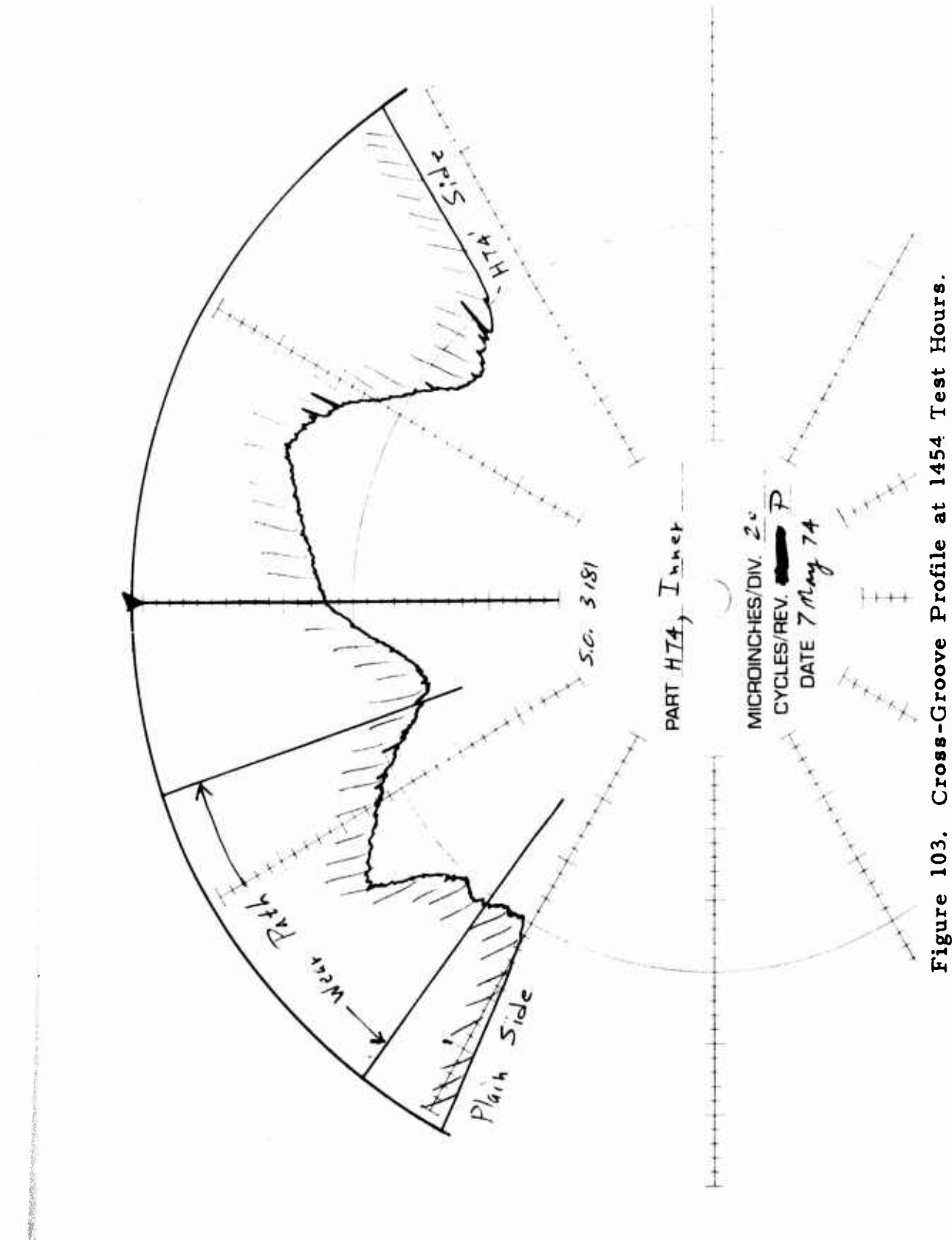
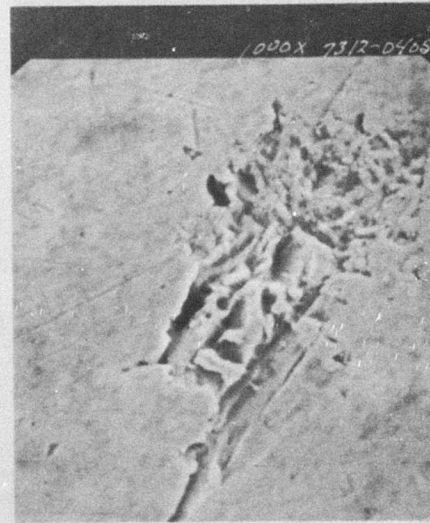
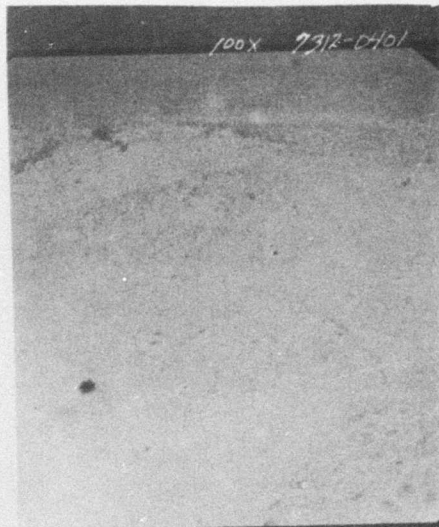


Figure 103. Cross-Groove Profile at 1454 Test Hours.



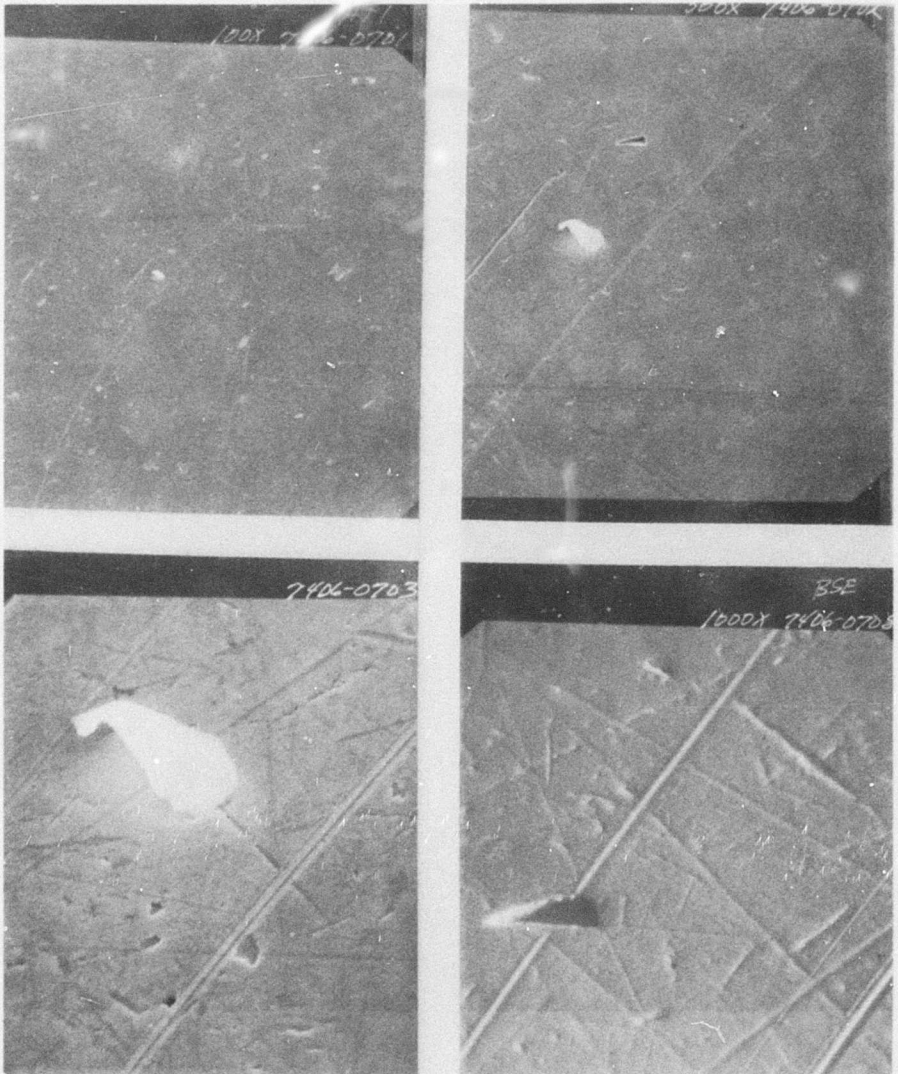
Top: 300 X, Zero Hours

Bottom: 300 X, 877 Hours

Top: 100 X, 877 Hours

Bottom: 300 X, 877 Hours

Figure 104. SEM Micrographs of HT-1 (Zero, 877 Hours).



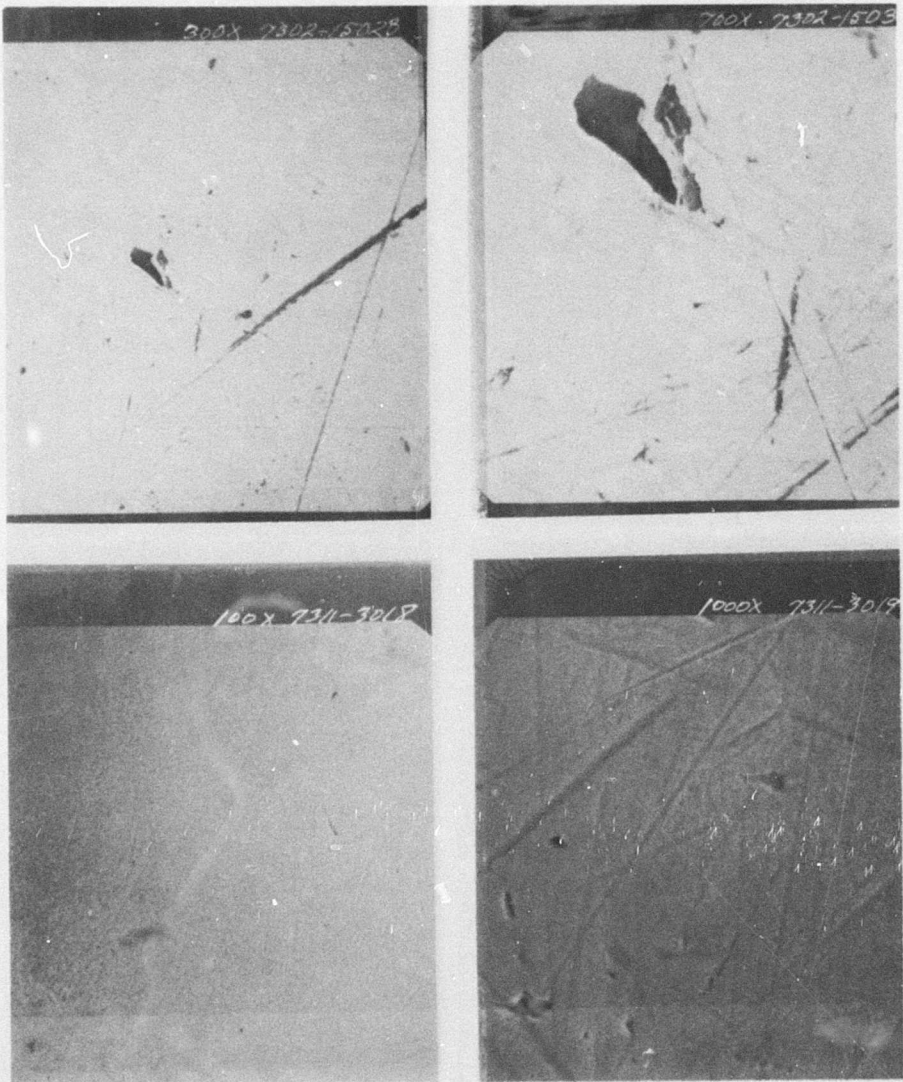
Top: 100 X

Bottom: 1000 X

Top: 300 X

Bottom: 1000 X BSE

Figure 105. SEM Micrographs of HT-1 (1454 Hours).



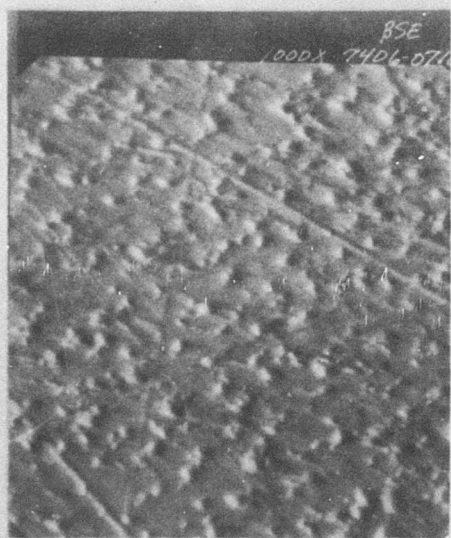
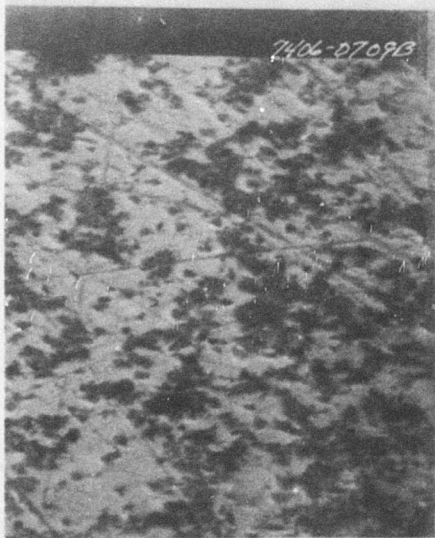
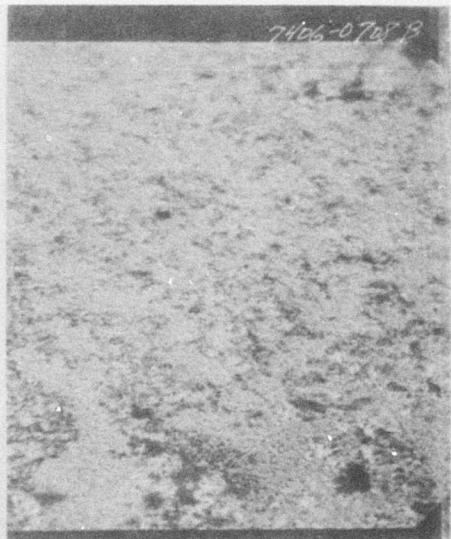
Top: 300 X, Zero Hours

Bottom: 100 X, 877 Hours

Top: 700 X, Zero Hours

Bottom: 1000 X, 877 Hours

Figure 106. SEM Micrographs of HT-2 (Zero, 877 Hours).



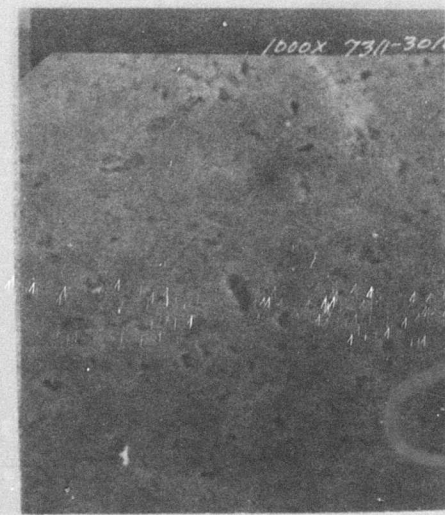
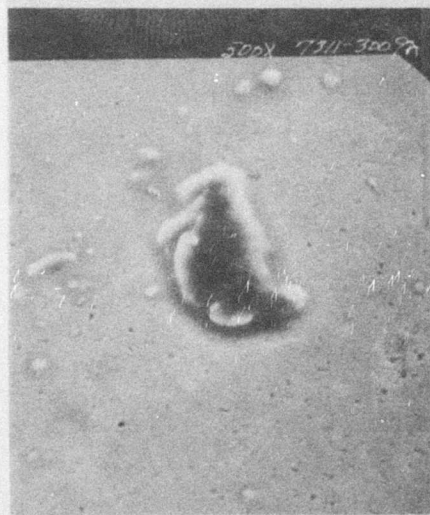
Top: 100 X

Bottom: 1000 X

Top: 300 X

Bottom: 1000 X, BSE

Figure 107. SEM Micrographs of HT-2 (1454 Hours).



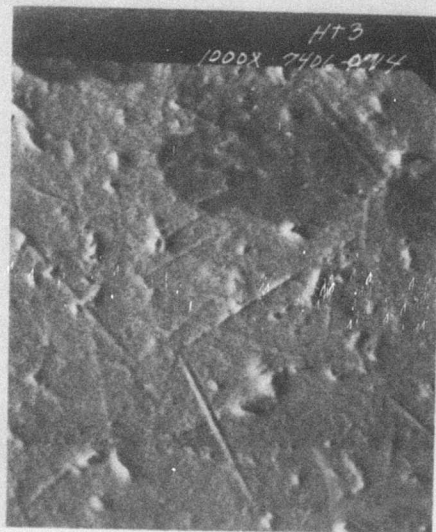
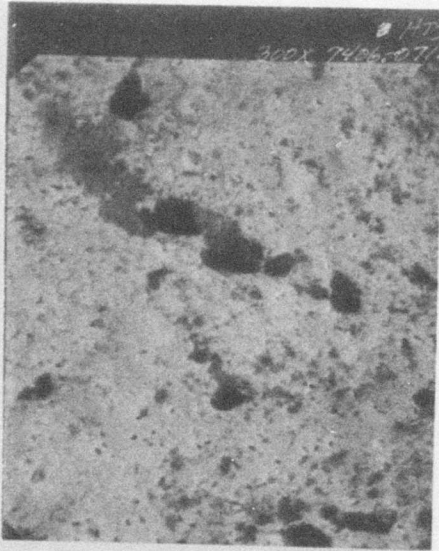
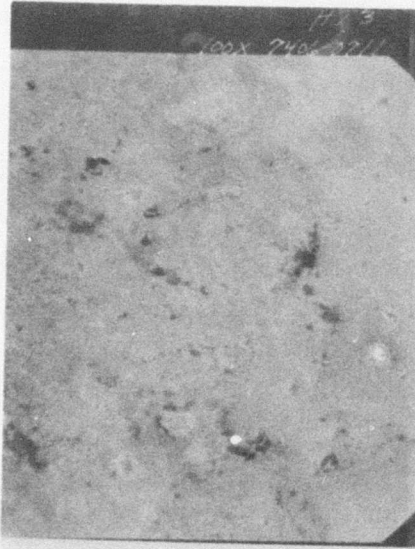
Top: 230 X, Zero Hours

Bottom: 500 X, 877 Hours

Top: 100 X, 877 Hours

Bottom: 1000 X, 877 Hours

Figure 108. SEM Micrographs of HT-3 (Zero, 877 Hours)



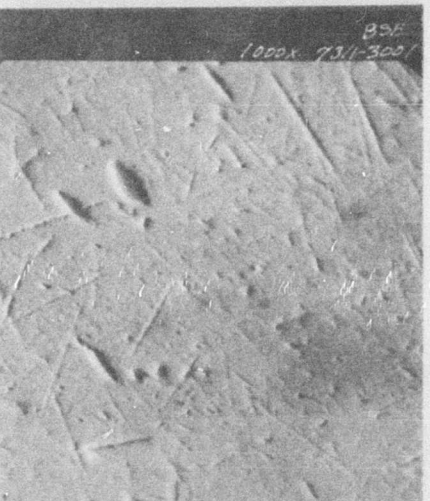
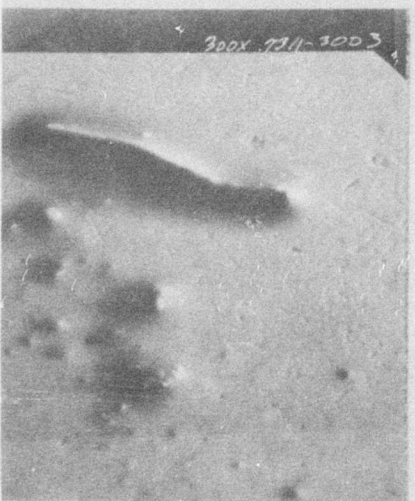
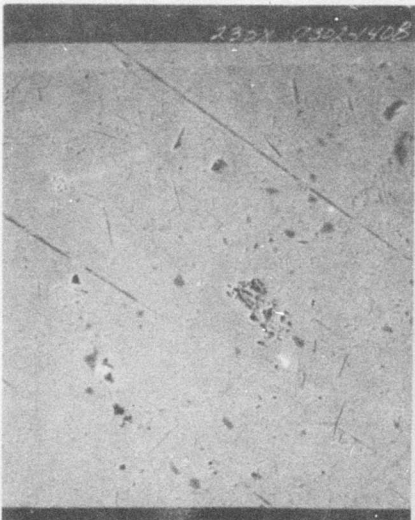
Top: 100 X

Bottom: 1000 X

Top: 300 X

Bottom: 1000 X, BSE

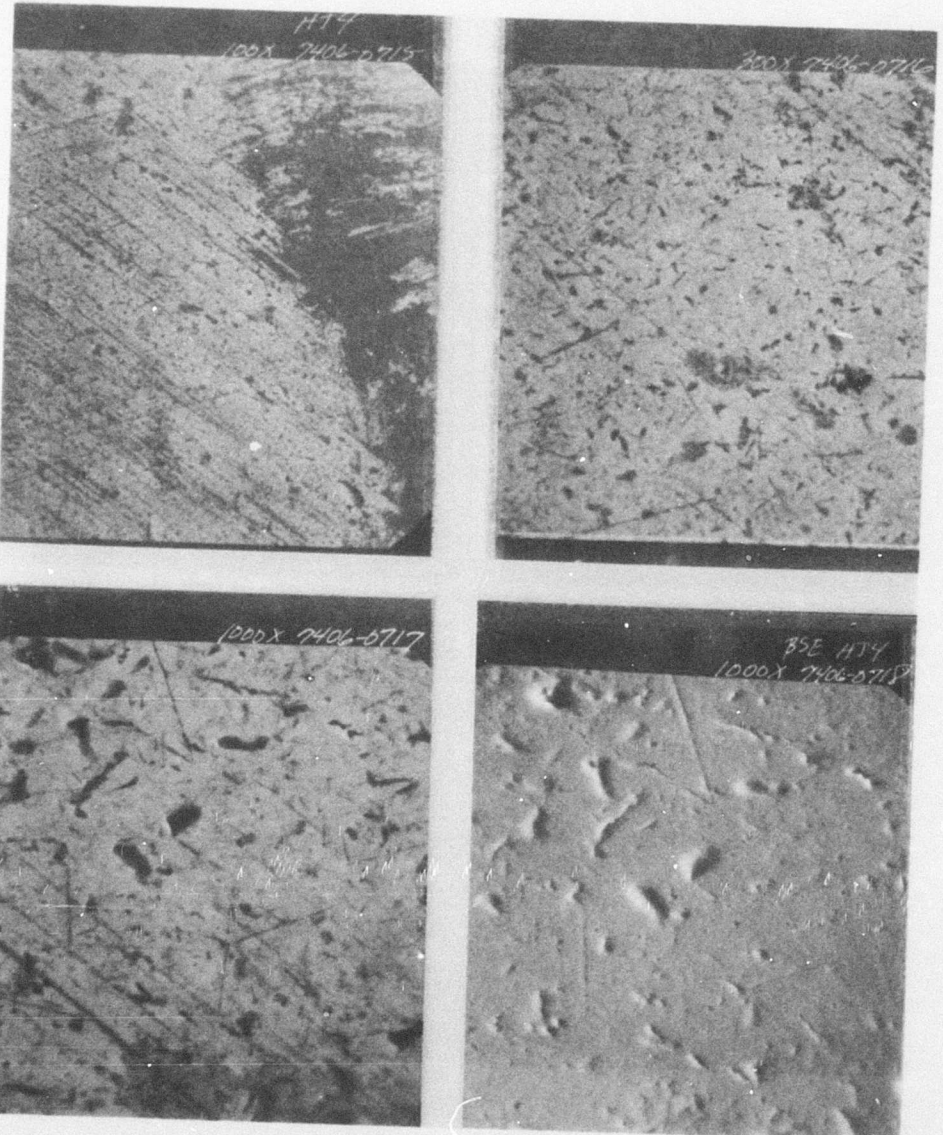
Figure 109. SEM Micrographs of HT-3 (1454 Hours).



Top: 20 X, Zero Hours
Bottom: 300 X, 877 Hours

Top: 100 X, 877 Hours
Bottom: 1000 X, BSE, 877
Hours

Figure 110. SEM Micrographs of HT-4 (Zero, 877 Hours).



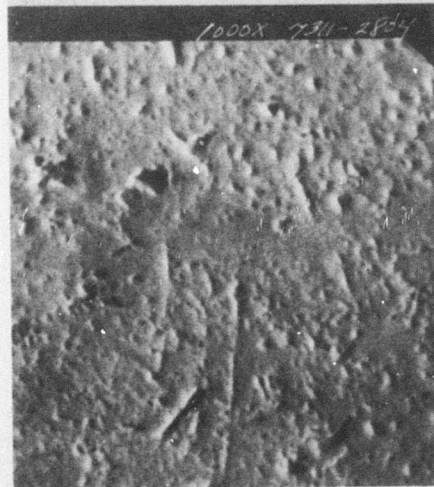
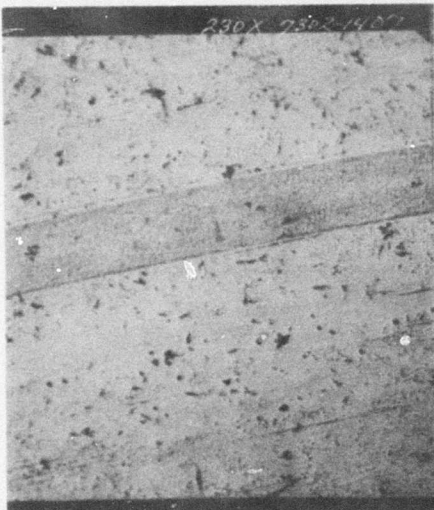
Top: 100 X

Bottom: 1000 X

Top: 300 X

Bottom: 100 X, BSE

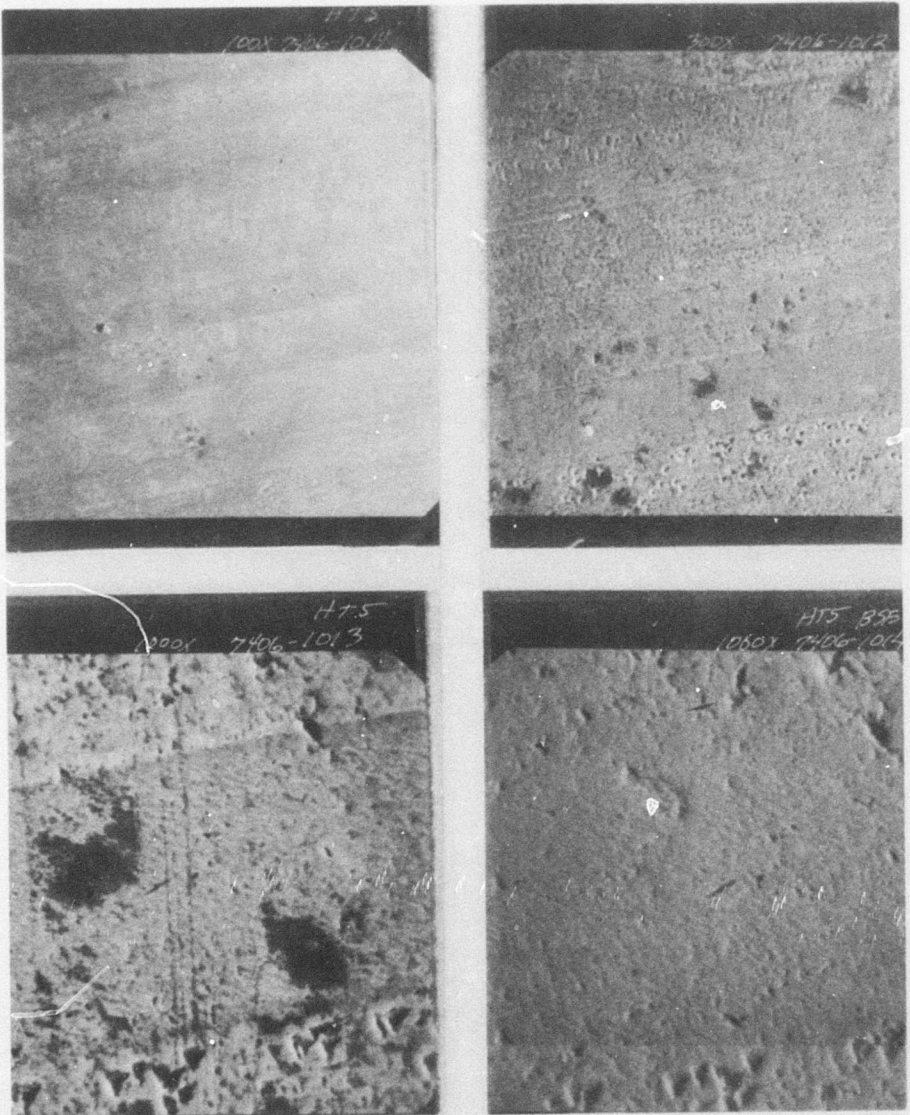
Figure 111. SEM Micrographs of HT-4 (1454 Hours).



Top: 230 X, Zero Hours
Bottom: 1000 X, 877 Hours

Top: 100 X, 877 Hours
Bottom: 300 X, 877 Hours

Figure 112. SEM Micrographs of HT-5 (Zero, 877 Hours)



Top: 100 X

Bottom: 1000 X

Top: 300 X

Bottom: 100 X, BSE

Figure 113. SEM Micrographs of HT-5 (1454 Hours).

BAD BEARING (BB) GEARBOX (ABC-3398)

This gearbox had reached TBO of 1200 hours and had shown signs of an incipient failed output duplex bearing (BB3, BB4). The manufacturer and serial number for each bearing are listed below:

BB1:	Fafnir 7207PW2	S/N 92154-1
BB2:	Fafnir 7207PW2	S/N 92154-2
BB3:	Fafnir 9108W1-3	S/N 37093-1
BB4:	Fafnir 9108W1-3	S/N 37094-2
BB5:	MRC R110KD	S/N 33338
BB6:	-- (not available)	

Visual Inspections of BB Gearbox Bearings

BB-1 Ball Bearing

ZERO TEST HOURS

Outer Race: Fair. 0.11" wide ball track, moderate wear, small dents.
Inner Race: Fair. 0.12" wide ball track, moderate wear, some corrosion outside ball tract.
Balls: Fair. Some dents and cuts.
Retainer: Good. Normal appearance.

166 TEST HOURS

Outer Race: Fair. 0.11" wide ball track, moderate wear, small dents.
Inner Race: Fair. 0.12" wide ball track, moderate wear, some light-brown-to-dark heat coloration on raceway outside of ball path extending to opposite end face.
Balls: Fair. Some dents and cuts.
Retainer: Good. Normal appearance.

BB-2 Ball Bearing

ZERO TEST HOURS

Outer Race: Fair. 0.11" wide ball track, moderate wear, small dents.
Inner Race: Fair. 0.12" wide ball track moderate wear, some corrosion outside ball track.

Balls: Fair. Some dents and cuts
Retainer: Good. Normal appearance.

166 TEST HOURS

Outer Race: Poor. 0.11" wide ball track, heavy wear, some dents.
Inner Race: Poor. 0.12" wide ball track, extreme wear in ball path; light brown coloration all about raceway.
Balls: Poor. Some dents and cuts, 0.13" wide circumferential heat coloration bands.
Retainer: Good. Normal appearance.

BB-3 Ball Bearing

ZERO TEST HOURS

Outer Race: Fair. 0.08" wide ball track, moderate-to-heavy denting, some large dents.
Inner Race: Fair-to-Poor. 0.09" wide ball track, heavy wear and denting.
Balls: Poor. Heavy wear and denting.
Retainer: Fair-to-Poor. Wear burrs (feathered edge) on lead edge of ball pocket.

166 TEST HOURS

Outer Race: Failed. Shoulder-to-shoulder fatigue 1/4 of raceway (circumferentially).
Inner Race: Failed. Off-square, variable fatigue path continuous - circumferentially.
Balls: Failed. Heavy fatigue.
Retainer: Poor. Heavy wear on leading edges of ball pockets; heavy wear on O. D. surface from raised edge on outer raceway shoulder

BB-4 Ball Bearing

ZERO TEST HOURS

Outer Race: Fair. 0.05" wide ball track, moderate small denting.
Inner Race: Fair-to-Poor. 0.08" wide ball track, moderate denting with heavy denting at 180° intervals.

Balls: Fair-to-Poor. Moderate-to-heavy small denting.
Retainer: Fair. Wear in leading edge of ball pocket.
Inner Race: Failed. Variable-width ball path with shoulder-to-shoulder fatigue, 1/4 (circumferentially) of raceway.
Balls: Failed. Heavy fatigue
Retainer: Failed. Just short of total separation into two halves due to thru-wear between pockets.

BB-5 Ball Bearing

ZERO TEST HOURS

Outer Race: Fair. Abrasive wear over 180°, moderate denting, several circumferential cuts.
Inner Race: Fair. Small-to-large particles denting with light electric pitting.
Rollers: Fair. Small-to-large particles denting with light electric pitting.
Retainer: Good. Normal

166 TEST HOURS

Outer Race: Poor. Heavy denting, over 180° of raceway, thermal coloration.
Inner Race: Fair. Small-to-large particle denting with light electric pitting.
Rollers: Fair. Small-to-large particle denting with light electric pitting.
Retainer: Poor. Light wear, damaged on plain side; distorted by impact load.

BB-6 Roller Bearing

ZERO TEST HOURS

Outer Race: Good. Slight abrasive wear and some small denting.
Inner Race: Fair. Moderate abrasive wear with some electric pitting.
Retainer: Good. Film of oxidized or deteriorated oil.

166 TEST HOURS

Outer Race: Fair. Slight abrasive wear, scoring and small-to-large particle denting.
Inner Race: Fair. Moderate abrasive wear and denting.
Rollers: Fair. Small-to-large particle denting.
Retainer: Poor. Film of oxidized or deteriorated oil, cracked at second rivet (CW from 'BB6' as viewed from 'BB6' side).

BB Gearbox Mechanical Condition Summary

Table IX summarizes the results of the mechanical measurements of the ball bearings in the BB gearbox. Table X summarizes the mechanical measurements for the roller bearings.

BB Gearbox Bearing Photographs and Cross-Groove Profiles

Figures 114 through 121 show the cross-groove profiles for the BB gearbox at various testing intervals.

Figures 122 through 127 show the scanning electron photomicrographs of the bearings taken before and after testing.

TABLE IX. MECHANICAL MEASUREMENTS FOR BB BALL BEARINGS

Bearing	Test Time (hr)	Noise Level (dB)	Peak Rise (dB)	General Condition (Wear)	Local Damage	Raceway Wear Depth (μ in.)	Radial Play (in.)
BB-1	0 166	2.5 5	18 1	light moderate	extreme light	20 20	.0070 .0070
BB-2	0 166	6.5 20.5	- 0.5 2	moderate extreme	negligible light	20 21.6	.0070 .0070
BB-3	0 166	20.5 **	2 *	extreme *	light *	160 **	.0032 **
BB-4	0 166	18.5 **	- 2 *	extreme *	negligible **	13.6 **	.0031 **

* Note: Catastrophic Failure

TABLE X. MECHANICAL MEASUREMENTS FOR BB ROLLER BEARINGS

Bearing	Time (hr)	Axial Clearance of Roller in Inner Race (in.)	Roller Contour	Roller Crown Drop (μ in.)	Crown Length (in.)
BB-5	0 166	.0027 .0027	10 Concave 30 Concave	64 91	.062 .064
BB-6	0 166	.0025 .0026	15 Concave 30 Convex	182 175	.113 .084

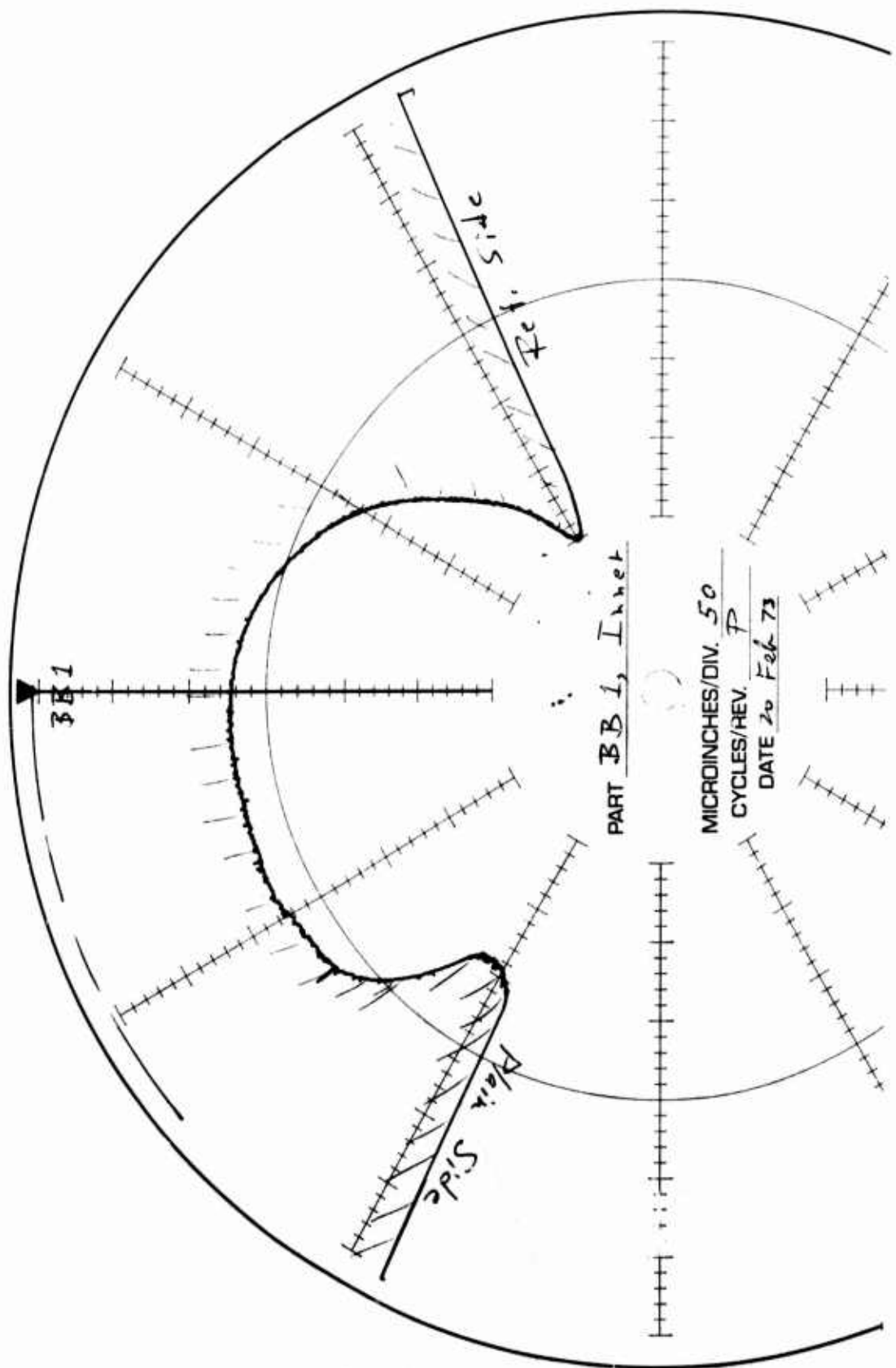


Figure i14. BB-1 Cross-Groove Profile at Zero Test Hours.

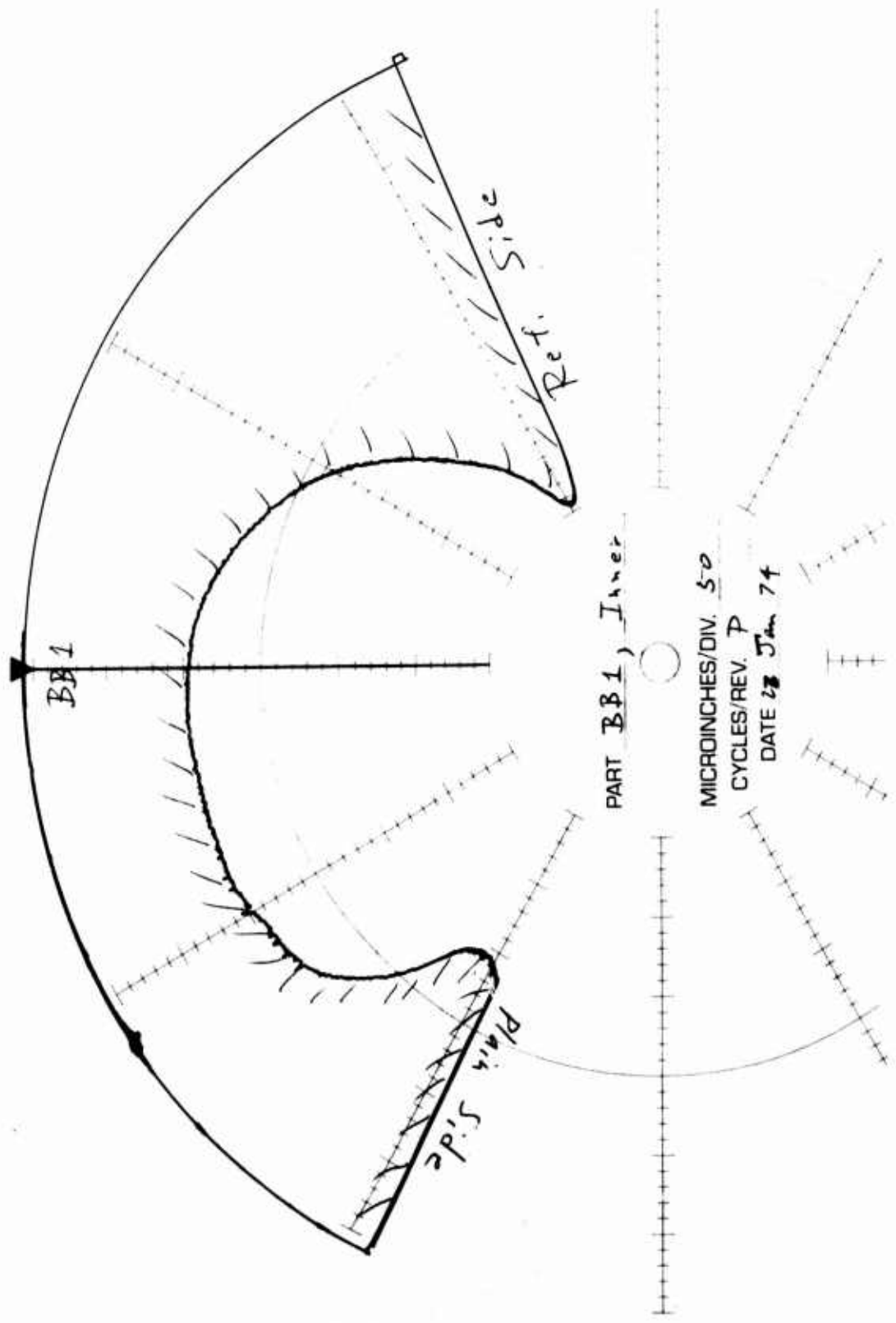


Figure 115. BB-1 Cross-Groove Profile at 166 Test Hours.

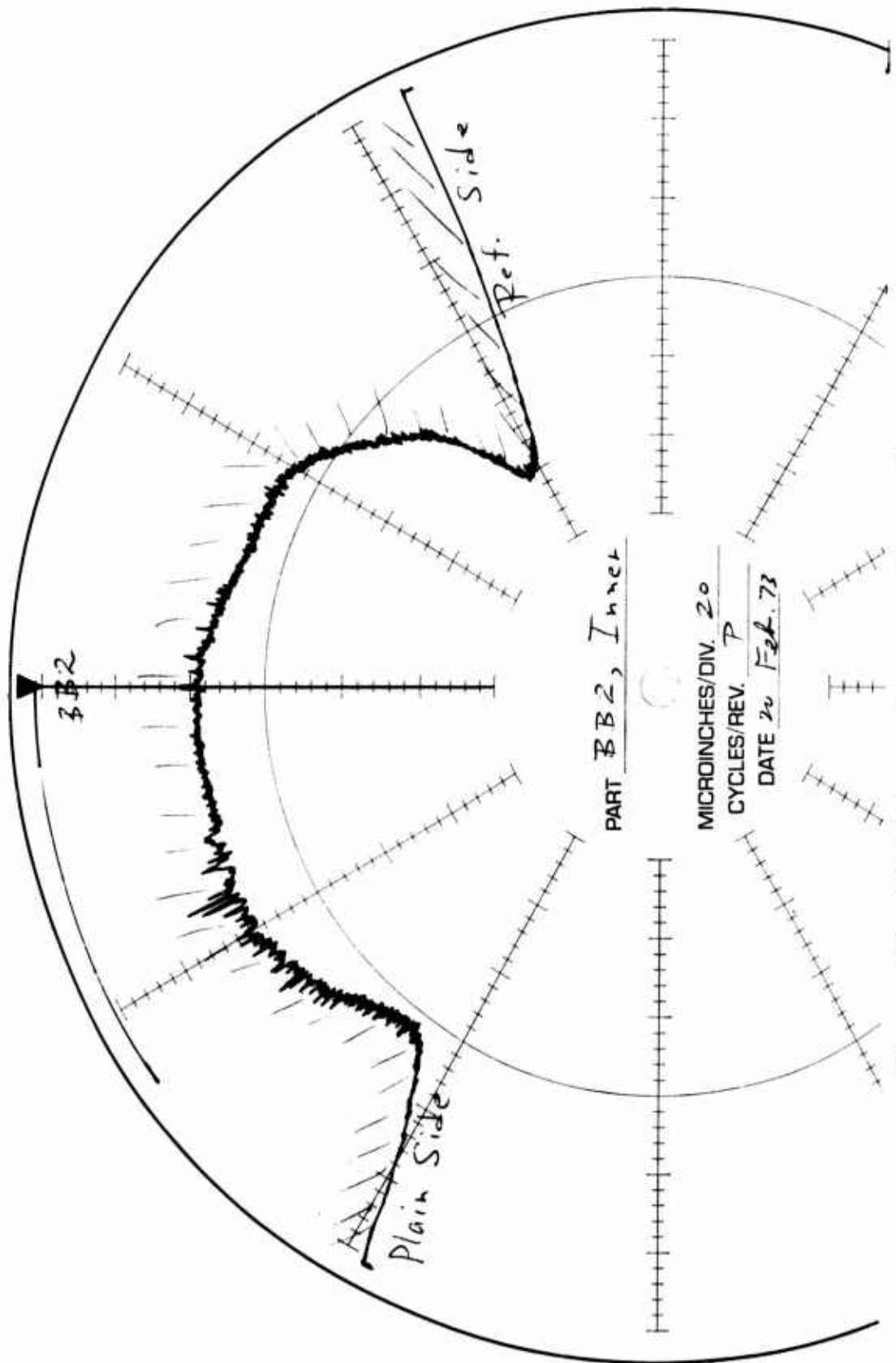


Figure 116. BB-2 Cross-Groove Profile at Zero Test Hours.

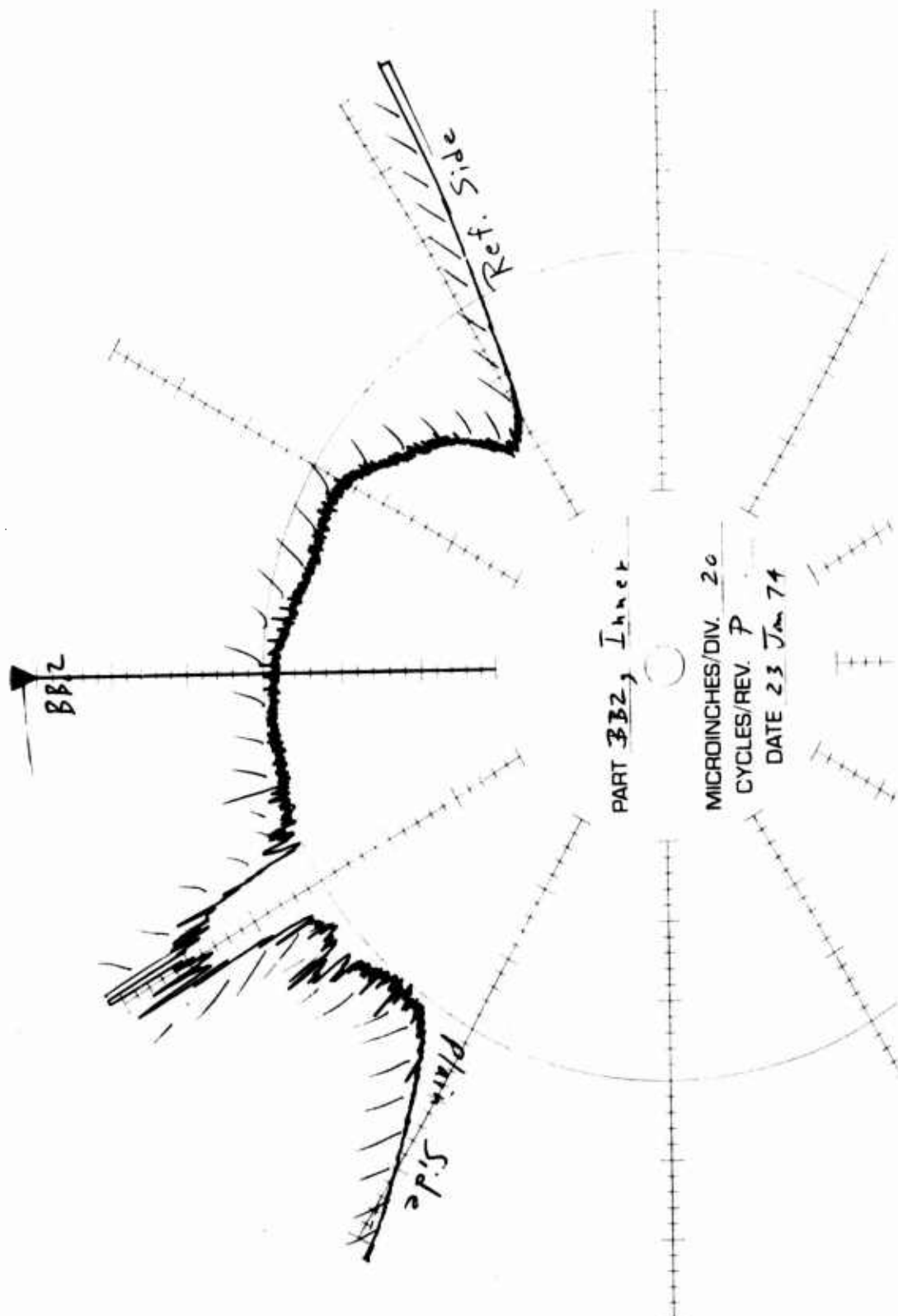


Figure 117. BB-2 Cross-Groove Profile at 166 Test Hours.

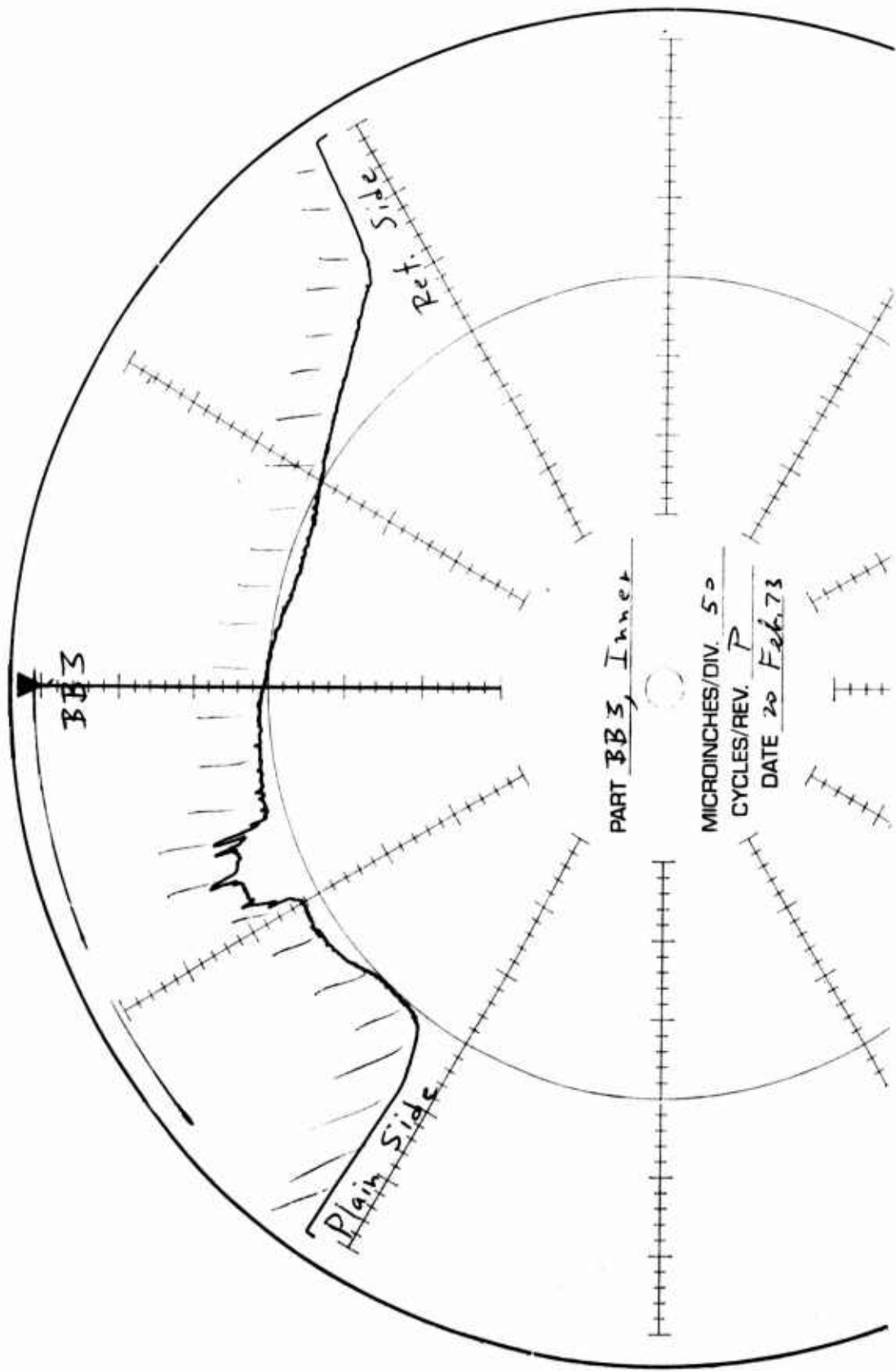


Figure 118. BB-3 Cross-Groove Profile at Zero Test Hours.

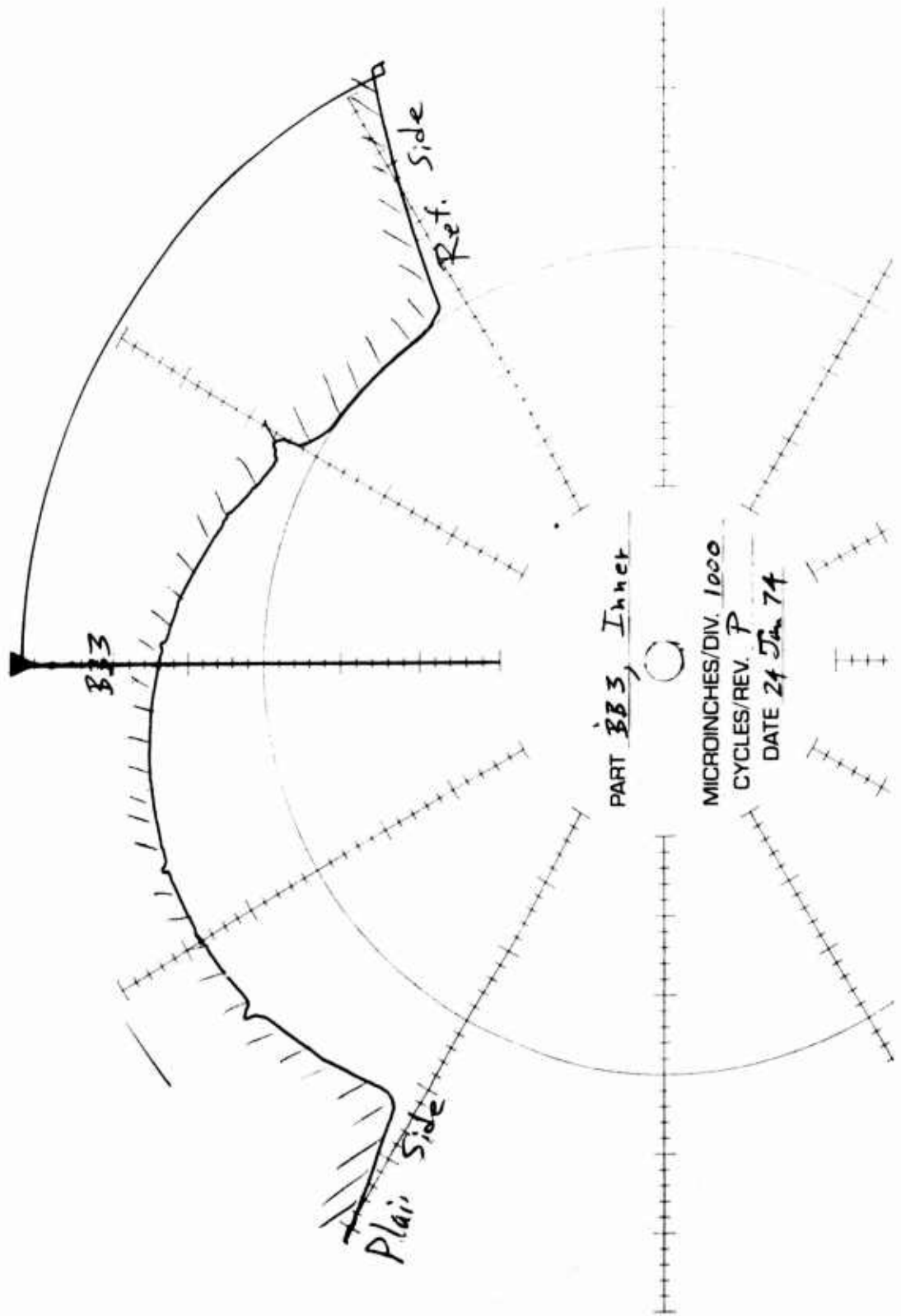


Figure 119. BB-3 Cross-Groove Profile at 166 Test Hours.

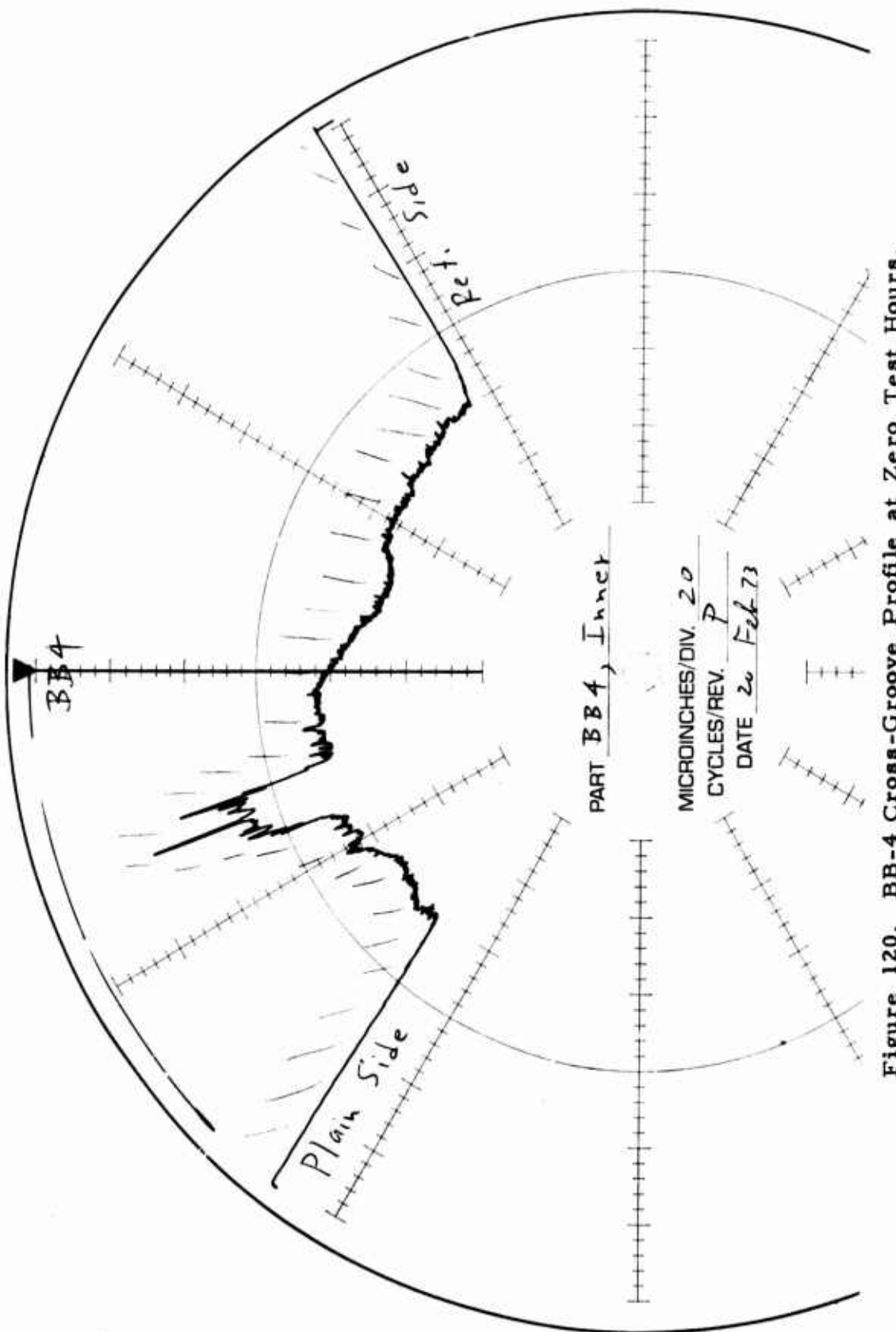


Figure 120. BB-4 Cross-Groove Profile at Zero Test Hours.

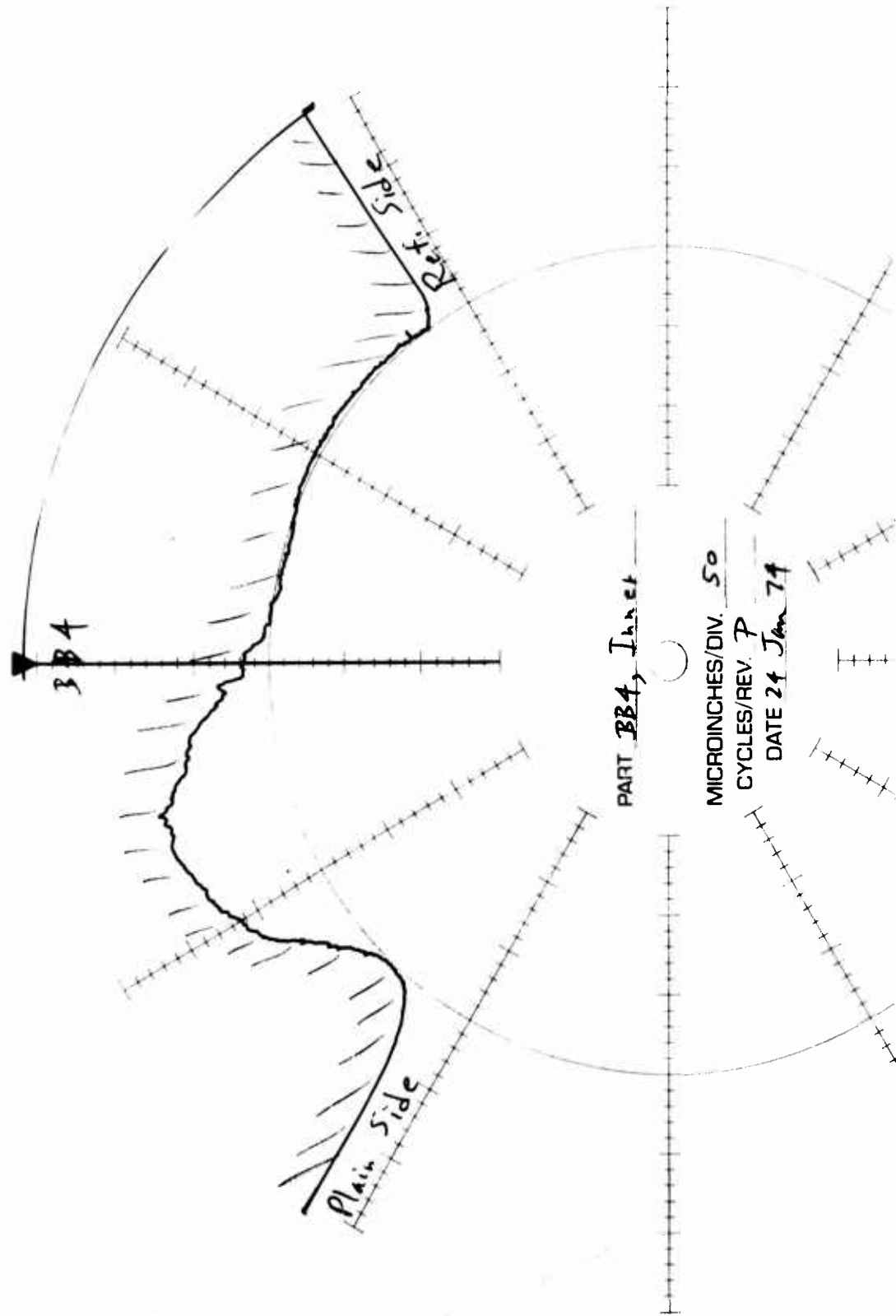
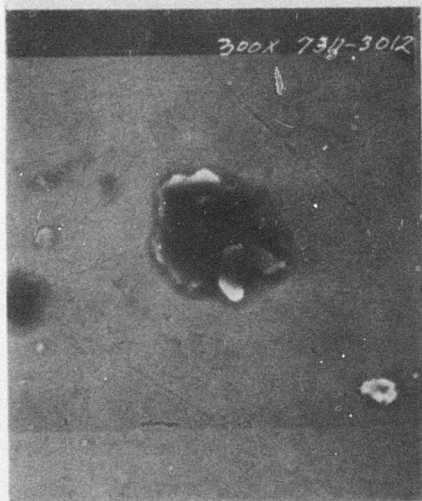
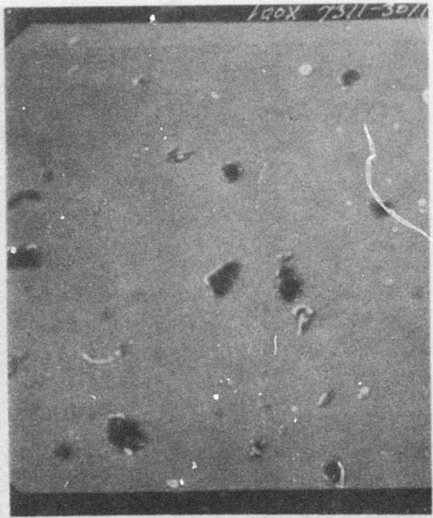


Figure 121. BB-4 Cross-Groove Profile at 166 Test Hours.



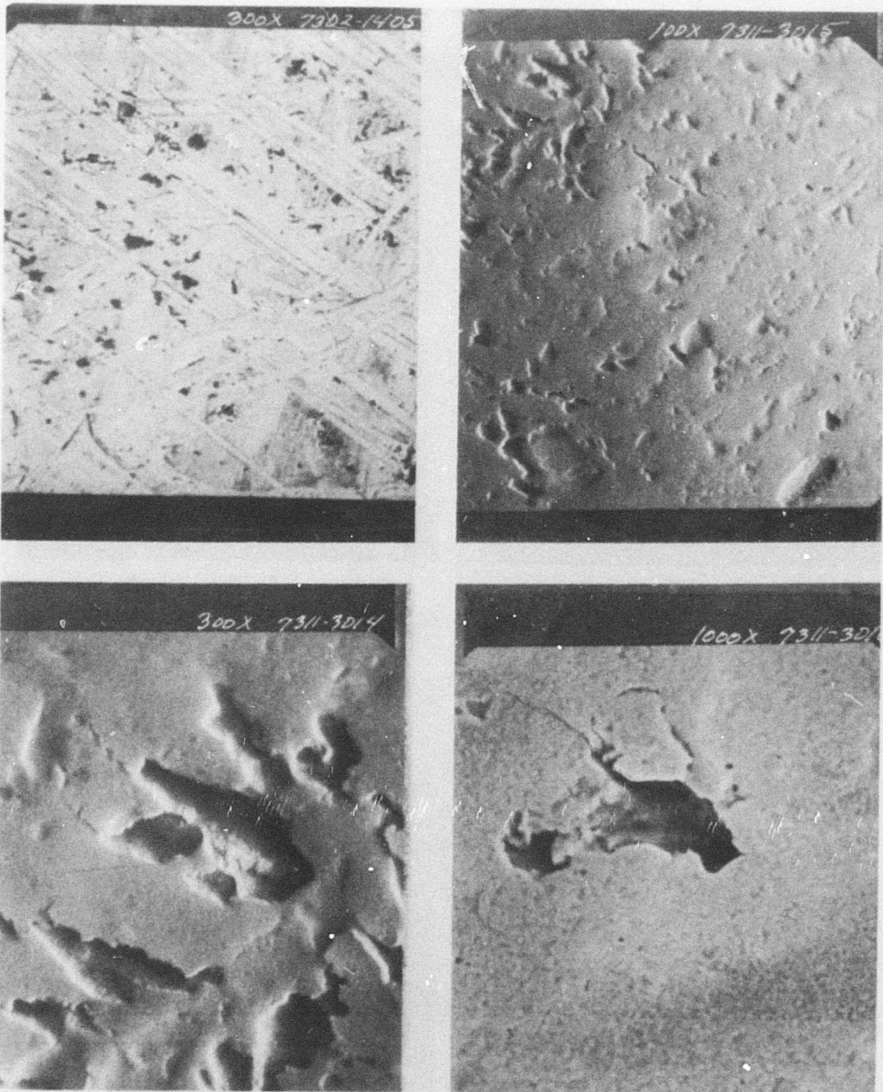
Top: 300 X, Zero Hours

Bottom: 300 X, 166 Hours

Top: 100 X, 166 Hours

Bottom: 1000 X, 166 Hours

Figure 122. SEM Micrographs of BB-1 (Zero, 166 Hours).



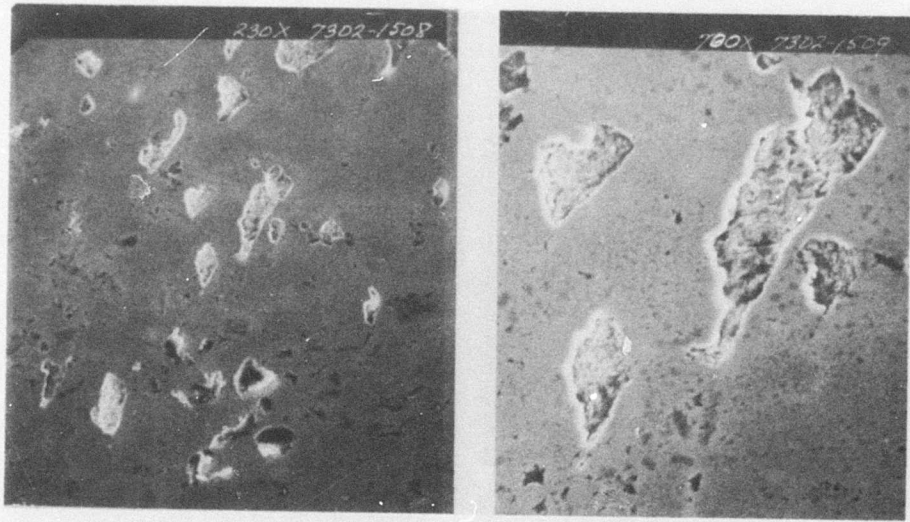
Top: 300 X, Zero Hours

Bottom: 300 X, 166 Hours

Top: 100 X, BSE, 166 Hours

Bottom: 1000 X, 166 Hours

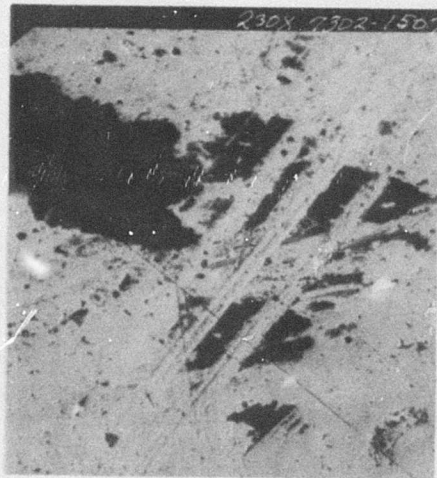
Figure 123. SEM Micrographs of BB-2 (Zero, 166 Hours).



230 X

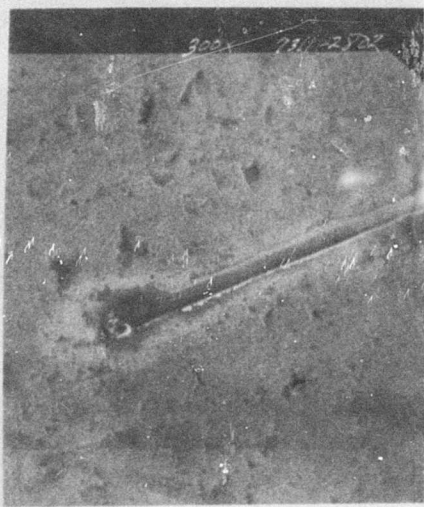
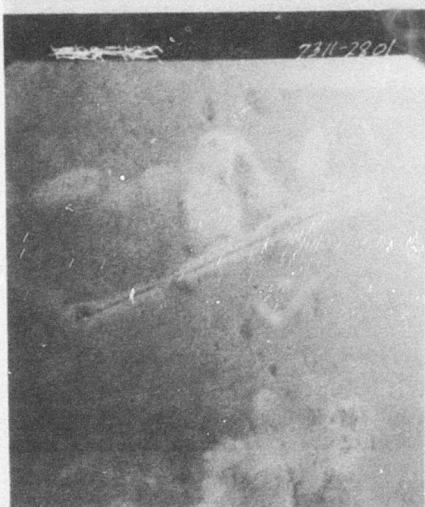
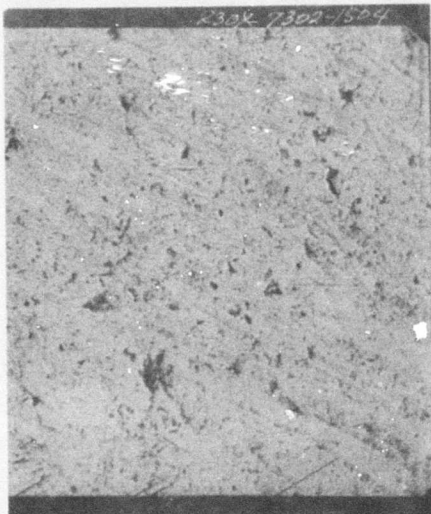
700 X

Figure 124. SEM Micrographs of BB-3 (Zero Hours).



230 X

Figure 125. SEM Micrograph of BB-4 (Zero Hours).



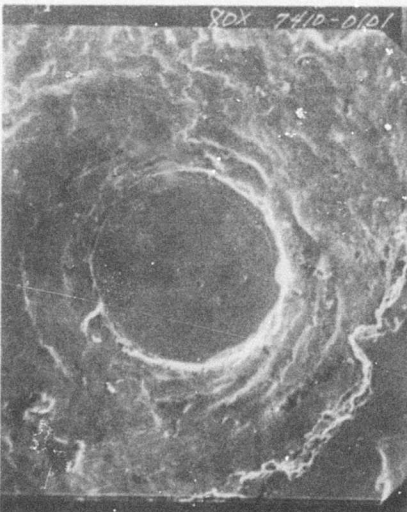
Top: 230 X, Zero Hours

Bottom: 100 X, 166 Hours

Top: 100 X, 166 Hours

Bottom: 300 X, 166 Hours

Figure 126. SEM Micrographs of BB-5 (Zero, 166 Hours).



Deep Circular Pit



Top: 80 X
Bottom: 100 X

Top: 300 X
Bottom: 1000 X, BSE

Figure 127. SEM Micrographs* of BB-3 or BB-4 (166 Hours).

*Exact identity of this ball is not known since the duplex pair fell apart upon gearbox disassembly.

BAD GEAR (BG) GEARBOX (B13-6884)

This gearbox had reached a TBO of 1200 hours and had shown signs of significant gear wear. The starting gear wear pattern showed signs of metal transfer between the pinion and ring gears. Apparently this gearbox had been badly overloaded.

Attempts were made during the early phases of this contract to obtain gear profiles to ensure complete documentation. The gearbox manufacturer, Bell Helicopter Company, was contacted in this regard, but was unable to help. The problem lies in the fact that the 90° gearbox utilizes spiral bevel gears for which profiles cannot be made.

It is interesting to note, however, that after nearly 1000 hours of testing, no significant differences were observed in BG gear wear patterns.

The bearings were documented by the same procedures used with the other gearboxes. The manufacturer and serial number for each bearing are listed below:

BG1	MRC	7207POS	S/N 46376-1
BG2	MRC	7207POS	S/N 46376-2
BG3	SKF	456607	S/N M99-A
BG4	SKF	456607	S/N M99-B
BG5	MRC	R110KD	S/N 6623
BG6	(not available)		

Visual Inspection of BG Gearbox Bearings

BG-1 Ball Bearing

ZERO TEST HOURS

Outer Race: Fair-to-poor. 0.09" wide ball track, moderate-to-heavy wear with many small dents.
Inner Race: Fair-to-poor. 0.12" wide ball track, heavy wear with many small dents and some large dents.
Balls: Poor. Heavy abrasive wear and denting.
Retainer: Good. Oxidized or deteriorated oil film.

1000 TEST HOURS

Outer Race: Fair-to-poor. 0.11" to 0.18" wide variable width ball track, moderate-to-heavy wear with many small dents.
Inner Race: Fair-to-poor. 0.14" wide ball track, heavy wear with many small dents and some large dents.

BG-2 Ball Bearing

ZERO TEST HOURS

Outer Race: Fair-to-poor. 0.11" wide ball track, moderate-to-heavy wear with many small dents and several large dents.
Inner Race: Poor. 0.12" wide ball track, heavy abrasive wear with many dents.
Balls: Poor. Heavy denting and pitting (pits are deep and black).
Retainer: Good. Oxidized or deteriorated oil film.

1000 TEST HOURS

Outer Race: Fair-to-poor. 0.13" wide ball track, moderate-to-heavy wear with many small dents and several large dents.
Inner Race: Poor. 0.14" wide ball track, heavy abrasive wear with many dents.
Balls: Poor. Heavy denting and pitting (pits are deep and black).
Retainer: Good. Oxidized or deteriorated oil film.

BG-3 Ball Bearing

ZERO TEST HOURS

Outer Race: Poor. 0.09" wide ball track, heavy abrasive wear with many small dents.
Inner Race: Poor. 0.09" wide ball track, heavy abrasive wear with many small dents, high contact angle, ball track goes to top edge of raceway.
Balls: Poor. Heavy abrasive wear.
Retainer: Good.

1000 TEST HOURS

Outer Race: Poor. 0.10" wide ball track, heavy abrasive wear with many small dents.
Inner Race: Poor. 0.10" wide ball track, heavy abrasive wear with many small dents, high contact angle.
Balls: Poor. Heavy abrasive wear.
Retainer: Good.

BG-4 Ball Bearing

ZERO TEST HOURS

Outer Race: Poor. 0.09" wide ball track, heavy abrasive wear with many small dents.
Inner Race: Poor. 0.09" wide ball track, heavy abrasive wear with many small dents, high contact angle, ball track goes to top edge of race-way, purple or lavender deposit on surface.
Balls: Poor. Heavy abrasive wear.
Retainer: Good.

1000 TEST HOURS

Outer Race: Poor. 0.10" wide ball track, heavy abrasive wear with many small dents.
Inner Race: Poor. 0.10" wide ball track, heavy abrasive wear with many small dents, high contact angle.
Balls: Poor. Heavy abrasive wear.
Retainer: Good.

BG-5 Roller Bearing

ZERO TEST HOURS

Outer Race: Fair. Abrasive wear over 180°, fine denting, several slightly larger dents in wear area.
Inner Race: Poor. Heavy denting, fine abrasive wear.
Rollers: Poor. Heavy denting, fine abrasive wear.
Retainer: Fair. Moderate wear.

1000 TEST HOURS

Outer Race:	Poor. Moderate wear, fine electrical pitting and small-to-large particle denting.
Inner Race:	Poor. Heavy denting, fine abrasive wear.
Rollers:	Poor. Heavy denting, fine abrasive wear.
Retainer:	Fair. Moderate wear.

BG-6 Roller Bearing

ZERO TEST HOURS

Outer Race:	Good. Slight abrasive wear, slight denting.
Inner Race:	Fair. Many small dents.
Rollers:	Fair. Many small dents.
Retainer:	Good.

1000 TEST HOURS

Outer Race:	Fair. Slight denting and fine electrical pitting.
Inner Race:	Fair. Many small dents.
Rollers:	Fair. Many small dents, light wear, some pitting, fatigue band at extreme edge (nut end) of some rollers. Some end wear, greatest at spline end.
Retainer:	Good.

BG Gearbox Mechanical Condition Summary

Table XI summarizes the results of the mechanical measurements of the ball bearings in the GB gearbox. Table XII summarizes the mechanical measurements for the roller bearings.

BG Gearbox Bearing Photographs and Cross-Groove Profiles

Figures 128 through 135 show the cross-groove profiles for the BG gearbox at various testing intervals.

Figures 136 through 140 show the scanning electron photomicrographs of the bearings taken before and after testing.

TABLE XI. MECHANICAL MEASUREMENTS FOR BG BALL BEARINGS

Bearing	Test Time (hr)	Noise Level (dB)	Peak Rise (dB)	General Condition (Wear)	Local Damage	Raceway Wear Depth (μ in.)	Radial Play (in.)
BG-1	0	5.5	3.0	moderate heavy	light	2.0	.0086
	1000	7.0	0.5		light	4.0	.0090
BG-2	0	5.0	1.0	moderate heavy	light	9.0	.0085
	1000	9.0	1.5		light	10.0	.0093
BG-3	0	10.5	0.0	heavy extreme	negligible light	6.5	.0036
	1000	15.0	1.5			9.3	.0030
BG-4	0	16.5	-20.0	extreme extreme	negligible light	14.0	.0029
	1000	18.5	0.5			15.0	.0030

TABLE XII. MECHANICAL MEASUREMENTS FOR BG ROLLER BEARINGS

Bearing	Time (hr)	Axial Clearance of Roller in Inner Race (in.)	Roller Contour (μ in.)	Roller Crown Drop (μ in.)	Roller Crown Length (in.)
BG-5	0	.0030	5 concave	165	.087
	1000	.0030	20 convex	124	.082
BG-6	0	.0030	5 convex	228	.103
	1000	.0030	20 concave	178	.089

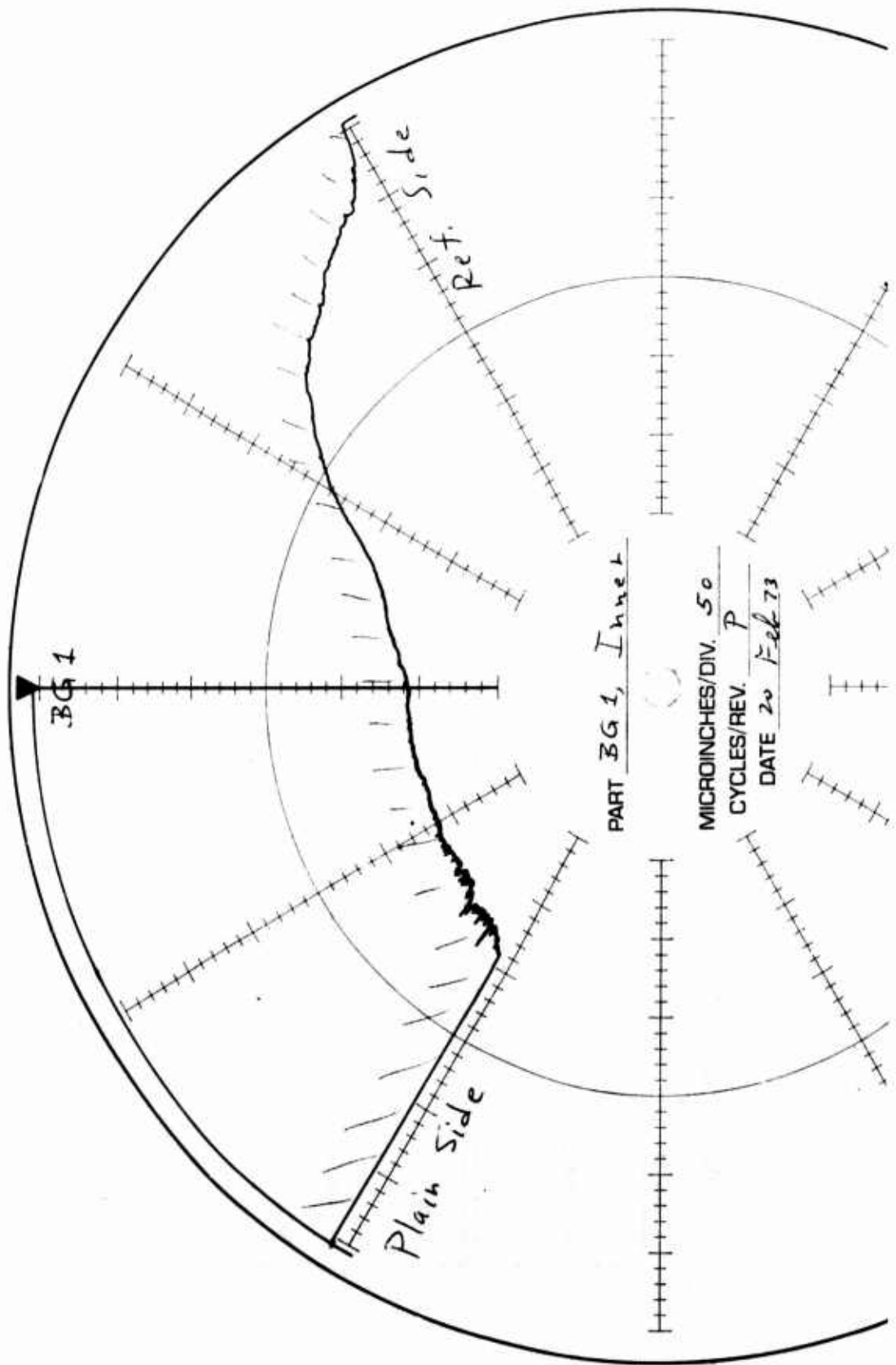


Figure 128. BG-1 Cross-Groove Profile at Zero Test Hours.

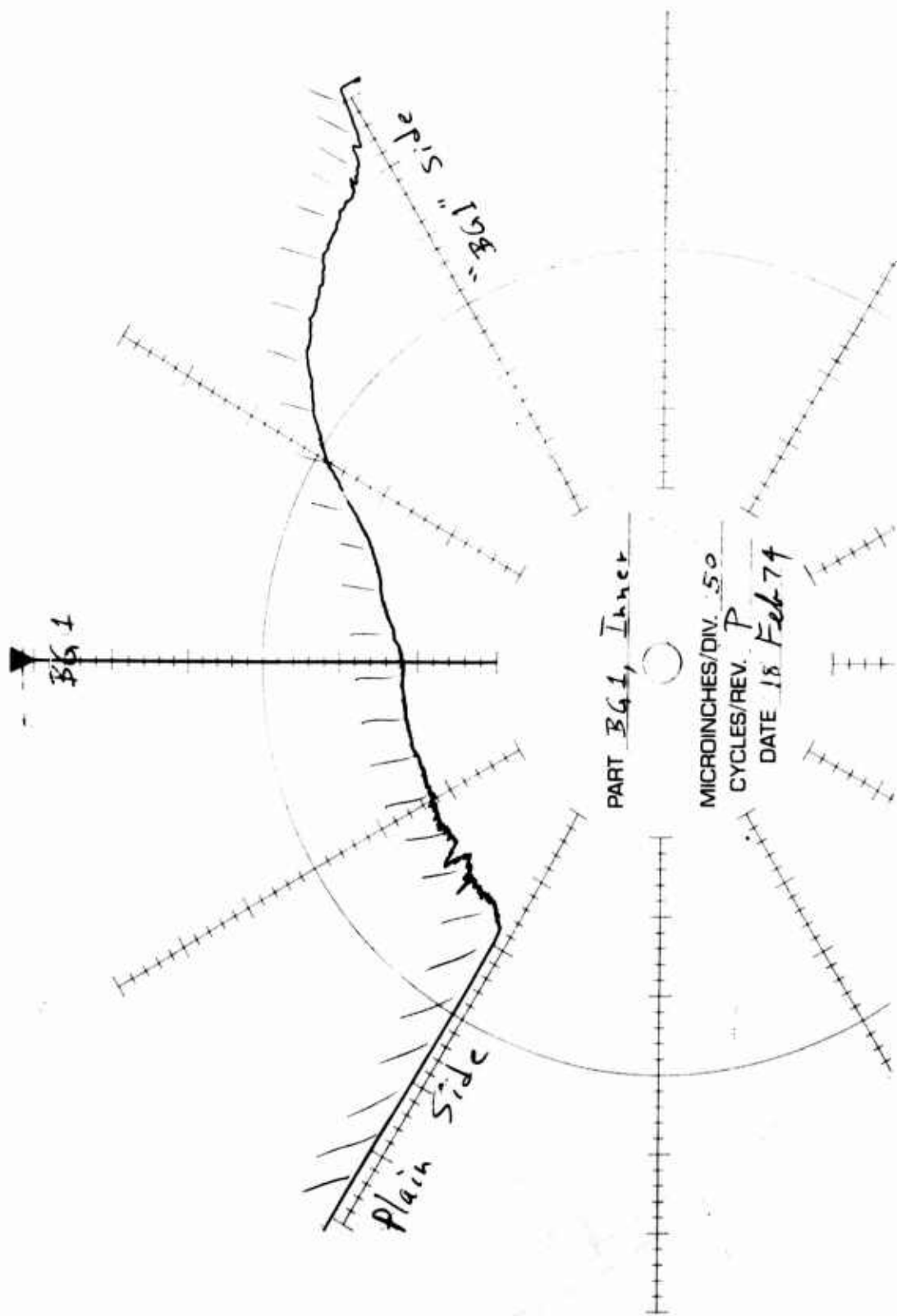


Figure 129. BG-1 Cross-Groove Profile at 1000 Test Hours.

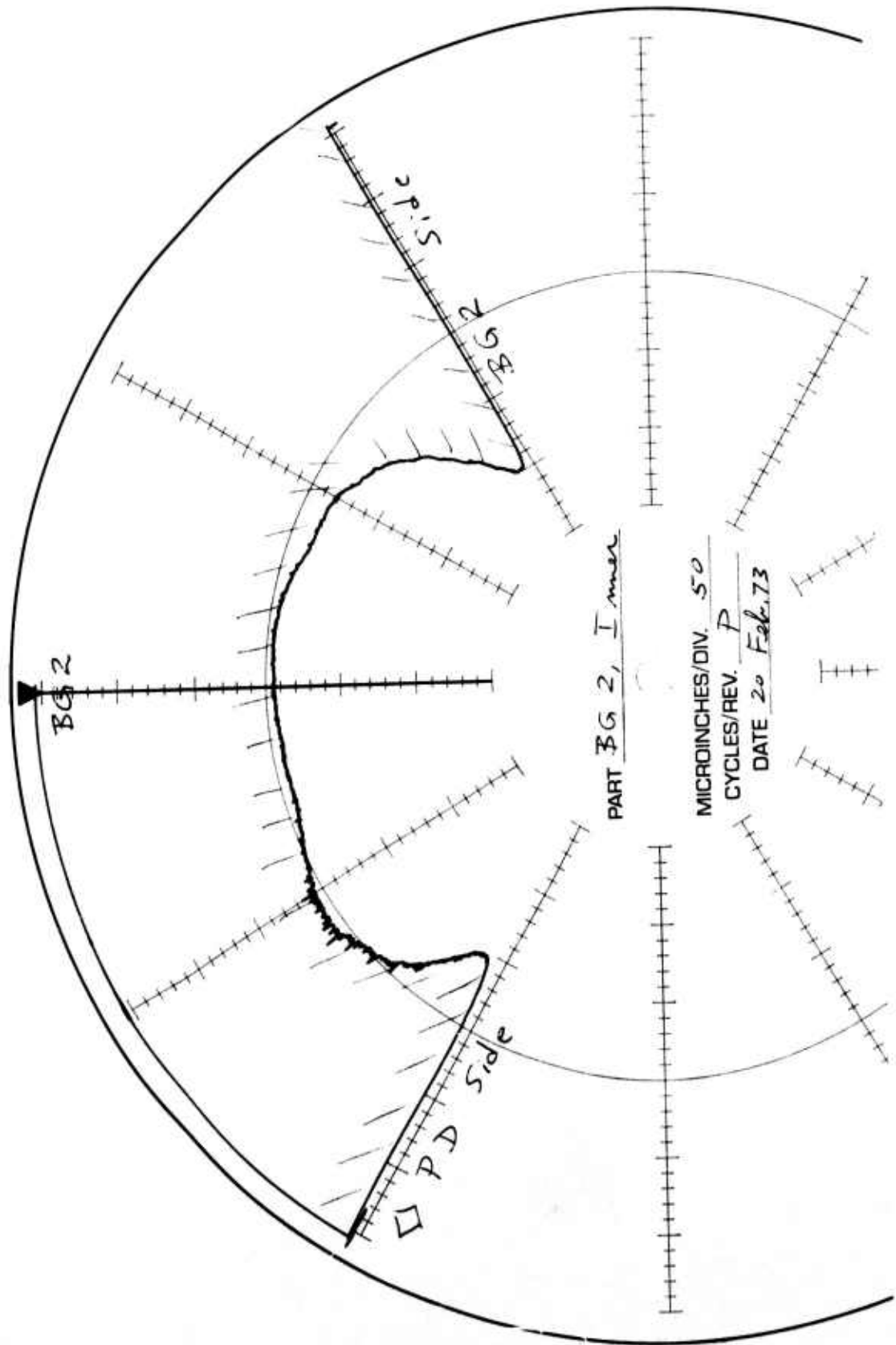


Figure 130. BG-2 Cross-Groove Profile at Zero Test Hours.

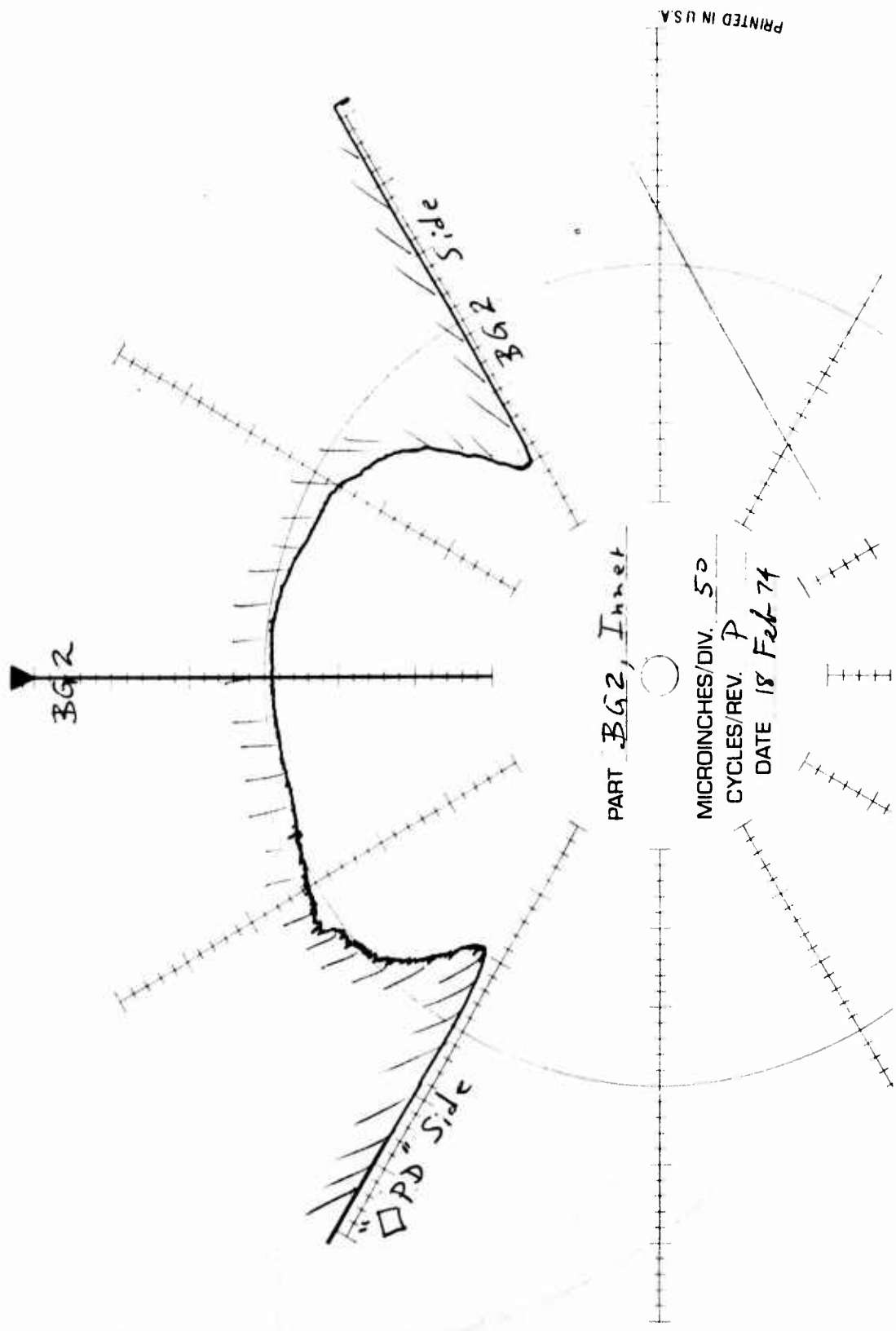


Figure 131. BG-2 Cross-Groove Profile at 1000 Test Hours.

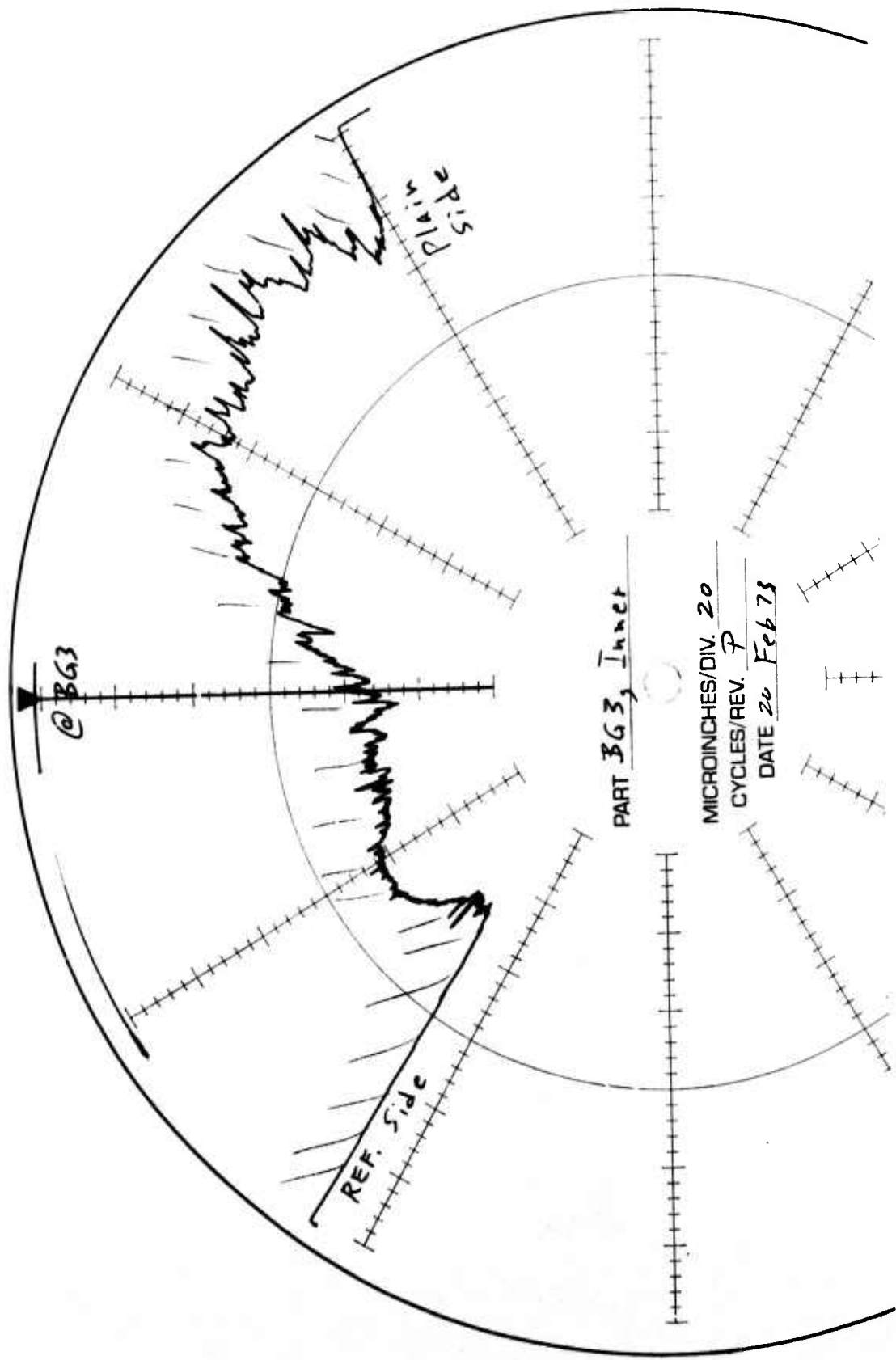


Figure 132. BG-3 Cross-Groove Profile at Zero Test Hours.

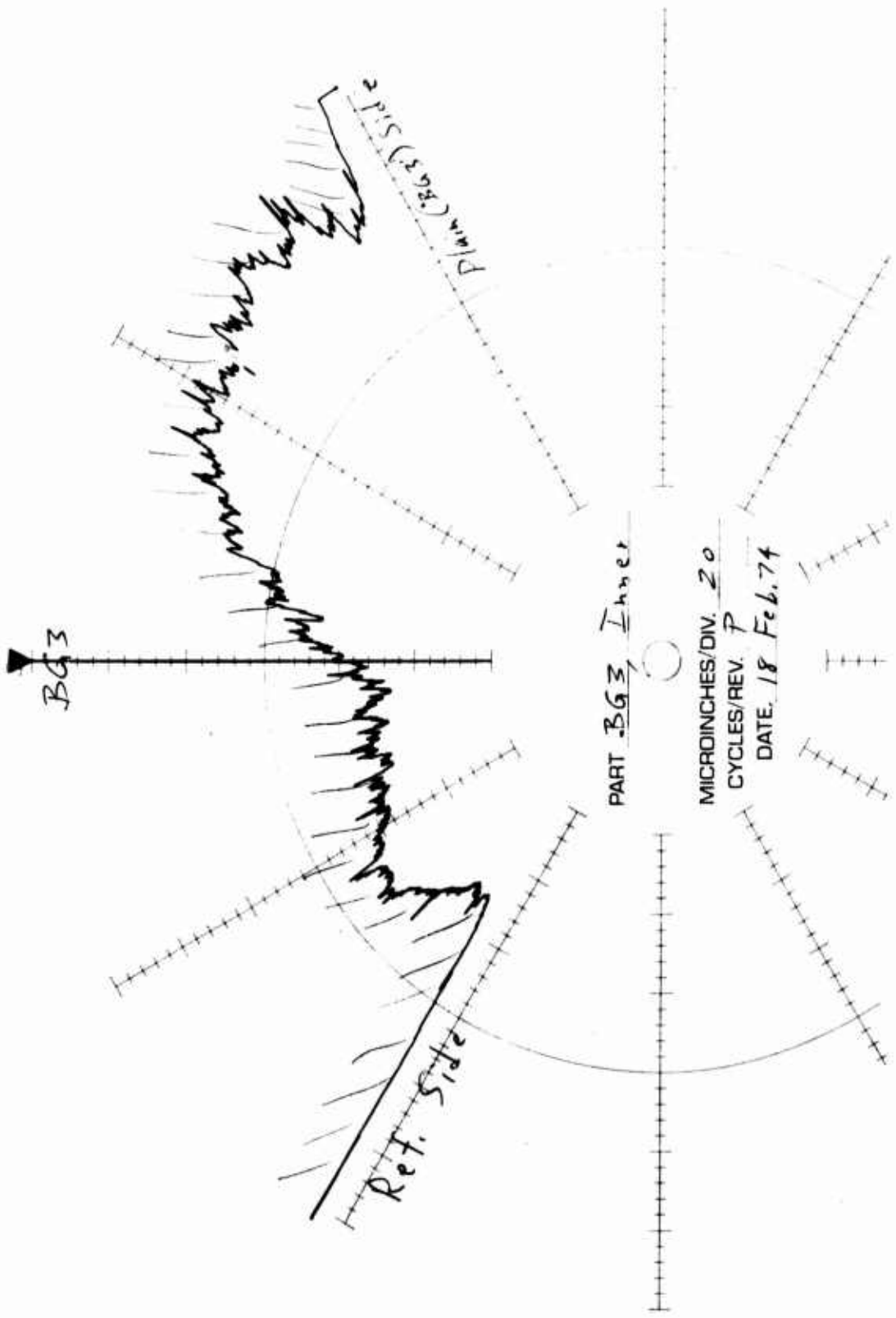


Figure 133. BG-3 Cross-Groove Profile at 1000 Test Hours.

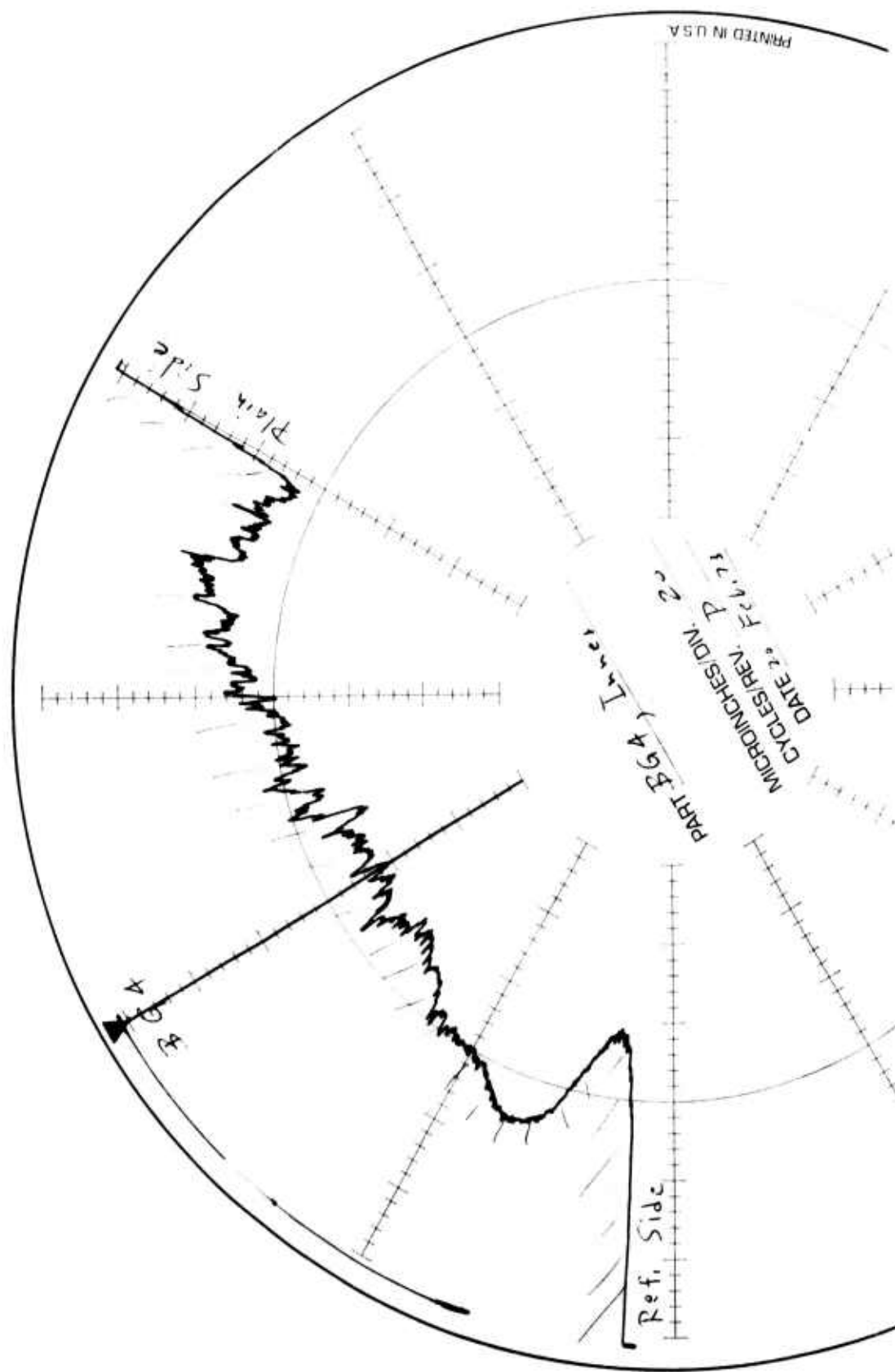


Figure 134. BG-4 Cross-Groove Profile at Zero Test Hours.

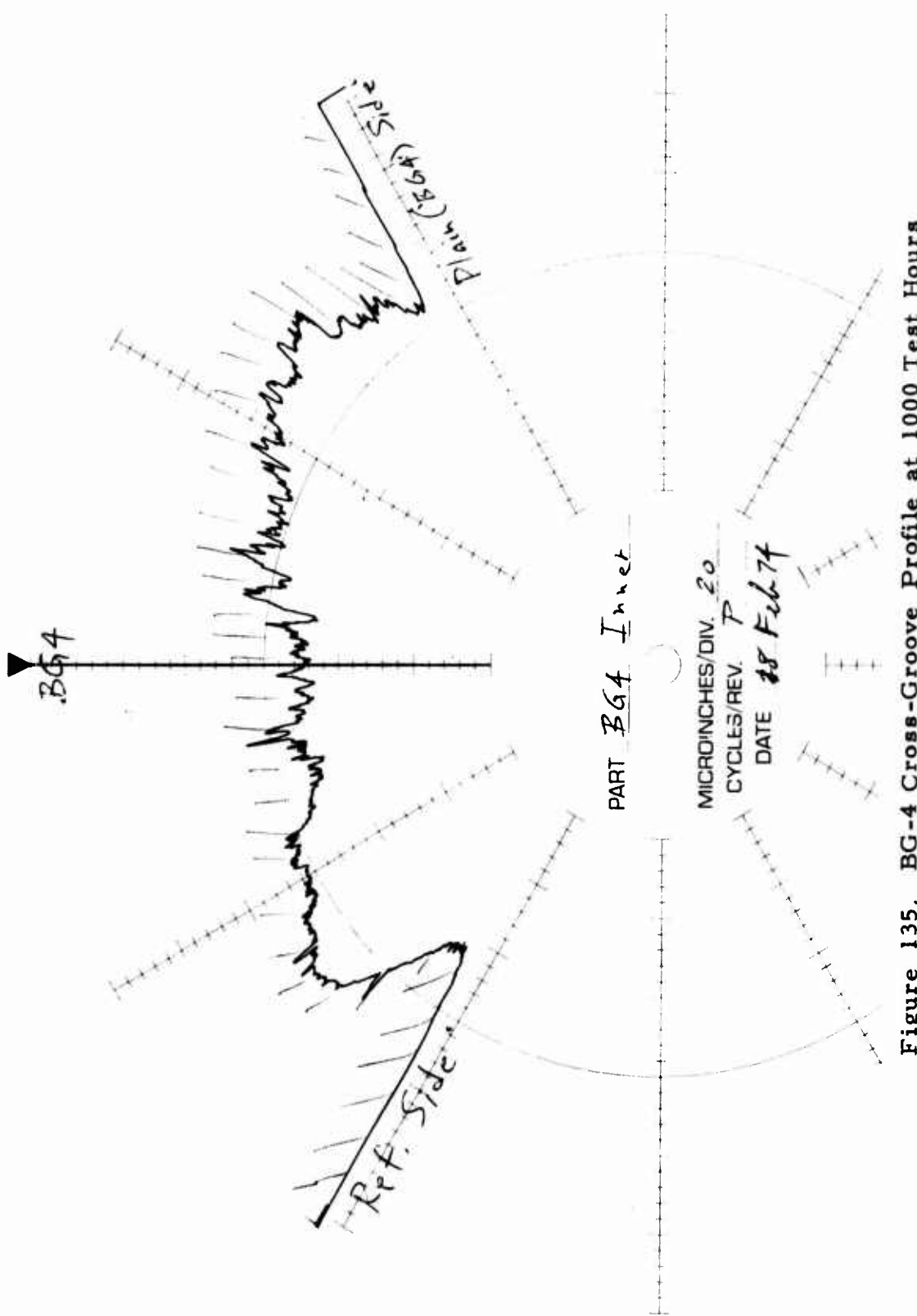
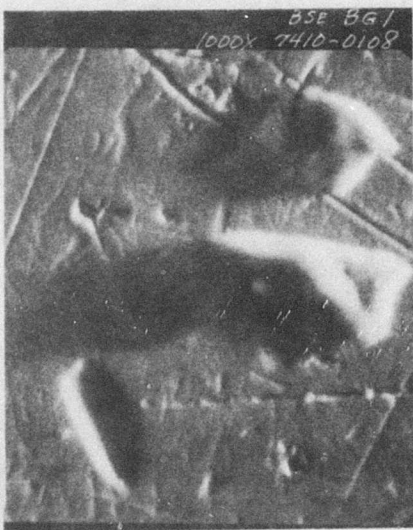


Figure 135. BG-4 Cross-Groove Profile at 1000 Test Hours.



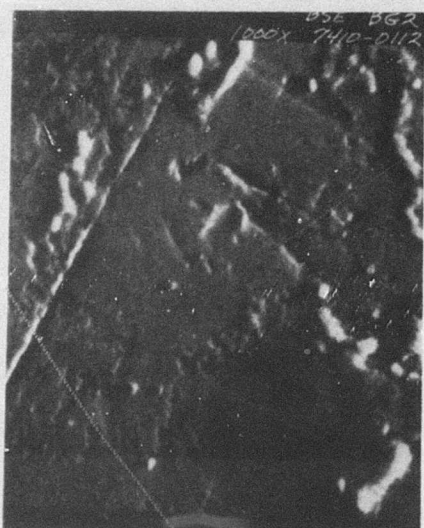
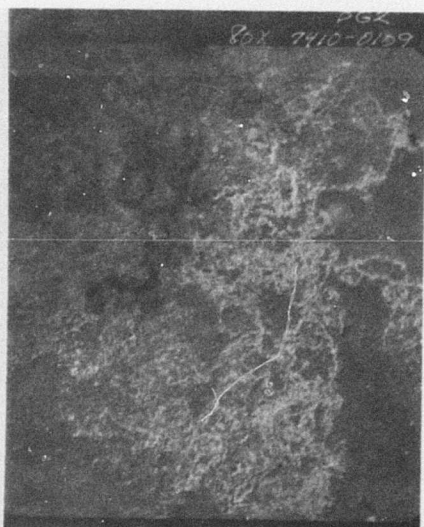
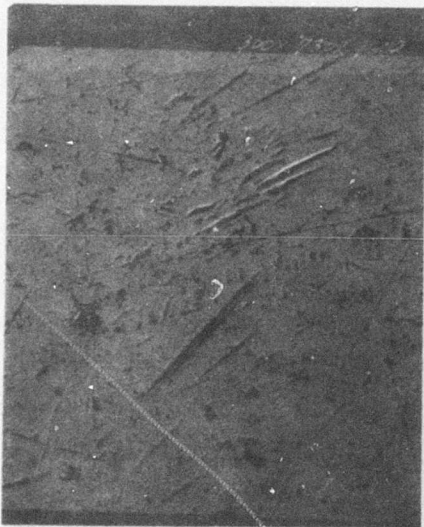
Top: 300 X, Zero Hours

Bottom: 1000 X, 1000 Hours

Top: 300 X, 1000 Hours

Bottom: 100 X, BSE, 1000 Hours

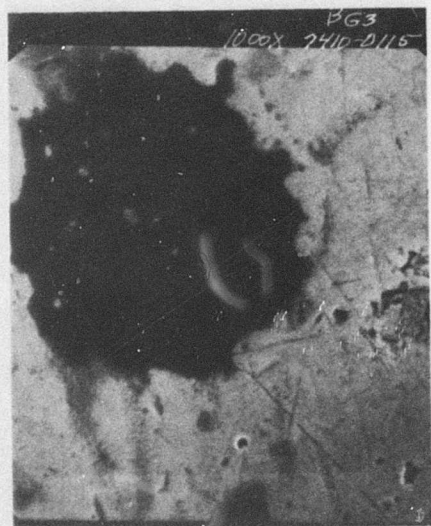
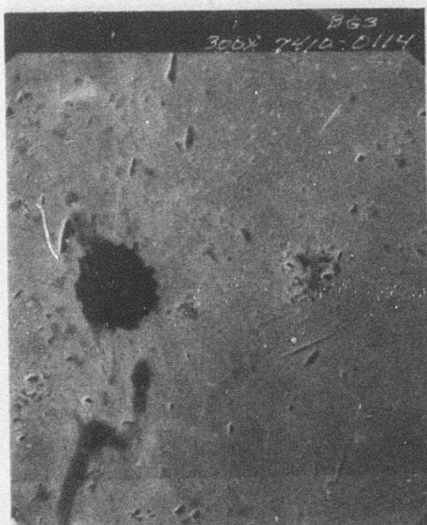
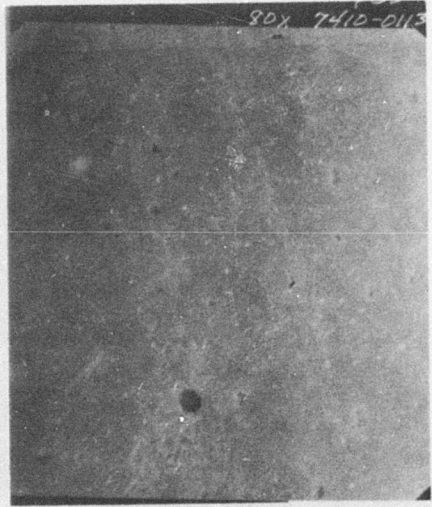
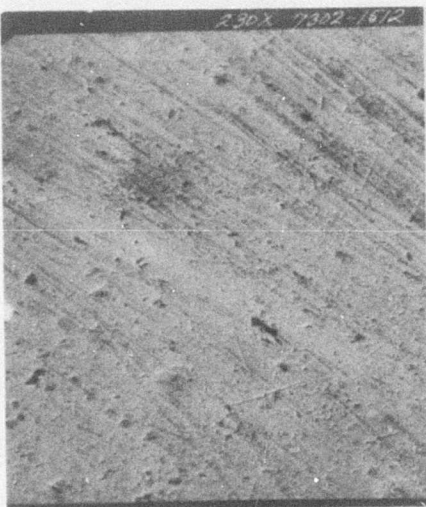
Figure 136. SEM Micrographs of BG-1.



Top: 300 X, Zero Hours
Bottom: 300 X, 1000 Hours

Top: 80 X, 1000 Hours
Bottom: 1000 X, BSE, 1000
Hours

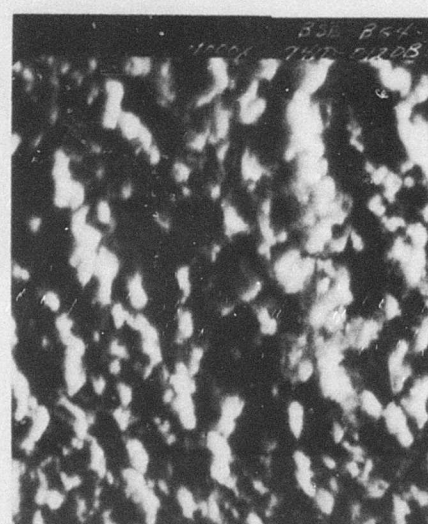
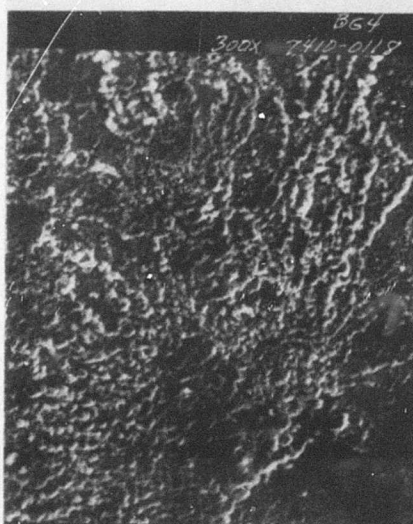
Figure 137. SEM Micrographs of BG-2.



Top: 230 X, Zero Hours
Bottom: 300 X, 1000 Hours

Top: 80 X, 1000 Hours
Bottom: 1000 X, 1000 Hours

Figure 138. SEM Micrographs of BG-3.



Top: 230 X, Zero Hours
Bottom: 300 X, 1000 Hours

Top: 80 X, 1000 Hours
Bottom: 1000 X, BSE, 1000
Hours

Figure 139. SEM Micrographs of BG-4.



230 X, Zero Hours

Figure 140. SEM Micrograph of BG-5.

BAD BEARING TWO (BBT) GEARBOX (B13-3395)

This gearbox had reached a TBO of 1200 hours and had shown signs of an incipient failed output duplex pair (BBT-3, BBT-4). The manufacturer and serial number for each bearing are listed below:

BBT-1	Fafnir 7207 PW2	S/N 22612-1
BBT-2	Fafnir 7207 PW2	S/N 22612-2
BBT-3	SKF 456606	S/N F24-A
BBT-4	SKF 456607	S/N F24-B
BBT-5	MRC R110KD	S/N 7854
BBT-6	(Not available)	

Visual Inspections of BBT Gearbox Bearings

BBT-1 Ball Bearing

ZERO TEST HOURS

Inner Race: Fair. 0.1" wide ball track, electrical pitting and denting, light wear.
Outer Race: Generally similar to inner; ball track width varies from 0.08" to 0.11".
Balls: Fair. Light scratches, pits and dents.
Retainer: Good. Light pocket wear.

407 TEST HOURS

Inner Race: Fair. 0.12" wide ball track. Moderate wear. Electrical pitting and denting. Transverse vibratory markings. Light stain marks on side opposite ball track; may be corrosive.
Outer Race: Generally similar to inner. 0.12" wide ball track.
Balls: Poor. Scoring, pitting and denting.
Retainer: Very good. Light pocket wear.

1022 TEST HOURS

Inner Race: Poor. 0.12" wide ball track. Moderate wear. Electrical damage (pitting and denting). Transverse vibratory markings. Light stains (possibly corrosive) on side opposite thrust.

Outer Race: Generally similar to inner. 0.10" wide ball track.
Balls: Poor. Pits, dents, scratches, wear.
Retainer: Good. Light-to-moderate pocket wear.

BBT-2 Ball Bearing

ZERO TEST HOURS

Inner Race: Fair. 0.08" wide ball track, electrical pitting and denting, some straw heat coloration in ball track, light wear.
Outer Race: Generally similar to inner; ball track width varies from 0.08" to 0."
Balls: Fair. Light scratches, pits and dents.
Retainer: Good. Light pocket wear.

407 TEST HOURS

Inner Race: Poor. 0.1" wide ball track. Heavy wear. Pitting and denting. Electrical pitting. Transverse vibratory markings and stains, some of which may be corrosive.
Outer Race: Generally similar to inner. 0.105" wide ball track. Some heat coloration.
Balls: Poor. Scoring, pitting and denting.
Retainer: Very good. Light pocket wear.

1022 TEST HOURS

Inner Race: Poor. 0.10" wide ball track. Heavy wear. Electrical damage (pitting and denting). Transverse vibratory markings and stains (possibly corrosive).
Outer Race: Generally similar to inner; 0.1" wide ball track.
Balls: Poor. Pits, dents, scratches, wear.
Retainer: Good. Light wear in pockets.

BBT-3 Ball Bearing

ZERO TEST HOURS

Inner Race: Fair. 0.08" wide ball track, electrical

Outer Race: pitting and denting, heat coloration in ball track, light-to-moderate wear.
Balls: Generally similar to inner; ball track width varies from 0.06" to 0.08".
Retainer: Fair. Light pitting and denting.
Good condition. However, shape has been deformed by impacts of some type as evidenced by indentations on one side.

407 TEST HOURS

Inner Race: Poor. 0.09" wide ball track. Heavy wear. One large (0.015") fatigue pullout in ball track. Pitting and denting. Electrical pitting. Some heat coloration in ball track.
Outer Race: Generally similar to inner. 0.09" wide ball track.
Balls: Poor. Pitting and denting.
Retainer: Poor. Distorted (out-of-round).

1022 TEST HOURS

Inner Race: Poor. 0.09" wide ball track. Very heavy wear. Fatigue pullout. Electrical damage (pitting and denting). Some heat coloration.
Outer Race: Generally similar to inner. 0.09" wide ball track.
Balls: Poor. Pits, dents, frosted or film-covered appearance.
Retainer: Poor. Visibly out-of-round. Several indentations on one side due to impact or excessive pressure by some implement.

BBT-4 Ball Bearing

ZERO TEST HOURS

Inner Race: Fair. 0.08" wide ball track, electrical pitting and denting and heat coloration in ball track.
Outer Race: Generally similar to inner; ball track width varies from 0.07" to 0.09".
Balls: Fair. Light pits and dents.
Retainer: Good. Normal appearance.

407 TEST HOURS

Inner Race: 0.105" wide ball track. Moderate wear. Some heat coloration in ball track. Pitting and denting. Electrical pitting. Some transverse vibratory markings.
Outer Race: Generally similar to inner. 0.075" wide ball track.

1022 TEST HOURS

Inner Race: Poor. 0.105" wide ball track. Heavy wear. Light heat color in ball track. Electrical damage (pitting and denting).
Outer Race: Generally similar to inner. 0.105" wide ball track.
Balls: Poor. Pits, dents, wear.
Retainer: Fair. Visibly out-of-round.

BBT-5 Roller Bearing

ZERO TEST HOURS

Inner Race: Fair. Small-to-large particle denting with electrical current pitting.
Outer Race: Fair. Light-to-moderate wear.
Rollers: Fair. Similar to inner race with slight end wear.
Retainer: Good condition.

407 TEST HOURS

Inner Race: Poor. Moderate-to-heavy wear. Pitting and denting.
Outer Race: Generally similar to inner.
Rollers: Poor. Similar to raceway. Circumferential wear lines. Very light end wear.
Retainer: Good. Moderate pocket wear.

1022 TEST HOURS

Inner Race: Poor. Moderate-to-heavy wear. Pitting and denting.
Outer Race: Generally similar to inner.

Rollers: Poor. Similar to raceways. Wear bands.
Some end wear.
Retainer: Fair. Some wear in pockets.

BBT-6 Roller Bearing

ZERO TEST HOURS

Inner Race: Unable to examine.
Outer Race: Fair. Light-to-moderate wear, pitting and denting. Variable contact; probable radial offset of loading.
Rollers: Light-to-moderate pitting and denting, metal smear or scuff marks at gear end of several rollers. Light end wear.
Retainer: Good. Normal appearance of outside surfaces.

407 TEST HOURS

Inner Race: Unable to examine; disassembly not authorized.
Outer Race: Fair. Moderate-to-heavy wear.
Rollers: Moderate-to-heavy wear. Light end wear.
Retainer: Good condition as observed from outside in fully assembled condition.

1022 TEST HOURS

Inner Race: Unable to examine; disassembly not authorized.
Outer Race: Poor. Moderate-to-heavy wear.
Rollers: Poor. Moderate-to-heavy wear (banding). Some end wear. Some heat coloration.
Retainer: Good as observed externally while in fully assembled condition.

BBT Gearbox Mechanical Condition Summary

Table XIII summarizes the results of the mechanical measurements made upon the ball bearings in the BBT gearbox. Table XIV summarizes the mechanical measurements for the roller bearings.

BBT Gearbox Bearing Photographs and Cross-Groove Profiles

Figures 141 through 152 show the cross-groove profiles for the BBT gearbox at the start, the middle, and the end of testing.

Figures 153 through 169 show the scanning electron photomicrographs of the bearings taken before, during, and after testing.

Figure 161 shows the presence of a fatigue pit on the inner race of BBT3. The ball track in this picture is the approximately 1-inch-wide dark band which passes horizontally through the upper portion of the photograph. The arrow identifies the pit, which is a 3/32-inch dark spot just to the right of the center of the picture. The magnification in Figure 161 is 8.9X.

Figure 162 is an enlargement of the pit shown in Figure 161. The maximum diameter of the pit is .0134 inch. The sharp edge on the right side and broken edge on left side suggest that the ball passed from right to left. Spacing is .005 inch.

TABLE XIII. MECHANICAL MEASUREMENTS FOR BBT BALL BEARINGS

Bearing	Test Time (hr)	Noise Level (dB)	Peak Rise (dB)	General Condition (Wear)	Local Damage	Raceway Wear Depth (in.)	Radial Play (in.)
BBT-1	0	7	21.5	heavy moderate heavy	extreme light light	22 80 66	.0073 .0071 .0074
	407	4	2				
	1022	9.5	2.5				
BBT-2	0	8	14.5	heavy heavy moderate	extreme moderate moderate	30 50 30	.0078 .0077 .0076
	407	7	3.5				
	1022	5.5	5				
BBT-3	0	11.5	0.5	heavy extreme heavy	light negligible light	33 50 75	.0032 .0029 .0032
	407	18	-1.5				
	1022	11.5	3				
BBT-4	0	10.5	0	heavy extreme extreme	negligible negligible moderate	50 80 130	.0032 .0031 .0034
	407	13.5	-0.5				
	1022	13	-3.5				

TABLE XIV. MECHANICAL MEASUREMENTS FOR BBT ROLLER BEARINGS

Bearing	Time (hr)	Axial Clearance of Roller in Inner Race (in.)	Roller Contour (μ in.)	Roller Crown Drop (μ in.)	Roller Crown Length (in.)
BBT-5	0	.0016	20 convex	195	.090
	407	.0025	240 convex	-	full
	1022	.0020	50 convex	140	.075
BBT-6	0	-	flat	112	.080
	407	.0030	140 convex	-	full
	1022	.0028	120 convex	N/A	full

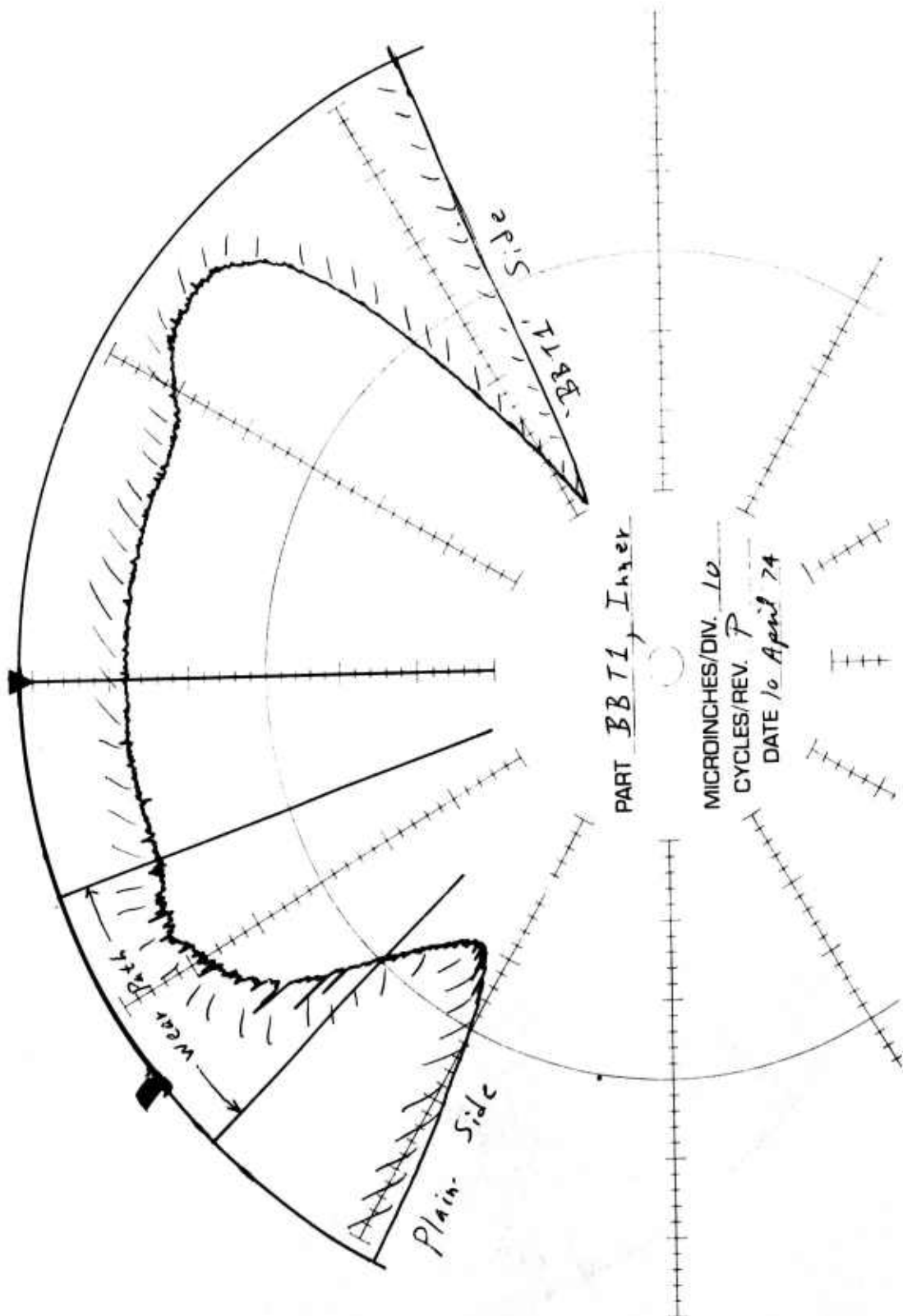


Figure 141. BBT-1 Cross-Groove Profile at Zero Test Hours.

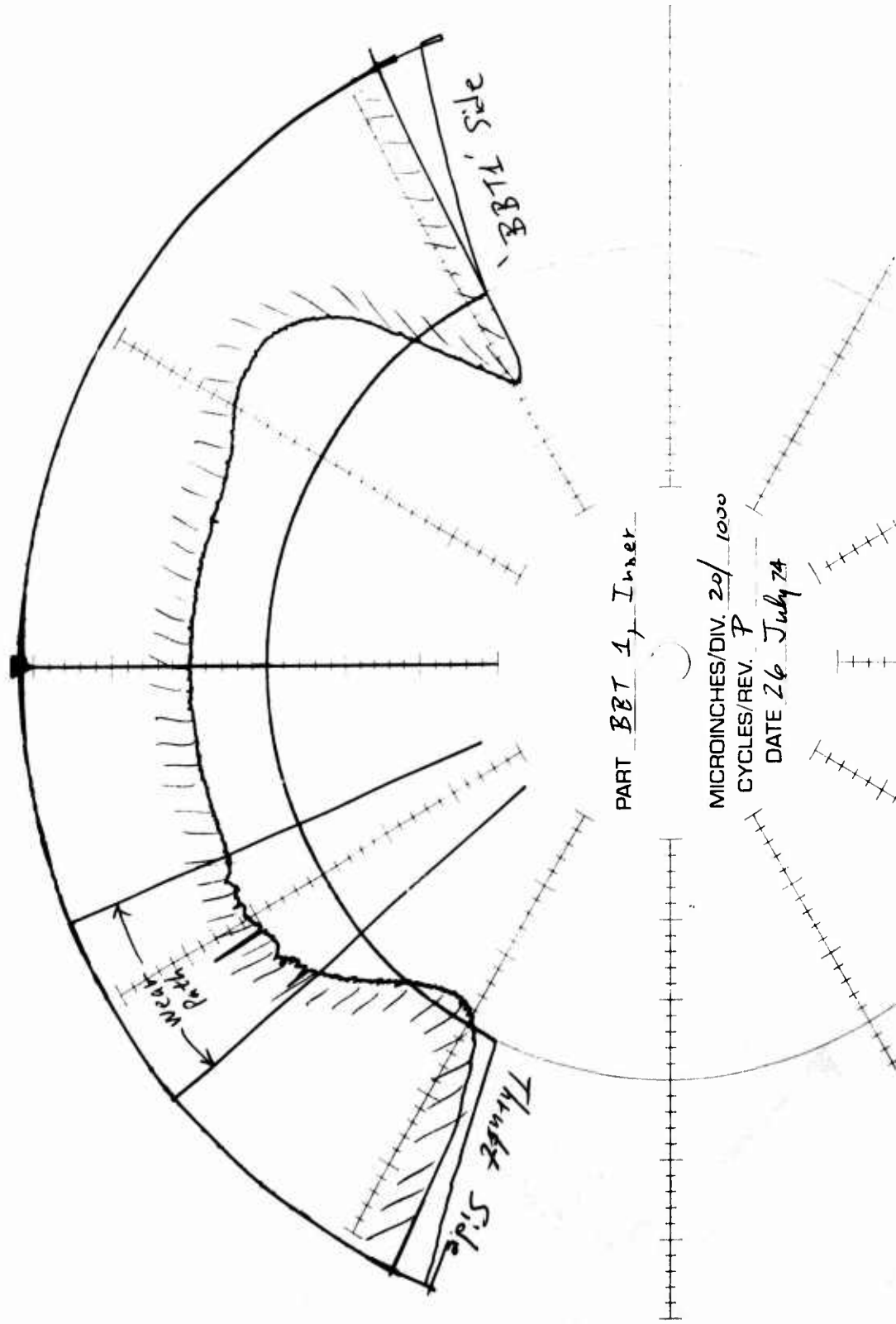


Figure 142. BBT-1 Cross-Groove Profile at 407 Test Hours.

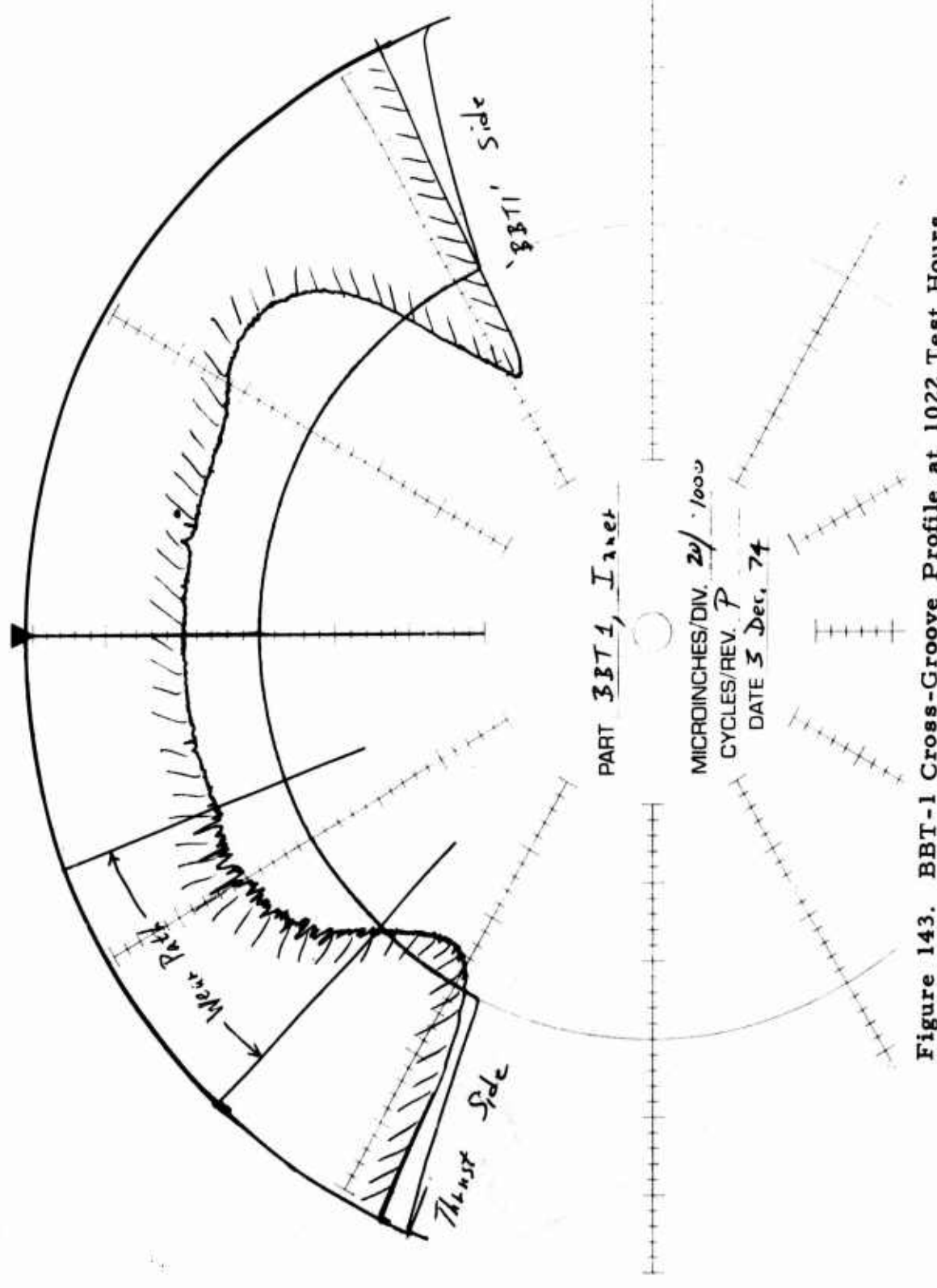


Figure 143. BBT-1 Cross-Groove Profile at 1022 Test Hours.

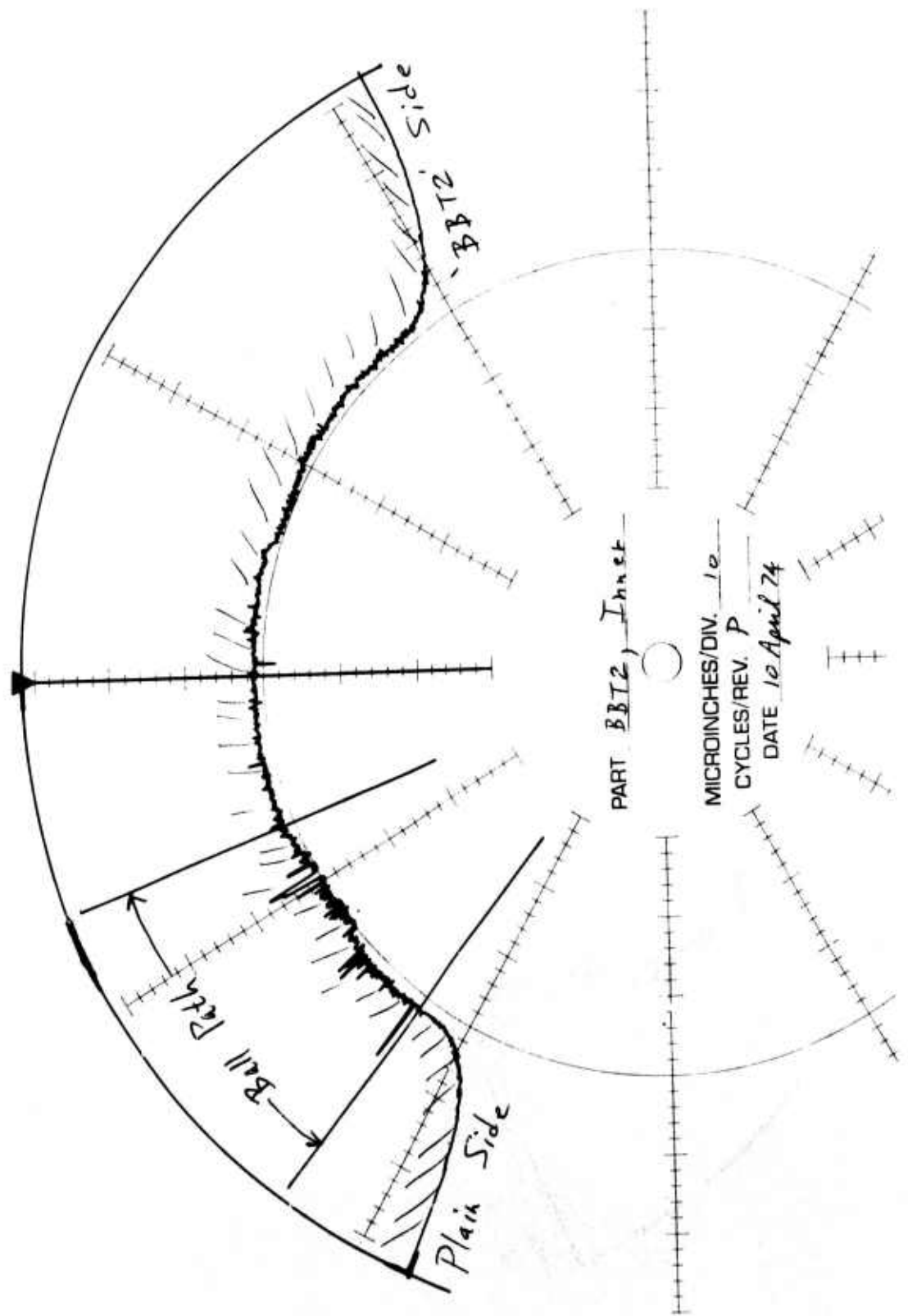


Figure 144. BBT-2 Cross-Groove Profile at Zero Test Hours.

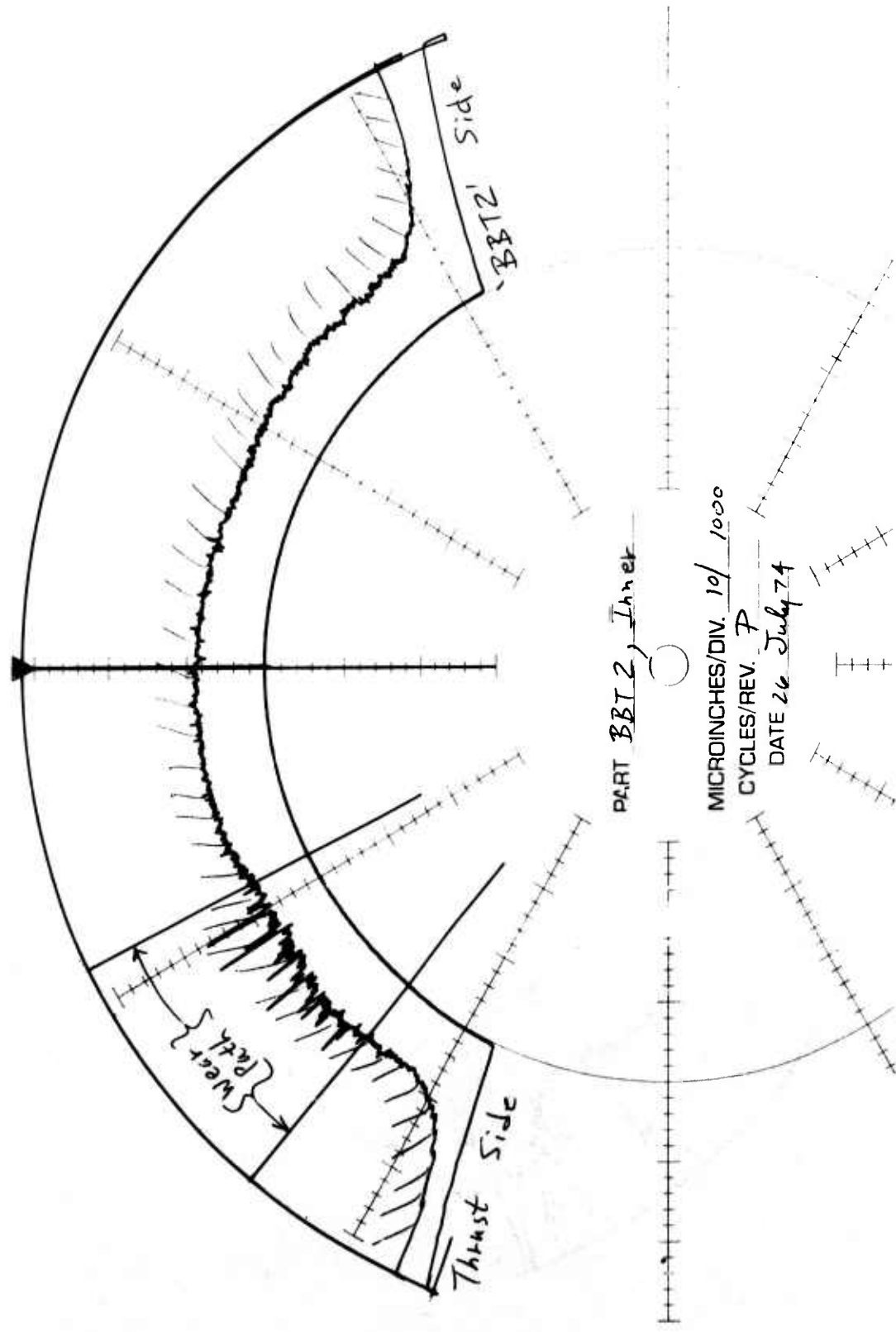


Figure 145. BBT-2 Cross-Groove Profile at 407 Test Hours.

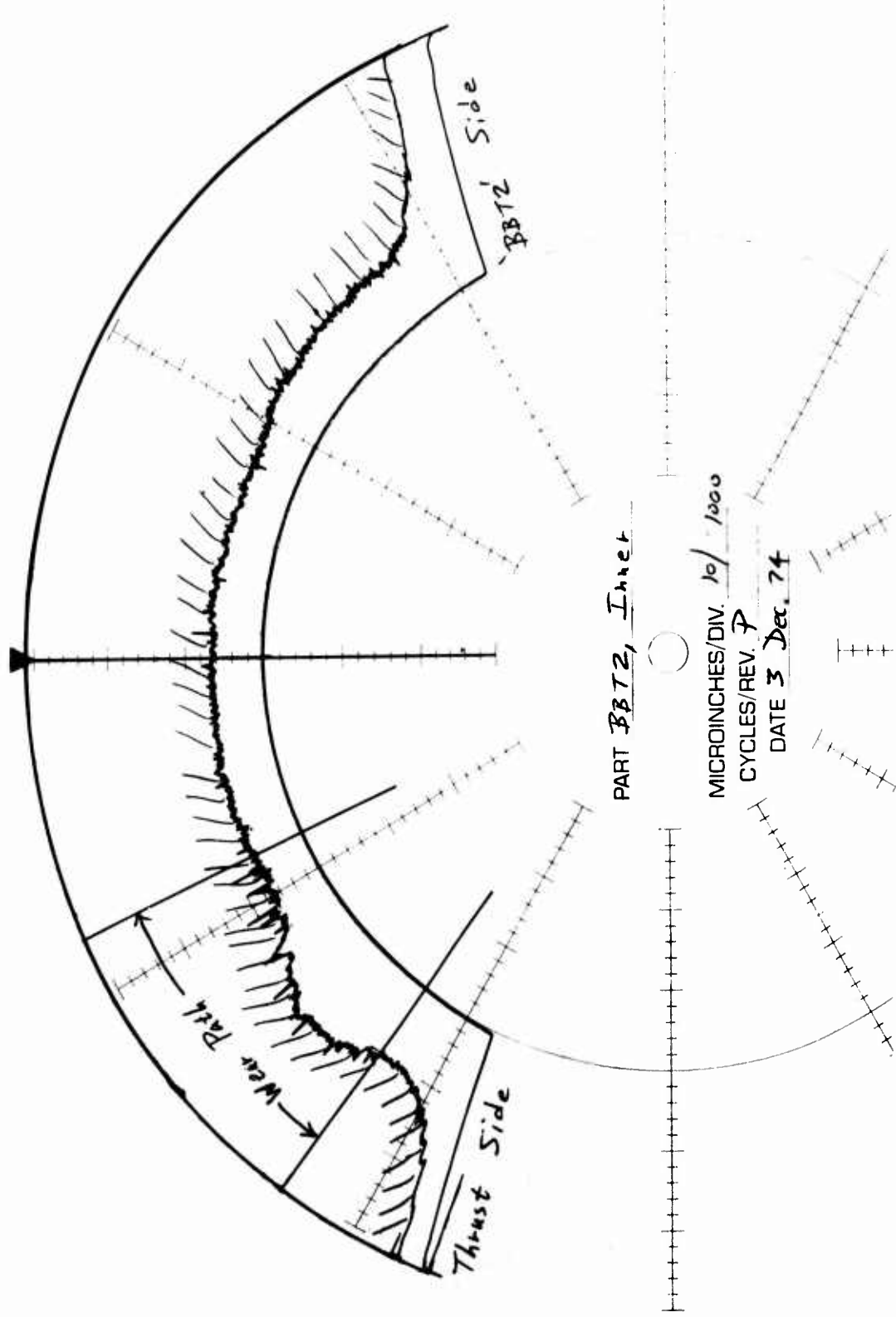


Figure 146. BBT-3 Cross-Groove Profile at 1022 Test Hours.

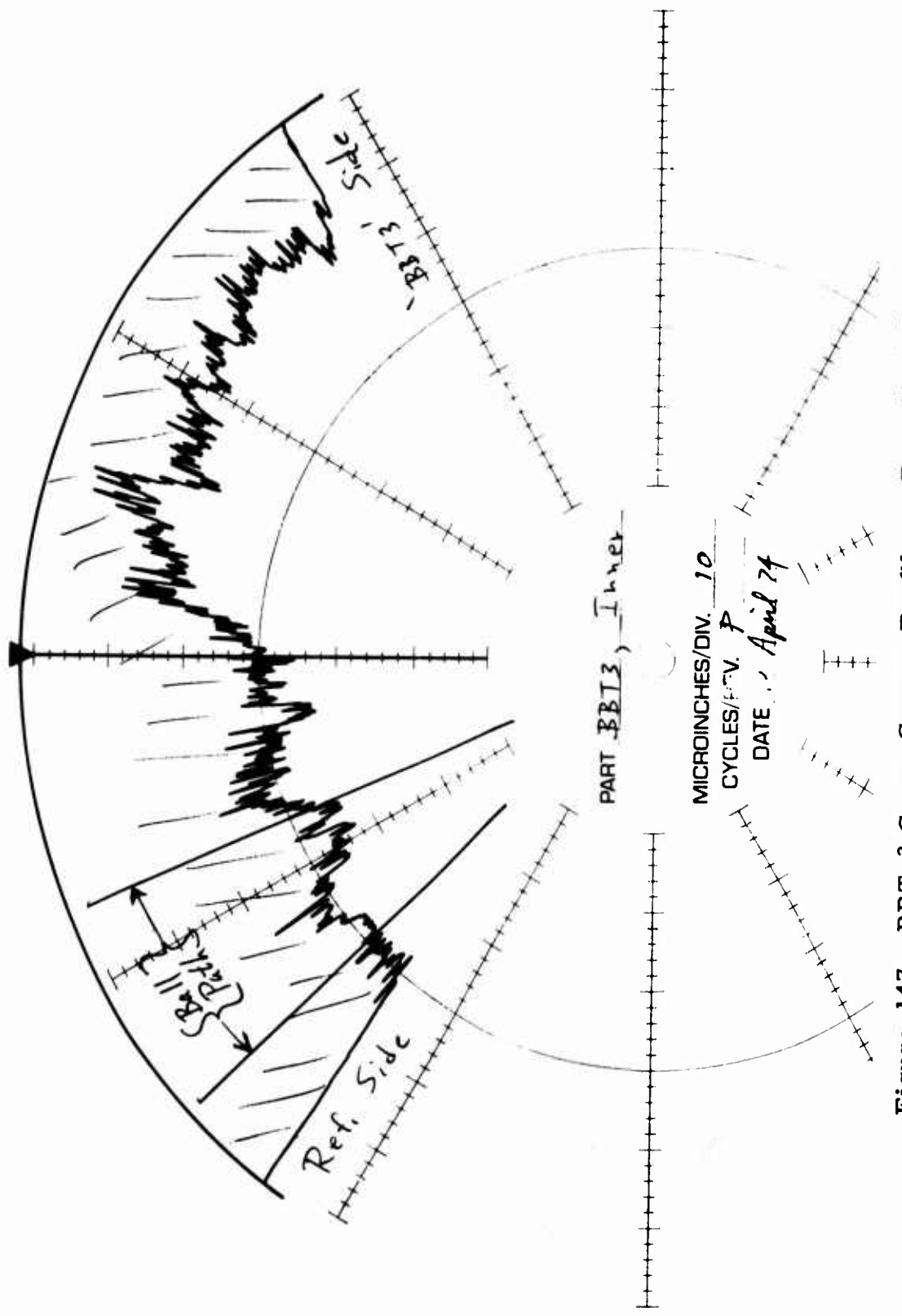


Figure 147. BBT-3 Cross-Groove Profile at Zero Test Hours.

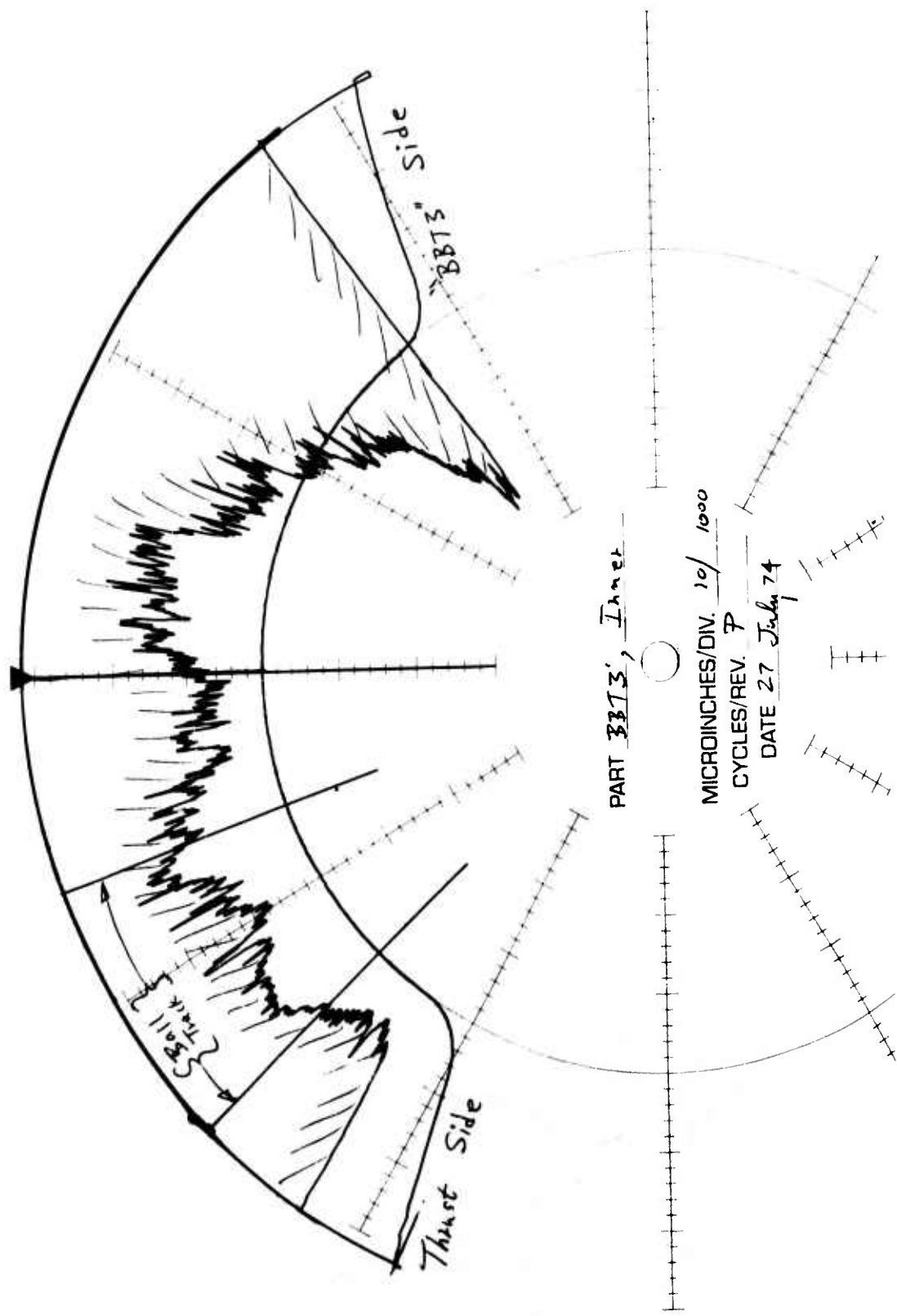


Figure 148. BBT-3 Cross-Groove Profile at 407 Test Hours.

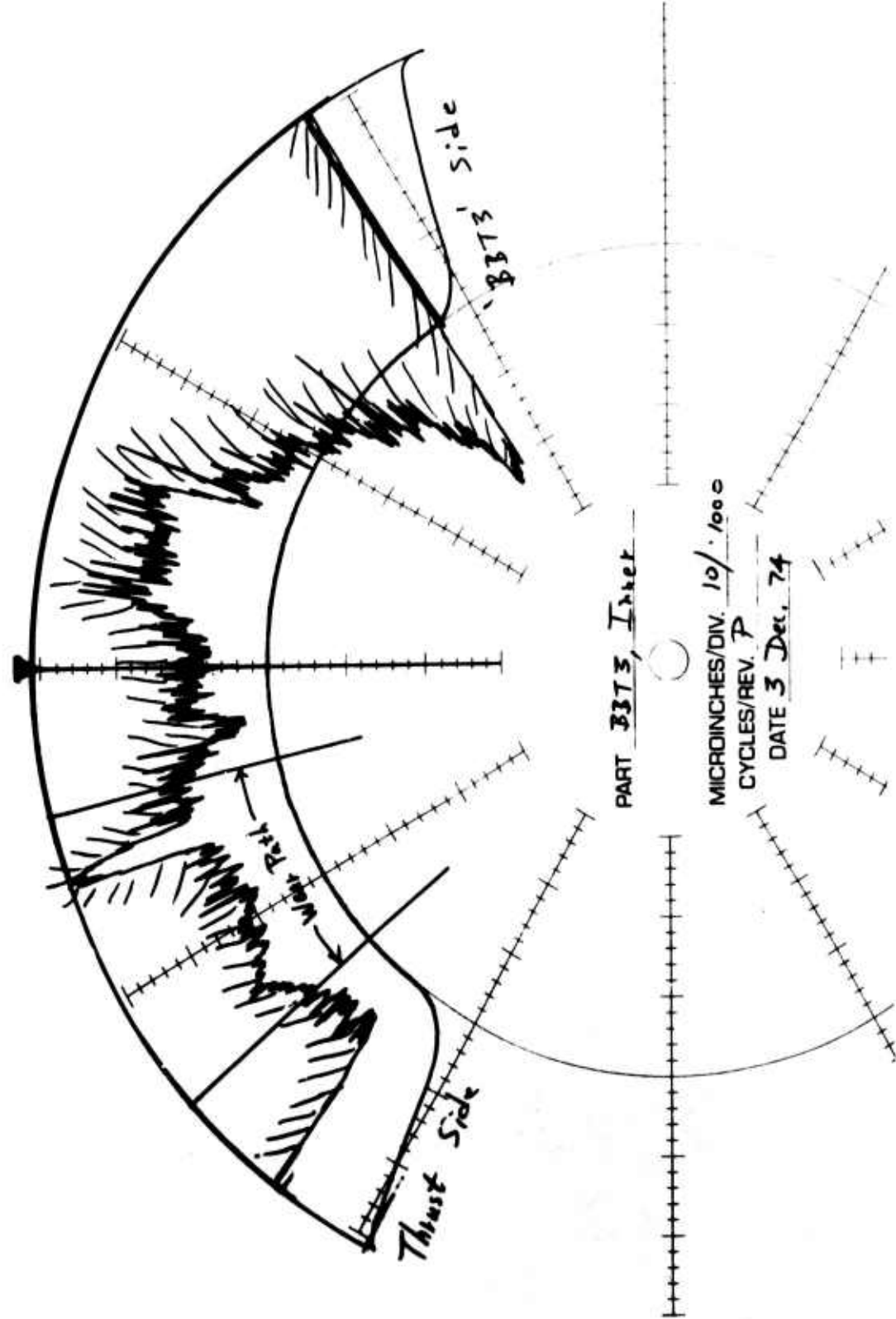


Figure 149. BBT-3 Cross-Groove Profile at 1022 Test Hours.

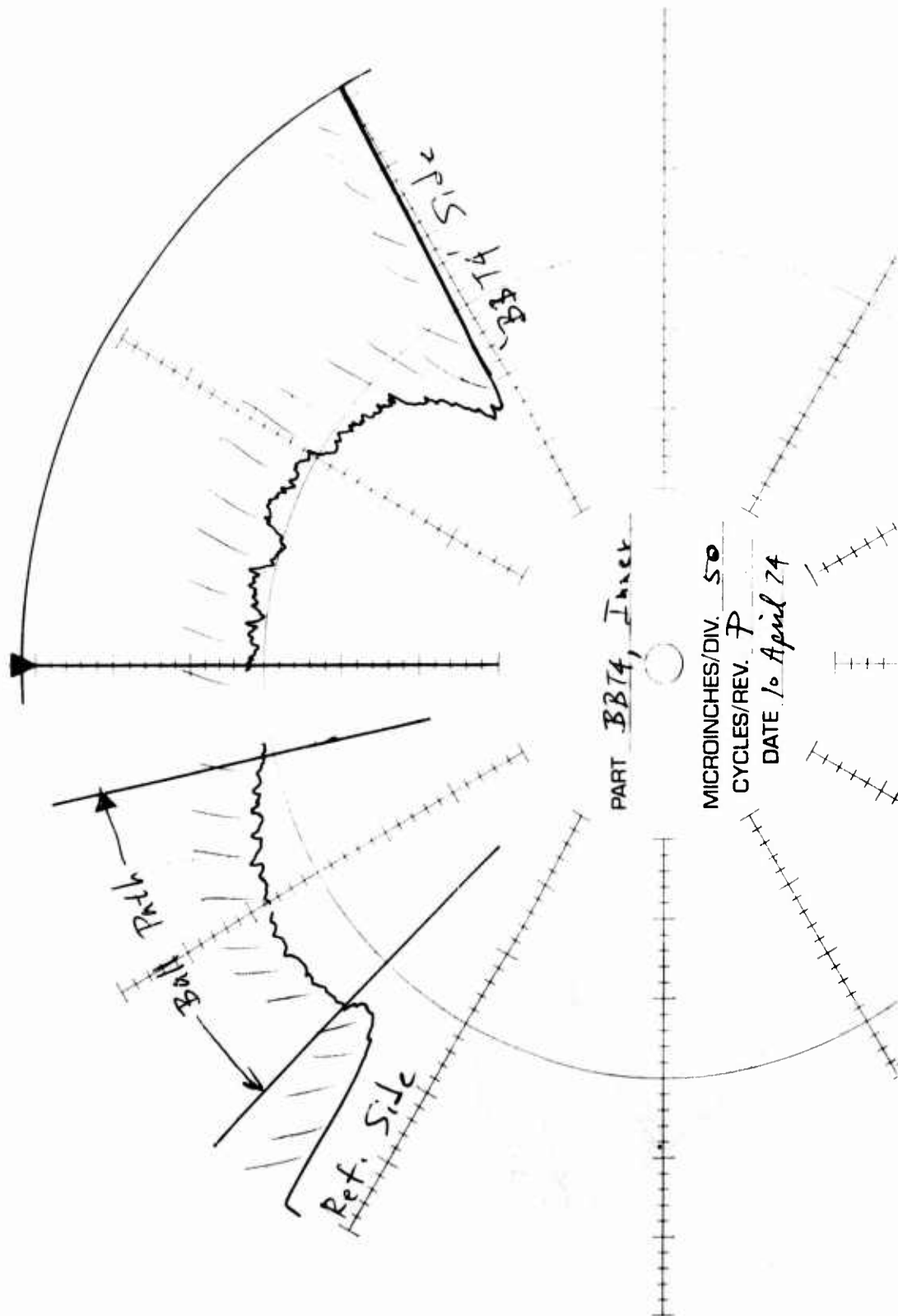


Figure 150. BBT-4 Cross-Groove Profile at Zero Test Hours.

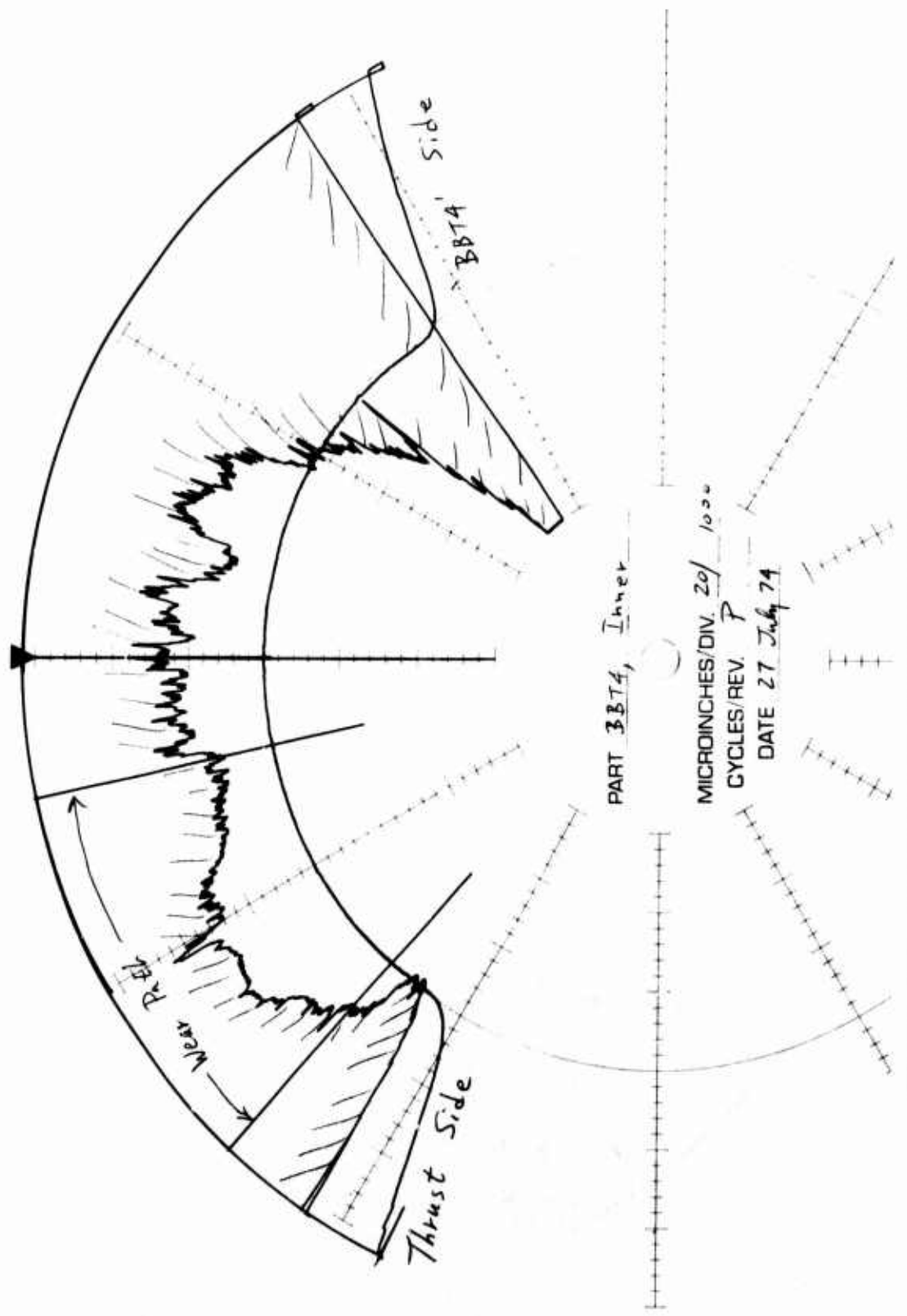


Figure 151. BBT-4 Cross-Groove Profile at 407 Test Hours.

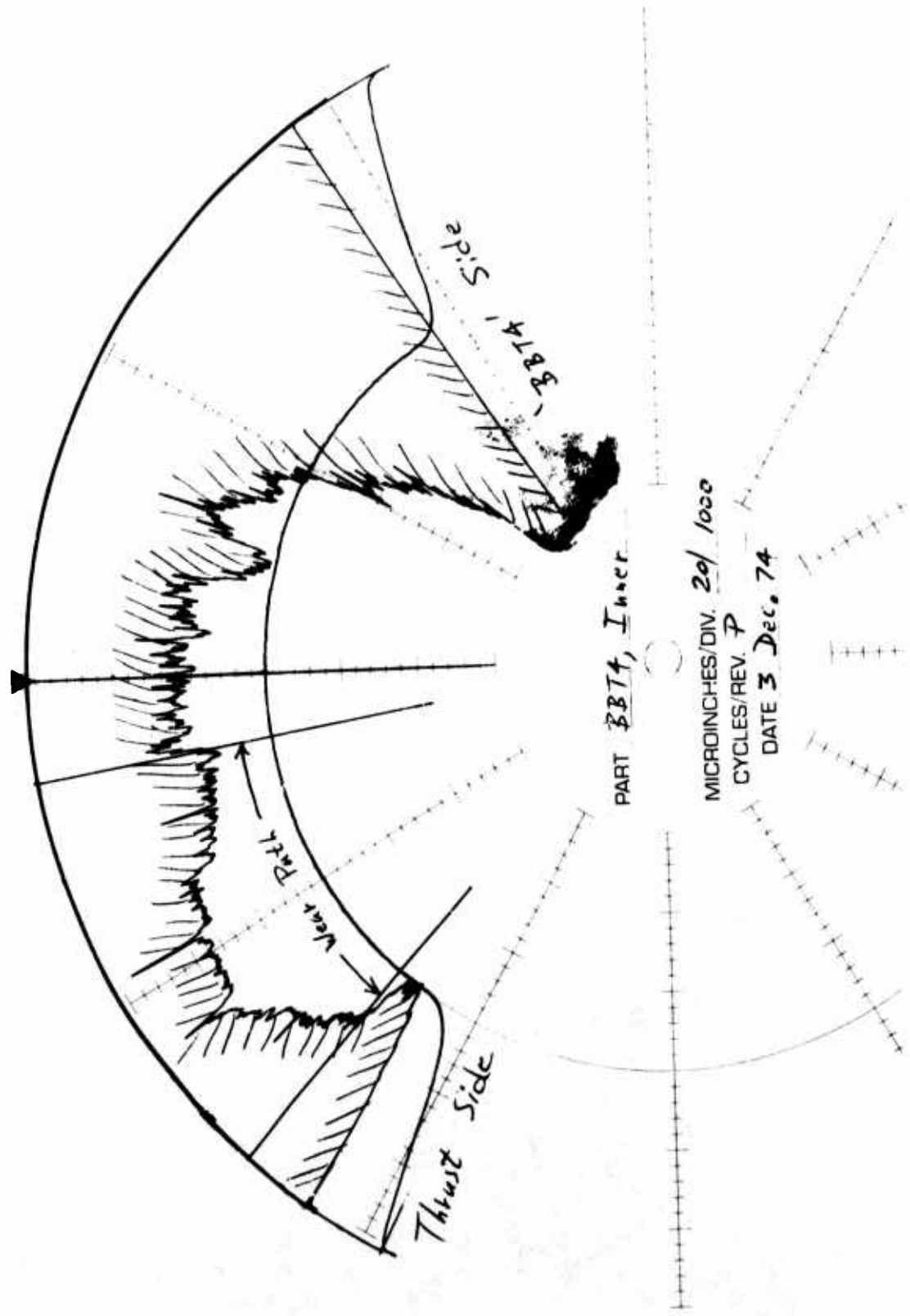
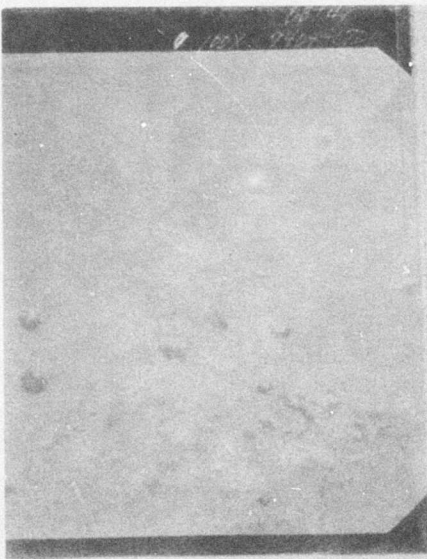


Figure 152. BBT-4 Cross-Groove Profile at 1022 Test Hours.



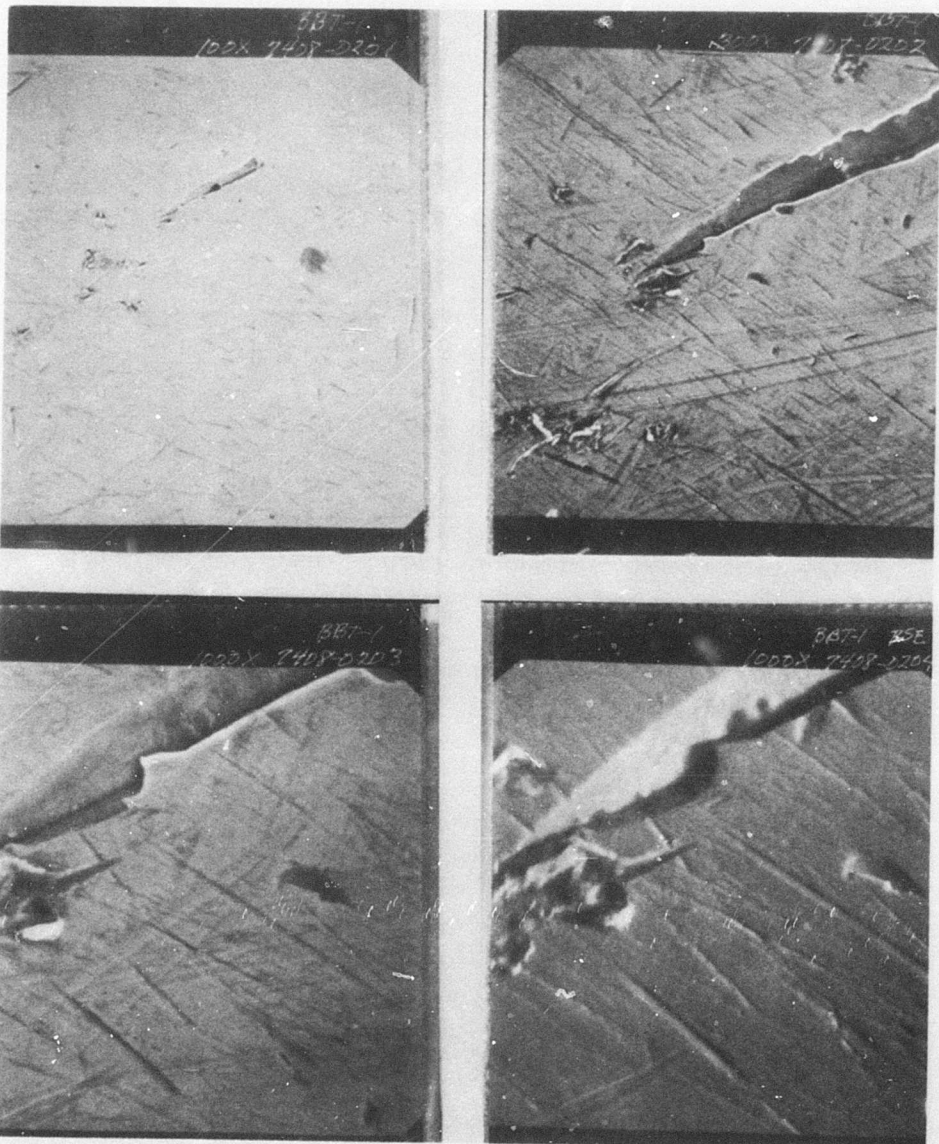
Top: 100 X

Bottom: 1000 X

Top: 300 X

Bottom: 1000 X, BSE

Figure 153. SEM Micrographs of BBT-1 (Zero Hours).



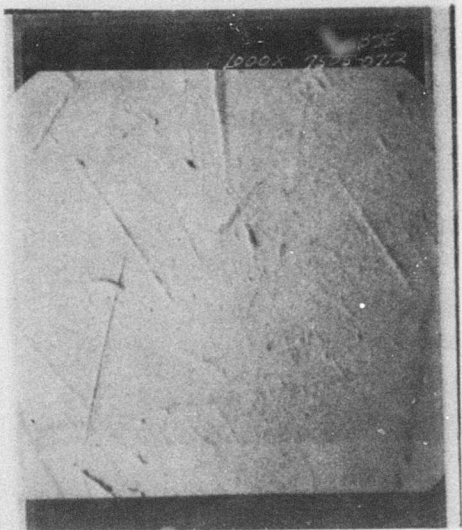
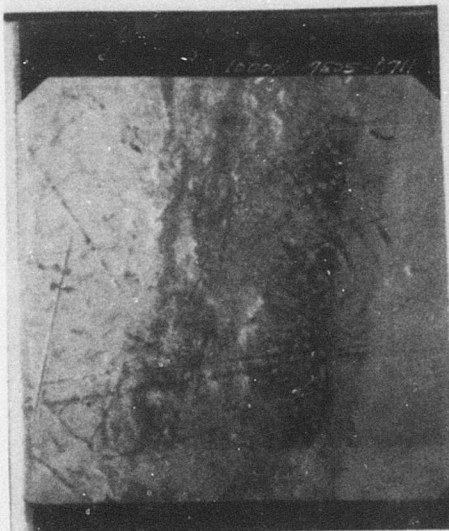
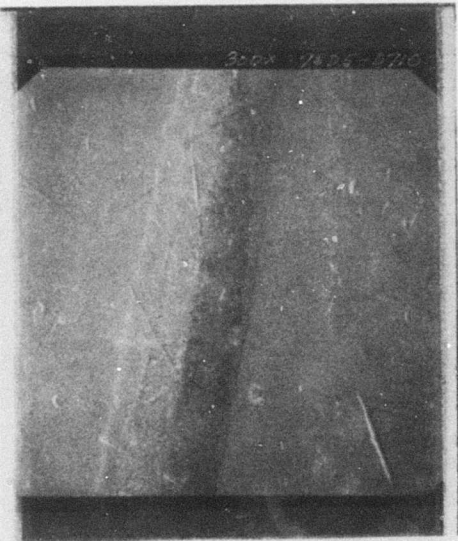
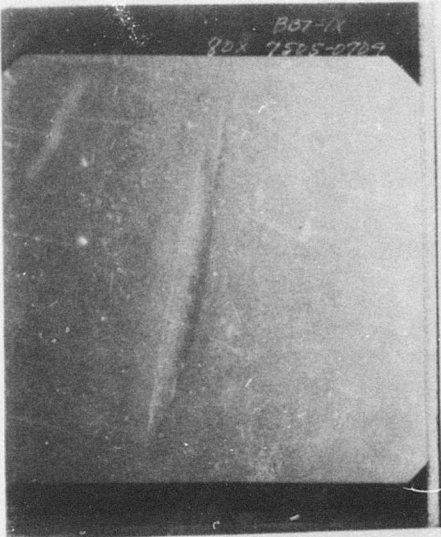
Top: 100 X

Bottom: 1000 X

Top: 300 X

Bottom: 1000 X, BSE

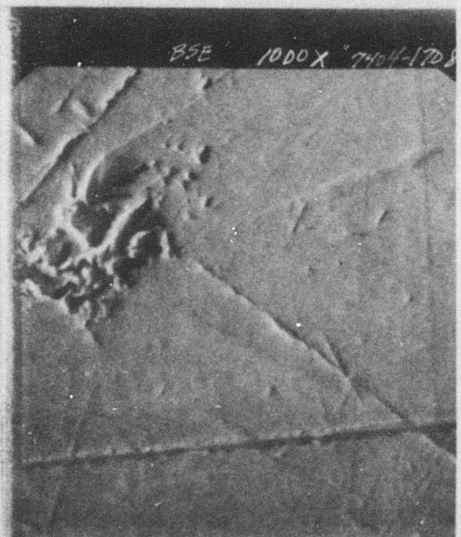
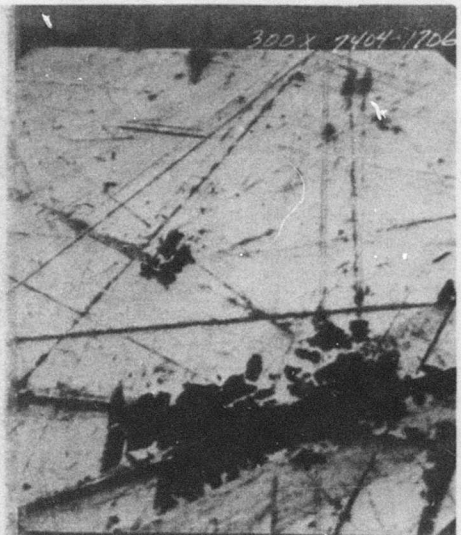
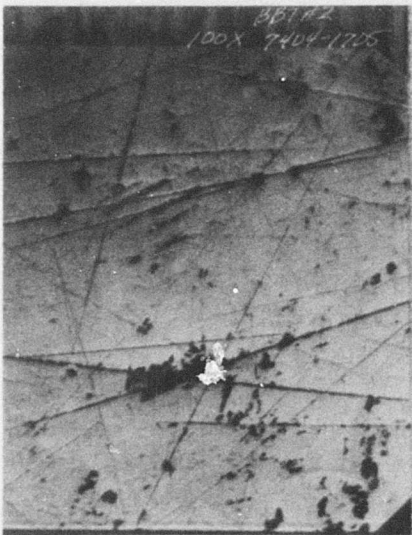
Figure 154. SEM Micrographs of BBT-1 (407 Hours).



Top: 80 X
Bottom: 1000 X

Top: 300 X
Bottom: 1000 X, BSE

Figure 155. SEM Micrographs of BBT-1 (1022 Hours).



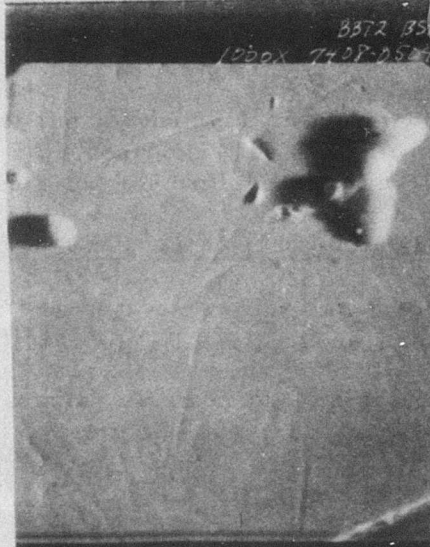
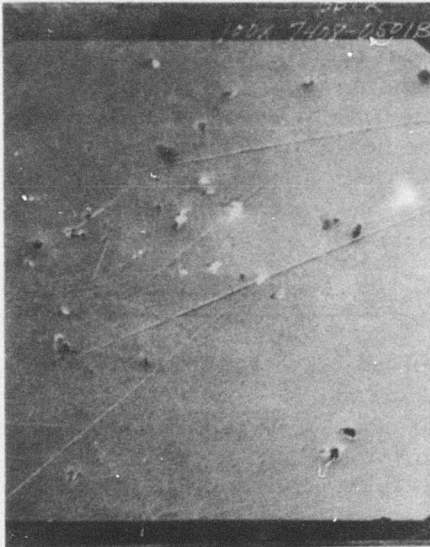
Top: 100 X

Bottom: 1000 X

Top: 300 X

Bottom: 1000 X, BSE

Figure 156. SEM Micrographs of BBT-2 (Zero Hours).



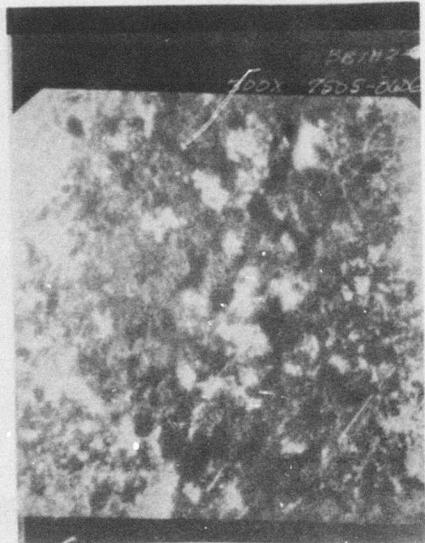
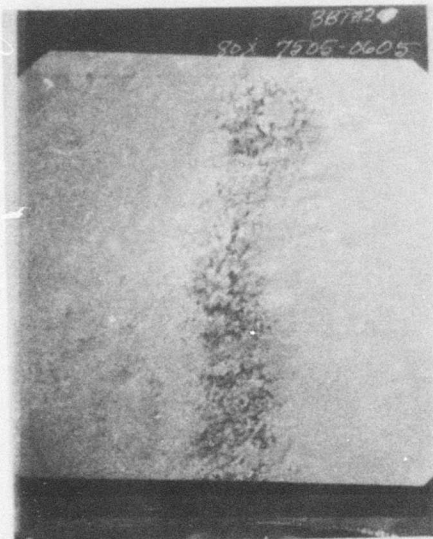
Top: 100 X

Bottom: 1000 X

Top: 300 X

Bottom: 100 X, BSE

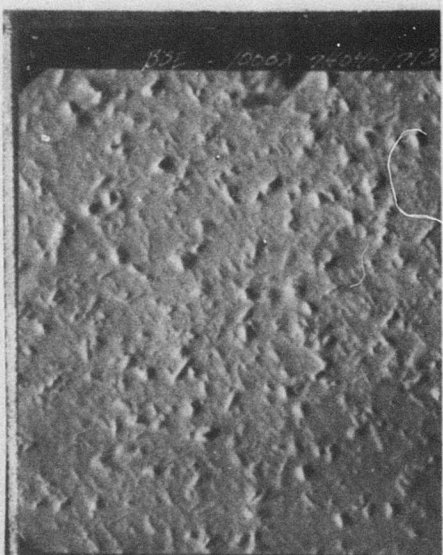
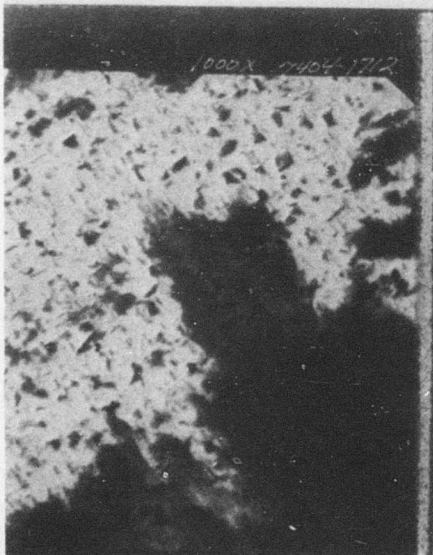
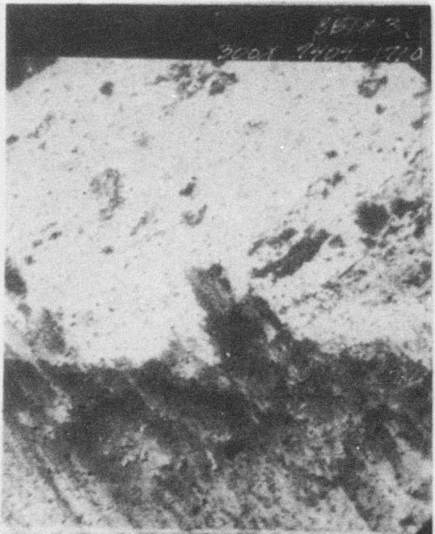
Figure 157. SEM Micrographs of BBT-2 (407 Hours).



Top: 80 X
Bottom: 1000 X

Top: 300 X
Bottom: 1000 X, BSE

Figure 158. SEM Micrographs of BBT-2 (1022 Hours).



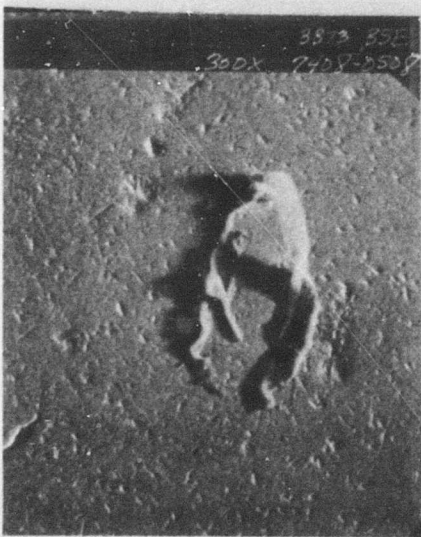
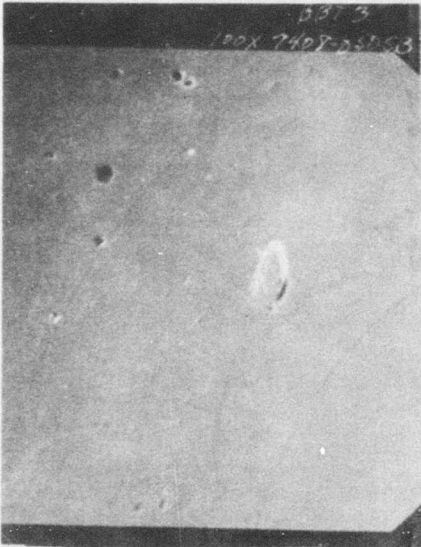
Top: 100 X

Bottom: 1000 X

Top: 300 X

Bottom: 1000 X, BSE

Figure 159. SEM Micrographs of BBT-3 (Zero Hours).



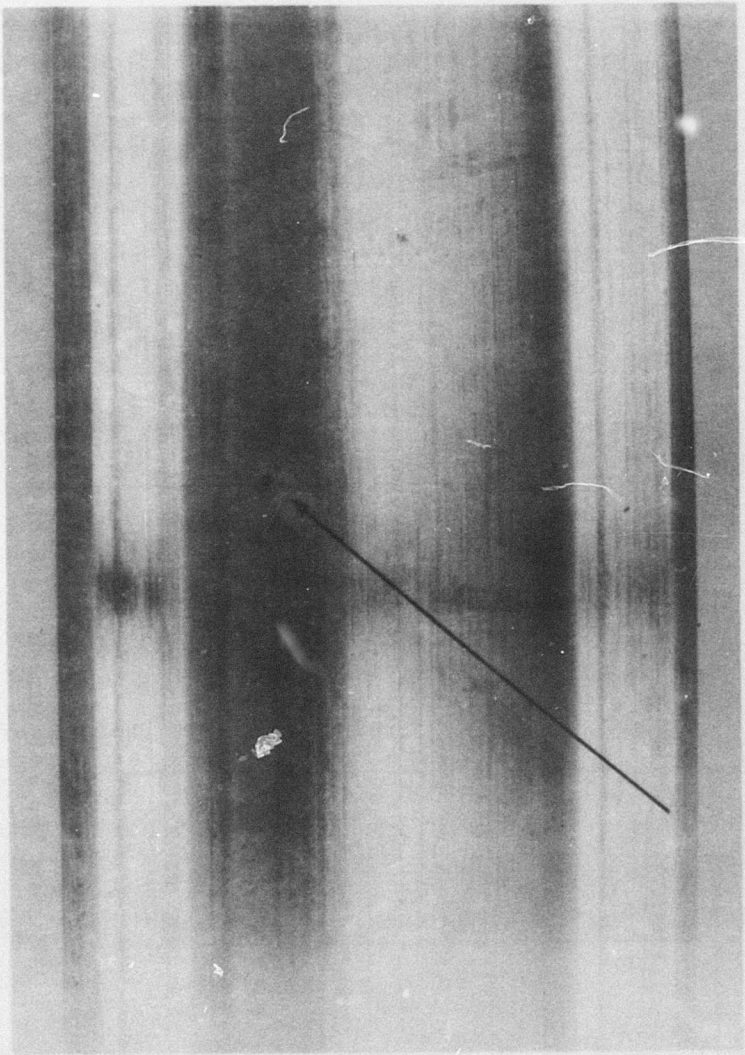
Top: 100 X

Bottom: 300 X, BSE

Top: 300 X

Bottom: 1000 X

Figure 160. SEM Micrographs of BBT-3 (407 Hours).



8.9X

Figure 161. Fatigue Pit on Inner-Ring Raceway, BBT-3 (407 Hours).

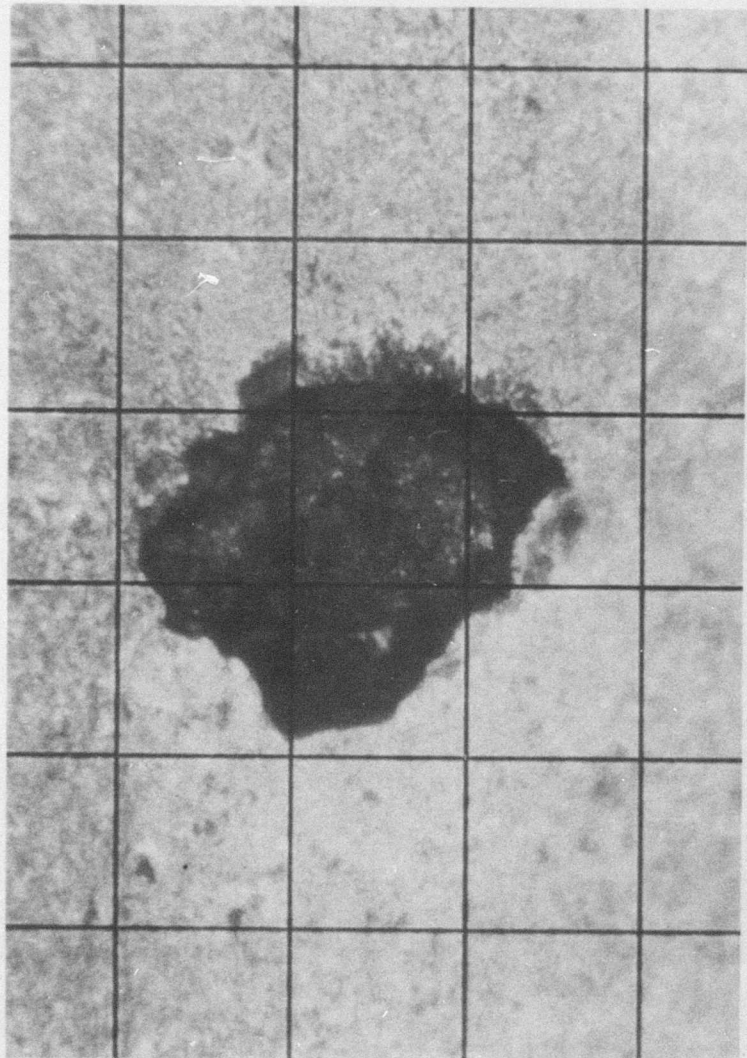
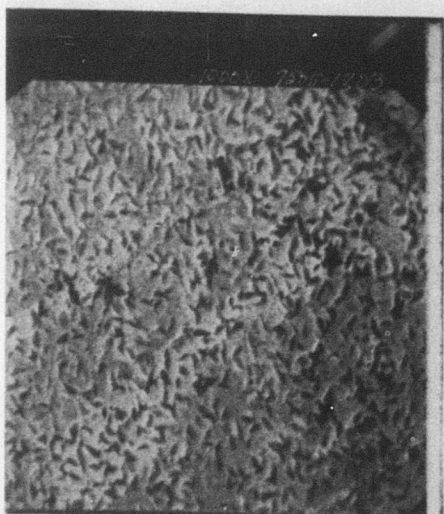
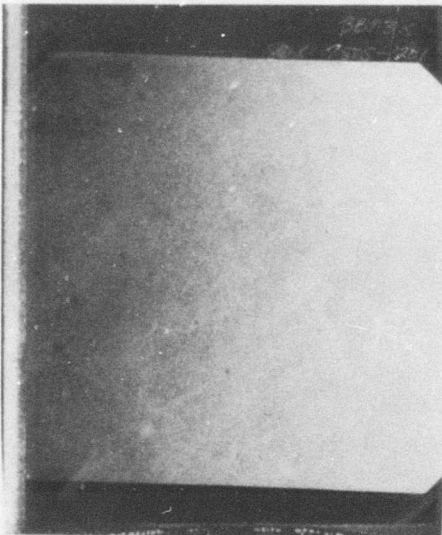


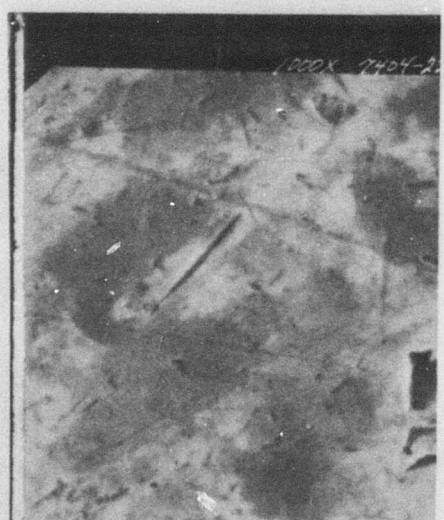
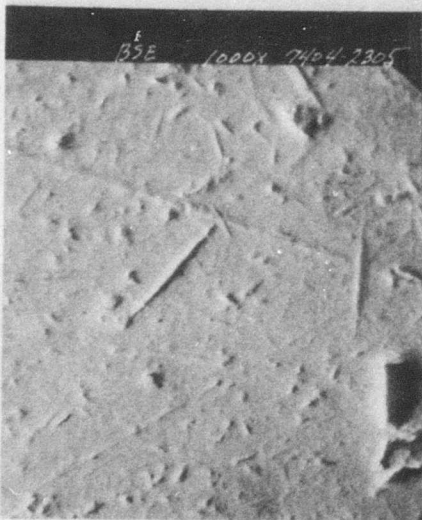
Figure 162. Magnified View of Fatigue Pit, S/N BBT-3.



Top: 80 X
Bottom: 1000 X, BSE

Top: 100 X
Bottom: 1000 X

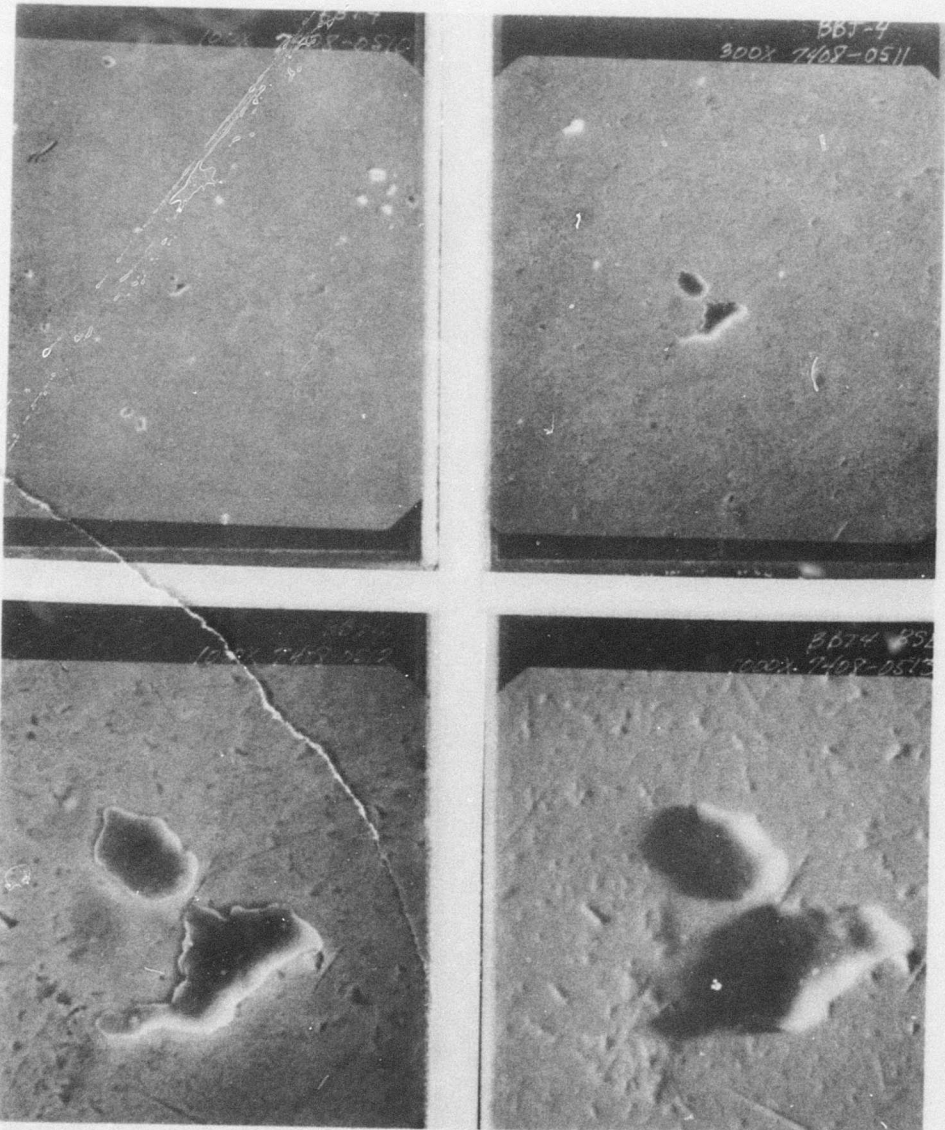
Figure 163. SEM Micrographs of BBT-3 (1022 Hours).



Top: 100 X
Bottom: 1000 X, BSE

Top: 300 X
Bottom: 1000 X

Figure 164. SEM Micrographs of BBT-4 (Zero Hours).



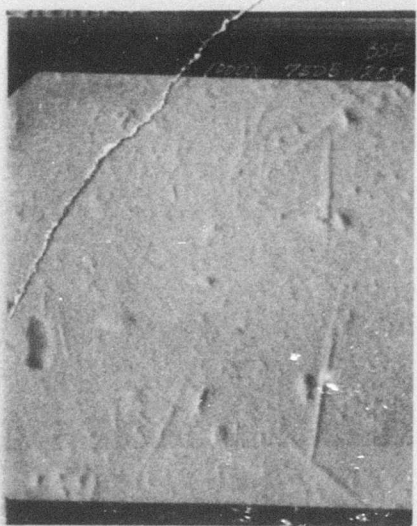
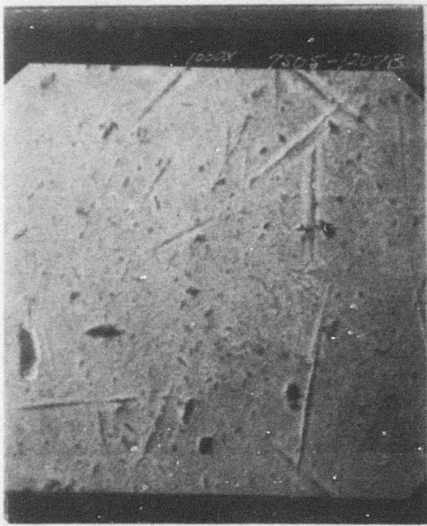
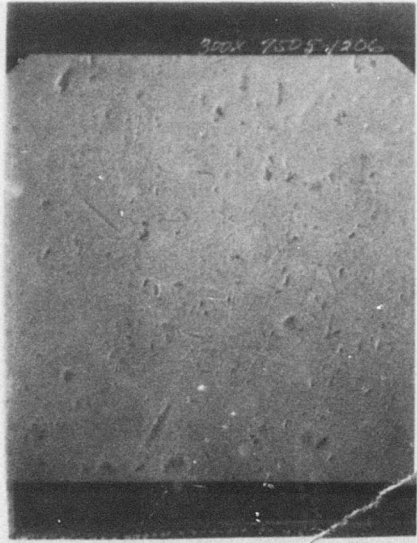
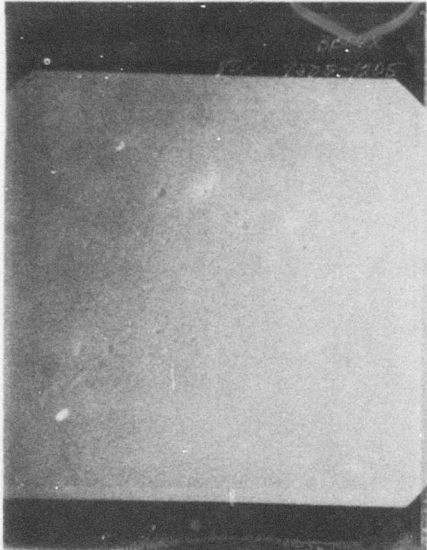
Top: 100 X

Bottom: 1000 X

Top: 300 X

Bottom: 1000 X, BSE

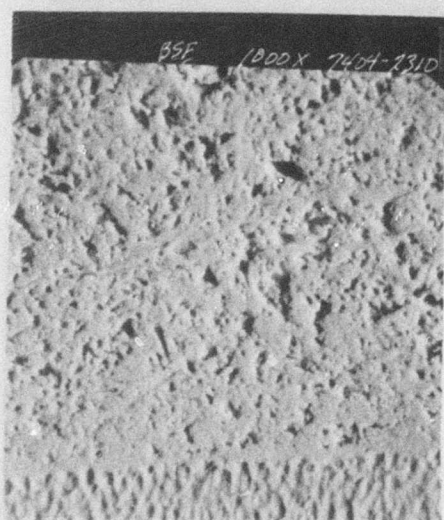
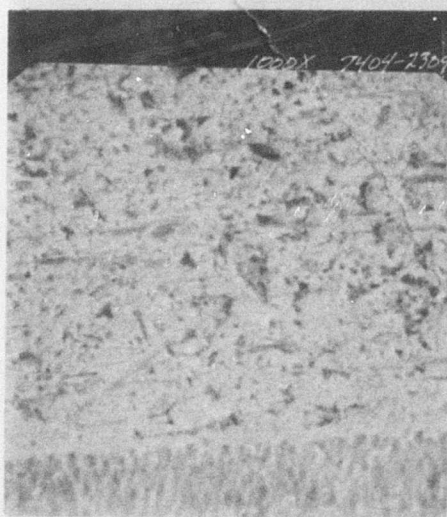
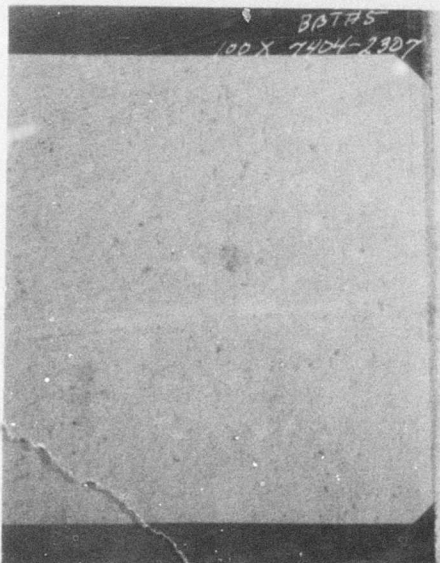
Figure 165. SEM Micrographs of BBT-4 (407 Hours).



Top: 80 X
Bottom: 1000 X

Top: 300 X
Bottom: 1000 X, BSE

Figure 166. SEM Micrographs of BBT-4 (1022 Hours).



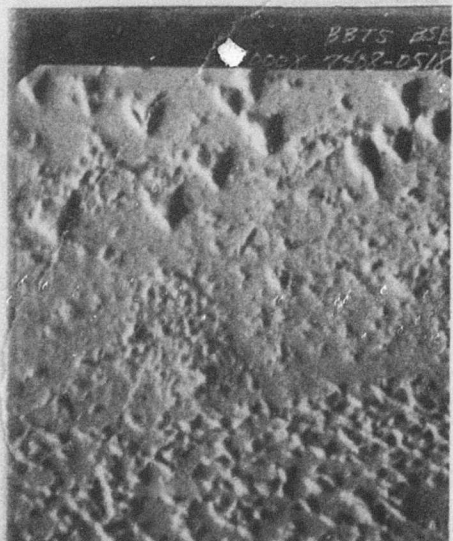
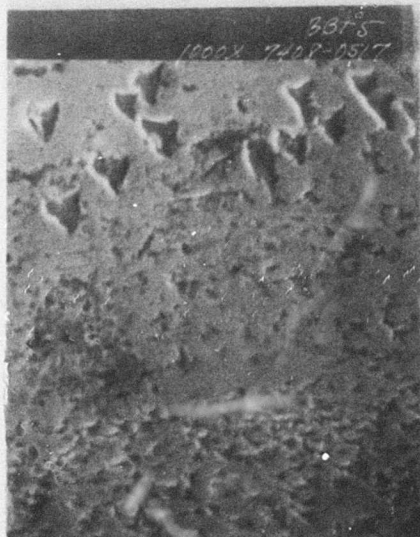
Top: 100 X

Bottom: 1000 X

Top: 300 X

Bottom: 1000 X, BSE

Figure 167. SEM Micrographs of BBT-5 (Zero Hours).



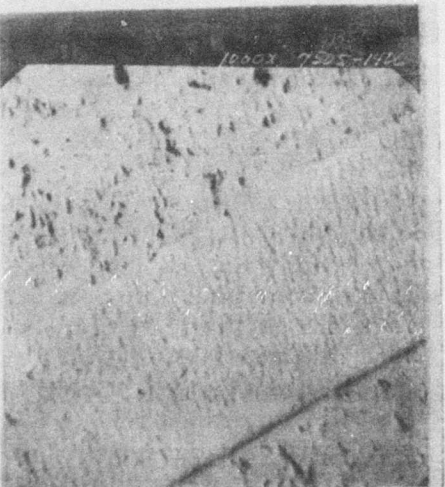
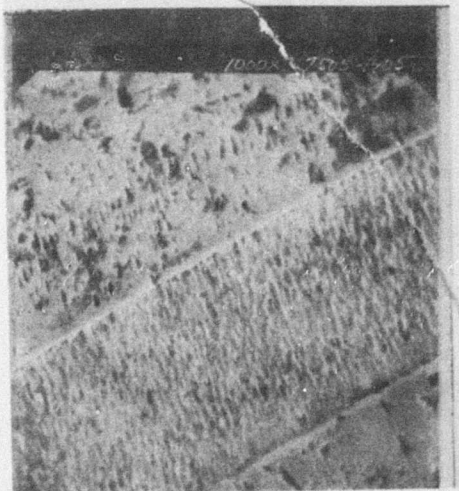
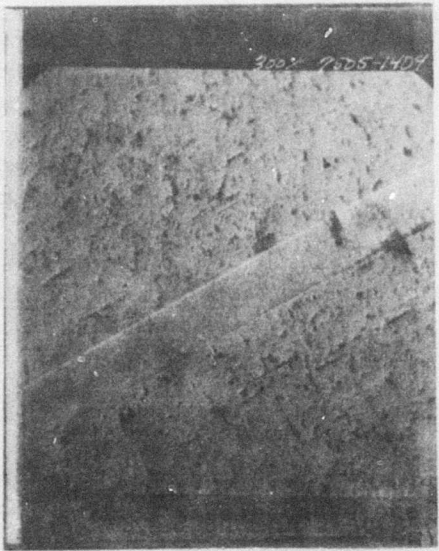
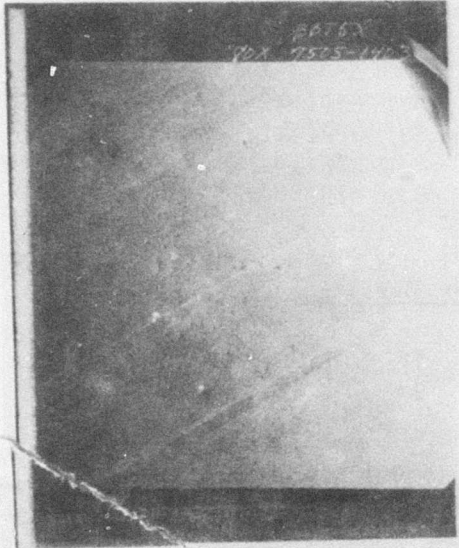
Top: 100 X

Bottom: 1000 X

Top: 300 X

Bottom: 1000 X, BSE

Figure 168. SEM Micrographs of BBT-5 (407 Hours).



Top: 80 X
Bottom: 1000 X

Top: 300 X
Bottom: 1000 X, BSE

Figure 169. SEM Micrographs of BBT-4 (1022 Hours).

BAD BEARING THREE (BB3) GEARBOX (B13-9974)

This gearbox had reached a TBO of 1200 hours and had shown signs of incipient failure in the output duplex pair (BB3-3, BB3-4). The manufacturer and serial number for each bearing are listed below:

BB3-1	Fafnir	7207 PW 2	S/N 65045-1
BB3-2	Fafnir	7207 PW 2	S/N 65045-2
BB3-3	Fafnir	9108 WI-3	S/N 32814-1
BB3-4	Fafnir	9108 WI-3	S/N 32814-2
BB3-5	MRC	R110KD	S/N 2702
BB3-6	(Not available)		

Visual Inspections of BBT Gearbox Bearings

BB3-1 Ball Bearing

ZERO TEST HOURS

Inner Race: Fair. 0.09" to 0.12" wide ball track; electrical damage (pitting and denting), moderate wear.
Outer Race: Generally similar to inner; 0.10" wide ball track.
Balls: Fair. Light scratches, pits and dents.
Retainer: Good. Moderate pocket wear.

1086 TEST HOURS

Inner Race: Fair. 0.10" to 0.12" wide ball track; electrical damage (pitting and denting), moderate wear.
Outer Race: Generally similar to inner; 0.10" wide ball track.
Balls: Fair. Light scratches, pits and dents.
Retainer: Good. Moderate pocket wear.

BB3-2 Ball Bearing

ZERO TEST HOURS

Inner Race: Fair. 0.09" to 0.135" wide ball track; electrical damage (pitting and denting), moderate wear.

Outer Race: Generally similar to inner; 0.10" wide ball track.
Balls: Fair; light scratches, pits and dents.
Retainer: Good. Light-to-moderate pocket wear.

1086 TEST HOURS

Inner Race: Fair. 0.10" to 0.135" wide ball track; electrical damage (pitting and denting), moderate wear.
Outer Race: Generally similar to inner; 0.10" wide ball track.
Balls: Poor. Light scratches, pits and dents.
Retainer: Good. Light-to-moderate pocket wear.

BB3-3 Ball Bearing

ZERO TEST HOURS

Inner Race: Poor. 0.075" wide ball track; electrical damage (pitting and denting), moderate-to-heavy wear.
Outer Race: Generally similar to inner; 0.075" wide ball track.
Balls: Poor. Considerable pitting and denting.
Retainer: Fair. Visibly out-of-round; light pocket wear.

1086 TEST HOURS

Inner Race: Poor. 0.10" wide ball track; electrical damage (pitting and denting), moderate-to-heavy wear. Some heat coloration in ball path.
Outer Race: Generally similar to inner; 0.075" wide ball track.
Balls: Poor. Considerable pitting and denting; heat color banding on most balls.
Retainer: Fair. Visibly out-of-round: light pocket wear.

BB3-4 Ball Bearing

ZERO TEST HOURS

Inner Race: Poor. 0.08" wide ball track; electrical damage.
Outer Race: Generally similar to inner; 0.075" wide ball track.
Balls: Poor. Considerable pitting and denting.
Retainer: Fair. Out-of-round, light pocket wear.

1086 TEST HOURS

Inner Race: Poor. 0.08" wide ball track; moderate to heavy wear, electrical damage, some heat coloration in ball path.
Outer Race: Generally similar to inner; 0.075" wide ball track. Considerable fretting corrosion on O.D. surface.
Balls: Poor. Considerable pitting and denting.
Retainer: Fair. Out-of-round, light pocket wear.

BB3-5 Roller Bearing

ZERO TEST HOURS

Inner Race: Fair-to-poor. Electrical damage (pitting and denting); light-to-moderate wear.
Outer Race: Fair-to-poor. Electrical damage (pitting and denting); light-to-moderate wear.
Rollers: Poor. Moderate-to-heavy wear; some banding; fatigue spots on some rollers; end wear.
Retainer: Fair condition. Light pocket wear.

1086 TEST HOURS

Inner Race: Fair-to-poor. Electrical damage (pitting and denting); light to moderate wear.
Outer Race: Poor. Moderate wear; some discoloration.
Rollers: Poor. Moderate-to-heavy wear; some banding; fatigue spots on some rollers; end wear.
Retainer: Fair condition. Moderate pocket wear.

BB3-6 Roller Bearing

ZERO TEST HOURS

Inner Race:	Unable to examine. Disassembly not authorized.
Outer Race:	Fair-to-poor. Light-to-moderate wear.
Rollers:	Moderate-to-heavy wear. Pitting and denting, some banding; few small fatigue spots; end wear.
Retainer:	Good condition as viewed externally.

1086 TEST HOURS

Inner Race:	Unable to examine. Disassembly not authorized.
Outer Race:	Fair-to-poor. Moderate wear; some discoloration.
Rollers:	Moderate-to-heavy wear. Pitting and denting; some banding; few small fatigue spots; end wear.
Retainer:	Good condition as viewed externally.

BB3 Gearbox Mechanical Summary

Table XV summarizes the results of the mechanical measurements made upon the ball bearings in the BB3 gearbox. Table XVI summarizes the mechanical measurements for the roller bearings.

BB3 Gearbox Bearing Photographs and Cross-Groove Profiles

Figures 170 through 177 show the cross-groove profiles for the BBT gearbox at the start and end of testing.

Figures 178 through 186 show the scanning electron photomicrographs of the bearings taken before and after testing.

TABLE XV. MECHANICAL MEASUREMENTS FOR BB3 BALL BEARINGS

Bearing	Test Time (hr)	Noise Level (dB)	Peak Rise (dB)	General Condition (Wear)	Local Damage	Raceway Wear Depth (in.)	Radial Play (in.)
BB3-1	0 1086	4 4.5	0.5 4	moderate moderate	light moderate	67 77	0.0078 0.0082
BB3-2	0 1086	4 9.5	2 2.5	moderate heavy	light light	60 50	0.0075 0.0081
BB3-3	0 1086	10 17.5	0.5 3.5	heavy extreme	light moderate	64 50	0.0029 0.0031
BB3-4	0 1086	16.5 18.5	0 0.5	extreme extreme	negligible light	70 60	0.0030 0.0032

TABLE XVI. MECHANICAL MEASUREMENTS FOR BB3 BALL BEARINGS

Bearing	Time (hr)	Axial Clearance of Roller in Inner Race (in.)	Roller Contour (μ in.)	Drop (μ in.)	Roller Crown Length (in.)
BB3-5	0	0.0020" 0.0028"	10 Concave 15 Compound	38 38.5	0.071 0.078
	1086				
BB3-6	0	0.0037" 0.0043"	40 Convex 40 Convex	340 310	0.048 0.045
	1086				

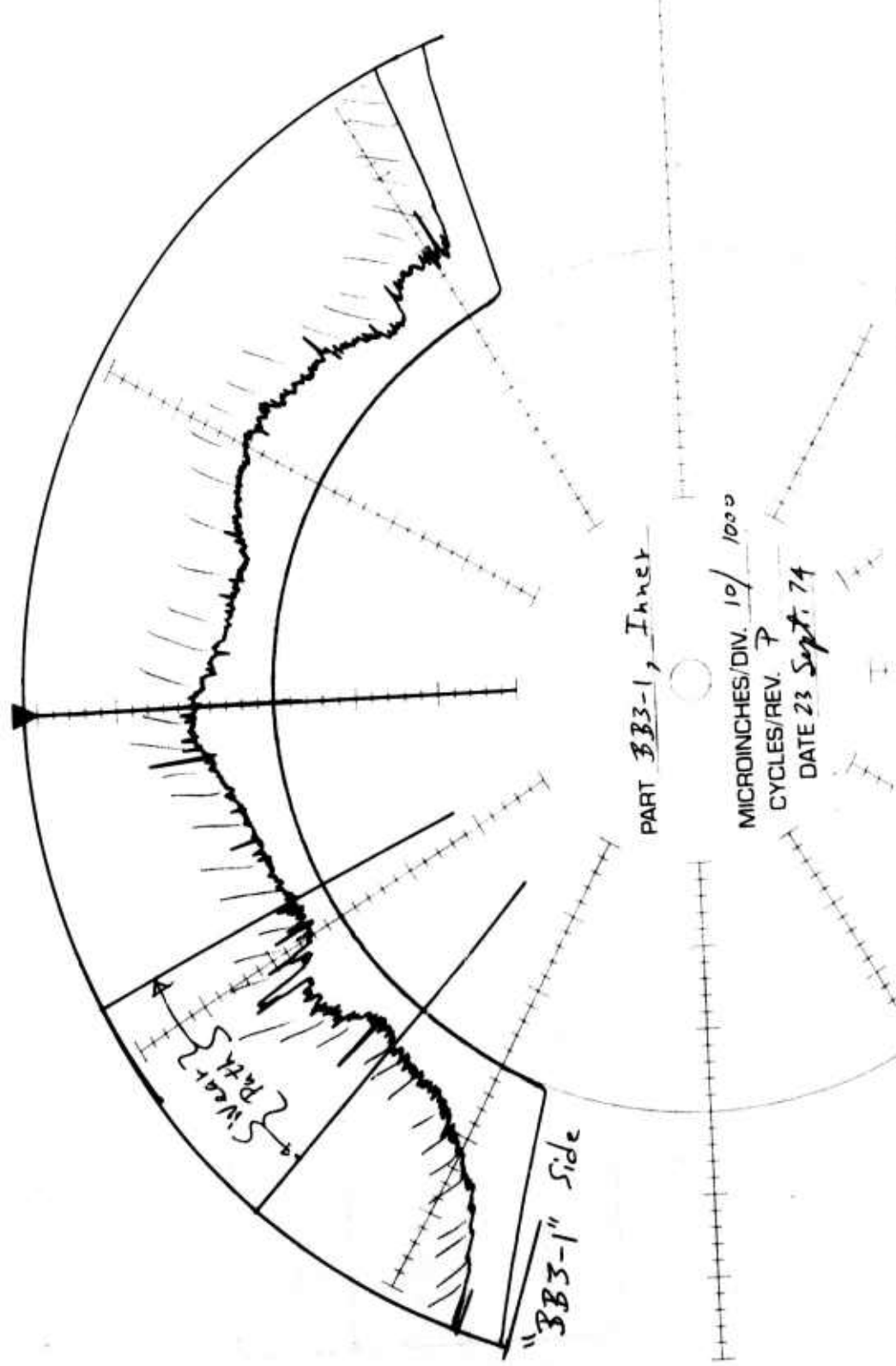


Figure 170. BB3-1, Cross-Groove Profile at Zero Test Hours.

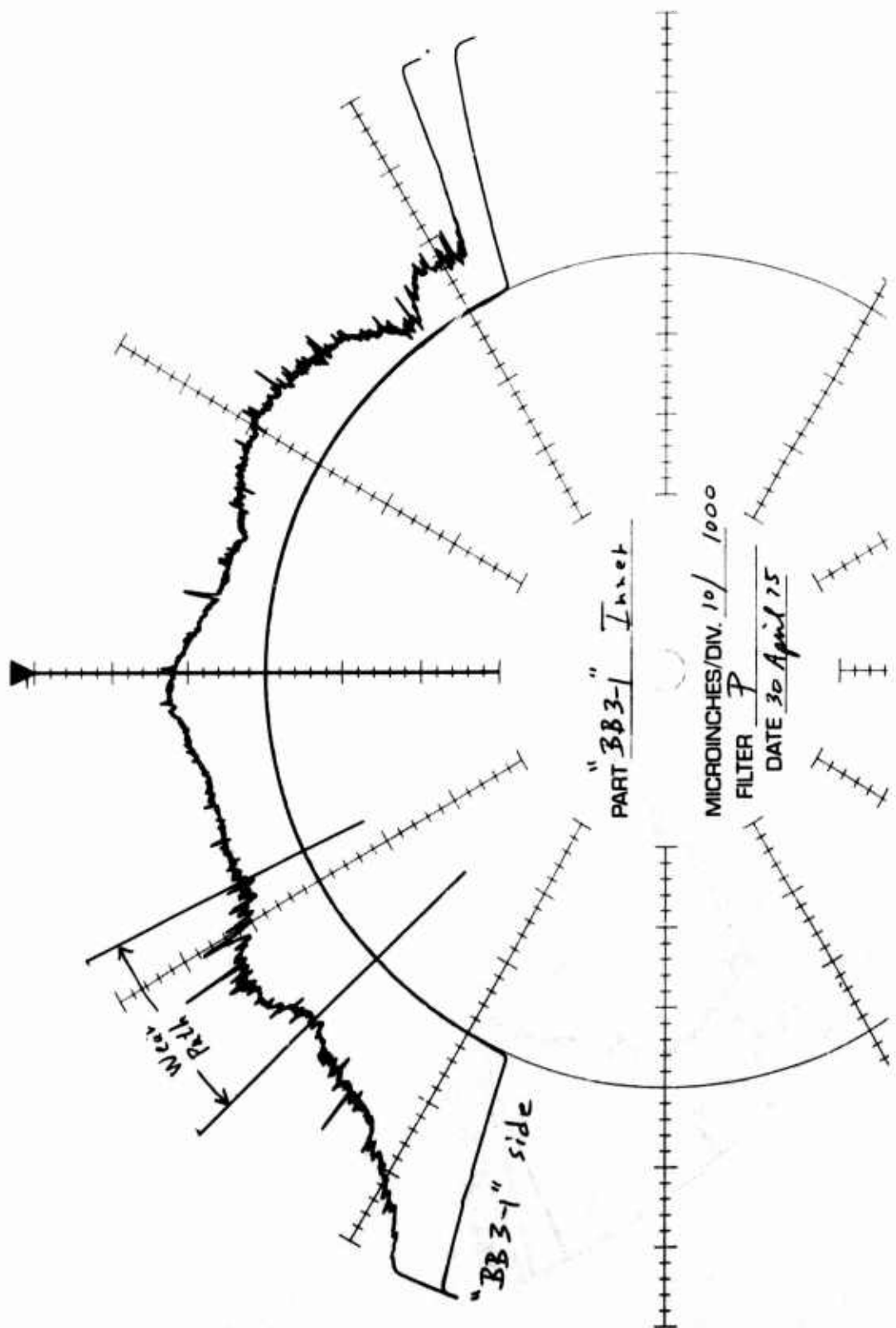


Figure 171. BB3-1, Cross-Groove Profile at 1086 Test Hours.

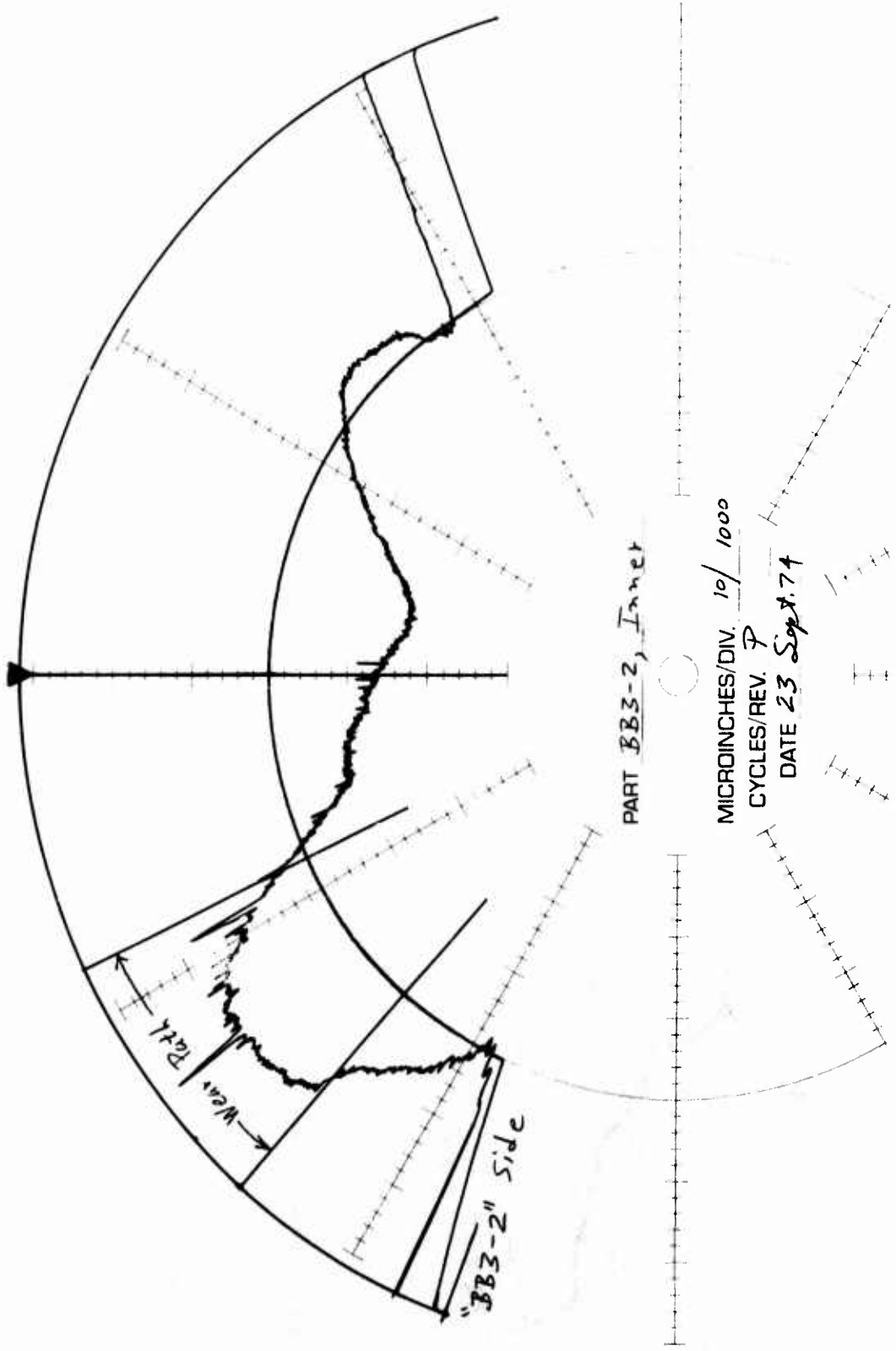


Figure 172. BB3-2, Cross-Groove Profile at Zero Test Hours.

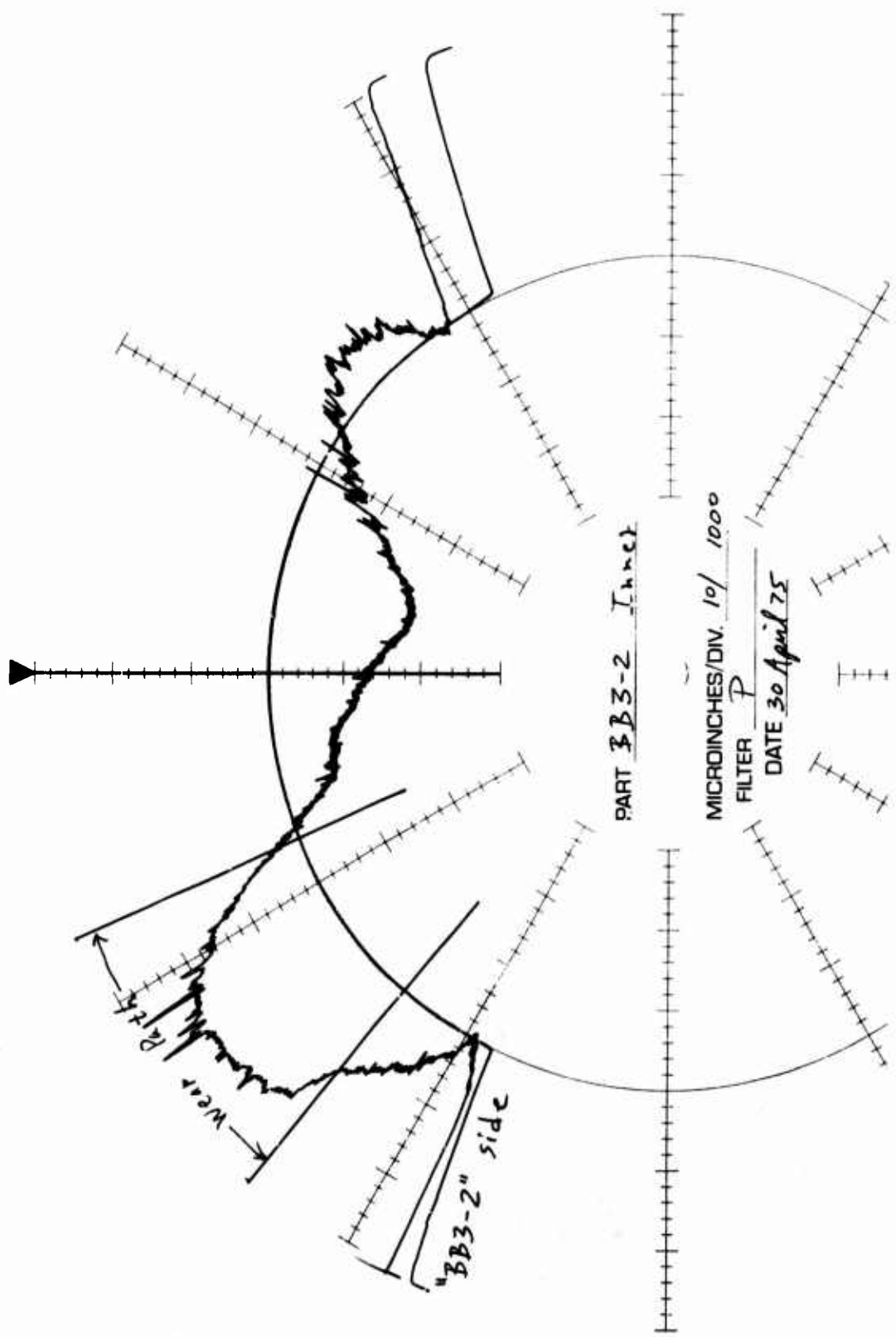


Figure 173. BB3-2, Cross-Groove Profile at 1086 Test Hours.

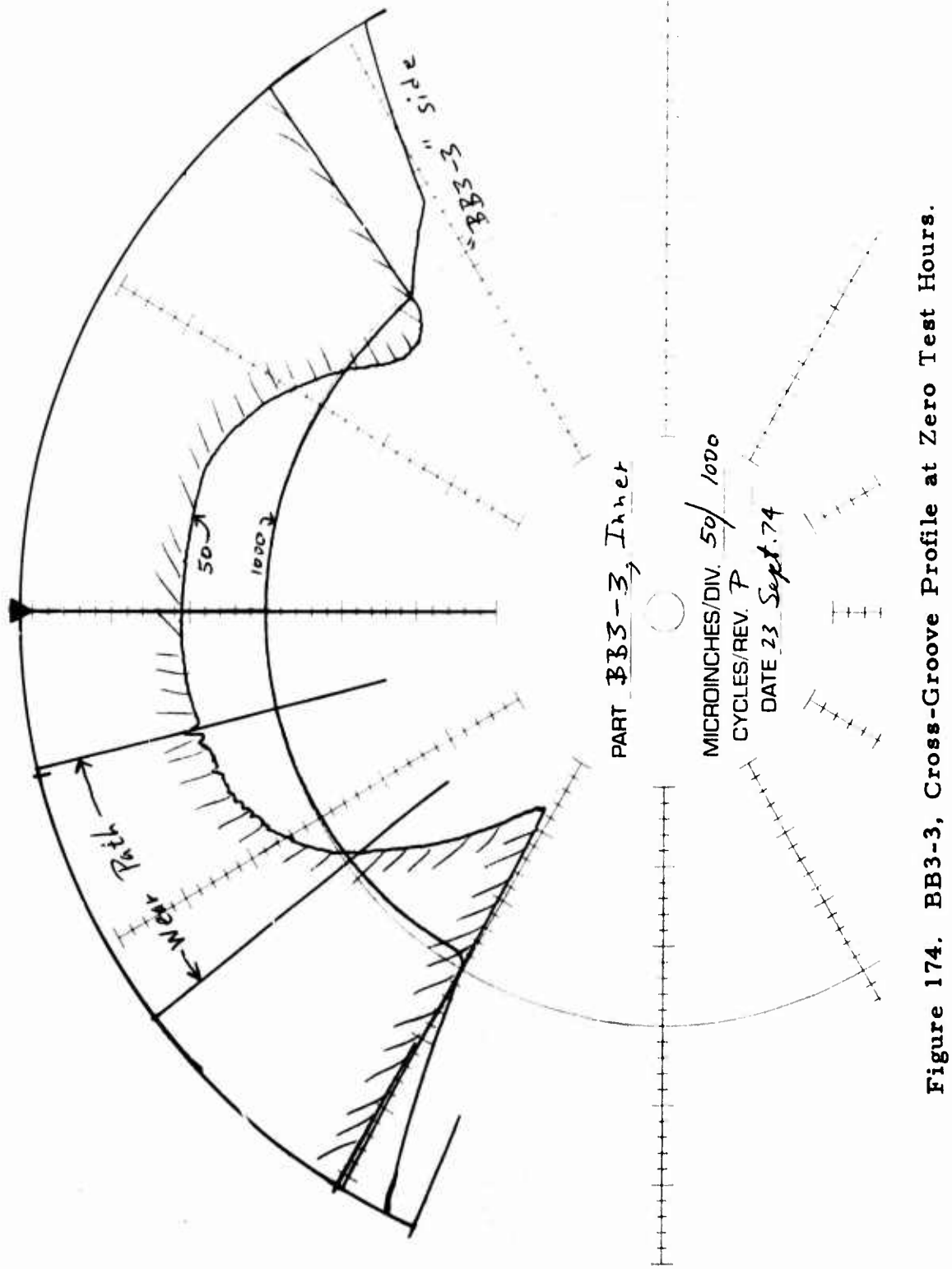


Figure 174. BB3-3, Cross-Groove Profile at Zero Test Hours.

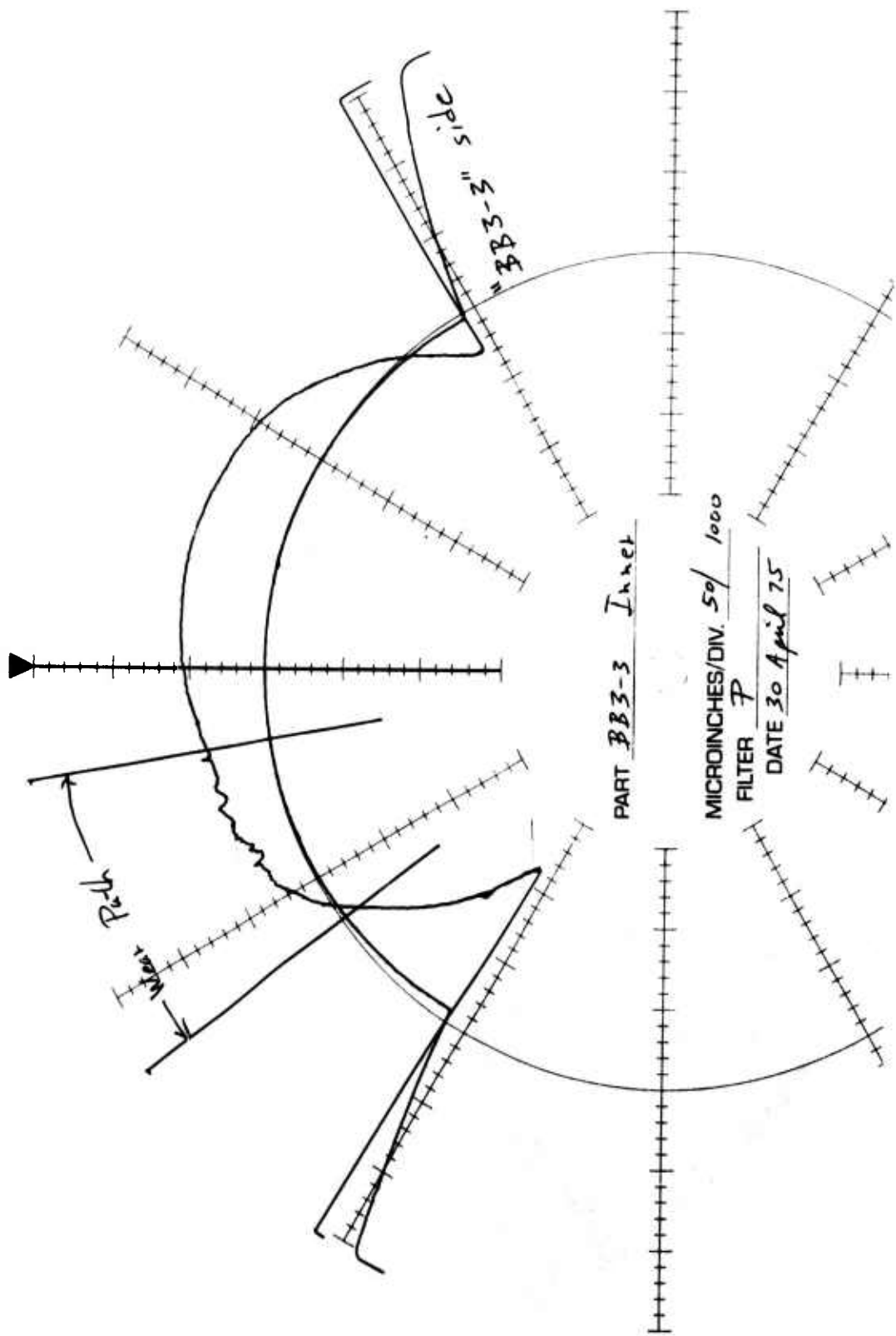


Figure 175. BB3-3, Cross-Groove Profile at 1086 Test Hours.

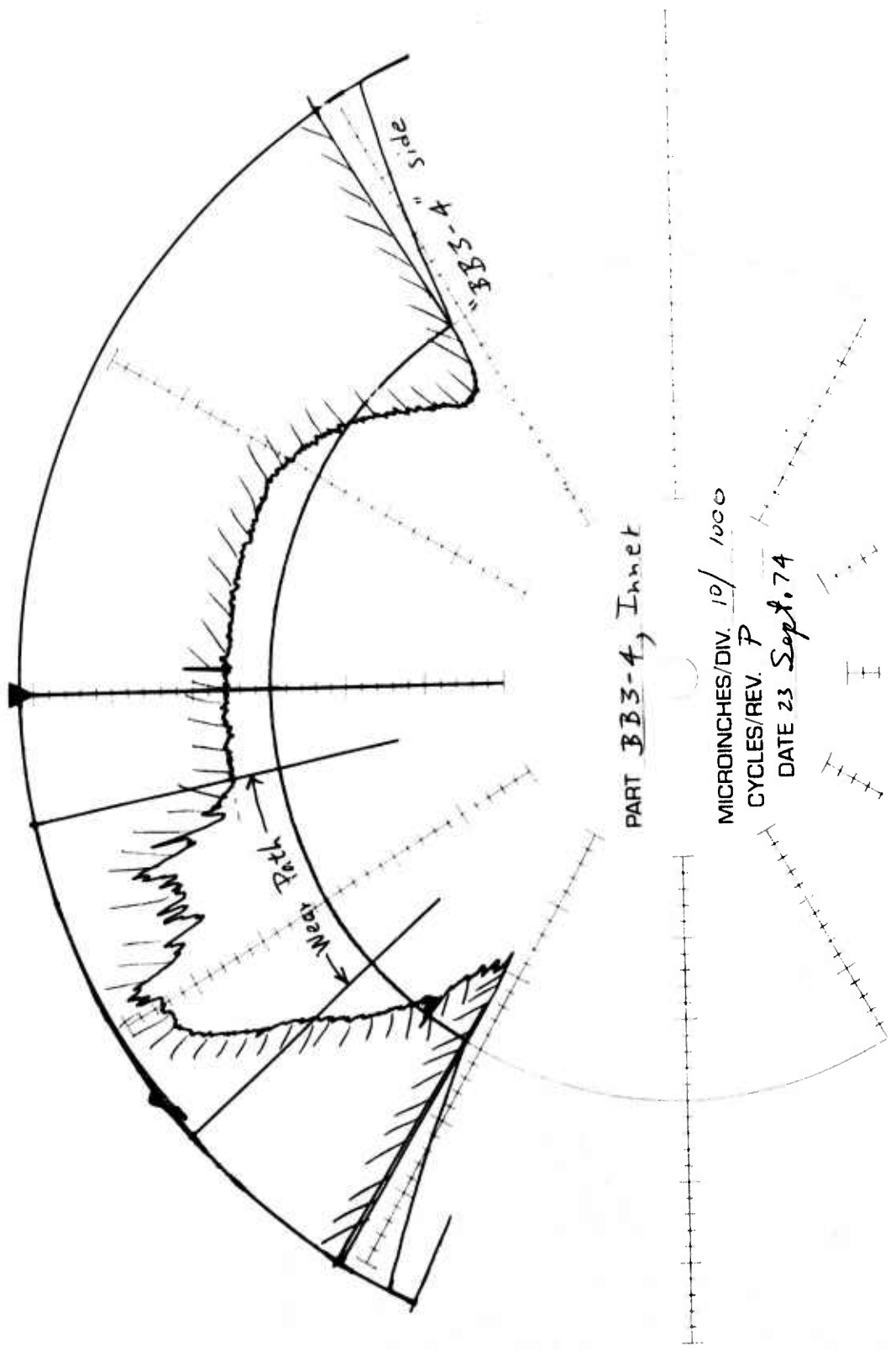


Figure 176. BB3-4, Cross-Groove Profile at Zero Test Hours.

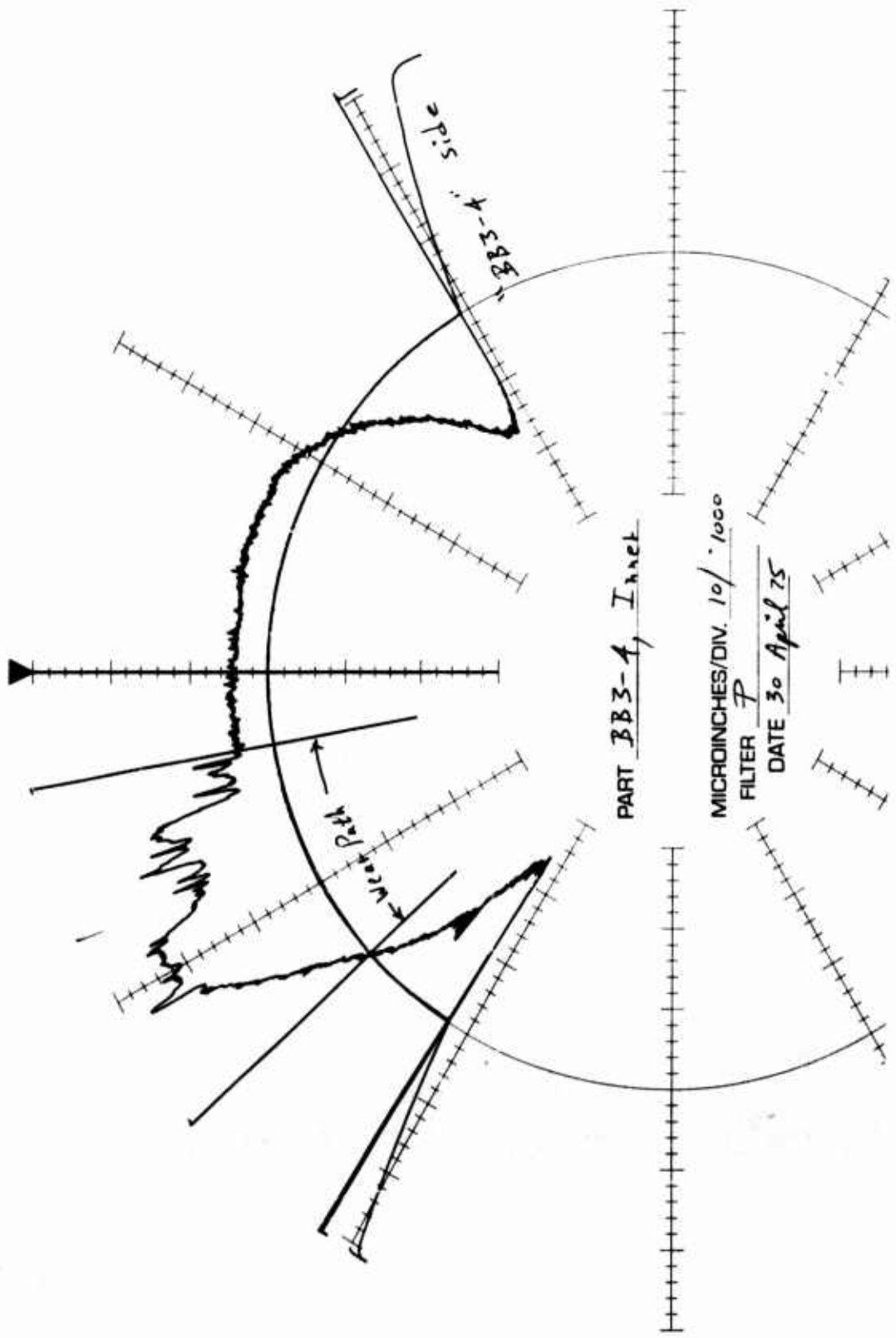
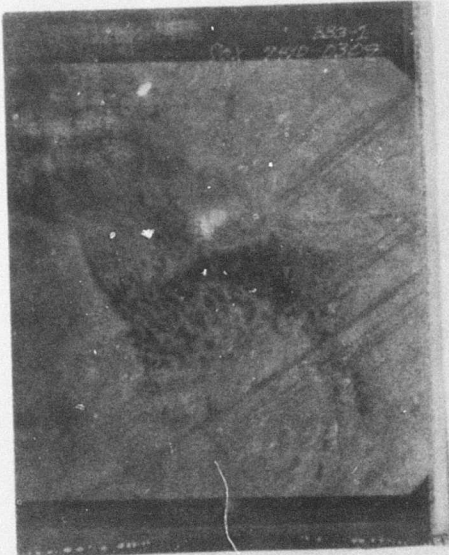


Figure 177. BB3-4, Cross-Groove Profile at 1086 Test Hours.



Top: 80 X
Bottom: 1000 X

Top: 300 X
Bottom: 1000 X, BSE

Figure 178. SEM Micrographs of BB3-1 (Zero Hours).



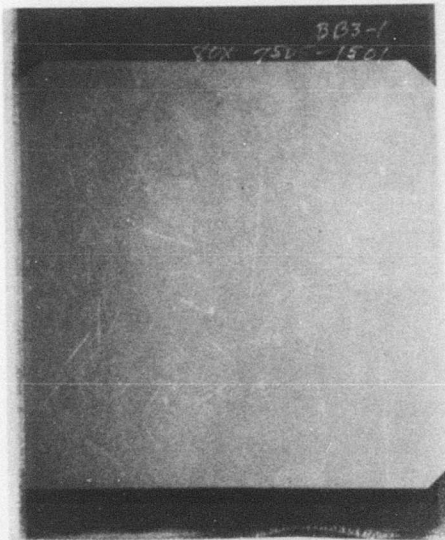
Top: 80 X

Bottom: 1000 X

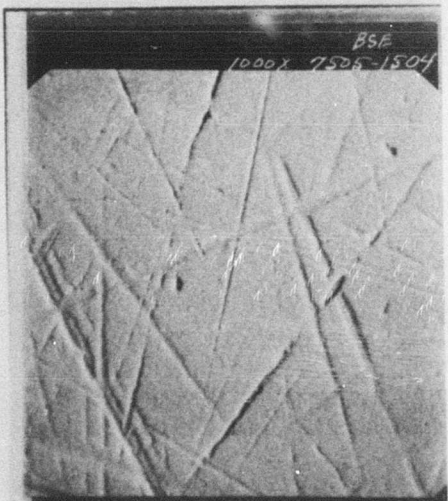
Top: 300 X

Bottom: 1000 X, BSE

Figure 179. SEM Micrographs of BB3-1
(Additional View, Zero Hours).

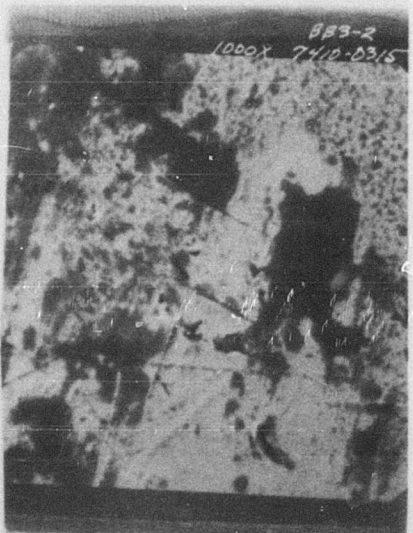
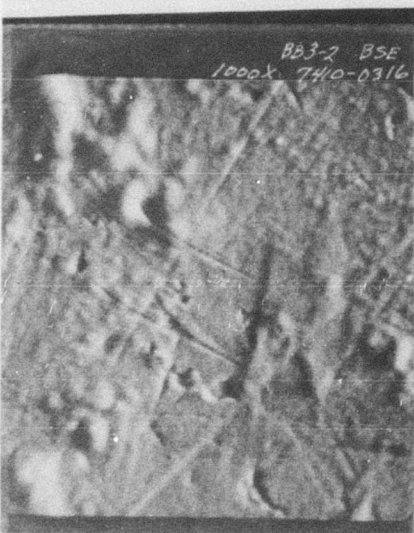
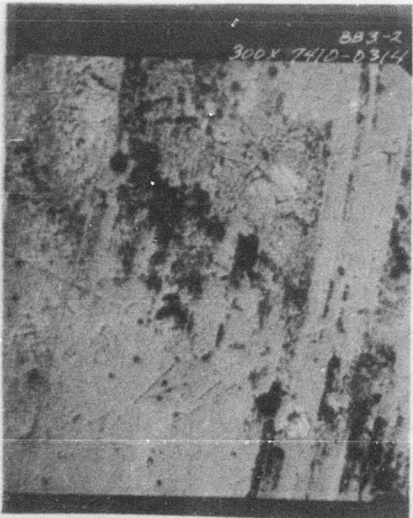


Top: 80 X
Bottom: 1000 X



Top: 300 X
Bottom: 1000 X, BSE

Figure 180. SEM Micrographs of BB3-1 (1086 Hours).



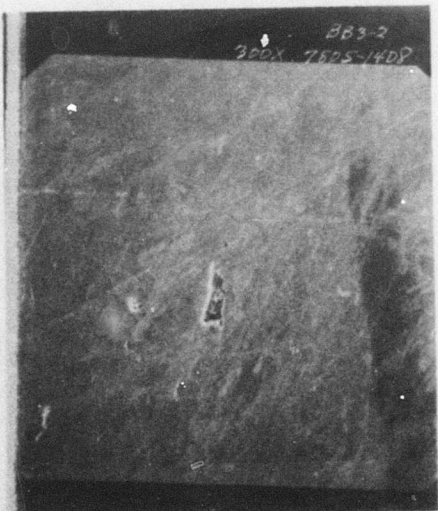
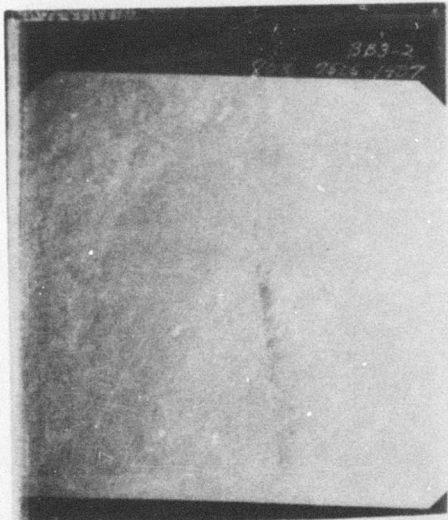
Top: 80 X

Bottom: 1000 X

Top: 300 X

Bottom: 1000 X, BSE

Figure 181. SEM Micrographs of BB3-2 (Zero Hours).



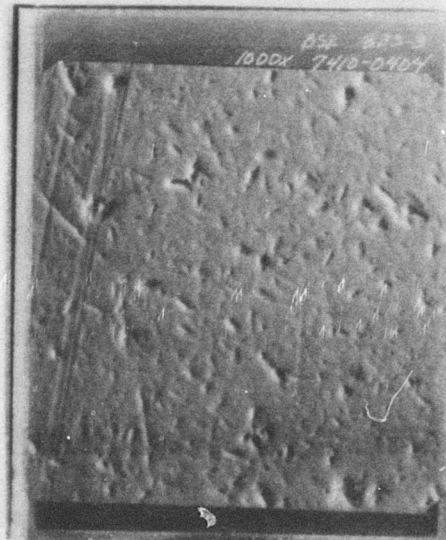
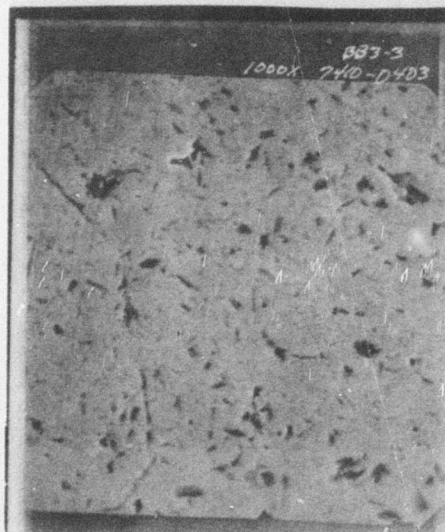
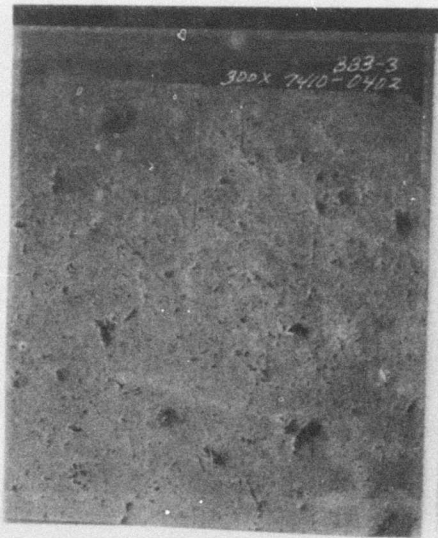
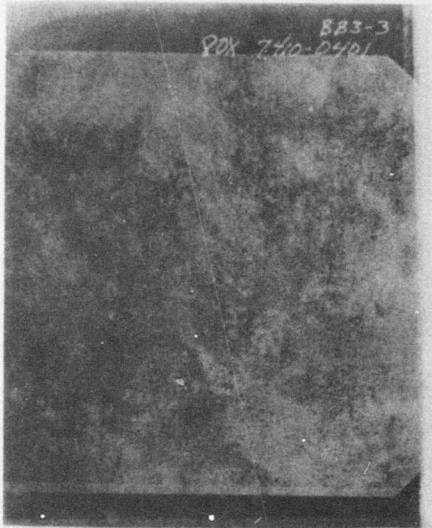
Top: 80 X

Bottom: 1000 X

Top: 300 X

Bottom: 1000 X, BSE

Figure 182. SEM Micrographs of BB3-2 (1086 Hours).



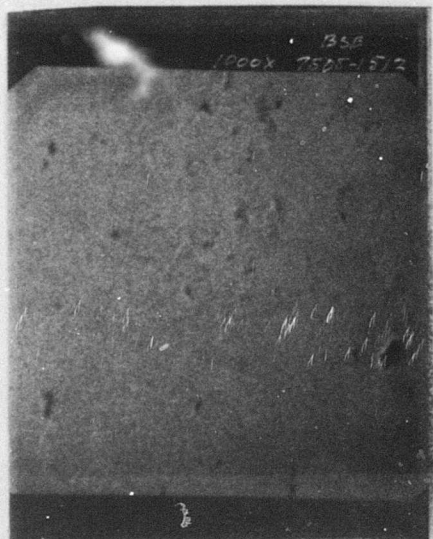
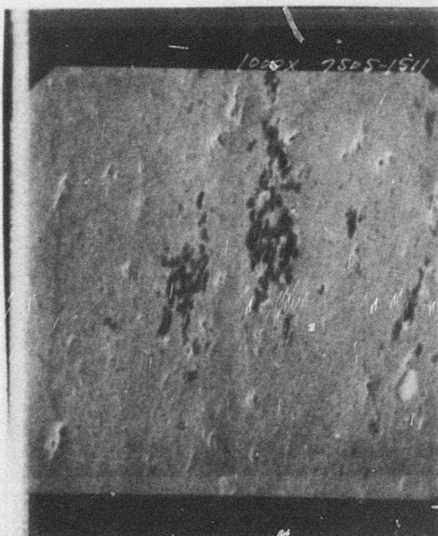
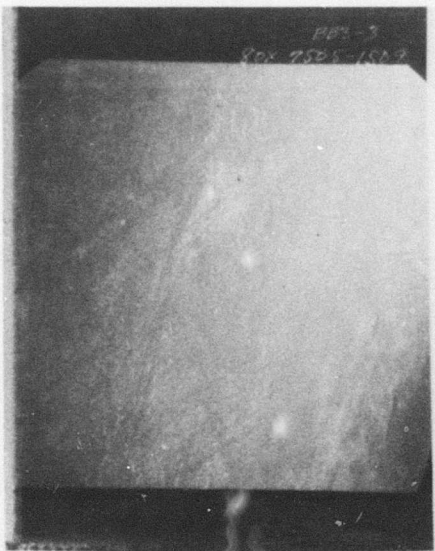
Top: 80 X

Bo. om: 1000 X

Top: 300 X

Bottom: 1000 X, BSE

Figure 183. SEM Micrographs of BB3-3 (Zero Hours).



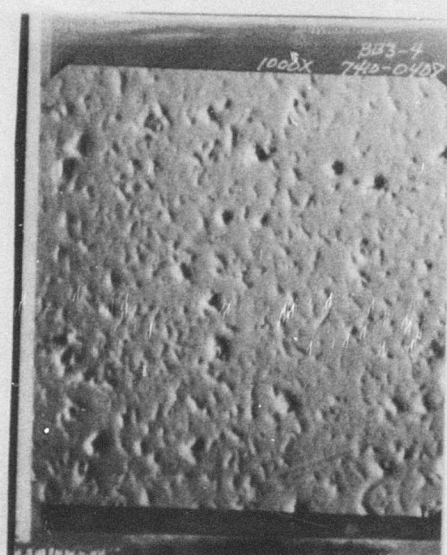
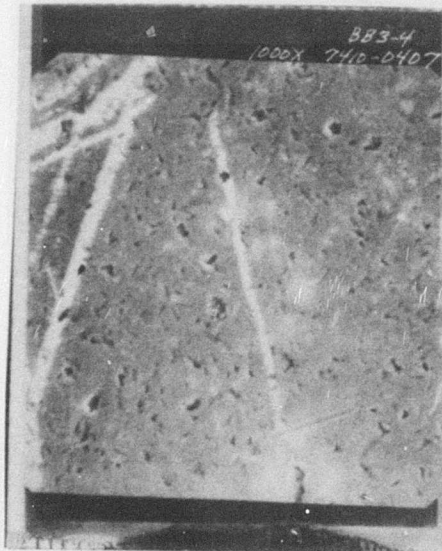
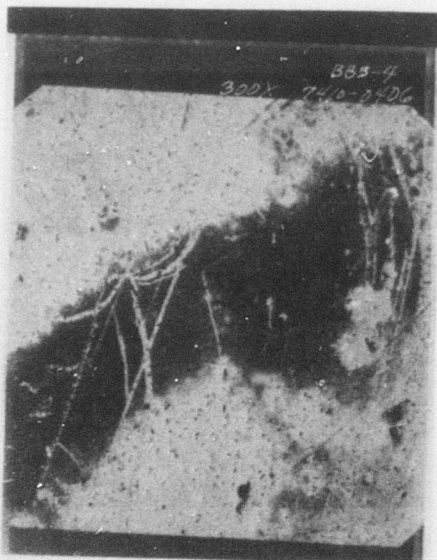
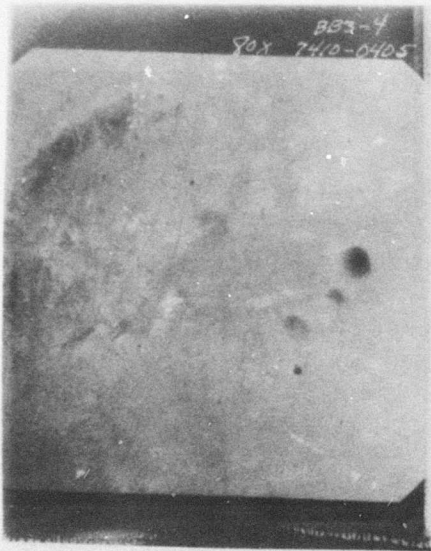
Top: 80 X

Bottom: 1000 X

Top: 300 X

Bottom: 1000 X, BSE

Figure 184. SEM Micrographs of BB3-3 (1086 Hours).



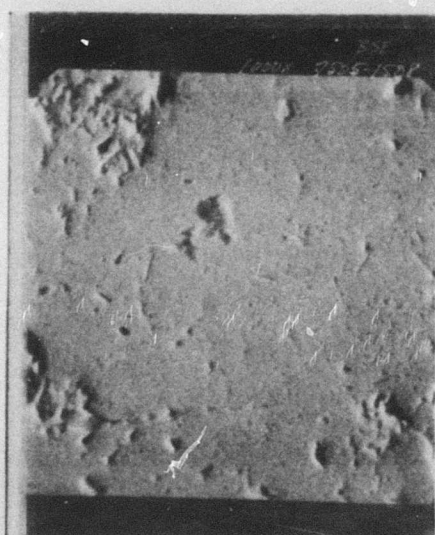
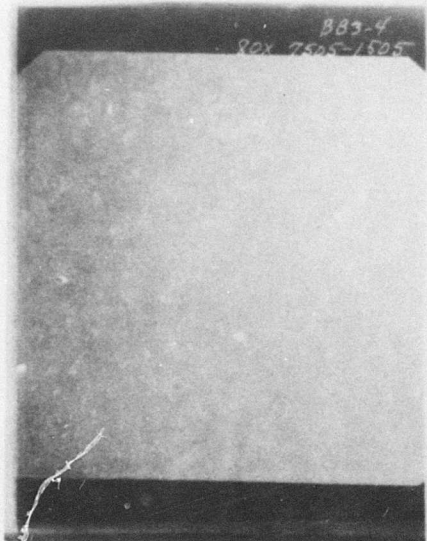
Top: 80 X

Bottom: 1000 X

Top: 300 X

Bottom: 1000 X, BSE

Figure 185. SEM Micrographs of BB3-4 (Zero Hours).



Top: 80 X

Bottom: 1000 X

Top: 300 X

Bottom: 1000 X, BSE

Figure 186. SEM Micrographs of BB3-4 (1086 Hours).

LIST OF SYMBOLS AND ABBREVIATIONS

SYMBOLS

a	starting time in hours
α	level of significance
b	stopping time in hours = $a + T$
β	confidence level
$F(k)$	Fourier transform coefficient k
$F(k)^*$	complex conjugate of $F(k)$
$f(i)$	time domain signal, sample i
k	frequency bin index
l	time index for statistically reduced PSD data = $(a+b)/2$
M	statistical mean over T hours
N	transform size, population size
$P(k)$	power contained in frequency bin k
P_t	PSD at hour t
S	statistical standard deviation of M , adjusted for sample size, T
$sgn(X)$	"Sign of X "
T	number of hours being averaged = sample size
t	time index for hourly PSD data
τ	torque
$W(i)$	hamming weighting function

LIST OF SYMBOLS AND ABBREVIATIONS - Continued

SYMBOLS

Z	Z-Score
Z_C	confidence coefficient
\hat{Z}	worst case \hat{Z}
ζ	confidence correction factor
$\hat{Z} _{w.c.}$	corrected Z-Score which includes confidence limits

TRENDING SYMBOLS

a_i	coefficients of a polynomial
k	frequency bin index
m	time index
$P_m(k)$	average PSD value of frequency bin k at time m
y_3	third-degree polynomial

ABBREVIATIONS

ADC	analog-to-digital converter
BSE	backscatter mode of the SEM
I/O	input/output
LED	light emitting diode
ODM	oil debris monitor
PSD	power spectral density
SEC	secondary emission mode of the SEM

LIST OF SYMBOLS AND ABBREVIATIONS - Continued

ABBREVIATIONS

SEM	scanning electron microscope
SUS	start-up sequence
TCC	test cell controller
TBO	time between overhauls
SOA	spectroscopic oil analysis